NTIA Special Publication SP-07-445

Proceedings of the International Symposium on Advanced Radio Technologies

February 26–28, 2007

Patricia J. Raush, General Chair
Kristen E. Davis, Publications

special publication

U.S. DEPARTMENT OF COMMERCE · National Telecommunications and Information Administration

NTIA Special Publication SP-07-445

Proceedings of the International Symposium on Advanced Radio Technologies

February 26–28, 2007

Patricia J. Raush, General Chair
Kristen E. Davis, Publications

U.S. DEPARTMENT OF COMMERCE
Carlos M. Gutierrez, Secretary

John M. R. Kneuer, Assistant Secretary
for Communications and Information

February 2007

DISCLAIMER

Certain commercial equipment, components, and software are identified to adequately present the underlying premises herein. In no case does such identification imply recommendation or endorsement by the National Telecommunications and Information Administration, nor does it imply that the equipment, components, or software identified is the best available for the particular applications or uses.

INTERNATIONAL SYMPOSIUM
ON
ADVANCED RADIO TECHNOLOGIES

February 26 - 28, 2007 · Boulder, Colorado

Sponsored by:

National Telecommunications and Information Administration (NTIA)

Institute for Telecommunication Sciences (ITS)

National Institute of Standards and Technology (NIST)

U.S. Department of Commerce, Boulder Laboratories

University of Colorado Department of Interdisciplinary Telecommunications

2007 ISART Technical Committee:

Patricia J. Raush, General Chair, NTIA/ITS

Carolyn G. Ford, Technical Chair, NTIA/ITS

Timothy Brown, University of Colorado

Nicholas DeMinco, NTIA/ITS

Paul McKenna, NTIA/ITS

Alakananda Paul, NTIA/OSM

CONTENTS

Page

Science, Engineering and Regulation – Support for Future Radiocommunications
An Australian View

Mrs Carol Wilson
Chairman, ITU-R Working Party 3M
CSIRO ICT Centre, PO Box 76, Epping NSW 1710 Australia
Phone: +61 2 9372 4222, Fax +61 2 9372 4106, carol.wilson@csiro.au

The radio spectrum used by a myriad of systems, providing a range of services to the public, is already crowded, and demand is growing. New approaches are needed to make better use of the spectrum. These approaches include extending our fundamental understanding of radiowave propagation through science, developing more effective and efficient radio systems through engineering, and managing the competing demands by innovative spectrum management techniques. This paper discusses the Australian context of radiocommunication use as well as the developments in science, engineering and regulation within Australia and elsewhere to support the continued growth of radiocommunications for future generations. The necessity for scientists, engineers and regulators to understand each other and work together is also detailed through examples.

1. Introduction

It is traditional to start a paper such as this by noting that the past few decades have seen a phenomenal growth in the number and type of radio devices that are a part of everyday life for millions of people.

Although such a statement is typically a justification in itself for the importance of radio technology research, I'd like to take a closer look at the radio devices and systems in common use. An obvious example is mobile telephones and wireless computer networks, which have been the main force in moving radio technology into consumer-grade products. While traditional television and radio broadcasting have been ubiquitous for quite some time, electronic news-gathering with a range of radio systems has enhanced the broadcasting experience with real-time coverage of sports, weather, traffic, emergencies and live entertainment. Air travellers rely on a number of communication and sensing systems, including air-traffic control, guidance systems, GPS and several types of radar. Drivers make use of keyless entry, garage door openers, traffic alerts and warnings, electronic toll payments, collision avoidance radar, hands-free headsets, and police radar. Office workers use an RFID tag for entering the building, and perhaps another for the parking lot, and collaborate over video-conferencing systems using fixed radio links. Retailers rely on checkout scanners, wireless inventory control, and RFID security systems. At home, remote control toys entertain older children while baby monitors watch the infants. The weather forecast on the evening news comes to us thanks to a huge range of active and passive sensing systems collecting data from the earth's surface as well as from space.

These are some of the radio technologies that an ordinary person in Australia (or America, France, Brazil…) might encounter in a typical day. Beyond this, specialist uses of radiocommunications, such as defence, emergency services, radioastronomy, amateur radio, taxi and fleet dispatch and maritime operations, would add significantly to the list of radio systems and services which have become essential, or at least highly desirable, to life in the developed world.

While this paper presents an Australian viewpoint, my key points are not unique to the Australian situation. First, I am convinced that innovation in science, in engineering, and in the regulation of spectrum are all essential to the continued success and growth of these important technologies. Indeed these three disciplines need to work together and understand each other better as radio technology becomes integral to more aspects of our lives. Following from this, I believe it is important that experts working on radiocommunications technology have an understanding of the broad reach of the whole field, in addition to their specialist view of a particular area.

2. Australian challenges for radiocommunications

From the description given above, it is clear that everyday life for a city-dweller in Australia is much like that in any other part of the world. Australians have typically been early adopters of new technologies; in a country of 20 million people, there were nearly 9 million mobile handsets sold last year. There are, however, some features of Australia that present particular challenges for radiocommunications, and also provide some interesting opportunities.

2.1 Australian geography and demographics

One of the defining differences between Australia and countries with a similar standard of living is the population density and distribution. Table 1 shows a comparison of Australia to the USA and the UK in some population statistics [1,2,3].

Table 1
Demographic comparison of Australia, USA and UK

	Australia	USA	UK
Population (millions)	20.7	301	60.6
Area (,000 sq km)	7,687	9,631	245
Population density (per sq km)	2.7	31.3	247.6

The distribution of population in Australia is quite sharply divided. About 85% of Australian live within 50 km (31 miles) of the coast, consequently, the major cities are also coastal. Most of the population is based on the eastern and south-eastern coasts. Three quarters of Australians live in major cities, with only 2.5% living in the remote areas through the centre of the continent. Figure 1 shows the sharp contrast between population centres and remote regions [4].

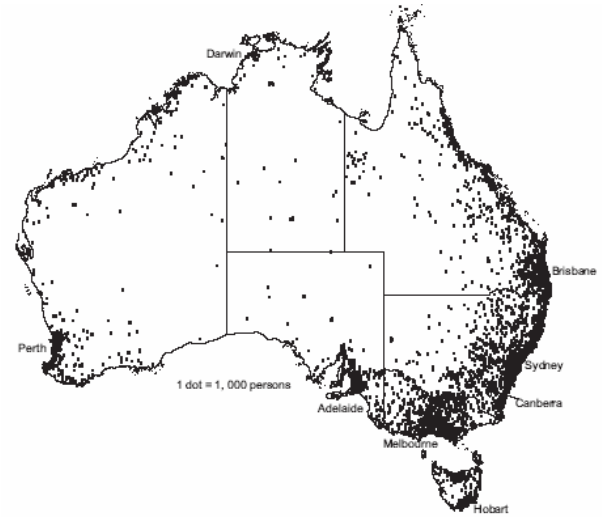

Figure 1
Population distribution of Australia, 2004

Australia has no land boundaries with another country. Papua New Guinea, East Timor, and Indonesia are near neighbours to the north, but our major trading partners: Japan, China, the US and Europe, are distant.

The population density of Australian and its geographic isolation has created both challenges and opportunities in relation to radiocommunications. The need to provide services to all Australians, even those in remote areas, has become a major political and economic issue. GSM and CDMA mobile phone systems currently service 97.5% of the population by covering 13.7% of Australia's landmass. However, reaching the last few percent in the extremely remote areas remains a technical and economic challenge. A new initiative to increase this to "more than 98%" will require increasing the area coverage to 18%.

Similarly, wired and wireless broadband services are available to many Australians in the cities, but "broadband to the bush" continues to be a highly charged political issue. Satellite is used to provide telephony, television and sound broadcasting, and a range of other services to remote areas, but it is expensive and the quality of service is generally poorer than that available in the cities.

On the other hand, Australia's geographic isolation, and particularly the lack of land borders with other countries, has traditionally provided some flexibility in the use of radio spectrum, as there is no requirement to coordinate terrestrial systems with adjacent countries. Australia is therefore an ideal place to evaluate new approaches to spectrum. These will be discussed in section 3.4.

2.2 Australian weather

As a large continent stretching from the tropics into cool temperate regions, Australia has a wide range of climates, and a number of very extreme weather conditions. The northern parts of the country are prone to cyclones and floods, while the central part of the country has large deserts. The areas of heavy population represent the traditional farming regions, but these are subject to frequent and prolonged drought. Coupled with high summer temperatures, this often leads to large scale bushfires. The state of Victoria is, along with southern California and the south of France, one of the three worst bushfire regions in the world; in January 2007, over a million hectares burned in a period of 48 days.

There is a misconception that Australia is such a dry continent that it never rains! Even in the midst of drought, many of the major cities experience heavy thunderstorms. A hail storm in Sydney in 1999 caused about $1.5 billion in damages, including 20,000 homes, 40,000 vehicles and 25 aircraft.

The implications of these weather characteristics for radiocommunications are two-fold. First, Australia

relies heavily on accurate and timely weather forecasting, which requires a number of passive and active radio sensing systems across a wide range of frequencies. In March 2006, Cyclone Larry hit a populated region of the Queensland coast. Satellite-based systems allowed the Bureau of Meteorology to predict the eye of the storm to within 30 km two days before landfall. Although the category 5 storm caused $360 million in damage to property, evacuations ensured there were no lives lost, and the potential for property damage would have been much higher without the warning.

Fire-fighters are dependent on the prediction of wind speed and direction as they battle bush-fires, and the information must be relayed to fire crews by reliable radio networks.

In the longer term, passive and active radio systems provide a record of climate patterns over decades, to predict future trends and influence policies for water usage, agriculture and environmental protection.

Secondly, the characterisation of weather patterns, particularly rain, is important in predicting the performance of radiocommunication systems. Australia's extremes of drought and floods make it challenging to measure and characterise "typical" rainfall patterns. Outside the major cities, there is little data at the level of detail required for propagation prediction, but the interest in providing broadband services to regional and remote areas of Australia, through terrestrial or satellite systems, has highlighted the urgent need for this information. There has been some interest from a few universities, and some data from operational links run by a telecommunications company, but much more is needed.

2.3 Australian industry

Australia does not have a major manufacturing industry, but has traditionally relied on primary industries such as agriculture and mining. In technology, there is a focus on innovation and value-added products rather than mass-production; we supply research and development for multinational companies, or develop small spin-offs which are taken over by international players.

In the radiocommunications area, this means that Australia buys in technology from Europe, from Asia and from North America. A major benefit of this approach is that Australia can consider different technologies from these regions and choose among them. With Australia's geographic isolation and lack of land borders, we have considerable independence in choosing a mobile telephony or digital television standard without concerns of cross-border interference.

The other side of this situation, however, is that while Australia has choice, it does not have full flexibility in the use of the spectrum. We rely on systems built for the national or regional requirements of other parts of the world. One example is the range of communications, surveillance and radar systems used by the Australian military. They often purchase a few units from a large production run by a manufacturer in, for example, the USA. The frequency range is therefore determined by the country of manufacture, and the Australian spectrum usage has to accommodate such systems. Similar situations occur for a range of professional and consumer systems, as Australia is typically not a large enough market to justify a separate product line.

One outcome of this position is that Australia is very active in international spectrum management activities in the ITU. We have a strong interest in ensuring that radiocommunication systems developed overseas will provide appropriate technology for the Australian market. We also support global harmonisation of spectrum, which will reduce the difficulties with competing regional standards, as well as the development of adaptive radio technologies which accommodate a range of standards.

2.4 Australian radioastronomy

Another significant user of spectrum in Australia is the radioastronomy community, which has a high international profile both for their research output and for operating several large radiotelescope facilities. The Australia Telescope National Facility is part of CSIRO, and works closely with the ICT Centre. It operates the Parkes telescope, a 64 metre instrument, as well as the Narrabri Compact Array of 6 22 metre antennas, and another 22 metre dish at Mopra. Requirements of radioastronomy instruments have created significant technical challenges for engineers over many years. In addition, the high sensitivity of radioastronomy receivers has required protection from radio interference caused by other systems.

Australia is also part of an international collaboration to build a new radiotelescope, the Square Kilometre Array (SKA), named for the equivalent collecting area of the proposed instrument. It is intended to operate over a frequency range of about 100 MHz to 20 GHz and provide 100 times more sensitivity than current radiotelescopes. In addition to contributing to the technical development of this telescope, Australia is one of the possible sites for its construction. A major factor in the siting, construction, and data processing of the SKA will be the prediction and mitigation of interference from active radio services. Australian

scientists and engineers have been working very closely with regulators on this issue. A demonstrator system is now being developed in Australia to evaluate a number of technology choices, including interference issues. A decision on the site for the SKA will be made in 2009.

3. Addressing the challenge for spectrum

The Chairman of the Australian Communications and Media Authority, which regulates radiocommunications within Australia, recently summarised the spectrum situation [5]:

Talk to any big user of spectrum, as we do – to telecoms operators, defence, space scientists, meteorologists, and you, the practitioners in this very room – and they (and you) will all say that more and more spectrum is needed every year. However, unlike demand, our ability to 'supply' spectrum, to make it available for use, is increasing very slowly. Even the higher bands, while able to carry more data, can only carry it over very short ranges. In effect, then, we will indeed run out of spectrum, unless we do something about it.

As stated earlier, I believe the three components of "doing something about it" are radio science, radio engineering, and radio spectrum management. These three components are strongly interconnected. Before going into detail, it is useful to review the framework of international spectrum management as undertaken by the Radiocommunication Sector of the International Telecommunication Union (ITU-R).

3.1 ITU-R and its Study Groups

The International Telecommunication Union (ITU) is an international organization within the United Nations System where governments and the private sector coordinate global telecom networks and services. One major function of the ITU is the management of the radio spectrum and the geostationary orbit, as limited resources to be shared in an efficient and fair manner. This activity is carried out by the Radiocommunication Sector (ITU-R) which maintains a treaty-level agreement, the Radio Regulations [6], to serve as a framework for international spectrum usage. National radio spectrum management within individual countries is then based on the Radio Regulations.

Across the frequency spectrum 9 kHz to 275 GHz, regulated internationally by the ITU and nationally by government agencies, most frequency segments are shared by at least two and often three or four different services. New technologies and growing technologies seek new spectrum allocations, requiring methods for sharing the spectrum with existing services.

Technical work to support decisions on spectrum management is carried out by ITU-R Study Groups [7]. Most of these Study Groups consider the operational characteristics and requirements of a particular type of radio system. For example, Study Group 4 addresses fixed satellite services, and Study Group 8 covers mobile services, including mobile-satellite systems. Study Group 3, however, considers propagation issues relating to all radiocommunication services. As a result, Study Group 3 has developed and continues to improve internationally agreed propagation prediction methods for all types of radio systems, in the form of Recommendations.

3.2 Science approaches – radiowave propagation

A major theme of this conference is propagation modelling for a range of applications and in a variety of environments. It is well-known that propagation prediction methods are used in system design, for example, to calculate the required link margin of a satellite service, or the expected coverage area of a mobile system. Improvements in such methods can lead to more accurate system design, utilising lower power or making better use of the allocated bandwidth.

Another important aspect of spectrum management is understanding and predicting the potential for interference between different services in the same band. There is therefore a need for propagation prediction methods to estimate the likelihood of signal levels able to cause interference. Supporting these prediction methods are models of the natural variability of the environment, including climate and its effects, terrain, building materials and vegetation.

Propagation prediction methods developed within Study Group 3 are based on inputs from researchers around the world. Extensive measurement campaigns coupled with modelling of the underlying physical processes have been used to develop step-by-step methods for calculation of impairment levels such as attenuation or depolarisation. The methods are tested against a database of measurements which is maintained by Study Group 3.

Study Group 3 Recommendations are intended to contain the most accurate and comprehensive advice at the time, but are also subject to frequent improvement and extension. It is therefore important for users of the Recommendations to consult the most recent version.

The key criteria in developing the prediction methods are, in order of importance: accuracy, clarity, simplicity and fit to the underlying physical phenomena. Prediction methods are selected which give the best match to measurements, not just for the database as a

whole, but also for specific subsets (low/high latitudes, low/high elevation angles, low/high frequency bands, etc) to ensure that the prediction method is uniformly accurate. In most cases, the prediction method is given as a step-by-step procedure for clarity. Simpler methods which are equally accurate and clear are preferred over more complex methods. Ultimately, Study Group 3 is working towards prediction methods which are more clearly based on physical processes, rather than empirical methods, where this is possible without sacrificing accuracy.

Research results and measurements which can assist in these activities are urgently needed and always welcomed. There is only space to note a few areas that may be of particular interest.

3.2.1 Short-range services

Recommendation ITU-R P.1238[1] provides advice and prediction methods for indoor communication systems, intended particularly for WLAN and mobile phone services. It covers the range 900 MHz to 100 GHz, and has specific data for 900 MHz, 1–2, 4–5, 60 and 70 GHz, based on measurements. The prediction methods include a site-general model for loss, including loss between floors of a building, and for delay spread. The Recommendation also provides extensive advice on the use of site-specific (e.g. ray-tracing) models, the effect of polarisation and antenna pattern, the effect of building materials and furnishings (including a table of the complex permittivity of a number of materials at a wide range of frequencies) and the effect of the movement of people in the room.

Current work to extend Recommendation P.1238 includes a model for angular spread, particularly for MIMO (Multiple-Input Multiple-Output) systems, and further measurements of path loss coefficients at the frequencies of interest. In addition, there is a need to address diversity (space, polarization, antenna sector and frequency) and the reflection characteristics of rough surfaces. For the purposes of interference analysis, there is also a requirement to consider indoor interference arising from distributed emissions, such as those which may be caused by Digital Subscriber Line (DSL), broadband-over-powerline systems and high speed data networks.

Recommendation ITU-R P.1411 gives prediction methods and advice for short-range (up to 1 km) outdoor environments, including urban high-rise, urban/suburban low-rise, residential and rural. It covers the frequency range 300 MHz to 100 GHz, with specific measurement results at key frequency bands. Prediction methods are provided for path loss and delay spread on line-of-sight and non-line-of-sight scenarios, including over rooftops and urban street canyons. General advice is given on the effects of vegetation, with reference to a more detailed Recommendation. Finally, the Recommendation provides some measured results, provided by CSIRO, of indoor-to-outdoor building material loss at 5.2 GHz. This information was used in evaluating the potential interference from WLANs to satellite-based receivers, prior to the decision of the ITU to allow WLANs in the 5.15–5.35 GHz band.

Work is underway within Study Group 3 to extend Recommendation P.1411 to cover more frequency bands and a more comprehensive set of environments. Measurements are needed to evaluate and refine the prediction methods.

3.2.2 Ultrawideband

With the growing interest in ultrawideband systems, both from potential developers who need to understand the performance of UWB and from regulators who need to estimate the interference to other services, Study Group 3 has recently developed a new Recommendation on ultrawideband propagation. It represents an initial step to characterise the basic transmission loss for typical indoor and outdoor systems up to a range of 20 metres. This is useful for establishing a link budget or planning system coverage. For interference analysis, the Recommendation indicates that other models should be used, depending on the narrowband system (mobile, satellite, WLAN, radar, etc) that may receive interference from UWB transmitters.

Study Group 3 plans to extend this Recommendation to cover distance beyond 20 metres, indoor-to-outdoor losses, and to extend the path loss parameters to more specific environments.

3.2.3 Land mobile and broadcasting systems

In the past, Study Group 3 maintained separate Recommendations to predict coverage for land-mobile systems (including mobile phones) and for broadcasting, but as the geometries and frequencies involved are similar, these have been merged into a single Recommendation ITU-R P.1546. It covers the frequency range 30 MHz to 3 GHz. In contrast to other Recommendations which provide step-by-step equations, the core of Recommendation P.1546 is a series of curves, developed for the broadcasting and

[1] Current (numbered) Recommendations cited available at www.itu.int/rec/recommendation.asp?type=products&parent=R-REC-P . Three free Recommendations per year are available via ecs.itu.ch/cgi-bin/ebookshop .

mobile industry on the basis of very extensive measurement campaigns. The curves provide the field strength exceeded for 50%, 10% and 1% time, within an area of 500 m by 500 m, for a 1 kW ERP (equivalent radiated power) transmission at 100 MHz, 600 MHz or 2 GHz, for a range of transmitter antenna heights and a fixed receiver height. Procedures are then provided to extrapolate or interpolate to other time percentages, other frequencies, other antenna heights, and to take account of local terrain variations.

This Recommendation has been used by the ITU in replanning the allocation of broadcasting frequencies across Europe, North Africa and the Middle East.

3.2.4 Interference between systems

Recommendation ITU-R P.452 gives comprehensive prediction methods to calculate the interference between a transmitter and a receiver which are both on the surface of the Earth. It is applicable at frequencies above 700 MHz, and covers all types of interference paths.

Prediction methods for system design typically concentrate on losses due to propagation phenomena, in order to establish a link margin, but as the emphasis in these methods is on signal levels that potentially cause interference, it is necessary to consider propagation effects which enhance the average signal level. The Recommendation starts with interference mechanisms which can occur for large percentages of time: line-of-sight, diffraction over terrain or buildings, and tropospheric scatter. But it also considers those mechanisms which can occur for short periods of time: multipath enhancements of the line-of-sight signal, ducting from surface or elevated atmospheric layers, reflection and refraction from atmospheric layers, and scattering by raindrops or other hydrometeors.

The prediction method requires information about the transmitter and receiver: frequency, geographic location and height of the antennas above local ground and above mean sea level. A terrain profile between the transmitter and receiver is needed, as well as an estimate of what proportion of the path is over water. It also requires radiometeorological data, particularly statistics of the refractive index variation with height, as well as rain statistics for the rain scatter calculations.

Work is underway to increase the frequency range of Recommendation P.452 and to extend the minimum time percentage at all frequencies down to 0.001%. Measurements are needed to validate these extensions. One recent proposal relates to the method of predicting the statistics of super-refractivity events, which is important for low time percentage predictions.

3.2.5 Coordination distance

Key frequency bands used by fixed satellite services are also allocated to terrestrial services, leading to the potential for interference between earth stations and terrestrial systems. Before the installation of an earth station, a detailed analysis must therefore carried out. As the earth station of one country can potentially affect (or be affected by) terrestrial systems in another country, internationally approved procedures are required.

Recommendation ITU-R P.620 is used to calculate the coordination area around a fixed earth station, that is, a geographic area surrounding the station within which the possibility of interference between the earth station and terrestrial systems exceeds a certain threshold. Once this zone is defined, more detailed interference calculations are then carried out for the actual systems within the zone, using Recommendation P.452 described above. For economic and technical reasons, it is important that the zone be accurately estimated; if the zone is too small, potential interference sites may be overlooked, while if the zone is too large, an excessive number of detailed analyses must be performed.

There are two components to the calculation in Recommendation P.620. The first considers terrain shielding, the earth station antenna pattern and clear-air effects: line-of-sight propagation, diffraction, ducting and troposcatter. For each azimuth angle around the earth station, a distance is calculated at which the total clear-air loss exceeds a threshold value, and a contour is drawn. The second component is rain scatter, which produces a circular contour around a point offset from the earth station location along the direction of the main beam. The complete coordination zone is then defined by taking the larger distance at each azimuth.

There is a need to study whether Recommendation ITU-R P.620 can be revised to provide a better method for coordination contours for bidirectionally-operating earth stations.

3.3 Engineering approaches – technology

Another main theme of this conference is advanced radio technologies. While I don't intend to review these in detail, it is worth noting the range of technologies and their relationship to the science and regulation components of this paper. Within Australia, particularly at my organisation, CSIRO, we are developing a number of these technologies to address future radiocommunication requirements.

Some of these technologies are aimed at more efficient spectrum use in frequency bands already heavily used.

MIMO, for example, takes advantage of a cluttered indoor or urban environment to create multiple channels and increase data rates within a limited bandwidth. Ultrawideband, in contrast, uses a much wider bandwidth but at very low power levels to minimise interference to other users. Software-defined radios, leading eventually to cognitive radio systems, adapt to the physical environment as well as other radio users to take advantage of unused portions of the spectrum.

Other technologies seek to extend the limits of useful spectrum. CSIRO recently demonstrated an 85 GHz link which carried 6 Gbits per second across a 250 m distance – this could reasonably be extended to at least 1 km. We are also developing remote sensing systems for security applications at about 200 GHz. Within the ITU, there is a growing interest in the use of near-infrared and optical frequencies for both terrestrial and satellite links. Technologies at such high frequencies allow larger bandwidths and higher data rates, and can free up lower spectrum for longer-range systems.

These new technologies require an understanding of radiowave propagation for particular environments, therefore, it is essential for engineers in these areas to work with the propagation scientists to articulate the requirements for prediction methods and to understand the limits of propagation models. Technology development also requires an awareness of the competing demands on spectrum use. It is not uncommon for engineers to start development of a new system in a frequency band which is technically valid but not ideal from a regulatory point-of-view. One example in recent years is the introduction of WiFi in the lower part of the 5 GHz band (5.15 – 5.35 GHz). Unlike other WiFi frequency bands, this was not "un-licensed" or class-licensed spectrum, but is used for satellite uplinks. The ITU-R eventually approved the use of WLANs in this band, subject to constraints that are difficult to enforce, and has left, for future analysis, the question of how to manage rising interference into the satellite receivers.

It is particularly important that engineers describe the benefits of new technology in the context of the full range of spectrum users. For example, cognitive radio systems offer great benefits in sharing specific frequency bands among radio devices with similar power levels and usage patterns. Within a band, the spectrum can be used much more effectively by allowing each device to use any unoccupied channel. It is dangerous, though, to extrapolate this to all users across the entire spectrum, as the system would have to allow for high-power radars, consumer short-range devices, sensitive satellite receivers and passive services. The radioastronomy and remote sensing communities are justifiably concerned when someone describes spectrum as "unused" simply because no man-made transmission is detected! Nevertheless, some regulators and legislators have predicted that cognitive radio will bring an end to the need for spectrum management. Engineers need to be clear, not only about the benefits of technology, but about its limits as well. On the other side, regulators need to look carefully at engineering solutions and the assumptions behind them.

3.4 Regulatory approaches – spectrum management

Spectrum regulators in Australia, and everywhere else, face the difficult challenge of balancing competing demands to allow for efficient and effective use of the radio spectrum. The difficulty might be highlighted with an example. Within Australia, the frequency range 10.6 to 10.68 GHz is used by one of the carriers for about 1000 fixed links in the backhaul network for mobile phones, mostly near a few major cities. It is also a critical band for satellite-based passive sensing of biomass, which is used for monitoring environmental changes, predicting bushfire behaviour and evaluating soil moisture. The transmissions from the fixed links create noise to the remote sensing systems, and therefore no data can be collected from some points in Australia. Regardless of how this situation arose, the regulators now face a complicated choice between the continued value of meteorological predictions or the cost to industry of moving fixed services to another band (if, in fact, one can be identified). Australian legislation requires that regulators manage the spectrum for "overall public benefit", but when competing demands include the commercial goals of industry, the public value of weather forecasting, science services such as radioastronomy, entertainment and information through broadcasting, national defence and security, and many more, there are no clear-cut guidelines.

As noted earlier, Australia's geographic isolation has allowed experimentation with spectrum management techniques. Australia was the first to introduce spectrum licensing in the early 1990's as a way of allowing more flexibility. Prior to this, users of radio spectrum either operated under a class licence (for low power, ubiquitous devices such as garage door openers or cordless phones) or an apparatus licence, which was issued on payment of a fee and allowed the operation of a particular transmitter with specified characteristics (frequency, power, antenna type) at a specified location or with a specified area. Spectrum licences, on the other hand, give users the right to a specified frequency band in a nominated geographic area for a given period

of time. There are some minimal technical limitations to ensure that users do not interfere into adjacent spectrum or geographic space, but otherwise, licence-holders have considerable freedom in their use of the spectrum. These licences were issued through an auction process, another innovation at the time, and one which is independent of the spectrum licence concept. A number of other countries have since introduced spectrum licences via auction, notably for the 2 GHz spectrum identified for 3G mobile services, with mixed results. Nevertheless, spectrum licences in Australia have provided a useful level of flexibility in some key frequency bands.

In considering spectrum availability for new wireless access systems such as WiMax, IMT-Advanced and others, the Australian regulators are now considering a tiered approach to accommodate Australia's particular demographic distribution. In a discussion paper released in December 2006 [8], four tiers are described. The first would allow coverage of an entire state, including its capital city. Licences would be issued to at most two operators per state through an auction process. A second tier would allow access to one large regional town and the rest of the state, but not the other towns or the capital city. The number of operators in each town would be limited to three. These licences might be issued through an auction if there is high demand, otherwise they would sold at a set price. The third tier would give operators the right to offer services within a state, excluding all the large towns and capital city. An unlimited number of licences would be issued over the counter for a set price, as there is not expected to be much competition. The fourth tier would allow wireless access services in the remote areas of Australia under a free class licence. Discussions between the regulator and industry are still proceeding on this proposal.

In an ideal world, the role of a spectrum regulator would be to prevent harmful interference between radiocommunication systems. However, engineers are well aware that radio technology is not ideal. Therefore another role of the regulator is to investigate and resolve interference problems. These are often caused by a complicated combination of circumstances, and sometimes lead to surprising conclusions. A number of years ago, the ACMA regional office received repeated calls about widespread television interference, every evening from 7:10 pm, for about 5 minutes. The problem of isolating the source in a short time duration was made more difficult by the fact that the area of interference was a four hour drive from the regional office. Over several visits, the ACMA engineers got closer, and after two years, finally pinpointed the house. The residents were an elderly couple who only used their television to watch the evening news at 7 pm. The masthead amplifier had a fault which didn't occur until it warmed up, which took about 10 minutes. After that, it not only caused interference to the rest of the town, but to their own viewing, so they turned off the TV, and, being frugal, unplugged the power to the set and amplifier, thereby ending the interference. [9] Such incidents highlight the challenges of Australian geography, as well as the persistence of engineers!

4. Conclusions

Australia relies heavily on radio technology for a range of essential services, commercial opportunities, entertainment and science. Aware that spectrum is a valuable and limited resource, we are active in the areas of science, engineering and regulation to improve the use of radiocommunications and ensure adequate spectrum for the future. These three disciplines need to communicate and collaborate, as they are deeply dependent on each other.

This conference is an excellent venue for propagation scientists, technology engineers, and spectrum regulators to discuss the issues relating to the future of our industry. I hope that you will use the opportunity for cross-fertilisation and take home some new ideas.

I would like to extend my thanks to Patricia Raush: first, for organising such an interesting and important conference, second, for inviting me to be here, and last, but not least, for encouraging researchers from NTIA to be involved in the work of ITU-R and Study Group 3.

5. References

[1] Australian Bureau of Statistics, www.abs.gov.au
[2] United States Census Bureau, www.census.gov
[3] CIA World Fact Book, www.cia.gov/cia/publications/factbook/index.html
[4] Australian Bureau of Statistics, *Year Book Australia 2006*, Canberra, 2006.
[5] Chapman, Chris, *Radcomms: a day in the life*, Address at ACMA Radiocommunications Conference, Sydney, 11-12 December 2006.
[6] International Telecommunication Union, Radio Regulations. Geneva, Switzerland, 2004.
[7] www.itu.int/ITU-R/index.asp?category=study-groups&link=rsg&lang=en
[8] ACMA, *Strategies for Wireless Access Services: Spectrum Access Options*, Discussion paper SPP/10/06, Canberra, December 2006.
[9] ACMA, "Convergence in Action – the New ACMA", *ACMAsphere Issue 8, May 2006.*

Apartment Building RF Penetration Measurements Using an Ultra-Wideband Measurement System

Robert Johnk[1], Dennis Camell, Chriss Grosvenor,
Galen Koepke, David Novotny, Kate Remley
National Institute of Standards and Technology
1. Corresponding author phone: (303) 497-3737
Email: robert.johnk@nist.gov

This paper describes the use of a newly-developed ultra-wideband transmission measurement system that was used to perform electromagnetic penetration measurements of a local apartment building. Measurements were performed using a NIST-developed system in the 30 MHz - 18 GHz frequency range. Phase-coherent transmission measurements were performed at over 48,000 frequencies, and the data obtained were used to evaluate building penetration at 26 different locations inside the building. In addition, the data were post processed to obtain high-fidelity time-domain waveforms to facilitate the extraction of useful propagation parameters. This talk will provide a detailed summary of the measurement system, test procedures, and the results obtained. The data should be of great interest to the first-responder and wireless network systems design communities.

Indoor Navigation Test Results using an Integrated GPS/TOA/Inertial Navigation System

Alison Brown and Yan Lu
NAVSYS Corporation
Phone: 719-481-4877; Fax: 719-481-4908, e-mail: abrown@navsys.com

ABSTRACT

NAVSYS has developed a networked radionavigation approach for operating in urban environments where GPS signals can be significantly attenuated or completely blocked. The networked radionavigation approach is based on a Software Defined Radio (SDR) testbed, which combines Global Positioning System (GPS), wireless communications, and Time-of-Arrival (TOA) "Pseudolite" technology to provide location indoors for applications such as first responders, warfighters operating in urban terrain, and location-based services. This system has been integrated with a low-cost Micro-Electro-Mechanical System (MEMS) Inertial Measurement Unit (IMU) to provide an integrated GPS/TOA/inertial man-portable navigation system. The system architecture and test results showing its performance for indoor navigation are presented in this paper.

1. Introduction

A Software Defined Radio (SDR) provides a flexible architecture (Figure 1) that allows the same radio components to be reconfigured to perform different functions. NAVSYS has developed an SDR that includes the capability to operate both as a Global Positioning System (GPS) receiver and also as a 900 MHz transceiver operating within the Industrial, Scientific and Medical (ISM) band. Since both the GPS and communications functions reside within common radio hardware, this positioning and communications (POSCOMM) device can use the GPS and communications functionality to provide a positioning capability that leverages both the GPS-derived pseudorange and carrier phase observations and also Time-Of-Arrival (TOA) observations derived from the communications channel. The design of the POSCOMM Software Defined Radio is described in this paper.

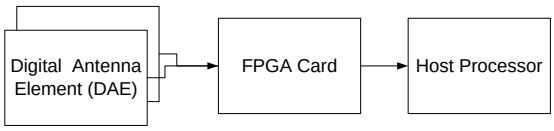

Figure 1 Software Defined Radio Architecture

The POSCOMM SDRs are designed to operate in a networked architecture, as shown in Figure 2, where "Master" units are designated as transmitters to provide TOA-augmented navigation to "Slave" units operating as receivers in a GPS-denied urban environment. The Master units transmit a TOA message that includes a pseudorandom sequence from which the time of arrival at the Slave unit can be precisely determined. A message is also sent which includes the precise time of transmission of the TOA message and the precise location of the Master unit based on the GPS observations. The time-of-arrival differenced with the time-of-transmission provides the Slave unit with a pseudorange observation from each of the Master units' locations. This can be used to solve for the position of the Slave either using the TOA updates alone or using a combination of both the GPS and TOA observations.

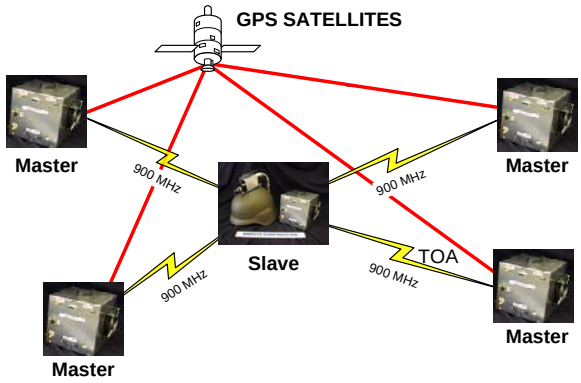

Figure 2 POSCOMM TOA Network[1]

We have integrated the GPS/TOA SDR with a Micro-Electro-Mechanical System (MEMS) Inertial Measurement Unit (IMU) to allow inertial aiding to be applied to the integrated GPS/TOA navigation solution. While the MEMS IMU used is relatively low power and inexpensive, the performance is such that the navigation solution degrades within a few minutes if aiding is not available[2]. However, when TOA updates are applied, the inertial navigation solution error growth is damped allowing this inertial unit to support indoor navigation. In this paper, we describe the design for this integrated system architecture and present initial test results on the TOA and inertial navigation.

2. POSCOMM Software Defined Radio

The POSCOMM GPS/TOA/inertial navigation system was implemented using NAVSYS' Software Defined Radio testbed shown in Figure 3[3]. This has been developed using a modular PC/104 configuration to facilitate rapid prototyping and testing of SDR software applications to support advanced positioning and communications functions. Previously, this SDR has been used for demonstrating a Software GPS Receiver (SGR) Application Programming Interface (API)[4], network assisted GPS operation using the military P(Y) code GPS signals[5], and also integrated GPS/inertial operation including Ultra-Tightly-Coupled (UTC) GPS/inertial tracking[6].

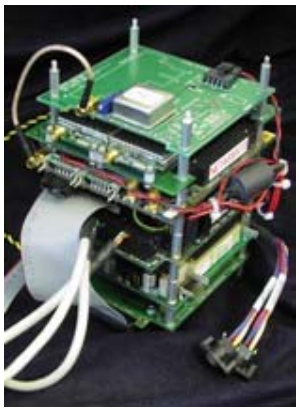

Figure 3 POSCOMM SDR Components

The POSCOMM SDR system is based on low-cost, commercial-off-the-shelf (COTS) hardware and software. The hardware can use any PC-based environment including desktop, laptop, PC/104, or CompactPCI form factors. Signal processing is performed by a Field Programmable Gate Array (FPGA) card and a Pentium-class CPU. The software is portable and developed for real-time flavors of Windows and Linux operating systems. A Software Communications Architecture (SCA)-based XML schema is used for system configuration.

The POSCOMM SDR PC/104-Plus stack shown in Figure 3 is packaged in the enclosure shown in Figure 4. The POSCOMM SDR PC/104-Plus stack includes the following primary components.

Figure 4 POSCOMM SDR

GPS Digital Antenna Element. Received RF signals for both GPS and TOA are converted to digital signals using Digital Antenna Elements (DAEs). The DAEs have a small 1"x4" size and can be easily modified for alternate frequencies and sampling rates and expandability. The DAE is responsible for RF down-conversion and up-conversion as well as high-speed analog-to-digital (A/D) and digital-to-analog (D/A) sampling. Each DAE uses a common sample clock and phase-locked reference local oscillator assuring a coherent sampling environment for all transmitted and received signals.

GPS 900 MHz Digital Antenna Element. This includes a 900 MHz receive and transmit channel that is used for either broadcasting or receiving the TOA-aided data. This could also be configured for use in communicating between the POSCOMM units. The 900 MHz channel was selected as it lies in the unlicensed ISM band. The DAE transceiver can also be configured to work at other frequencies.

PC/104 Correlator Accelerator Card (CAC). This NAVSYS designed card includes three Spartan FPGAs and a PCI bridge to the Host Computer. This interfaces directly with the DAE receive and transmit channels through an adapter board, as shown in Figure 5.

802.11b Data Link. The data link provides a transport mechanism for the Network Assist data as well as a remote login capability. In addition, real-time monitoring and navigation display data are transferred over the wireless link.

Host Computer, **Hard Drive, and Power Supply**. These are COTS components that include a PC/104 form factor Pentium-M Single Board Computer, power supply, and an 80 GB Hard Drive.

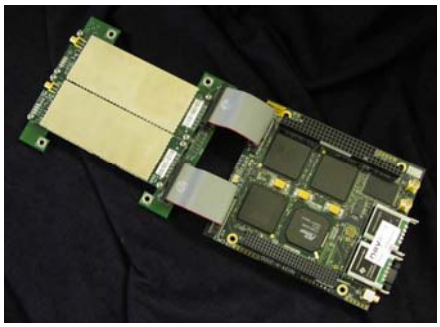

Figure 5 PC/104 CAC to DAE Interfaces

3. POSCOMM SDR Sensor Head

The POSCOMM SDR is integrated with a helmet mounted sensor head as shown in Figure 6. This includes a color digital camera, a MEMS-based IMU, and a dual GPS/900 MHz antenna. The IMU data is used to generate an inertial navigation solution that is updated with the GPS and TOA observations. The position and attitude data from the inertial updated solution is associated with the camera images and is passed back through the network for situational awareness. This imagery can be viewed through a web browser using NAVSYS' GeoReferened Information Manager (GRIM) (see Figure 7).

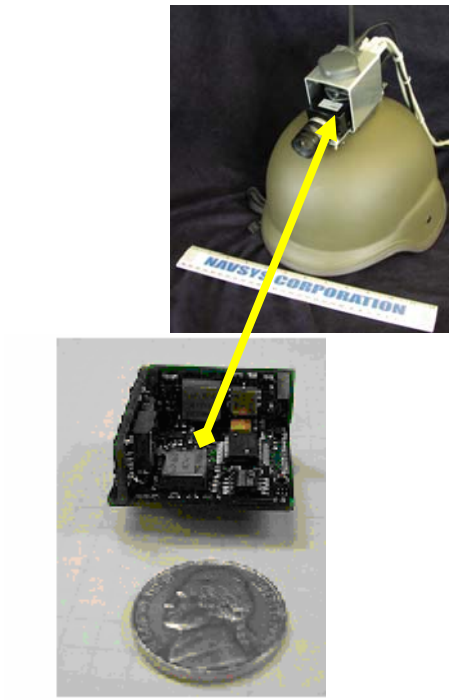

Figure 6 POSCOMM Sensor Head

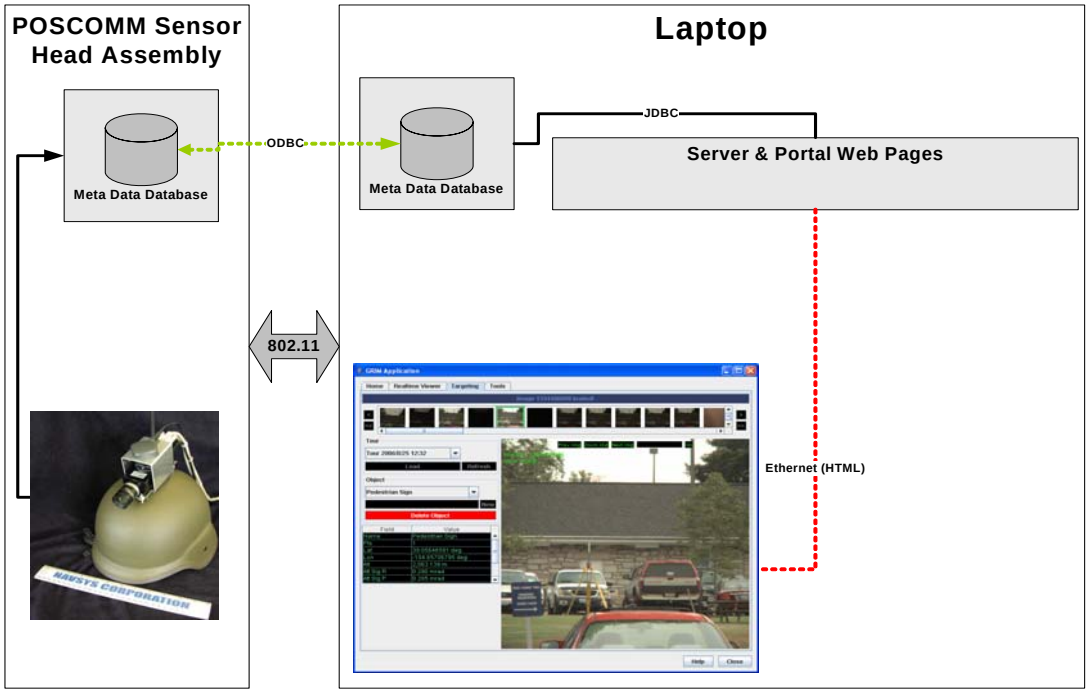

Figure 7 GeoReferenced Information Manager (GRIM) Web Interface

4. POSCOMM SDR Operation

The POSCOMM SDRs are configured through software to operate as either a Master (Transmit) or Slave (Receiver) mode of TOA operation.

Master units are required to be tracking at least one GPS satellite to allow the time of the TOA transmission to be synchronized precisely with GPS time. These units send TOA Assistance messages across the network which tells the Slave units what TOA observations are available for use in aided navigation and also provide the location of the Master units that are providing the TOA aiding.

Slave units will default to GPS tracking if satellites are in view, but do not require GPS tracking to operate. At start-up, the time on each unit is initialized across the network using Network Time Protocol (NTP). On receipt of the TOA Assistance messages from the Master units, the Slave unit will then initiate tracking of the TOA observations which will be used, in combination with any observed GPS satellites, to compute the aided navigation solution.

The SDR architecture allows for a variety of different waveforms to be used to provide TOA assistance. This provides maximum flexibility in configuring the POSCOMM TOA assistance network to optimize performance and share limited bandwidth for both positioning and communications functionality. The parameters that specify the TOA signal characteristics are all defined using configuration parameters and are defined in the TOA ACK Message sent by the Master Units (see Table 1).

Table 1 TOA Acknowledge Message

Field Name	Units	Description
Time	Week secs	GPS time of week of first TOA being transmitted
PRN		ID of PRN code
Period	ms	Interval between TOA signals
Duration	ms	Duration of TOA ranging signal
Freq	MHz	RF Frequency of TOA signal

The GPS/TOA solution accuracy is a function of the following components which are addressed in the POSCOMM SDR design[3].

- Accuracy of the GPS time and position mark at the Master unit.
- Geometry provided by the TOA observations.
- Accuracy of the TOA observations

In an indoor environment, the building can significantly attenuate the received signal power and strong multipath signals are present. To mitigate the multipath in the TOA measurement, a maximum likelihood estimation (MLE) algorithm is used. This algorithm models both the direct signal and closest multipath signal and detects the direct signal as the result of the maximum likelihood estimation. The MLE algorithm is also used to derive the TOA navigation solution. Field tests were performed at NAVSYS to evaluate the multipath environment and the ability of the TOA tracking loops in such conditions. Test data was collected from units operating both outside the building, where GPS could be used as a truth reference and inside the building. In both cases, the TOA signals were passing through multiple types of construction.

5. TOA Observations

The accuracy of the TOA observations is a function of the waveform characteristics, the tracking loops employed, and the environment. The main challenge faced for the TOA ranging signal design is to provide robust and accurate performance in the presence of multipath.

To evaluate the multipath environment and the ability of the TOA tracking loops to handle these errors, four Master units (Figure 9) were set up around the NAVSYS building shown in Figure 8 with the test layout shown in Figure 10. Test results were collected from units operating both outside the building, where GPS could be used as a truth reference, and inside the building. In both cases, the TOA signals were passing through multiple different types of construction. The west end of the building is metal construction while the center and east end is brick construction.

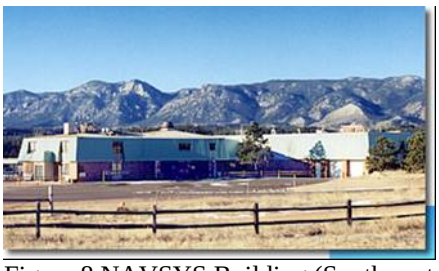

Figure 8 NAVSYS Building (Southwest View)

Figure 9 POSCOMM Master Unit

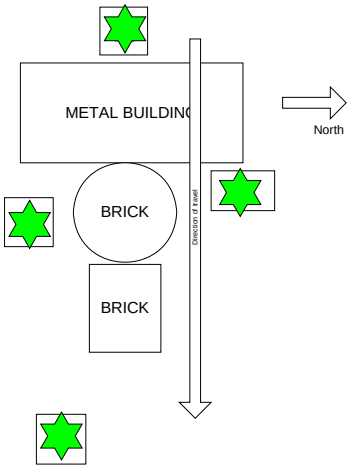

Figure 10 Indoor Test Pseudolite Layout

An MLE algorithm is used to estimate the TOA from the correlation results generated from the 900 MHz received signal correlated with the modulated PRN code. The algorithm detects the peak of the correlation from the closest in signal detected. This will result in detecting the correlation peak of the signal from the direct path from the transmitter rather than a multipath signal that arrived from an indirect path. Figure 11 shows the correlation results from four transmitters when the receiver has a direct line-of-sight to the transmitters. All four signals have a strong detected correlation peak with a received RF signal of around -16 dBm. Figure 12 and Figure 13 show the correlation results from signals received through the NAVSYS building. In these cases, the building can significantly attenuate the received signal power and also strong multipath signals are present, which appear as peaks showing to the left of the direct signal peak. The MLE algorithm used to perform the TOA tracking detects the closest peak in each case shown.

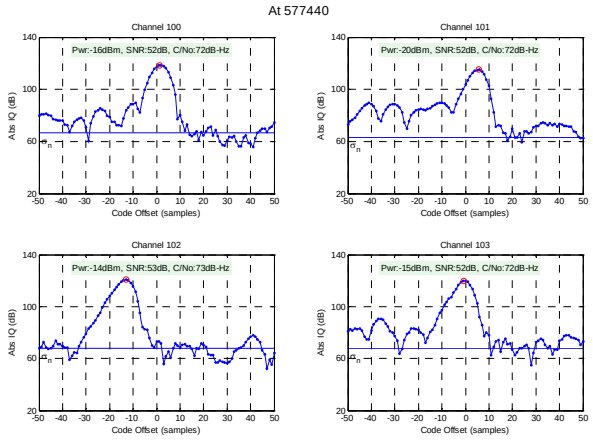

Figure 11 MLE Estimation of Shortest TOA Pseudorange (outdoor testing)

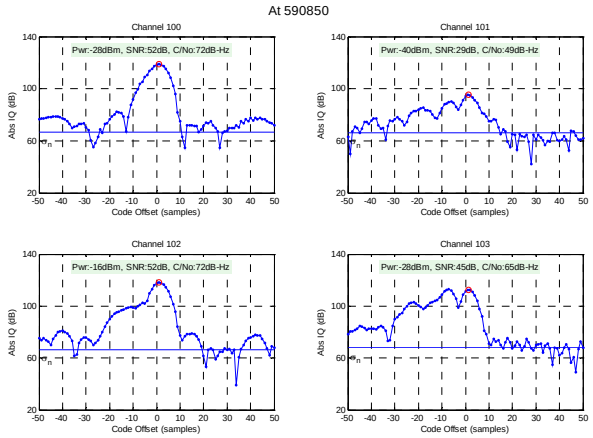

Figure 12 MLE Estimation of Shortest TOA Pseudorange (indoor testing)

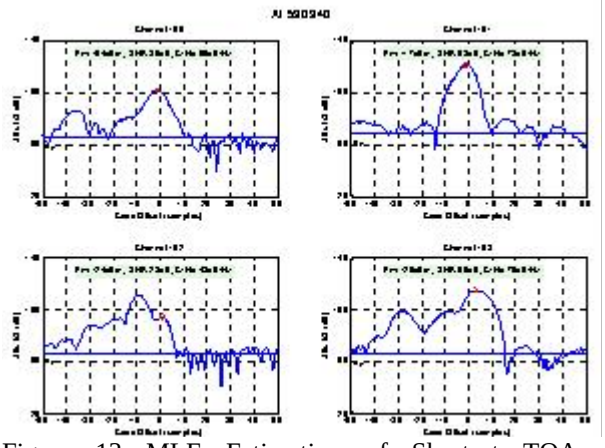

Figure 13 MLE Estimation of Shortest TOA Pseudorange (indoor testing)

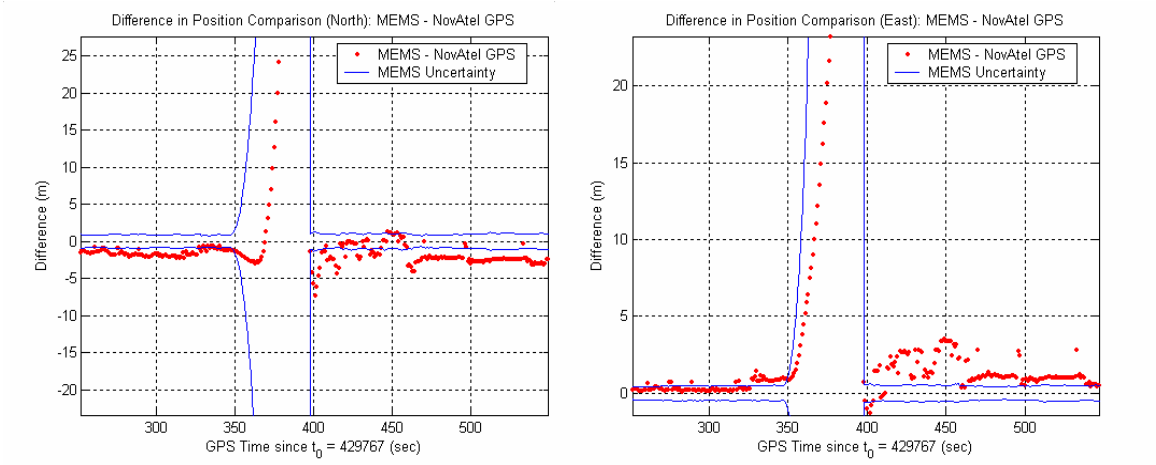

Figure 14 MEMS Inertial Navigation Results

6. MEMS Inertial Navigation

The MEMS IMU being used for the inertial navigation is based on low cost Analog Devices accelerometers and gyroscopes. These inexpensive instruments exhibit significant drift when operating as an unaided inertial navigation unit. Figure 14 shows the inertial navigation results during a short GPS drop-out. The navigation solution accuracy degrades very rapidly without updates. The POSCOMM approach is to continue to apply TOA updates to the inertial navigation solution which will bound the IMU error growth.

7. TOA-Aided Navigation Test Data

The TOA-aided navigation solution was first tested in an outdoor environment using GPS as truth data to analyze the performance of a TOA navigation solution. The results are shown in Figure 15. The POSCOMM navigation solution computed from four TOA observations agreed with the GPS truth solution to within 5 meters except for a few excursions. In Figure 16 the indoor test configuration is shown that was used to test the TOA solution. Five transmitters were set up at different sites around NAVSYS' building. This building uses brick construction on the east side and center and is a metal building with brick façade on the west side. The navigation test results are shown in Figure 19. The average position error at the test site locations was on the order of 7 m (RMS).

An example of the signal variation throughout the building is shown in Figure 17 and Figure 18. This data is shown for a Master transmitter located on the SE side of the building. The figures show that sometimes the received SNR of the TOA signals drops by as much as 20 dB as the unit is moved to the West of the building. These plots also compare the tracking performance achieved with the straight peak detection and the MLE estimation. The MLE estimation technique noticeably has fewer excursions demonstrating its improved performance in tracking the TOA signals in a strong multipath environment.

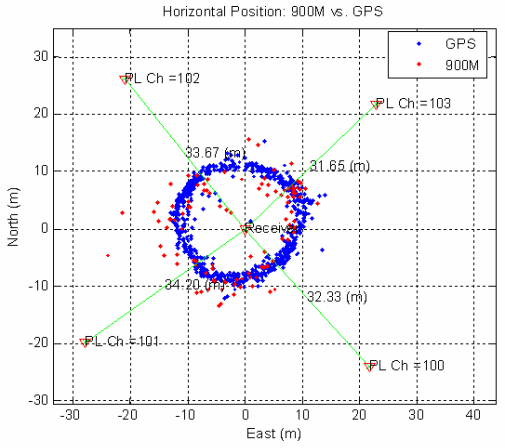

Figure 15 TOA Navigation Solution

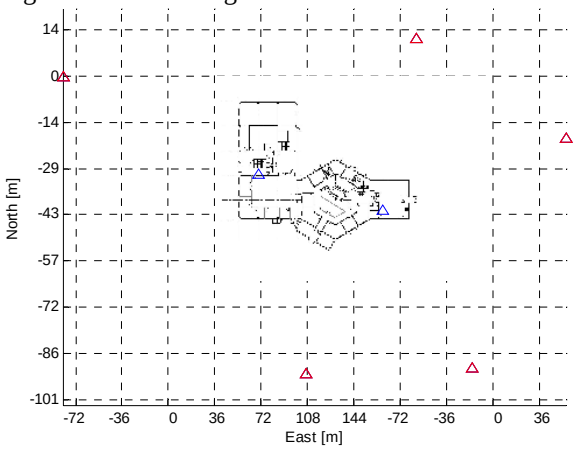

Figure 16 NAVSYS Building Transmitter Sites (Red) and Test Sites (Blue)

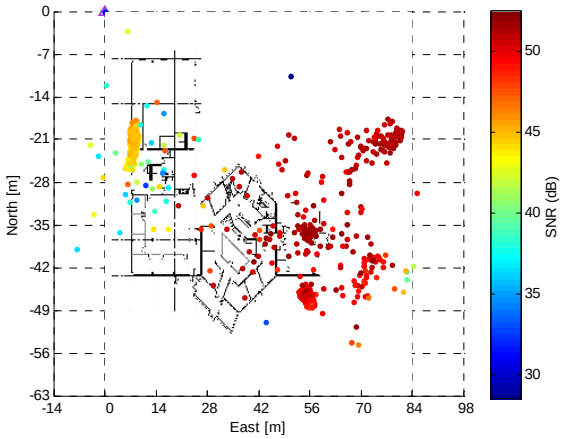

Figure 17 Signal Strength using TOA Peak Detection

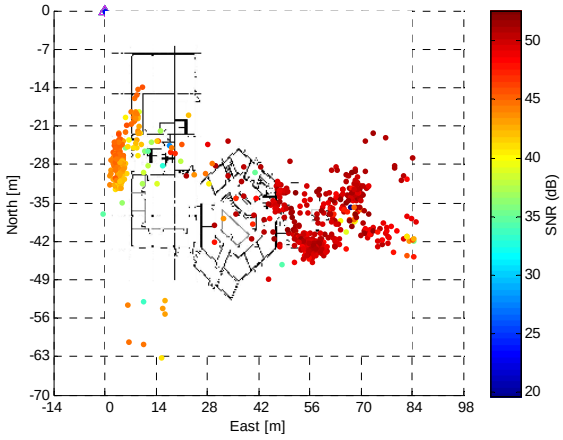

Figure 18 Signal Strength using MLE Detection

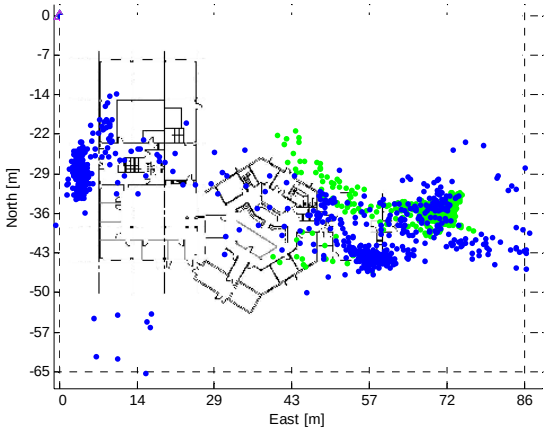

Figure 19 Navigation solution in mobile indoor test (Green=GPS, Blue=900M TOA)

8. Conclusion

The POSCOMM units are being developed to provide a robust urban navigation solution that can provide precise positioning inside buildings where the GPS signals cannot be received. The initial tracking and positioning results shown in this paper show the capability provided by the POSCOMM SDR to augment GPS signal tracking in the challenging urban environment with TOA aiding from an alternative RF source. This technology offers the capability to provide access to GPS-like quality of service both outside and inside buildings. The camera and inertial unit in the POSCOMM Sensor Head also provide the capability for real-time georeferenced situational awareness by networking the POSCOMM units with the GRIM web-based server.

Military applications for this technology include improved military operations in urban terrain (MOUT). Commercial applications include firefighters as well as other First Responders. This project will give firefighters, police officers and emergency officials an electronic vest and eyepieces that will provide their commanders with their location and their vital signs, as well as real-time georeferenced images of their surroundings.

9. Acknowledgments

The authors would like to acknowledge the support of CERDEC who have provided funding to support the development of this technology.

10. References

[1] Systems shown from Rex Systems Incorporated First Responder Program

[2] A. Brown, and Y. Lu, “Performance Test Results of an Integrated GPS/MEMS Inertial Navigation Package,” Proceedings of ION GNSS 2004, Long Beach, California, September 2004

[3] A. Brown, Y. Lu, and J. Nordlie, “Integrated GPS/TOA Navigation using a Positioning and Communication Software Defined Radio,” Proceedings of ION GNSS 2005, Long Beach, California, September 2005

[4] F. Carpenter, S. Srikanteswara, and A. Brown, “Software Defined Radio Test Bed For Integrated Communications And Navigation Applications,” Proceedings of 2004 Software Defined Radio Technical Conference, Phoenix, Arizona November 2004

[5] A. Brown and P. Olson, “Urban/Indoor Navigation using Network Assisted GPS”, Proceedings of ION 61st Annual Meeting, Cambridge, Massachusetts, June 2005

[6] A. Brown and Y. Lu, “Performance Test Results of an Integrated GPS/MEMS Inertial Navigation Package,” Proceedings of ION GNSS 2004, Long Beach, California, September 2004

Wideband Channel Characteristics for Indoor Reception of Satellite Transmissions at 2.4 GHz

Richard Rudd

Aegis Systems Ltd, UK

This paper describes an experimental campaign concerned with the evaluation of channel characteristics for indoor reception of satellite transmissions. A wideband channel sounder, operating at 2.4 GHz with a resolution of 10ns has been designed and constructed. Particular features of this equipment are the low cost and compact size.

This equipment has been used to gather statistics of the wideband outdoor-indoor slant-path channel in domestic and office environments. Values of RMS delay spread were generally found to be in the range 5-40ns, with no dependence on elevation angle. Statistics of building penetration loss have also been gathered.

1. BACKGROUND

With the inception of the European Galileo satellite navigation project, the potential for near-future satellite systems operating within IMT-2000, and the growing interest in satellite radio broadcast systems, there is a need for reliable data on the satellite-to-indoor transmission channel structure in L and S-band. This data should cover the range of building types for the likely users of these services.

It is important that satellite system designers are able to estimate the implications of transmission channel characteristics on satellite-to-indoor transmitted signals. This will allow the signal parameters to be chosen appropriately to minimise adverse channel effects and to improve in-building coverage. Such information will also be valuable in making commercial decisions regarding the competitiveness of the systems compared to other satellite or terrestrial systems.

In addition, the accurate estimation of transmission channel behaviour will be useful in both establishing regulations and standards and determining the spectrum requirements for delivering new satellite services to indoor receivers.

Although in recent years much effort has been put into the characterisation of the outdoor-to-indoor mobile channels at frequencies around 900 MHz and 1.8 GHz, there has been little data on transmission channel characterisation relating to satellite-to-indoor radiowave propagation. Most measurements, therefore, relate to low elevation angles. In addition, the building types concerned (which are mostly laboratories and office buildings) are not representative of the majority of UK building stock.

The study described in this report, which was funded by the British National Space Centre (BNSC), sought to address these issues through a limited measurement campaign, and built on related work undertaken in a previous study, which characterised the penetration loss of a selection of typical buildings for a number of frequencies and elevation angles.

2. THE WIDEBAND RADIO CHANNEL AND ITS CHARACTERISATION

A radio channel may be classified as 'narrowband' if the inverse of the signal bandwidth is much greater than the spread in propagation path delays. Equivalently, a narrowband channel is one in which fading affects all frequencies within the channel bandwidth equally, i.e. 'flat fading'. The previous Aegis study [1] examined the attenuation and fading characteristics of the outdoor-indoor channel.

In a wideband channel, by contrast, frequency selective fading becomes significant. Equivalently, multipath reflections will have time delays comparable to the reciprocal bit rate of a digital channel, potentially giving rise to intersymbol interference (ISI), and hence bit errors.

2.1. Channel characterisation

2.1.1. Power Delay Profile

The most intuitive characterisation of a radio channel is possibly in the time-domain, by way of the Power Delay Profile (PDP). The PDP can be classified by means of its statistical moments. The notation below follows ITU-R Recommendation P.1407.

The first moment is simply the 'Mean Delay' given by:

$$T_d = \frac{\sum_{i=1}^{n} P_i \tau_i}{\sum_{i=1}^{n} P_i}$$

where the denominator simply represents the total power (P_m) in the channel.

The second moment, the Delay Spread, gives the most often-used indicator of the performance of a channel. It is given by:

$$S = \sqrt{\frac{1}{P_t}\sum_{i=1}^{n} p_i \tau_i^2 - T_d^2} \ .$$

If the delay spread is much less than the symbol duration, little inter symbol interference (ISI) will occur.

Attention must be paid to the dynamic range and noise floor of the measurements. If samples that, actually, only represent noise are included in calculations, the T_d and S will be exaggerated.

2.1.2. Examples

Measurements made (in a separate study) in a small room produced the following PDP.

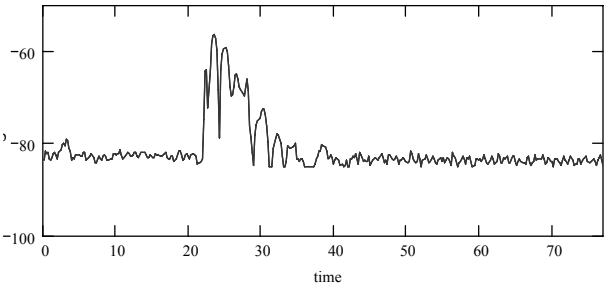

Figure 1: Raw data

If the expressions above are applied to the entire data set, the mean delay and delay spread are found to be 25.6 and 8.1 ns respectively.

If a window is applied, so that only samples between 21.5 and 40 ns are accounted for, these figures become 24.6 and 2.1 ns.

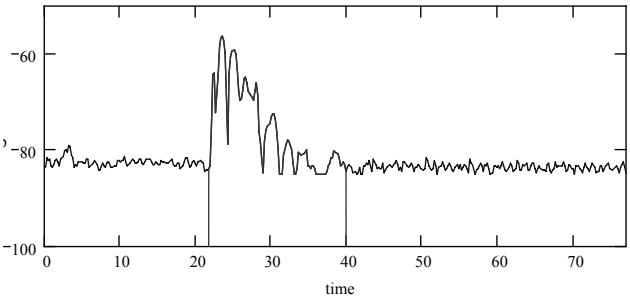

Figure 2: Application of window

Alternatively, a threshold may be set, so that only samples exceeding a given amplitude are accounted for in the calculations. From an examination of the data

(see figures below) a clipping value of –81 would appear to be realistic.

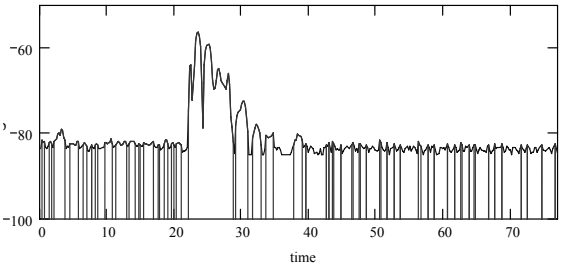

Figure 3: Clipping at –83 dB

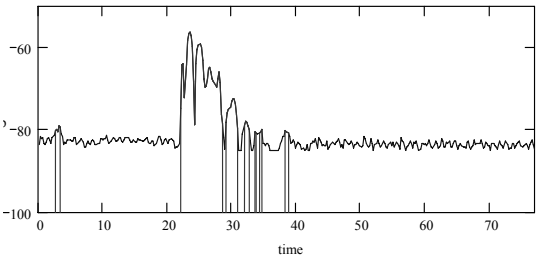

Figure 4: Clipping at –81 dB

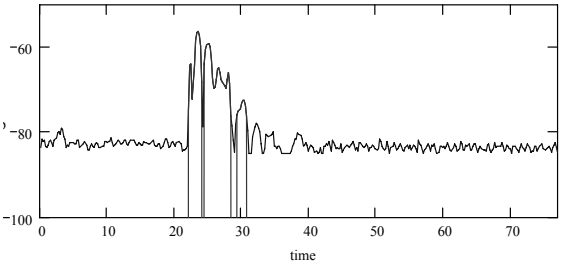

Figure 5: Clipping at –78 dB

3. PREVIOUS WORK

The majority of such studies have concentrated on the outdoor, generally urban channel. In the last decade or so, however, with increased interest in the use of wireless LANs, cellular radio picocells and other indoor radio systems, the indoor channel has received more attention. Very little work, however, has considered the outdoor-to-indoor path, particularly that from a satellite.

This section gives a brief summary of previous work undertaken in each of these categories, summarising the statistics gathered.

3.1. The outdoor channel

Following the work of Cox [3], a large number of measurement campaigns have been undertaken, to characterise urban, suburban and rural channels. Typical values of delay spread are ~1μS, with maximum delay values of ~10μS.

3.2. The indoor channel

Measurements of the indoor channel concentrated, initially, on mobile radio frequencies. More recently, much of the work has related to the bands used by Wireless LAN systems at 2.4 and 5.7 GHz. Typical values for delay spread are in the range 10-50nS.

3.3. The 'Outdoor to indoor' channel

There has been very little work reported in this category, and most relates to the indoor coverage obtained from the outdoor base stations of cellular radio systems. Some results are summarised in Table 1.

Frequency	**Area**	**Delay Spread**	**Max delay**	**ref**
850 MHz	Suburban/residential	100 ns	1.1μs	[6]
2.5 GHz	University	27ns	0.4 μs	[11]
1.6 GHz	University	30ns	0.2 μs	[13]

Table 1: Outdoor-indoor measurement results

Recent work at Leeds University [11], [13] is, however, comparable with the results of the current study, and this is discussed further in section 6.

4. EXPERIMENTAL EQUIPMEMT

This section describes the choice of measurement method, and provides details of the actual

implementation of the circuitry, with a discussion of some of the choices made, and problems encountered.

In order to keep within the limited budget available for the experimental equipment, commercial equipment has been modified and specialised modules constructed, in place of the use of expensive, general-purpose test equipment configured appropriately. The overall cost of the sounding system was less than £2,000.

It is possible that the compact equipment developed for this project may have applications in other work.

4.1. Sounding method

The measurements were made with a probing signal comprising a carrier spread over a large bandwidth by mixing it with a pseudo-noise (PN) sequence.

Alternative sounding signals, such as the use of a frequency-swept 'chirp' sequence, were also considered; the use of PN techniques offers the greatest flexibility and simplicity of implementation.

The pseudo-noise sequence, *m(t),* is so called because its autocorrelation function, given by $R_{mm}(\tau) = \frac{1}{T}\int_0^T m(t) \cdot M(t-\tau)dt$ and sketched in Figure 6, is similar to that of band-limited noise.

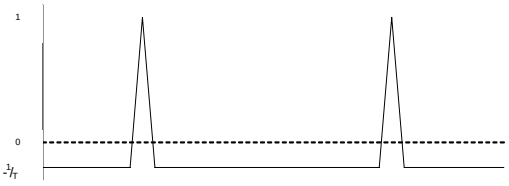

Figure 6: Autocorrelation function of PN sequence

The sequence used in the measuring system described here is a 'maximal length', or '*m*-' sequence, generated by a shift register with recursive taps. A shift register of n stages will generate a sequence of length 2^n-1.

Providing the spatial resolution required for the characterisation of the indoor channel requires a high bandwidth for the probing signal. The minimum useful resolution for this purpose is in the region of 3m, implying a chip rate of 100 Mb/s (chip duration = 0.01μs).

The *length* chosen for the PN sequence will determine two further parameters of the measurements: (i) the dynamic range of the observable multipath and (ii) the maximum, unambiguous, range measurement. A sequence of 511 bits will give a maximum theoretical dynamic range of 54 dB; as this range will unavoidably be degraded by practical implementation effects, this is the minimum sequence length felt to be acceptable. The maximum delay range implied by a 511-bit sequence is more than adequate, at 1.5km.

4.2. Measurement technique

Having established a format for the sounding signal, an appropriate technique for the recovery of the channel multipath information must be selected. The receiver must perform a correlation of the received signal with a 'clean' local copy of the original sounding sequence.

This correlation may be carried out in either the time or frequency domain, and in either hardware or software form. In the original study proposal, it was hoped that a software approach might be possible, in which the received signal would be digitised at an early stage, and all further processing be carried out in software. This approach would have the merit of requiring little in the way of hardware, and would potentially allow great flexibility. The processor power required would not necessarily be great, as the correlation might be carried out off-line.

The major difficulty with this approach is that a high speed analogue to digital converter (ADC) is required. Adequately to sample the sounding signal proposed, for example, would require a speed in excess of 200 M samples/second.

While such ADCs are available, it proved impossible to find a suitable device that fell within the equipment budget for the project.

A hardware solution based on the established method of the 'sliding correlator' has therefore been adopted. In this technique, the local PN sequence is clocked at a slightly different rate to that transmitted. This causes the two sequences to drift past each other, with the output of the correlator representing the multipath profile of the channel, dilated in time by a factor given by the ratio of the slip rate to the chip frequency. A particular advantage of this configuration is that the required IF bandwidth of the receiver is reduced to twice the slip rate, greatly simplifying the design, and increasing the processing gain of the system.

In the final design, this slip rate is ~12 kHz, with an IF bandwidth set at ~24 kHz by a crystal ladder filter.

In the classic 'sliding correlator' approach, as with most other sounding techniques, high stability clocks are used at transmitter and receiver, ensuring phase coherence during the measurements, and allowing Doppler channel characteristics information to retrieved.

For most of the applications likely to be used indoors, it is less important to recover Doppler information from the complex channel. Consequently, the usual rubidium frequency standards can be dispensed with, keeping hardware costs within the study budget.

4.2.1. System parameters

The frequency selected for the measurements was largely determined by the availability of a test & development licence. Satellite systems offering services to portable, possibly indoor, terminals are likely to operate below 3 GHz, while the required sounding bandwidth of 200 MHz places a further restriction on spectrum choice. The frequency band 2300-2500 MHz was eventually allotted for the measurements.

The choice of PN bit rate and sequence length has been discussed, above. The remaining parameter to be chosen is the scaling factor (i.e. the ratio of the sounding bandwidth to the slip-rate).

This might appear to be an arbitrary choice. However, to ensure maximum signal-to-noise ratio it is necessary to ensure that the integration period of the correlator corresponds to an integer number of PN sequences – if this is not the case, the correlation will only be carried out over part of the PN sequence. Thus the bandwidth of the integrating filter should be $\frac{1}{nT_{PN}}$, where T_{PN} is the PN sequence time (i.e. $\frac{511}{100MHz} = 5.11\mu s$). The filter must, also, have a bandwidth of at least twice the slip rate, but be as narrow as possible to exclude noise. For n=1, a filter bandwidth of 196 kHz is implied, giving a slip rate of 98 kHz.

This would result in a scaling factor of ~1000. As noted in [3], the use of such low slip rates results in considerable distortion of the correlator output. A higher value of *n* has therefore been selected; *n*=8 gives a slip rate of 12 KHz.

4.3. Detailed design

Block diagrams of the transmitter and receiver are shown in Figures 7 & 8, below.

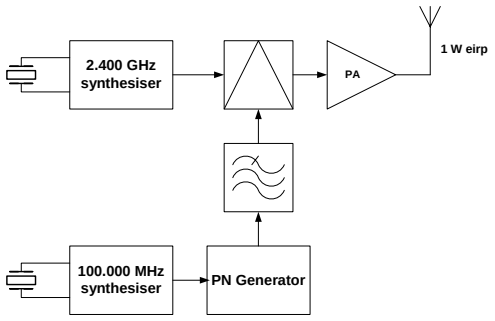

Figure 7: Transmitter

The transmitter is very simple, using a double balanced mixer (DBM) to BPSK modulate the 2.4 GHz carrier with the 511-bit PN sequence. The output of the DBM is amplified to a maximum value of 28 dBm. Low-pass filtering is applied to the output of the PN-generator, to limit out-of-band emissions.

In the receiver, a bandpass filter at 2.4 GHz reduces the potential for interference from out-of-band emissions. Following a low noise amplifier (LNA) the received signal is mixed with a replica of the transmitted PN sequence at the local oscillator frequency. This replica sequence is clocked at a slightly faster rate than the transmitted sequence.

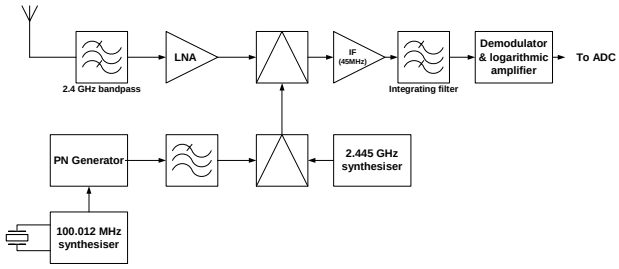

Figure 8: Receiver

Following decorrelation, the received signal collapses to a carrier at the IF frequency (45 MHz), modulated by the time-dilated power delay profile of the channel. This is demodulated and conditioned in a logarithmic amplifier before being passed to a laptop PC fitted with a simple analogue to digital converter (ADC) card.

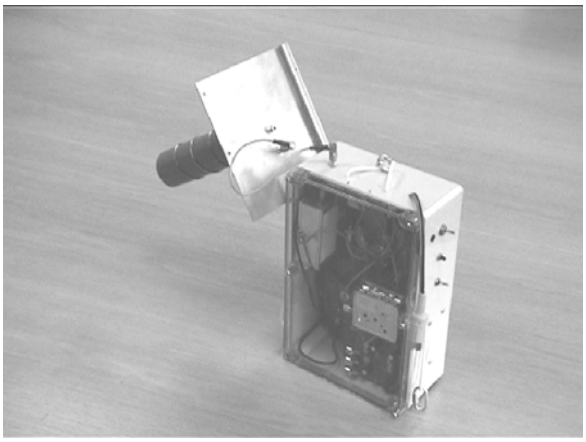

Figure 9: Sounding transmitter with CP antenna

4.3.1. ADC and data logging

A commercial analogue-to-digital converter (ADC) was used to capture the output of the logarithmic amplifier. Software was written to capture sequences of 100 power delay profiles (PDP) for each measurement.

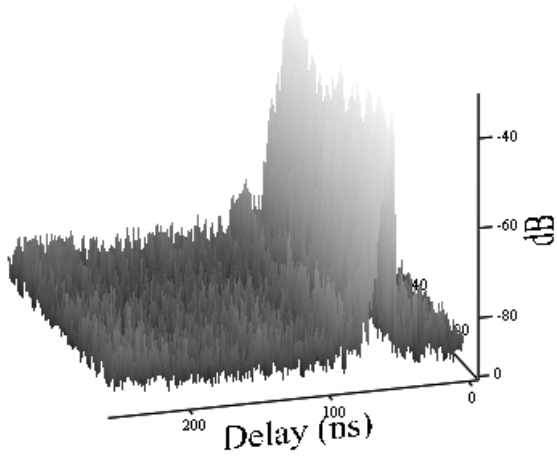

Figure 10: A sequence of power delay profiles captured during a single 'measurement'

Figure 10 illustrates a typical sequence of PDP's, clearly showing the variation over time of the power in the principal tap. The delay (τ) axis is from 0-250 ns, while the power axis is in dB (arbitrarily referenced).

5. MEASUREMENT METHODOLOGY

5.1. Balloon and sounding transmitter

The measurements made use of a tethered balloon to simulate a satellite source, an approach which necessarily introduces some errors in the channel measurements. The most serious potential problem with the method is that clutter and ground in the neighbourhood of the balloon transmitter may give rise to additional multipath that would have a different character than that experienced on a satellite path.

This inaccuracy has been minimised by the use of a directional aerial for the transmitter, so that radiation in directions other than the receiver is minimised. In practice, however, the directivity that can usefully be applied is limited by the (in)stability of the balloon platform. It had, initially, been proposed to make use of an automatically-steered platform to ensure correct pointing of the transmit aerial – in the event, it proved impossible to develop this equipment in the time available.

Figure 11: Helium balloon used for transmitter platform

Both circularly- and linearly-polarised antennas have been used at the transmitter with a gain of 8 dBi in both cases. For linear-polarisation, a commercial flat-plate antenna was used, while circular polarisation was radiated using a specially built helical antenna.

At each measurement site, the balloon was tethered at between 20-30m from the receiver location. Civil Aviation Authority regulations permit the balloon to be raised to a maximum height of 60m above ground level, allowing elevation angles of up to around 70˚ to be explored.

To achieve stable antenna pointing, it was necessary to carry out the tests on particularly calm days. For each measurement, a set of 100 power delay profiles (PDPs) from the correlating receiver were captured. Those profiles in which the overall received power fell by more than 3dB (due to transmit aerial misalignment) from the maximum were discarded

The receive antenna was either a vertical dipole or a second 8 dBi helical antenna.

6. ANALYSIS OF MEASUREMENT RESULTS

Measurements have been undertaken in eight locations at two sites. One site was a small, modern house in Guildford, the other a mixed development of apartments and small offices in Cobham. Both buildings were of traditional brick construction.

The individual results files were examined manually to determine an appropriate value of clipping. A clipping level of around –40dB with respect to the maximum response was generally chosen.

Figure 12, below, summarises the results obtained in the measuring campaign. The figure presents the median values of RMS delay spread for each measurement location, and for each path elevation angle explored.

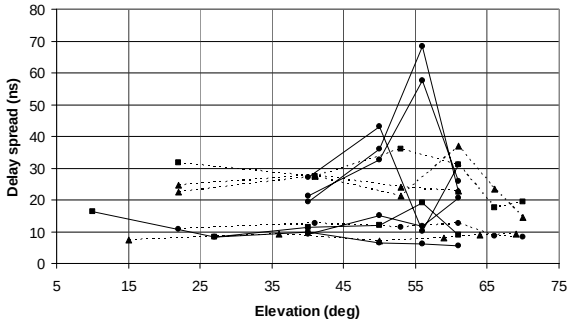

Figure 12: Overall median delay spread results

It is apparent that there is no clear dependence of RMS delay spread on elevation angle, or with either test site. The measurements at 56° elevation in Cobham appear to give anomalous results; two of the locations giving rise to high values of delay spread, and one to a particularly low value. It appears that this may reflect the internal structure of the building.

The expected dependence on antenna polarisation and gain was found, and is illustrated in Figure 13.

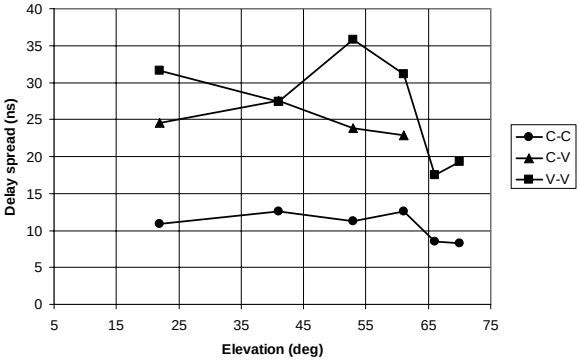

Figure 13: Dependence of delay spread on polarisation

It can be seen that the use of CP antennas for both transmit and receive gives rise to the lowest values of delay spread, owing to the high gain of the receive antenna and to the cancellation of odd-order reflections.

While Figure 13 shows the variation in median results for each location, the spread of results individual location is considerable, as illustrated in Figure 14.

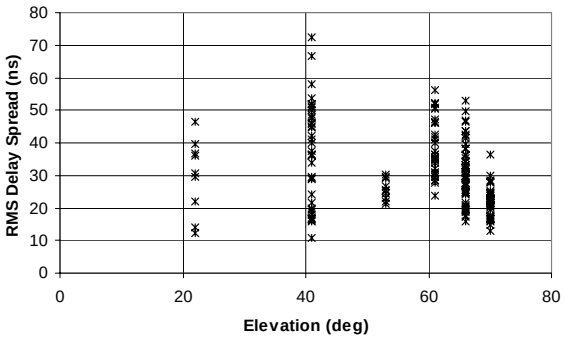

Figure 14: Spread of measurements

The variation in delay spread at each location reflects the detailed changes in multipath structure due to variations in balloon position, and movement of people within the rooms.

The cumulative statistics of RMS delay spread, for all measurements, are shown in Figure 15.

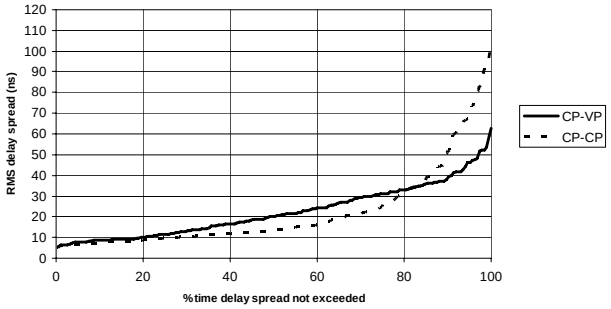

Figure 15: Overall cumulative statistics

Though the use of CP antennas at both terminals generally gives lower delay spreads, the highest values are greater than those for the CP-to-VP case. This appears to be the result of the higher gain receive antenna allowing long-delay multipath to be resolved.

The cumulative statistics are examined in more detail in Figure 16, where they are broken down for the three measurement locations at Guildford.

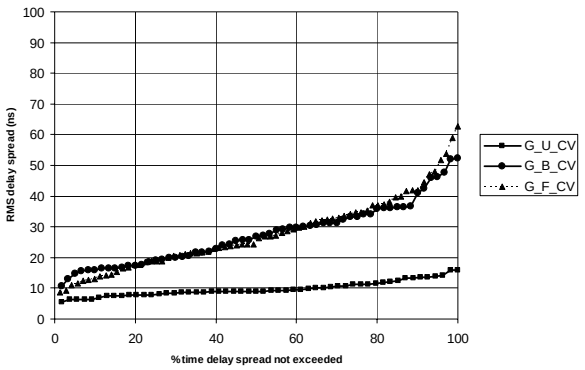

Figure 16: Statistics for CP (transmit) – VP (receive)

The cumulative statistics for the two locations on the ground floor are very similar. The delay spread experienced on the first floor is significantly reduced, however, as the result of a less strongly attenuated direct path.

6.1. Comparison with narrowband measurements

A previous study [1] undertaken by Aegis examined the statistics of building penetration loss at 1.5 GHz, 2.5 GHz and 5.8 GHz. The figure below is reproduced from the previous study report, and illustrates the values of building penetration loss measured in that study.

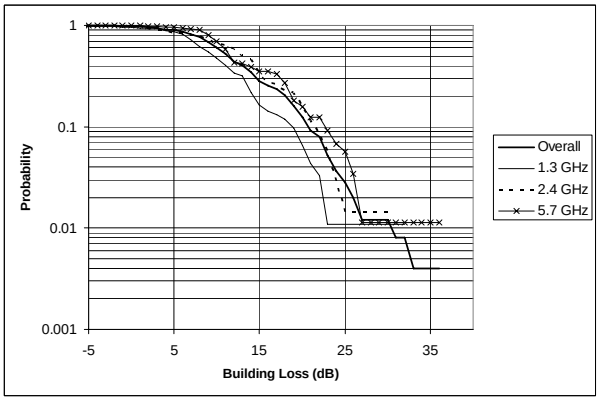

Figure 17: Measured building penetration loss

Although the correlating receiver, described above, was not designed with the intention of allowing precise measurement of received power, it has been possible to determine path loss values by integrating the individual power delay profiles.

The values of building penetration loss thus determined agreed well with those measured in the previous study.

6.2. comparison with other work

A separate BNSC-funded project, aimed at studying issues surrounding channel modelling for GALILEO terminals, has been undertaken jointly by Astrium, Roke Manor Research and Leeds University.

One aspect of the project was concerned with the simulation and measurement of the satellite-indoor path. A channel sounder was been constructed to operate at 1.6 GHz, with particular attention having been paid to the design of the radiated signal so as to minimise interference to GPS receivers. This equipment was used to make measurements of channel impulse response within the Leeds University campus. These measurements are described in [13]

Three measurement locations were used in the Leeds study, and median values of delay spread were found to be 30-65 ns, compared with 10-80ns in the current study.

The RMS Delay spread measured at the most benign location had a cumulative distribution from 11-60 ns, which is very similar to the values measured in this study on the ground floor of the terraced house in Guildford.

The delay spread at the worst Leeds location had a distribution that extended from 9 to 193 ns, significantly in excess of anything experienced in the current study, where the worst case was 105ns.

7. CONCLUSIONS

The main conclusions of the work are summarised below:

- Compact and cost-effective equipment has been designed and built to allow the investigation of wideband channel characteristics at 2.4 GHz.

- This equipment has been used, in conjunction with a tethered helium balloon to determine the RMS delay spread for slant paths into two typical UK building types.
- No dependence on path elevation angle was found.
- There is considerable variation of delay spread between locations, with values typically in the range 10-50ns.
- Results obtained are comparable with those from another UK study, that investigated the indoor propagation channel from the proposed Galileo constellation.

8. REFERENCES

[1] Rudd, R.F. "Measurements of the slant-path penetration loss into domestic buildings at L-, S- and C-band", *IEE Conference on Antennas and Propagation, (ICAP '03)*, Exeter, 2003.

[2] Bello, P.A. "Characterisation of randomly time-variant linear channels, *IEEE Trans*, CS-11 (4), pp.360-393, 1963.

[3] Cox, D.C., "Delay Doppler characteristics of multipath propagation at 910 MHz in a suburban mobile radio environment", IEEE Trans on Antennas & Propagation, AP-20(5), 1972, pp.625-635, 1972.

[4] Gurdenli, E and Huish, P.W. "Channel sounding results in London", Input to COST 207, TD(87)CO4, January 1987.

[5] Bajwa, A.S. and Parsons, J.D. "Small-area characterisation of UHF urban and suburban mobile radio propagation.

[6] Devasirvatham, D.M.J., "Time delay spread and signal level measurements of 850 MHz radio waves in building environments", IEEE Trans on antennas & propagation, AP-34(11), pp.1300-1305, 1986.

[7] Devasirvatham, D.M.J., "A comparison of the time delay spread measurements within two dissimilar office buildings, IEEE Conf. On Commun., Toronto, pp.852-856, 1986.

[8] Savage, N. *et al*, "Wideband wireless indoor communications", IEE Conference on Antennas and Propagation (ICAP), Exeter, 2003.

[9] Salous, S. and Hinostroza, V.,"Indoor and between building measurements with high-resolution channel sounder ", IEE Conference on Antennas and Propagation (ICAP), Exeter, 2003.

[10] Lukama, L.C. and Edwards, D.J., "Analysis of wideband indoor propagation measurements", IEE Conference on Antennas and Propagation (ICAP), Exeter, 2003.

[11] Jones, S.M.R. *et al*, "Wideband measurements across the outdoor-indoor interface at 2.5 GHz", Proc. Millennium Conf. On Antennas & Propagation, AP2000, Davos, Switzerland, 2000. (available on ESA CD-ROM)

[12] Shelswell P *et al* (1994) Wideband measurements of multipath propagation at 531 MHz and 1.265 GHz, BBC Research Department, Report RD1994/3.

[13] O'Donnell, M. *et al*, "A Study of Galileo Performance - GPS Interoperability and Discriminators for Urban and Indoor Environments", ION-GPS 2002, Portland, Oregon, September 2002 (see www.ion.org)

Measurement and Modeling of Indoor MIMO-OFDM Channels

Hajime Suzuki, Zhongwei Tang, and Iain B. Collings

CSIRO ICT Center
Phone: +61-2-9372-4121, Fax: +61-2-9372-4545, E-mail: Hajime.Suzuki@csiro.au

This paper compares measured and simulated multiple-input multiple-output orthogonal frequency division multiplexing (MIMO-OFDM) channels in indoor environments. Standard stochastic MIMO channel models (TGn channel models) are compared with real measurements made on a channel sounder with four transmitters and four receivers operating at 5.24 GHz with 40 MHz bandwidth. The channels are analyzed in terms of spatial fading Rician factors and MIMO subchannel cross correlation. While the standard models assume identical Rician factor for different MIMO subchannels, the measurement reveals that Rician factors can be different for different MIMO subchannels. Measured MIMO subchannel cross correlation is found to be frequency dependent. Comparisons are also made in terms of error rate of MIMO-OFDM packet transmission, which highlights a large variation of performance in typical indoor environments.

1 Introduction

Multiple-input multiple-output orthogonal frequency division multiplexing (MIMO-OFDM) is currently being considered as a strong candidate for the physical layer transmission scheme of next generation wireless communication systems [1]. A commercial product utilizing two transmit antennas and three receive antennas (denoted 2×3) achieving 6 bps/Hz bandwidth efficiency for wireless local area networks (WLAN) is currently available, while the WLAN standardization group is aiming to achieve 15 bps/Hz bandwidth efficiency using four transmitters (Txs) [2].

MIMO-OFDM channel models allow detailed assessment of the performance of different MIMO-OFDM transmission schemes such as spatial multiplexing, space-time-frequency coding, or beam forming [3]. For this purpose, the Task Group N of the IEEE 802.11 Working Group has developed a set of standard stochastic wideband MIMO channel models, called TGn channel models [4]. In this paper, we focus on comparing MIMO-OFDM channels produced by the TGn channel models with those obtained by the actual measurement performed in indoor environments. Our interest is to find whether the TGn channel models faithfully reproduce MIMO-OFDM channels which are encountered in typical indoor environments. The TGn channel models have been implemented as MATLAB codes by Schumacher and Dijkstra [5] which we utilized in this paper.

MIMO-OFDM channel measurements have been reported by several researchers (e.g. [6–11]). However, very few results have been reported for the scenario of using four transmitters and four receivers (4×4) with 40 MHz bandwidth. This is somewhat surprising considering that this is the combination which is suggested for providing the maximum data rate in the new IEEE 802.11n standard [2]. In this paper, we focus on this 4×4 MIMO-OFDM case using 40 MHz bandwidth at 5.24 GHz. We compare our actual measurement results with the TGn channel model results.

The paper is organised as follows: The wideband stochastic MIMO channel model developed in [4] is briefly reviewed in Section 2. Section 3 describes the measurement site and equipment. The analysis of measured and modeled MIMO-OFDM channels is presented in Section 4. Packet error rate (PER) performance based on the measured and modeled MIMO-OFDM channels is investigated in Section 5 followed by the conclusions in Section 6.

2 Wideband Stochastic MIMO Channel Model

The TGn channel model is based on the tapped delay line model incorporating multiple clusters [4]. The MIMO channel matrix $\mathbf{H}(l)$ of the lth tap ($l > 1$) is given by

$$\mathbf{H}(l) = \sqrt{P(l)}\mathbf{H}_V(l) \tag{1}$$

where $P(l)$ is the power of the lth tap. The stochastic random channel component $\mathbf{H}_V(l)$ is given by

$$\mathbf{H}_V(l) = \mathbf{R}_{\text{Rx}}(l)^{1/2}\mathbf{G}(l)\left(\mathbf{R}_{\text{Tx}}(l)^{1/2}\right)^T, \tag{2}$$

where $\mathbf{R}_{\text{Rx}}(l)$ and $\mathbf{R}_{\text{Tx}}(l)$ are the receive and transmit correlation matrices, respectively. $\mathbf{G}(l)$ is a matrix of independent zero mean, unit variance, complex Gaussian random variables. T indicates matrix transpose.

The receive and transmit correlation matrices for each tap are determined by the correlation model as a function of angle of arrival (AoA), angle of departure (AoD), and angle spread, as well as the antenna element spacing and arrangement. The model for uniform linear

array is given in [5]. We have extended the model to include uniform circular array [12]. In both cases, an omnidirectional antenna pattern is assumed for all antenna elements. The truncated Laplacian power angle spread (PAS) as defined in [4] is used in this paper.

Since different mean AoA/AoDs and angle spreads can be assigned to different clusters, $\mathbf{R}_{\text{Rx}}(l)$ and $\mathbf{R}_{\text{Tx}}(l)$ are specific for different taps. We note that it is not clear how the different correlation characteristics of different taps affect the correlation of the channels in frequency domain. In Section 4.3, we will investigate this by analyzing the MIMO channel correlation characteristics as a function of frequency.

The TGn channel model also incorporates the model for fixed component to support line-of-sight (LoS) scenarios. The MIMO channel matrix $\mathbf{H}(1)$ of the first tap is given by

$$\mathbf{H}(1) = \sqrt{\frac{P(1)}{\kappa+1}}\left(\sqrt{\kappa}\mathbf{H}_F + \mathbf{H}_V(1)\right) \qquad (3)$$

where κ is the Rician factor of the first tap (herein called the first tap Rician factor). Note that κ does not take into account the power of other taps and thus this value is typically different from the conventional Rician factor defined over a narrowband power distribution (denoted as K in the following analysis). The effect of κ on K is analyzed in Section 4.2. Non zero κ is defined in the case of LoS while $\kappa = 0$ in the case of non-LoS (NLoS). The fixed channel component $\mathbf{H}_F$ is specified in [4] with an assumption that AoA/AoD is 45°.

Six standard models, models A to F, are defined in the TGn channel models with deterministic parameters of AoA, AoD, and angle spreads for each cluster, as well as the delay and the power of each tap within a cluster. The model A contains only one tap and does not represent typical indoor MIMO channels, and thus it is excluded from the following analysis. Some parameters of the models are listed in Table 1.

The effects of active fluorescent lights [13] and a moving vehicle nearby are incorporated in the model, however these features are disabled in this paper in order to focus the analysis. (The fluorescent lights were turned off at the time of our measurement and there were no moving vehicles near our measurement sites.)

The time domain power delay profile of each MIMO subchannel is converted into frequency domain MIMO-OFDM channels. The number and the spacing of OFDM sub-carriers are as specified in [2], which are 117 (108 data sub-carriers, 6 pilot sub-carriers and 3 middle null sub-carriers) and 312.5 kHz, respectively.

3 Measurement Equipment and Site

The CSIRO ICT Centre has recently developed a 4×4 MIMO-OFDM hardware demonstrator [14, 15]. It operates at 5.24 GHz and supports an operational bandwidth of up to 40 MHz. The receiving antennas are connected to an antenna array positioner controlled by a PC. For channel measurements, the antenna positioner moves the receiving antenna array within a horizontal two-dimensional area of four wavelengths $\times$ four wavelengths with 0.05 wavelength increment, resulting in 6400 locations. We found that these parameters provided an adequate spatial sampling, based on our observation that from a statistical point of view the measured results are relatively insensitive to coverage area and wavelength spatial sampling distance.

Identical off-the-shelf omnidirectional loop antennas (SkyCross SMA-5250-UA) are used as both Tx and Rx antenna array elements for all MIMO-OFDM measurements. The antenna elements are arranged to form a uniform square array on the horizontal plane. The spacing of the antenna elements is set to 3 wavelengths at Tx and 2 wavelengths at Rx. The measurement was performed during the night or over the weekend in order to avoid possible temporal variation due to human activities. More details of the measurement can be found in [16].

The measurements were performed in the CSIRO ICT Centre Laboratory in Marsfield, Sydney. Six propagation links covering both LoS and NLoS scenarios were established as shown in Table 2. In the following analysis, the measured MIMO-OFDM channel scenarios are referred by the combination of the Rx environment and the path type, e.g. Atrium LoS.

4 Analysis on MIMO-OFDM Channels

4.1 Measured and simulated MIMO-OFDM channels

The measured MIMO-OFDM channels obtained in Atrium LoS and Atrium NLoS are shown in Fig. 1. Sets of MIMO-OFDM channels obtained at eight consecutive Rx antenna array locations with 0.05 wavelength spacing are plotted (from light gray curves to solid black curves) showing typical variation in space and in frequency. While severe frequency-selective fading, as expected from a multipath environment, is observed in most MIMO sub-channels in the case of NLoS, such fading is remedied in many MIMO sub-channels in the case of LoS.

Fig. 2 shows simulated MIMO-OFDM channels generated by the TGn channel models. Results for Model B LoS and Model F LoS are shown as an example. It is

Table 1: TGn channel model parameters.

Channel model	B	C	D	E	F
RMS delay spread (ns)	15	30	50	100	150
First tap Rician factor (κ) (dB)	0	0	3	6	6
Average correlation amplitude	0.15	0.14	0.14	0.10	0.10
Correlation amplitude standard deviation	0.13	0.13	0.14	0.07	0.06

Table 2: Measured channel parameters.

Tx environment	Lab	Office	Atrium	Office	Theatre	Office
Rx environment	Lab	Lab	Atrium	Atrium	Theatre	Office
Path type	LoS	NLoS	LoS	NLoS	LoS	NLoS
Distance (m)	5	5	7	10	9	9
RMS delay spread (ns)	28	32	29	37	28	42
Average correlation amplitude	0.22	0.22	0.62	0.23	0.36	0.20
Correlation amplitude standard deviation	0.11	0.11	0.16	0.11	0.16	0.10

well-known that the frequency selectivity is related to the longer delay of multipath components and hence severe frequency selectivity is observed in the case of Model F, which has a delay spread of 150 ns. However, a closer analysis on the LoS MIMO-OFDM channel results produced by the model B to model F did not show any signs of dominant component. An analysis on the cumulative distribution function (CDF) of the spatial fading for each OFDM sub-carrier and for each MIMO sub-channel reveals that the MIMO-OFDM channels generated by the TGn channel models are all close to Rayleigh distribution, even when the LoS component was added. This was surprising considering relatively large (6 dB) first tap Rician factor was used in some models. It turned out that the total power of the delayed components is much larger than the power of the first tap, and hence the addition of 6 dB to the first tap shows insignificant effect in terms of narrowband spatial fading. This aspect of the finding is further elaborated in the next section.

4.2 Rician Factor Analysis

Fig. 3 (a) shows the CDF of spatial fading generated by the model E LoS, denoted by the dots. The results are averaged over all OFDM sub-carriers and all MIMO sub-channels. (Little variation on CDFs was observed for different OFDM sub-carriers or MIMO sub-channels.) The first tap Rician factor κ was artificially increased from the original 6 dB to 10, 15, and 20 dB as shown in Fig. 3 (a). Shown also in the plot are the theoretical Rician distribution with the values of K determined by fitting the model E LoS CDFs. It can be seen that $\kappa = 6$ dB corresponds to the Rayleigh distribution while $\kappa = 20$ dB corresponds to Rician distribution with $K = 10.1$ dB. Hence in order to simulate LoS channel with Rician factor of $K = 6$ dB, the first tap Rician factor κ should be increased from $\kappa = 6$ dB to a value larger than $\kappa = 15$ dB in the case of model E. The amount of necessary increase of κ depends on the ratio of first tap power and the total power of other taps for each model.

Fig. 3 (b) shows the 16 CDFs of spatial fading, each corresponding to a single MIMO sub-channel, obtained in Atrium LoS. CDFs are averaged over OFDM sub-carriers. Contrary to the assumption of TGn channel model where an identical (first tap) Rician factor is applied to all MIMO sub-channels, it can be seen that the distribution of the measured channels can be specific to different MIMO sub-channels. The corresponding Rician factor ranges from $-\infty$ (Rayleigh) to 7.5 dB. The exact cause of the different Rician factor for different MIMO sub-channels is yet to be identified. One of the most likely causes is an effect of different antenna patterns due to the existence of other antennas and the effect of local environment at the proximity of the antennas. While further investigation is required to determine the exact cause of this phenomenon, it is reasonable to assume different Rician factor for different MIMO sub-channel when the radiation patterns of the antenna elements are different.

4.3 Correlation Analysis

As discussed in Section 2, it is not clear how the tap specific correlation characteristics of the TGn channel models affect the correlation of MIMO-OFDM channels in frequency. Fig. 4 shows the amplitude of complex correlation derived for each pair of MIMO sub-channels as a function of OFDM sub-carrier. x and y axes represent

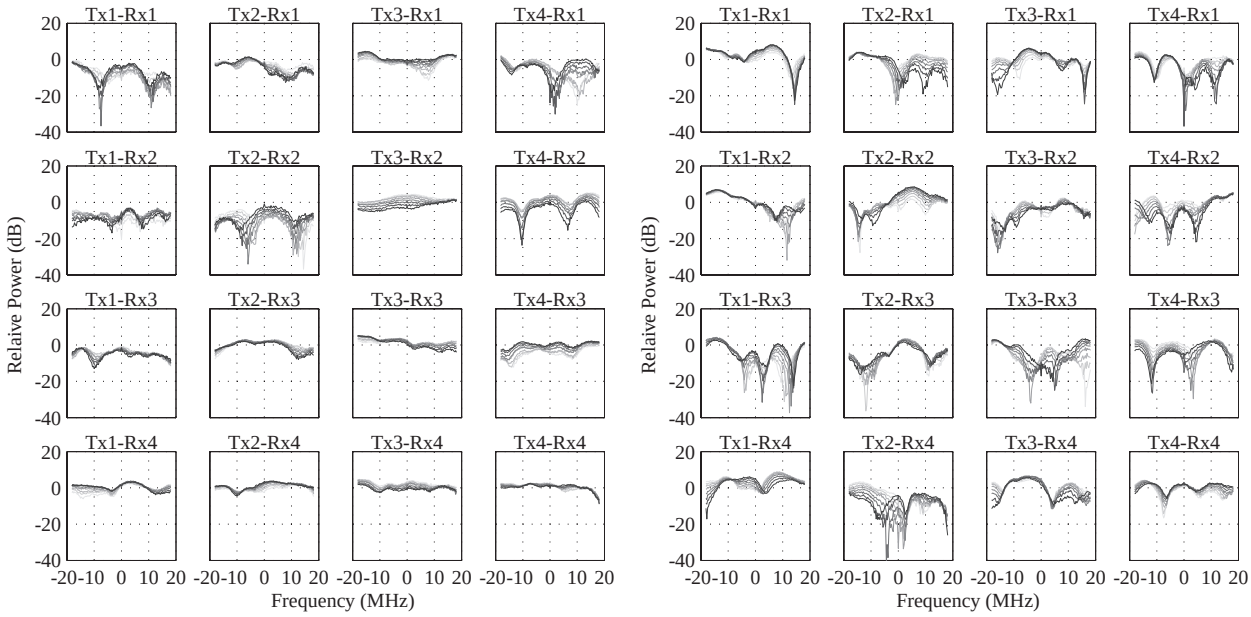

(a) Atrium LoS.

(b) Atrium NLoS.

Figure 1: Example of measured MIMO-OFDM channels.

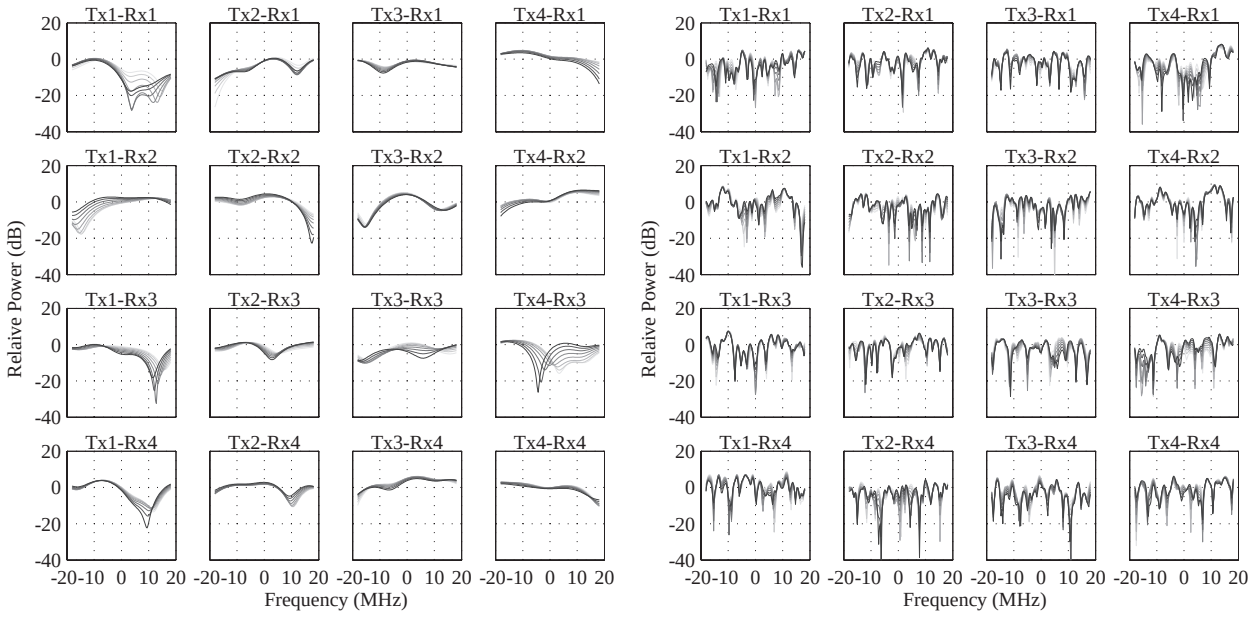

(a) Model B LoS.

(b) Model F LoS.

Figure 2: Example of simulated MIMO-OFDM channels.

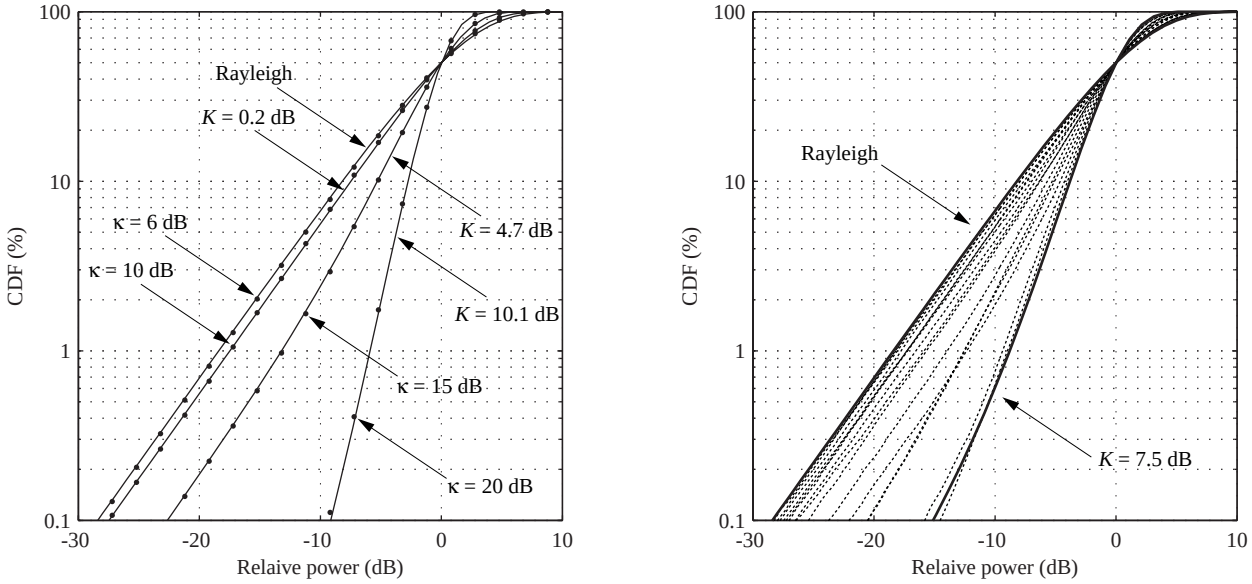

(a) Model E LoS. (b) Atrium LoS.

Figure 3: Example of spatial fading distribution of modeled and measured MIMO-OFDM channels.

frequency from -20 MHz to 20 MHz and correlation amplitude from 0 to 1, respectively. Since the correlation is the same for symmetric channels, e.g. (Tx1-Rx2, Tx3-Rx4) and (Tx3-Rx4, Tx1-Rx2), only the half of the total of $16 \times 16 = 256$ cases are shown in Fig. 4 in order to save the space. The lower triangle shows measured Atrium results and upper triangle shows Model C results as an example. The solid curves represent LoS results while the dotted curves represent NLoS results.

The measured correlation exhibits relatively large variation as a function of frequency while the model results show less variation. This tendency was observed in other measured and simulated results. The exact cause of this phenomenon is currently unknown, and further investigation is needed. It is also observed that the variation of mean correlation amplitude averaged over frequency exhibits relatively large variation as a function of MIMO sub-channel pairs in the case of model results. This is quantified by the standard deviation (STD) of the correlation amplitude as given in Table 1 and 2 for model and measurement results, respectively. The correlation amplitude STD is relatively large for models B, C, and D, while measured values for NLoS cases are 0.11 or less. We also note that while the first tap Rician factor of 0 dB does show apparent effects on the narrowband signal distribution of Channel C LoS results, the cross correlation of the MIMO sub-channels is strongly dependent on this value, as indicated by the differences between LoS and NLoS results in Fig. 4.

5 MIMO-OFDM-LDPC Packet Error Rate Performance Analysis

To assess the quality of the measured and modeled MIMO-OFDM channels, Monte Carlo simulation was performed to measure PER of MIMO-OFDM spatial multiplexing transmission using the low density parity check (LDPC) forward error correction coding. MIMO-OFDM-LDPC is defined in [2] as an an advanced optional mode and can provide approximately 3 dB coding gain over conventional convolutional code when applied to MIMO-OFDM transmission [17]. Here, the coding rate of $5/6$ is used, which provides the highest data rate in [2]. A packet consists of 30 OFDM symbols which contains $30 \times 6 \times 4 \times 108 = 77{,}760$ coded bits using 64 symbol quadrature amplitude modulation (QAM) with 6 bits per symbol, 4 transmitters, and 108 OFDM data sub-carriers. With $5/6$ coding rate, this corresponds to $77{,}760 \times 5/6 = 64{,}800$ information bits per packet. For each of 6400 measured MIMO-OFDM channels, one packet is sent and received to measure the number of uncoded and coded bit errors. If any information bit was found to be received in error, the packet was considered to be in error. For model results, 6400 MIMO-OFDM channels were generated by using the TGn channel models for each scenario. A set of 6400 packets were processed for each specified value of average signal to noise ratio (SNR) per receiver, while complex Gaussian noise was generated according to the specified SNR. A simple zero-forcing detection is used. The detail of the MIMO-

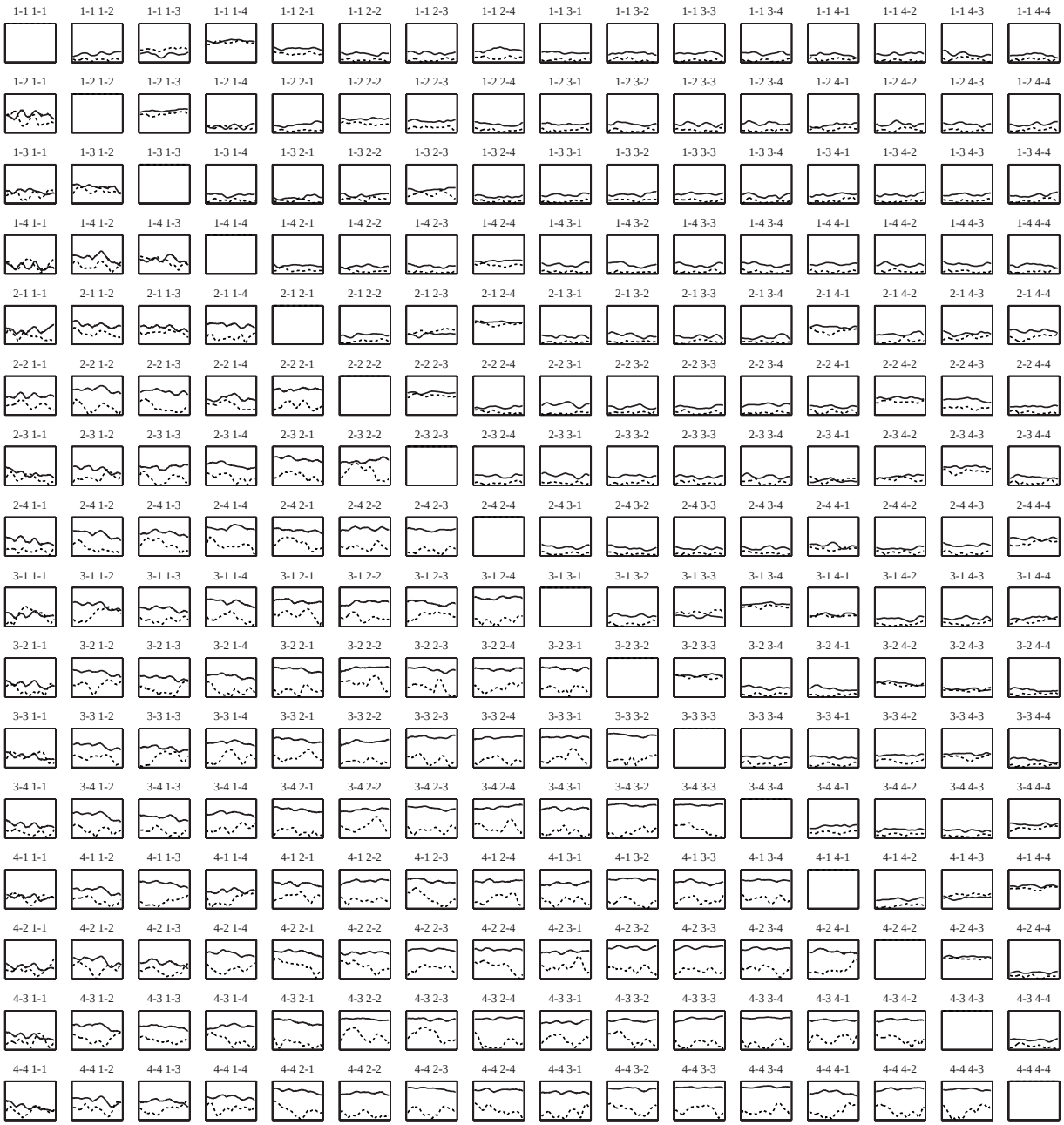

Figure 4: MIMO-OFDM correlation amplitude for Atrium (lower triangle) and Channel C (upper triangle). The solid curves represent LoS results while the dotted curves represent NLoS results. x axis is frequency (-20 to 20 MHz) and y axis is correlation amplitude(0 to 1). The numbers on the top of each plot indicates the pair of MIMO sub-channels. For example, 1-2 3-4 stands for the correlation of the channels between Tx1-Rx2 and Tx3-Rx4.

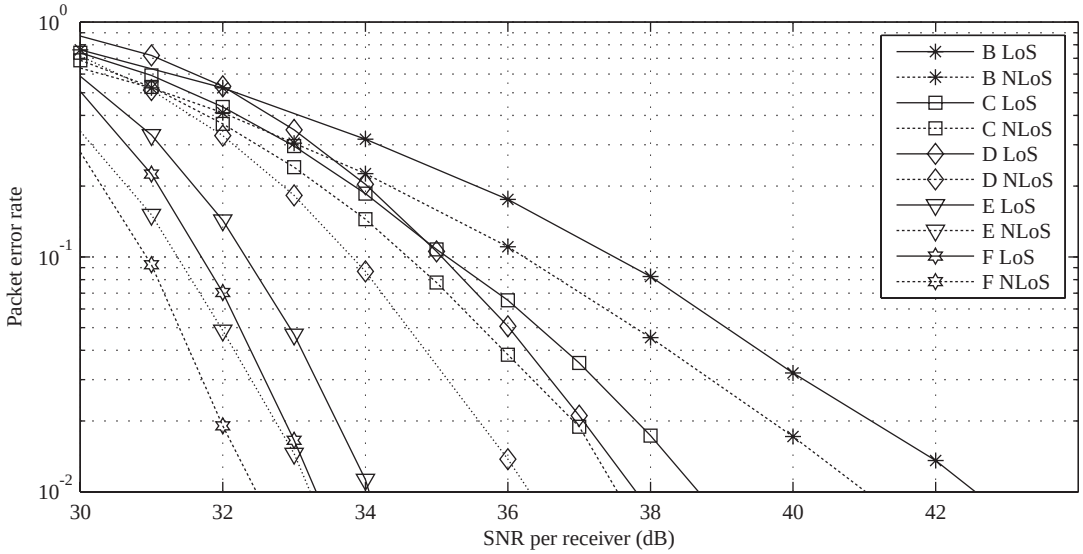

(a) Modeled MIMO-OFDM channel results.

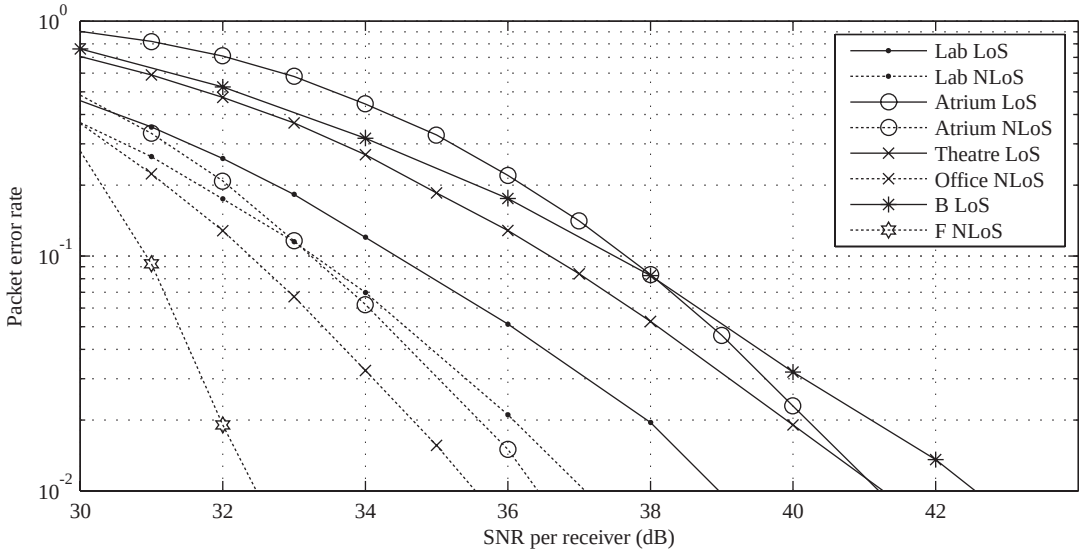

(b) Measured MIMO-OFDM channel results.

Figure 5: MIMO-OFDM-LDPC packet error rate performance.

OFDM-LDPC transmission and its implementation can be found in [15].

Fig. 5 shows the PER performance results based on modeled and measured MIMO-OFDM channels. As can be seen, a large variation in performance can result depending on the MIMO-OFDM channel condition. The Atrium LoS is found to be the least performing channel followed by the Theatre LoS. Both cases are within the scope of TGn channel models, i.e. model B LoS is performing worse than those two cases.

As discussed in Section 4.2, the spatial fading distribution of TGn channel models are all Rayleigh distributed both for LoS and NLoS cases. One might expect very little differences when comparing LoS and NLoS error performance. However, for all models, the NLoS always outperforms LoS, by approximately 1 to 2 dB. Similar PER improvement is observed from the measured results with close to 4 dB improvement observed in Atrium. However this is not to conclude that NLoS is always preferred over LoS in practice, since 4 dB improvement in SNR can also be easily obtained by the fact that LoS does not have blockage to attenuate the receivable power.

It is also observed that the required SNR to achieve PER of 10^{-2} ranges from approximately 32 dB to 42 dB. If the maximum supported SNR of a practical system is less than 42 dB, the results show that significant errors are expected in such a system. In this case, methods to reduce the required SNR are needed, such as employing more receivers to exploit diversity, or implement more advanced MIMO detection schemes.

6 Conclusions

In this paper, we have compared modeled and measured MIMO-OFDM channels expected in typical indoor environments. The standard TGn stochastic MIMO channel models are shown to be capable of generating realistic indoor channels, although the first tap Rician factor may need to be adjusted to support channels with larger Rician factor in some LoS environment, which was also found to be typical in our measurement. The exact cause of the measured frequency dependency of MIMO subchannel cross correlation as well as MIMO subchannel dependent Rician factor needs to be further investigated.

7 Acknowledgment

The authors acknowledge AAU-CSys' and FUNDP-INFO's parenthood on the MATLAB TGn channel model implementation [18]. The authors also acknowledge cooperation with IST project IST-2000-30148 I-METRA [19].

References

[1] G. L. Stüber, J. R. Barry, S. W. McLaughlin, Y. G. Li, M. A. Ingram, and T. G. Pratt, "Broadband MIMO-OFDM wireless communications,"*Proc. of the IEEE*, vol. 92, no. 2, pp. 271-294, Feb. 2004.

[2] S. Coffey, A. Kasher, and A. Stephens, "Joint Proposal: High throughput extension to the 802.11 Standard: PHY," IEEE 802.11-05/1102r4, Jan. 2006.

[3] R. W. Heath, Jr. and A. J. Paulraj, "Switching between diversity and multiplexing in MIMO systems," *IEEE Trans. on Comms*, vol. 53, no. 6, pp. 962-968, Jun. 2005.

[4] V. Erceg *et al.*, "TGn channel models," IEEE 802.11-03/940r4, May 2004.

[5] L. Schumacher and B. Dijkstra, "Description of a MATLAB implementation of the indoor MIMO WLAN channel model proposed by the IEEE 802.11 TGn channel model special committee: Implementation note version 3.2,"May 2004.

[6] M. D. Batariere, J. F. Kepler, T. P. Krauss, S. Mukthavaram, J. W. Porter, and F. W. Vook, "An experimental OFDM system for broadband mobile communications," *In Proc. of the IEEE Vehic. Tech. Conf.*, vol. 4, pp. 1947-1951, Oct. 2001.

[7] R. Piechocki, P. Fletcher, A. Nix, N. Canagarajah, and J. McGeehan, "A measurement based feasibility study of space-frequency MIMO detection and decoding techniques for next generation wireless LANs," *IEEE Trans. on Consumer Electronics*, vol. 48, no. 3, pp. 732-737, Aug. 2002.

[8] K. Yu, M. Bengtsson, B. Ottersten, D. McNamara, P. Karlsson, and M. Beach, "Modeling of wideband MIMO radio channels based on NLoS indoor measurements," *IEEE Trans. on Vehic. Tech.*, vol. 53, no. 3, pp. 655-665, May 2004.

[9] N. Kita, W. Yamada, A. Sato, D. Mori, and S. Uwano, "Measurement of Demmel condition number for 2x2 MIMO-OFDM broadband channels," *In Proceedings of the IEEE Vehic. Tech. Conf.*, vol. 1, pp. 294-298, May 2004.

[10] A. Gupta, A. Forenza, and R. W. Heath Jr., "Rapid MIMO-OFDM software defined radio system prototyping," *IEEE Workshop on Signal Processing Systems*, pp. 182-187, Oct. 2004.

[11] R. M. Rao, S. Lang, and B. Daneshrad, "Indoor field measurements with a configurable multi-antenna testbed," *In Proc. of the IEEE GLOBECOM*, vol. 6, pp. 3952-3956, Dec. 2004.

[12] J-A. Tsai, R. M. Buehrer, and B. D. Woerner, "Spatial fading correlation function of circular antenna arrays with Laplacian energy distribution," *IEEE Comms. Let.*, vol. 6, no. 5, pp. 178-180, May 2002.

[13] H. Suzuki, M. Hedley, G. Daniels, and C. Jacka, "Spatial distribution of temporal variation caused by active fluorescent lights in office environment," *In Proc. of the URSI Commission F Triennium Open Symposium*, pp. 181-186, June 2004.

[14] H. Suzuki, R. Kendall, M. Hedley, G. Daniels, and D. Ryan, "Demonstration of 4x4 MIMO data transmission on CSIRO ICT Centre MIMO testbed,"*In Booklet of Abstracts for 6th Aust. Comms. Theory Workshop*, p.35, Feb. 2005.

[15] H. Suzuki, M. Hedley, G. Daniels, and I. B. Collings, "Implementation of 4x4 MIMO-OFDM-LDPC achiving 600 Mbps packet transmission," *In Proc. of the Australian Telecommunication Networks and Applications Conf.*, pp. 440-444, Melbourne, Australia, Dec. 2006.

[16] H. Suzuki, T. V. A. Tran, and I. B. Collings, "Characteristics of MIMO-OFDM channels in indoor environments,"to appear in *EURASIP Journal on Wireless Comms. and Networking*, vol. 2007, Article ID 19728, Jan. 2007.

[17] H. Suzuki, M. Hedley, G. Daniels, and J. Yuan, "Performance of MIMO-OFDM-BICM on measured indoor channels,"*in Proc. of the IEEE Vehic. Tech. Conf.*, May 2006.

[18] J. P. Kermoal, L. Schumacher, K. I. Pedersen, P. E. Mogensen, and F. Frederiksen, "A stochastic MIMO radio channel model with experimental validation,"*IEEE Jour. on Sel. Areas in Comms.*, vol. 20, no. 6, pp. 1211-1226, Aug. 2002.

[19] http://www.ist-imetra.org.

Simulation and Modelling of Propagation Paths involving the Indoor/outdoor Interface

David Bacon
dB Spectrum Services Ltd, UK
tel: 07785 335871. email: dfbacon@btinternet.com

Nick Thomas
Rutherford Appleton Laboratory,
Didcot, UK

Ray-tracing simulation results at 1 to 10 GHz for representative building types and geometries were analysed primarily to derive a simple path-loss model for radio propagation involving the indoor/outdoor interface. This paper reports some general conclusions as to the nature of inter- and intra-building propagation.
Keywords: Propagation Modelling Ray-tracing Buildings

1 Motivation

A simple path-loss model was required for propagation involving the indoor/outdoor interface. Ray-tracing is suitable for indoor propagation [1],[2] and results are found to have the same statistical properties as measured data [3]. Thus a model was derived from ray-tracing results for representative buildings and geometries. We report initial progress and modelling issues which have arisen.

2 The ray-tracing tool

Only brief details of the ray-tracing software are given here. We used "Rapid Pipeline Development" produced by the Radio Communications Research Unit at the Rutherford Appleton Laboratory. This was originally developed for studies in broadcasting satellite coverage. It has since been used for broadband FWA studies. For this project it was set up to calculate ray geometries from one source ("Tx") to many field points ("Rx") for use by different frequencies as a speed-up technique. Losses were calculated due to spreading, reflection, penetration and diffraction. In the interests of speed knife-edge diffraction was used rather than UTD. Various techniques maximised the capture of significant rays and avoided duplication. An empirical correction was made to results close to the search depth.

3 Representative buildings

The model must require only simple classification of the environment, not specific building details. Models based on real buildings of the following representative types were used for ray tracing.

a) Blg 1: Open plan office building with reinforced-concrete floor slabs, relatively narrow columns, and lightweight external cladding.
b) Blg 2: Non-open-plan office building with brick external and some internal walls.
c) Blg 3: High-rise office building with central core surrounded by open-plan floors with glass external cladding.
d) Blg 5 Substantial Victorian-style dwelling with masonry external and internal walls.

Blg 3 represents high-rise commercial districts, Blgs 1 and 2 represent medium-rise urbanisation, and Blg 5 represents suburban, intermediate between modern lightweight housing and "high-street" shopping centres in the UK

4 Distance as a predictor

The variation of path loss with distance within a building must be modelled to establish frequency-sharing distances where required. This means that indoor distance must be a predictor. The model must also be suitable for use as an end correction to methods for earth-space or long terrestrial paths. Many indoor models use log(distance) as a predictor for indoor distance. For a path with extensive sections outside buildings this requires the building entry/exit distances, which is undesirable in a simple statistical model.

Thus one objective in the analysis was to test whether it is sufficiently accurate to predict horizontal indoor attenuation as $K_i \cdot d_i$, where K_i is an attenuation rate in dB/m and d_i is the indoors distance, m, .

Fig 1 shows one of the simulation geometries. There are two instances of Blg 5. A transmitter is in one building and a large number of receiver points are distributed across the same floor level in both buildings. For clarity, internal walls are not shown.

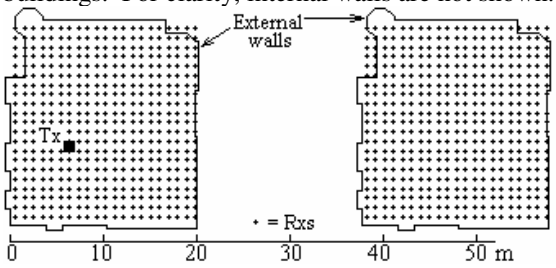

Fig 1. Geometry of distance-predictor test, Blg 5

Fig 2 shows the ray-traced excess path losses (i.e. path loss minus free-space path loss) plotted against the logarithm of total path length. There are two populations of results for receivers in the separate building. Each population could be modelled against distance in the form $N_p \cdot \log(d_p)$ where N_p is the additional exponent for indoor propagation and d_p is the path length, but different values of N_p would be

needed for the two buildings, despite their having the same internal structure.

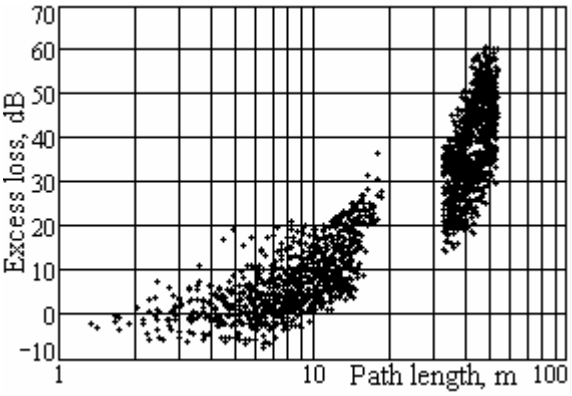

Fig.2. Excess losses vs log path length

Fig 3 shows the same excess losses plotted against the total indoor linear distance from the transmitter to each receiver position. In this case a single line can be fitted with a correlation coefficient of nearly 0.9.

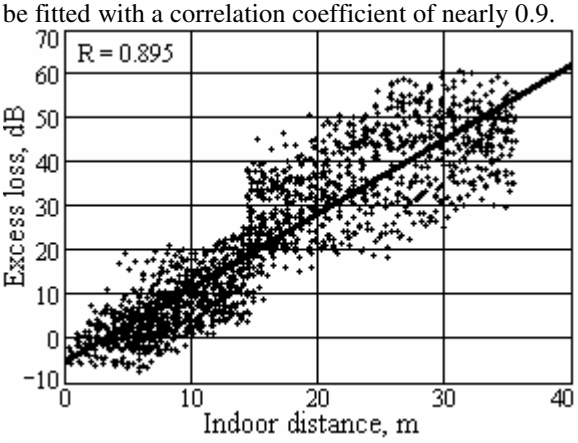

Fig.3. Excess losses vs indoor distance

Similar results to Fig. 3 were obtained for all of the other buildings. It thus seemed worthwhile to compare models based on both log and linear distance for various building types and overall geometries.

5 Room gain

The regression line in Fig.3 has a negative intercept. This was found to some extent in all of the building models.

Signal levels higher than free space in the same room as the transmitter are possible indoors . This is readily understood in terms of the combination of multiple rays due to reflection. Ray tracing calculations reproduce this effect.

Thus the negative intercept in Fig 3 can be expected, and appears to be significant despite the building concerned being sub-divided by brick walls into fairly small room.

The effect is more pronounced in corridors or open-open plan floors. Fig 4 shows a floor plan of Building 3, and Fig 5 excess losses from Tx 1 for a number of receiver locations distributed across the floor plus a regression fit..

Fig 4. Building 3

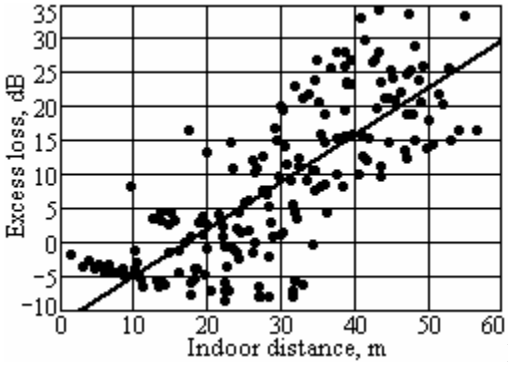

Fig

Fig 5. Excess losses at 2.4 GHz

In this less cluttered building there is a clear tendency for excess loss to decrease with increasing distance, reaching nearly -9 dB about 32 m from the transmitter. This is expected, since within the first few metres of the paths the direct ray will be strong compared to any reflected ray. At longer path lengths the direct and several reflected rays are more comparable in length, and thus significant reinforcement above free space is possible.

The other conspicuous feature is that, as the regression line shows, the effect of this initial reinforcement extends to the far corners of the floor.

Results from modelling ray-tracing results showed that this remains true for longer paths, including between floors and between different buildings.

A “room gain” term was thus included in the models tested against the ray-tracing results. Room gain is considered to exist for each indoor terminal.

6 Models

As commented in 4 above the model must be suitable for use with prediction methods for long paths, including earth-space. This implies a strong preference for a model based on losses simply added in dB, and proportional to linear indoor distance. A

model based on adjusting exponents for indoor sections of a path would be much less convenient to combine with other methods.

However, in view of the several existing models [4] in which log(distance) is a predictor, it was considered essential to perform quantitative comparisons of models based on the two methods.

The "Method 1" model was formulated for near-horizontal propagation as:

$$L_e = K_e \cdot N_e + K_{di} \cdot d_i - G_r \cdot N_{it} \quad (1)$$

where:

L_e = excess loss over the estimate of basic transmission loss for the entire path derived from an associated propagation model.

K_e = coefficient of loss, dB, per building entry/exit point, included because buildings vary in the type of external cladding.

N_e = number of entry/exit points.

K_{di} = coefficient of indoor attenuation, dB/m.

d_i = total indoor distance, m

G_r = room gain, dB, per indoor terminal

N_{it} = number of indoor terminals.

The "Method 2" model was formulated to give excess loss over free-space for near-horizontal propagation in the type of geometry shown in fig.1, where the Tx is inside a building and the path is allowed to leave that building and enter another. This model is conditional upon path length d as follows:

$$L_e = (N_p - 20) \cdot \log(d) - 2G_r \quad (d \le D_1) \quad (2a)$$

$$L_e = (N_p - 20) \cdot \log(D_1) + K_e - G_r \quad (D_1 < d \le D_2) \quad (2b)$$

$$L_e = (N_p - 20) \cdot \log(d \cdot D_1 / D_2) + 2K_e - 2G_r \quad (D_2 < d) \quad (2c)$$

where in addition to the symbols defined for eq(1):

N_p = indoor exponent, greater than 20

d = total path length, m

D_1 = path length to exit from first building, m

D_2 = path length to entry into second building, m

7 Testing method

Equations (1) and (2) were used to calculate predicted values for excess losses (above free-space loss) for each set of ray-traced results. For each individual path the prediction error, E, is defined as

$$E = L_{ep} - L_{er} \quad \text{dB} \quad (3)$$

where

L_{ep} = predicted excess loss

L_{er} = ray-traced excess loss

For any set, or combination of sets, of results, coefficients K_e, K_{di}, N_p and G_r in eqs (1) and (2) were varied to find the set which produced the lowest rms prediction error.

A steepest-descent search method was used to find the lowest rms prediction error. Most searches were restricted to 1 or 2 dimensions, and visualisation of the variation in rms error was employed extensively to ensure consistent results, It was found necessary to modify the most simple steepest-descent method in 2-dimensional searches, since in most cases the prediction error was much more sensitive to one variable than the other. This is illustrated in Fig 6.

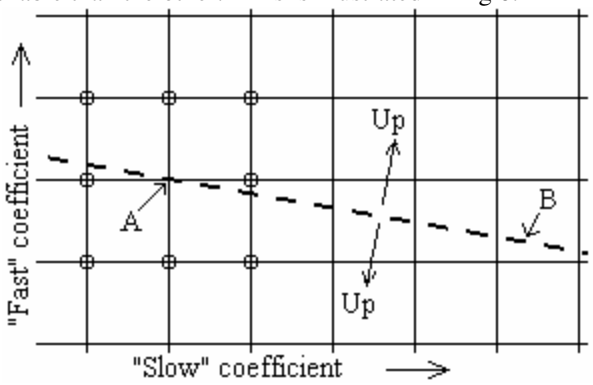

Fig 6. Search method

The intersections of the square grid represent possible values of the two coefficients being varied, at a given step size, and the height of these points the rms prediction error. Due to the difference in sensitivity to the two variables this surface forms a steep-side valley with the lowest values along the dashed line. With simple steepest descent the search process may find point 'A', for which all neighbouring points at a given step size are higher than the true minimum of point 'B' and the search is thus trapped at 'A'.

The modified search process first identifies the coefficient with the steeper slope ("fast") and every search in this direction always proceeds from largest to smallest step size for each step in the "slow" direction at any step size. This was found to produce consistent search results for two dimension.

For more than two variables it was found to be practicable to vary the additional coefficients manually and search by inspection.

Having found a coefficient set producing the lowest rms prediction error, the performance of the model with respect to its distance predictor was considered an important measure of quality. The was evaluated by plotting prediction errors against the appropriate distance and also noting the slope of a regression fit to them, a low slope indicating that the predictor is working well. The mean and standard deviation of the prediction errors was finally taken as the normal indication of the model's performance.

8 Separating entry/exit loss and room gain

For some of the urban geometries studied the sets of Rx positions were in the same building, and thus both N_e and N_{it} in eqs (1) and (2) were constants. This means that the search process described above

cannot separate the two coefficients, since a change in one is automatically balanced by a change in the other.

Thus some geometries were designed to give different values of N_e and N_{it} in the same data set for the different types of buildings used in the study. Fig 1 shows one of these using Blg 5. The coefficient K_e is zero for the rx points in the left-hand building and 2 for those in the right-hand building, whereas N_{it} is 2 in all cases. This allows the search procedure to separate the two.

9 Near-horizontal propagation

Using the geometry in Fig 1, where propagation is predominately horizontal within one floor of a building and to a floor at the same level in an adjacent building, eqs(1) and (2) were used as predictors to find the coefficients giving lowest rms prediction errors. Fig 7 plots prediction errors against indoor distance for the optimum coefficients using eq(1) with Blg 5. A regression line fitted to the errors almost coincides with zero error.

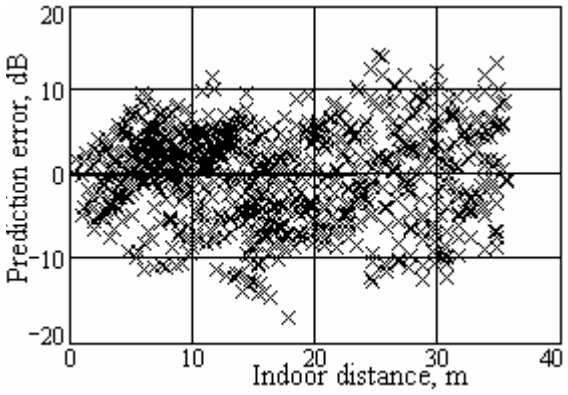

Fig 7. Building 5, eq(1)

Fig 8 plots prediction errors plotted against path length for the optimum coefficients using eq(2).

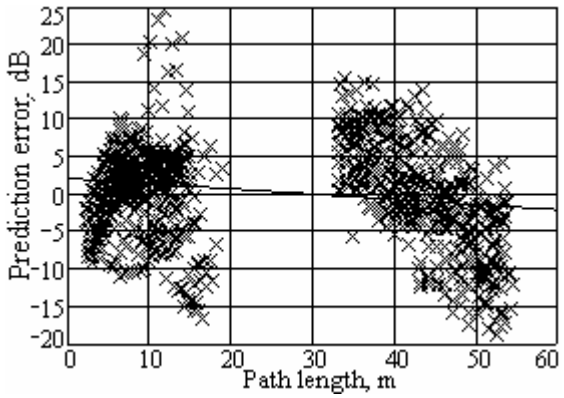

Fig 8. Building 5, eq(2)

There is a marked difference in appearance between Figs 7 and 8, since they must be plotted against different distances. But prediction errors in Fig 8 have a wider scatter and show clear trends with distance, reflected by the regression slope, which are not present in Fig 7.

Similar results were obtained for three other building types. In all cases eq(1) produced the lower means and standard deviations, and indoor distance worked more successfully as a predictor than log(d) in eq(2).

Tables 1 and 2 give optimum coefficients and the associated error statistics for eqs(1) and (2) respectively.

Table 1. Results from eq(1)

	Coefficients			Error statistics	
Blg	K_e	K_{di}	G_r	Mean	S.D.
1	5.3	0.27	3.5	0.02	8.67
2	4.6	0.64	4.6	0.01	7.96
3	0.8	0.61	3.5	0.01	8.35
5	4.0	1.14	2.4	-0.03	5.45

Table 2. Results from eq(2)

	Coefficients			Error statistics	
Blg	K_e	N_{it}	G_r	Mean	S.D.
1	6.7	44.0	16	0.08	9.47
2	13.8	24.9	1	0.46	8.61
3	8.53	39.6	8	0.81	11.04
5	9.36	42.9	8	0.14	6.75

In addition to poorer error statistics, the coefficients in Table 2 vary more, and sometimes have unrealistic values, particular G_r for Blg 1.

It was concluded that although models based on log(distance) may be suitable for propagation entirely within buildings, losses which are added in dB and are proportional to indoor distance are more accurate when paths have both indoor and outdoor sections. This also has the major advantage of making it much simpler to utilise excess losses resulting from the indoor/outdoor interface in conjunction with signal-strengths predicted by other methods.

10 Inter-floor propagation

A simple loss-per-floor coefficient can be used between floors, but a non-linear loss for traversing large numbers of floors may be more accurate. This aspect is included in tests reported in [5] Section 4.7.1, in which a floor-loss model is proposed given by $K_f \cdot N_{fm}$ where K_f is the loss due to propagation between one floor and an adjacent floor, and N_{fm} is a modified number of floor transitions given by

$$N_{fm} = N^{[(N+2)/(N+1)]-b} \qquad (3)$$

where b is a parameter

A comparison was made between linear floor losses, and non-linear floor losses using eq(3), for 5 floors of building 3 at 2.4 and 10 GHz. Two different Tx positions were used on the lowest floor, as shown in Fig 4. Ray tracing was used to obtain signal levels for arrays of Rx positions covering all 5 floors.

To model the ray-tracing results eq(1) was extended to alternative forms given by:

$$L_e = K_e \cdot N_e + K_{di} \cdot d_i + K_f \cdot N_f - G_r \cdot N_{it} \qquad (4a)$$

$$L_e = K_e \cdot N_e + K_{di} \cdot d_i + K_f \cdot N_{fm} - G_r \cdot N_{it} \qquad (4b)$$

where N_f is the number of floors traversed ($N_f = 1$ for an adjacent floor) and N_{fm} is the modified number of floors obtained by substituting N_f for N in eq(3).

Parameter b in eq(3) was investigated by plotting the mean and median excess loss (relative to free-space) from the ray-tracing results and fitting losses for floors 2 to 5. It was found that, although irregularities existed, reasonable fits could be obtained for both Tx positions and at both 2.4 and 10 GHz with $b = 0.54$.

Figs 9 and 10 show these fits for the most and least satisfactory cases respectively.

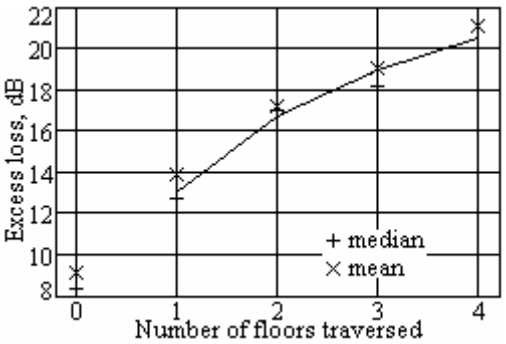

Fig 9. Inter-floor losses, Tx 1, 2.4 GHz, $b = 0.54$

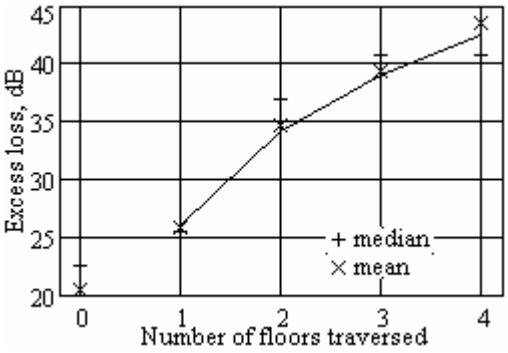

Fig 9. Inter-floor losses, Tx 2, 10 GHz, $b = 0.54$

Although better fits could be obtained with different values of parameter b for each Tx position and frequency, it is advantageous to have single value for all cases. Thus b was set to 0.54 for all cases in comparing eqs (4a) and (4b).

Although some rays may travel outside the building and re-enter, for modelling purposes N_e is considered to be zero since all terminals are in the same building, and thus the coefficient K_e is immaterial in this case.

Indoor distance d_i is in the horizontal plane, ignoring the vertical separation of the terminals. This can produce the case where d_i is zero and the extra losses are due purely to the floor-loss term. This is consistent with the tendency for indoor propagation to be confined between floors and ceilings.

As usual in these tests, free-space loss was calculated using the slope path length, that is, as calculated in 3 dimensions.

Tables 3 to 6 give the coefficients K_f and K_{di} averaged over the floors, and the error statistics for each floor and averaged over floors, for each combination of Tx position and frequency, for both eqs(4a) and (4b).

These show that eq(4b) produces the better error statistics, particularly at 10 GHz, although the differences are small. Extending the comparison over more floors might produce a larger difference. Both losses and prediction errors are higher at the higher frequency.

Table 3. Inter-floor, 2.4 GHz, Tx 1

GHz	Eq(4a)		Eq(4b)	
2.4	Kf=3.17, Kdi=0.57		Kf=4.80, Kdi=0.55	
Floor	Mean dB	S.D. dB	Mean dB	S.D. dB
1	1.01	7.72	0.36	7.79
2	-0.61	7.92	0.37	7.92
3	-1.01	7.38	0.32	7.4
4	-0.05	7.23	0.27	7.22
5	0.78	6.68	-0.54	6.63
Avs	**0.02**	**7.39**	**0.16**	**7.39**

Table 4. Inter-floor, 2.4 GHz, Tx 2

GHz	Eq(4a)		Eq(4b)	
2.4	Kf=3.61, Kdi=0.60		Kf=5.41, Kdi=0.58	
Floor	Mean dB	S.D. dB	Mean dB	S.D. dB
1	0.26	9.75	-0.46	9.81
2	-0.42	8.81	0.66	8.78
3	-0.78	8.98	0.67	8.97
4	-0.28	8.61	0	8.6
5	0.78	8.57	-0.81	8.53
Avs	**-0.09**	**8.95**	**0.01**	**8.94**

Table 5. Inter-floor, 10 GHz, Tx 1

GHz	Eq(4a)		Eq(4b)	
10	Kf=7.03, Kdi=0.65		Kf=10.8, Kdi=0.60	
	Mean	S.D.	Mean	S.D.
Floor	dB	dB	dB	dB
1	-3.24	12.87	-4.89	12.99
2	-2.35	11.61	-0.26	11.51
3	-3.22	10.09	-0.25	9.88
4	-0.65	10.36	0.18	9.94
5	3.1	11.26	0.3	10.76
Avs	**-1.27**	**11.24**	**-0.98**	**11.02**

Table 6. Inter-floor, 10 GHz, Tx 2

GHz	Eq(4a)		Eq(4b)	
10	Kf=8.81, Kdi=0.76		Kf=12.6, Kdi=0.70	
	Mean	S.D.	Mean	S.D.
Floor	dB	dB	dB	dB
1	-3.24	12.87	-4.89	12.99
2	-2.35	11.61	-0.26	11.51
3	-3.22	10.09	-0.25	9.88
4	-0.65	10.36	0.18	9.94
5	3.1	11.26	0.3	10.76
Avs	**-1.27**	**11.24**	**-0.98**	**11.02**

11 Horizontal illumination with shielding

In this case the Tx is outdoor and distant, such that illumination can be viewed as coming from a given direction rather than a given point. Losses are required for paths entering different floors of a building where there is a degree of shadowing by an intervening building.

Figure 10 shows a plan view of the general layout. Three transmitters are located 10 km or more away. The azimuths of their illumination directions are spaced at 22.5° such that rays from Tx 1 are incident at 45° to Blg 3 walls in the horizontal plane.

Figure 11 shows an elevation of the geometry, viewed from the "south" of Fig 10. Blg 1 has a lower roof than Blg 3, and thus shields only the lower floors of Blg 3.

Arrays of Rx points were defined across all 5 floors of Blg 3, and ray tracing calculations run for 1, 2, 5 and 10 GHz.

It was found that the mean and median excess losses on the upper 2 floors of Blg 3 were very similar, and thus shadowing losses on these floors were taken as zero.

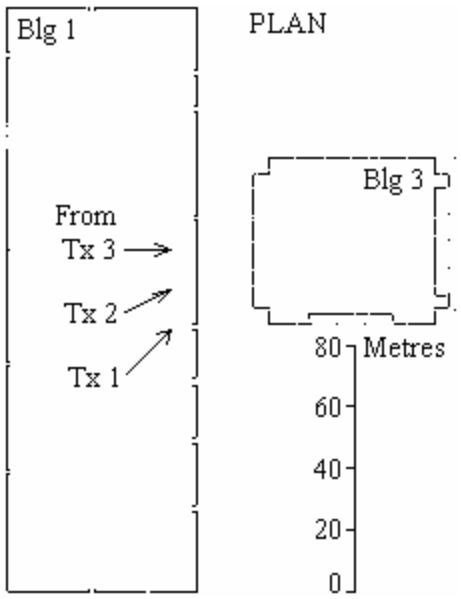

Fig 10. Blg 3 shadowed by Blg 1, plan

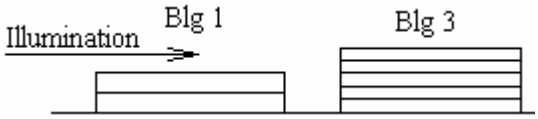

Fig 11. Blg 3 shadowed by Blg 1, elevation

The lower 3 floors showed progressively higher losses due to shadowing by Blg 1. Using eq (1) and coefficients from Table 1 to calculate the losses of signals passing through the 2 floors of Blg 1and then into the lower floors of Blg 3 showed that they would be comparable with signals diffracted over and around Blg 1.

The model under development could be used to predict losses through a complete building but the result would have to be compared with diffraction around it. The target model must require only simple urban classifications, and thus it was decided to derive a statistical shadowing model taking floor height into account.

As an alternative to using either the mean or median excess losses for the different floors, a search was conducted for the value of K_e and K_{di} giving the lowest rms prediction error for each combination of floor, Tx and frequency, without at this stage making any separate allowance for shadowing. Since $N_e = 1$ for all results, the values of coefficient K_e reflected the additional losses on lower floors. These were averaged over the floors, and converted to shadow loss L_{sn} for the n-th floor for floors 1 to 3 by:

$$L_{sn} = K_{en} - 0.5\cdot(K_{e4} + K_{e5}) \quad \text{dB} \quad (5)$$

where

K_{en} = Coefficient K_e for n-th floor averaged over the transmitters

Fig 12 shows L_{sn} plotted as solid traces against the number of shadowed floors for each frequency. Data only exists at integer values of the number of floors, but lines are used to facilitate visualisation.

L_{sn} varies with the number of shielded floors with an 'S' shaped curve, and as expected increases with frequency. It was found that L_{sn} can be approximately modelled by:

$$L_{sn} = (18 + 1.4\cdot f)\,[\tanh(N_s)]^{4} \quad \text{dB} \quad (6)$$

where

f = frequency in GHz

N_s = number of shadowed floors

Fig 12 shows the model values as dashed traces. In addition to being approximate, the fit is special to the geometry shown in figures 10 and 11.

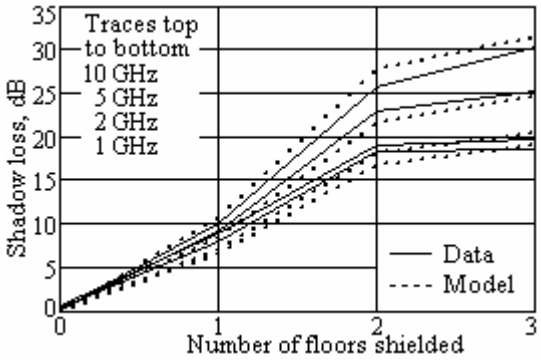

Fig 12. Shielding loss data and model

Thus eq(1) can be extended for a shielded building:

$$L_e = K_e\cdot N_e + K_{di}\cdot d_i + L_{sn}\cdot N_s - G_r\cdot N_{it} \quad (7)$$

where: L_{sn} is given by eq (5), and in this case both N_e and N_{it} are always 1.

This permits a complete model for the shielded building to be formulated. Table 7 gives values of the coefficients K_e and K_{di} obtained from the fits for each transmitter, floor and frequency, averaged over the floors and transmitters, and with a small amount of smoothing.

Table 7. Coefficients for shielded building 3.

GHz	1	2z	5	10
K_e	2.27	3.31	4.79	5.72
K_{di}	0.20	0.21	0.24	0.27

Tables 8 and 9 give the minim, average and maximum mean and standard deviation prediction error when the resulting model is applied to each combination of transmitter, floor and frequency. This is a more useful assessment than the mean and standard deviation of all ray-tracing results taken as a single dataset, since it shows the spread of results when the model is applied to different situations.

Table 8. Mean prediction errors

	Means, dB		
GHz	Min	Av	Max
1	-1.3	1.5	7.9
2	-0.4	2.2	9.3
5	-0.9	2.0	10.6
10	-0.9	3.2	16.3

Table 9. Standard deviations of errors

	Std deviations, dB		
GHz	Min	Av	Max
1	3.9	6.8	12.0
2	4.6	7.2	11.4
5	5.7	9.9	16.7
10	5.7	12.0	19.0

It will be necessary to derive coefficients for different combinations of the representative buildings before such could be used for practical purposes, but the above results indicate that a model based on simple urban classifications is practicable.

12 Indoor distance

Although the results are not yet ready for publication, ray-tracing simulations for earth-space paths at 40° elevation incident on a multi-floor building have indicated that significant rays enter floors via both illuminated and non-illuminated external walls. As a result losses tend to increase with distance from the nearest external wall rather than in the direction of illumination. This is particularly true for the upper two floors of Blg 3. There have also been some results which indicate that the trend can exist to a smaller degree for terrestrial paths in the presence of shielding by other buildings.

This means that for certain situations, and particularly for high-angle paths, distance d_i in eqs(1) and (7) should be distance from the nearest external wall.

13 General form of model

A potential model for propagation involving the indoor/outdoor interface based on simple urban classifications can now be given. It calculates the extra loss, L_e, dB, produced by a path entering or leaving a building and propagation within it. It can be used where the straight-line propagation path is

wholly within the same building, or either or both terminals are outdoors. Under these conditions L_e is given by:

$$L_e = K_e \cdot N_e + K_{di} \cdot d_i + K_f \cdot N_{fm} + L_{sn} - G_r \cdot N_{it} \quad (8)$$

where the symbols are as defined for eqs(1),(4b) and (7), N_{fm} is calculated using eq(3) and L_{sn} by eq(6).

If the path is between floors of the same building N_e is zero and thus the entry/exit loss term is zero. If the path is not between floors of the same building N_{fm} is zero and thus the floor-loss term is zero. If there is no shielding by an intervening building L_{sn} is zero. Otherwise the model can be used for near-horizontal propagation within and between buildings and for building penetration.

The coefficients in eq(8) should apply to buildings representing the required urban classification, as discussed in Section 3 above. A sufficiently representative set are not yet ready for publication; the purpose of this paper is to describe the principle.

The basic transmission loss for the path not taking the indoor/outdoor interface into consideration should use the most appropriate method. For paths wholly within the same building, or between adjacent buildings, free-space is a suitable model. For longer terrestrial paths suitable models should be used. Examples of appropriate ITU-R Recommendations are [6] and [7].

The potential model is not suitable at present for paths between floors at substantially different heights in different buildings or for high-angle paths.

In some situations, particular when scattering from adjacent buildings might be significant, if may be more accurate for indoor distance d_i to be the distance of the indoor terminal from the nearest external wall. When the model is used for evaluating interference it would be conservative to predict losses using both interpretations of indoor distance and take the lower-loss result.

14 Conclusions

Ray-tracing results have been analysed to study propagation involving the indoor/outdoor interface. The following general principles have been noted.

Although actual rays can take a complicated set of indirect paths the overall effect can be estimated by simple statistical models.

Account must be taken of "room gain" due to signal reinforcement by multi-path propagation within buildings. This applies for all paths, not only those wholly within the room or corridor concerned.

Losses due to propagation into, within, or out of buildings can be added in dB to the basic transmission loss predicted for longer paths not taking the buildings into account. Propagation within buildings can be characterised by a horizontal attenuation rate in dB/m, thus making indoor losses proportional to horizontal indoor distance.

Indoor distance should either be interpreted as indoor path projected into the horizontal plan parallel to the direction of the straight-line path, or as distance from the nearest external wall.

15 Acknowledgements

The Authors acknowledge the support of the Office of Communications (Ofcom), London, as sponsor of this activity.

16 References

1 Li et al "Experimental verification of a ray-launching model used for the prediction of indoor wideband directional radio channel at 5.8 GHz" Proceedings of the European Conference on Wireless Technology 2004 , Amsterdam, pp. 341-344, Oct. 2004

2 Hassan-Ali and Pahlaven "A new statistical model for site-specific indoor radio propagation prediction based on geometric optics and geometric probability" IEEE Trans Wireless Comms, Vol.1, No.1, 2002

3 Smulders et al "60 GHz Indoor radio propagation – Comparison of simulation and measurement results" Proc. IEEE 11th Symposium on Communications and Vehicular Technology in the Benelux, Nov. 2004.

4 Recommendation ITU-R P.1238-4 "Propagation data and prediction methods for the planning of indoor radiocommunication systems and radio local area networks in the frequency range 900 MHz to 100 GHz" 2005

5 COST Action 231 "Digital mobile radio towards future generation systems" (EUR 18957) 1999

6 Recommendation ITU-R P.1411-3 "Propagation data and prediction methods for the planning of short-range outdoor radiocommunication systems and radio local area networks in the frequency range 300 MHz to 100 GHz", 2005

7 Recommendation ITU-R P.452-11 "Prediction procedure for the evaluation of microwave interference between stations on the surface of the Earth at frequencies above about 0.7 GHz", 2003

Potential Cognitive Radio Denial-of-Service Vulnerabilities and Countermeasures

Timothy X Brown, Amita Sethi
Interdisciplinary Telecommunications
Electrical and Computer Engineering
Boulder, CO 80309
{timxb,sethi}@colorado.edu

Abstract: Unlike traditional radios, cognitive radios sense spectrum activity and apply spectrum policies in order to make decisions on when and in what bands they may communicate. This paper examines how such activities make CR's vulnerable to denial-of-service attacks. The goal is to assist cognitive radio designers to incorporate effective security countermeasures now, in the early stages of cognitive radio development.

1. Introduction

The radio spectrum is a valuable resource. However, at any given time it consists largely of unused bands, so-called white space [PeS05]. Cognitive radios (CR) sense white space and adapt the radio's operating characteristics to operate in the white space while limiting interference to other devices [ALV06]. Consequently, spectrum regulators such as the Federal Communications Commission (FCC) in the United States (US), recognize that CRs can be applied to dynamically reuse white spaces in licensed spectrum bands, thereby efficiently utilizing under-utilized spectrum [FCC02]. CR technology is still early in its development. Cognitive radio concepts are being developed by a number of research efforts such as the Defense Advanced Research Projects Agency (DARPA) Next Generation (XG) project in the United States [DXG03a,DXG03b] and the End-to-End Reconfigurability (E2R) program in Europe [E2R06]. The technological advances in CRs are of such a magnitude that the FCC takes the view that none of the other advances "holds greater potential for literally transforming the use of spectrum in the years to come than the development of software-defined and cognitive or "smart" radios" [FCC05]. Commercial, military, and public safety users all stand to benefit from CR technology. Consequently, the FCC has also been actively reviewing its rules and procedures to support and accommodate cognitive radio advancements [FCC05].

Cognitive radios may be susceptible to actions that prevent them from being able to communicate effectively, so-called denial-of-service (DoS) attacks. These actions might also induce an otherwise legitimate cognitive radio to interfere with a licensed transmitter. These threats, if significant, will prevent the widespread adoption of CR technology and will prevent the anticipated benefits to spectrum management from being realized.

In this paper we do not identify the motives for such actions. They could be from one or more malicious agents who wish to prevent a CR from communicating; from a valid CR that is malfunctioning; or a CR that is misconfigured. Whether they are due to malicious, malfunctioning, or misconfigured behavior, the actions have the same detrimental outcome and are treated equally. Actions such as direct jamming of the CR communication would affect any radio and so is not of interest here. What we seek to understand are the attack vulnerabilities that are enabled because of the CR functionality. Our goal is to identify these vulnerabilities early in the development of CR so that countermeasures can be incorporated into their design by engineers, standards groups, and regulators. To this end, we outline potential countermeasures for each identified vulnerability.

2. Cognitive Radio Architectures

Figure 1 shows the basic components of the cognitive radio. The *operating system* represents the higher-layer communication functionalities above the radio Physical and Link layers. This generates and receives the traffic information which is to be sent and received by the CR. If appropriate, it includes the end-user interface. A *sensor* measures information about the radio environment. The *policy database* contains information about what kinds of transmissions are and are not allowed. CR policies depend on knowledge of the transmitter location, which is provided by a *geolocator* such as the GPS. The *cognitive engine* combines sensor and

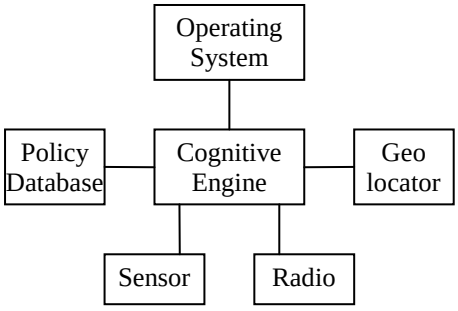

Figure 1: Cognitive radio components.

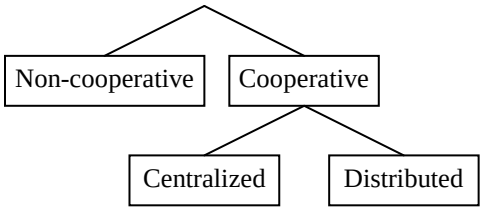

Figure 2: Cognitive radio network architectures.

location information with policy information to make decisions about when and how it will communicate using the radio transmitter and receiver.

CRs can be broadly classified into one of three network architectures as shown in Figure 2. They can range from architectures that encompass all six components in a single non-cooperating device to networked architectures where none of the CR components may be co-located with each other. This model includes multiple instances of each component. For example, there may be dedicated sensing nodes that communicate with a centralized cognitive engine that then directs remote transmitters on how they can communicate. Furthermore, several distributed CR may choose to share information such as measurements, location, or policies in order to make more informed and coordinated communication decisions. To the cognitive engine, the other CRs are effectively sensing, geolocation, or communication extensions. Many cooperative schemes (centralized or distributed) envision a common control channel that is a well known link to shared information [MHS05, SPM05]. The operational advantages or disadvantages for any architecture in this range are not considered. Rather, we consider the security vulnerabilities when any of these components may or may not be collocated with each other.

The cognitive radio can operate as an overlay or an underlay. In an overlay the CR searches for white space bands with which to communicate and generally avoids transmitting power in occupied licensed channels. In an underlay the CR uses spread spectrum or ultra-wideband techniques along with careful power control so as to ensure that no licensed band receives a strong enough signal to cause interference.

The CR can operate in several licensed models. Some bands may be unlicensed and so free for use by any radio. Some bands may be licensed, but allow unlicensed secondary use by any CR under some policy-defined rules and limitations. Yet other licensed bands may allow secondary CR use, but only to a specific licensed set of users under specific conditions. Licensing provides more control over who can operate. Regardless of the model we refer to primary protected users as licensed users, secondary or unlicensed spectrum sharing user as CRs, and misbehaving users that are threatening the CR as attackers.

With this overview of types of CR we turn to jamming and the types of vulnerabilities that are possible beyond direct jamming.

3. Direct Jamming and Jamming Gain

Direct jamming is a simple denial-of-service attack where an attacker transmits a continuous high-power signal that prevents usable reception. This brute-force approach can be applied to any type of radio transmission. In general there are approaches such as spread spectrum that can make a radio more resistant to direct jamming. The greater the spreading of the signal, the harder the signal is to detect and the more robust it is to direct jamming.[1] A cognitive radio has a disadvantage and related advantages to this attack. Because the cognitive radio is operating in available spectrum, the signal bandwidth may be constrained limiting the protective spreading that is possible. However, the cognitive radio is designed to operate in many different bands. Further the CR generally has robust mechanisms for choosing which band to communicate in the presence of licensed and other users. With these capabilities, an attacker would need to jam many different communication bands simultaneously or have reliable techniques for detecting the CR as it switches among the many bands. A potential complication for the attacker is the presence of the licensed users. The attacker may need to avoid these users as it attempts to detect and attack a target CR. We are especially interested in attacks that use transmission that is not per se prohibited. For instance, an attacker may be able to transmit otherwise legitimate packets that prevent CR communication.

A direct attack on the signal can be effective; however, such an attack makes the attacker easier to be detected and countermeasures to be taken. Therefore an attacker will seek techniques to limit its exposure to countermeasures by reducing the fraction of time and power needed to prevent communication. The effectiveness of this technique is denoted *jamming gain* [BJS06]. The attacker has greater jamming gain as it reduces the time or power that it needs to transmit in order to achieve the same effect as with direct jamming. For this paper we will discuss this only in general terms. However, we should be clear that the attacker wants to maximize the jamming gain. The question then is what elements of a CR—its architecture; how it networks with other CR; and its operation—open up jamming gains to the attacker.

4. Types of Vulnerabilities

A DoS attack can prevent communication through

[1] But, an attacker that is close enough or has a powerful enough transmitter can always detect or attack a spread spectrum signal.

placing the CR in one or more of the following states:

1. All available spectrum appears to be occupied by licensed transmitters
2. No policy is available that enables it to transmit.
3. The location is unavailable or has too low accuracy.
4. The sensor is unavailable or has incorrect measurements.
5. The cognitive engine cannot connect to the radio.
6. The operating system cannot connect to the cognitive engine.

Another class of vulnerabilities occurs when the CR causes interference with a licensed transmitter. While the result is not an immediate DoS, it may cause permission policies to be tightened or eliminated, potentially denying service over the long term. A CR may cause interference with a licensed transmitter under one or more of the following conditions:

1. The licensed spectrum appears unoccupied.
2. The policy is incorrect.
3. The location is incorrect.
4. The sensor provides incorrect measurements.
5. The commands to the TX/RX are incorrect.

These conditions parallel the DoS states except the 6th since, by design, no command from the operating system should induce the radio to transmit in an interfering channel.

The subsequent sections describe in more detail these six avenues of attack and the relative effectiveness of each.

4.1 Spectrum occupancy failures

A cognitive radio will not communicate on a channel that is being used by a licensed transmitter. A CR that detects such licensed use may be required to avoid the licensee for long periods of time. An attacker might mimic a licensed carrier. In this case there is a potentially large jamming gain for the attacker. Occupying each licensed channel for a brief time can prevent any channel from being used. For example, some CR will measure the channel it is using often. An attacker that detects a CR transmission can produce a signal with characteristics of the licensed transmitter until the CR radio detects the signal and ceases transmission. The attacker's signal need not be strong enough to physically jam the CR signal at the receiver. It needs only to be strong enough to be detected by the CR transmitter.

This provides gains in two dimensions. First, the CR's signal power and the attacker's signal power are independent of each other. The attacker's signal can be many orders of magnitude weaker than the CR's signal and yet still be detectable and thus prevent the CR transmitter from communicating. Second, once detected, a short jamming period from the attacker can yield a long period of inactivity for the CR. CR can renegotiate new transmission bands if a licensed transmitter is detected, a so-called spectrum handoff [ALV06]. This typically takes time and some effort to negotiate a new channel between CR transmitter and receivers. Even if the CR could change instantaneously, there would always be the potential for the attacker exploiting a large differential between the power required by the attacker and CR transmitters.

Interestingly, if the attacker is near the transmitter, the power required to generate a detectable false signal can be below Part 15 limits so that it is possible the attacker's behavior does not directly violate any regulations.

The attacks can be further leveraged if the CR transmit channel is wider bandwidth than the licensed channel. In this case the attacker only needs to mimic a subset of licensed transmitters so that only small unusable white space segments are left.

Alternatively, the attacker may try to mask licensed users so that the CR will mistakenly communicate. In one approach the attacker may broadcast noise which raises the noise floor so that feature detectors tuned to the licensed service will fail. However, if the attacker generates too much noise, other more general power detectors will trigger. The level of noise power in order to mask the licensed transmitter may be low, and for some cognitive radios, the intervals when measurements are made are known and occupy only a fraction of the total time. Together the average power for this attack may be low. However, the attack is fragile in the sense that strong licensed signals cannot be masked in this way and the attack must mask the signal on every detection attempt to be successful. Further, if a CR is cooperating with other CR radios, then every CR radio must be masked in this way.

4.2 Policy failures

A cognitive radio requires some policy that permits it to communicate. Policy failures include the lack of any policy or the use of false policies.

If the CR can be prevented from receiving any policy, then it will not communicate. This effect is difficult to achieve. The policy database is not necessarily monolithic. The CR may draw on some general policies provided at time of manufacture (e.g. for unlicensed operation). A radio beacon may announce local policies. The CR may be able to make specific queries to a remote policy database. Or the CR may be able to transfer policies from other CR. Furthermore, policies can be distributed in the form of certificates with a period of validity. A CR may already have such certificates from an earlier access to the database. Each of these mecha-

nisms is an opportunity to introduce false policies or modify valid policies.

At any given time, several policy certificates may be valid. These policies can be positive (permitting communication) or negative (preventing communications) and include conditions under which they apply. The cognitive engine must reason through these to find a sufficient policy for its intended communication or scale back its communication. An attacker can try to inject false policies into the CR policy database. Negative policies will prevent communication; positive policies may cause the radio to cause interference. An attacker can also intercept policies applicable on a victim CR to gain knowledge of the CR's operating carrier. It can then launch a DoS attack by forcing the CR to vacate its operating carrier by mimicking licensed carriers (as explained in 4.1).

4.3 Location failures

Almost all policies require some location reference. Even when using a pure sensing strategy, the CR must as a minimum know in which country or region it is operating in order to know which regulatory policy regime to apply. A greater number of policies can be applied as more specific location information is available. For instance, every TV channel is used somewhere in the United States. So, some other communication band must be used unless location information more specific than the country is available. Knowing that one is in a localized region may create some opportunities. However, in some regions, such as New York City, the location must be known accurately, to within a few kilometers, for the CR to be sure it will not interfere with any of the many TV transmitters in the New York metropolitan area [BrS06]. From this example, it should be clear that any location information is useful. But, any degradation in location accuracy can limit or prevent communication.

Location information can come from standard geolocation techniques such as GPS or LORAN; user input of country, zip code, or street address; identifying known radio sources like FM radio or TV signals and finding their transmitter locations in a database; or known location beacons such as from a cellular system base stations that broadcasts its GPS coordinates. This diversity of sources enables a CR to always have some level of location awareness.

However, many of these sources are vulnerable. GPS signals are weak and easily jammed [Vol01]. GPS often fails in indoor, dense urban, or rough terrain environments. Manual entry is open to misconfiguration by intended users or malicious entry by users with access to the user interface. If the attacker is in close proximity, false "known" transmitters can be generated that can be stronger than other transmitter signals. These attacks can cause the CR to have incorrect location estimates or increase the uncertainty in its estimates, both of which are effective at reducing the location specificity [Bro05].

If the geolocator is networked, then the CR is gaining location information from outside sources such as a locator beacon or it infers its location from other CR radios. Attackers can generate false reports purported to be from these sources. Or it can try to compromise these sources using one of the above techniques; in this way, leveraging the number of nodes affected by a single location failure.

4.4 Sensor Failures

Section 4.1 already described failures that could be caused by false or masking inputs provided to sensors. A malfunctioning sensor could simply report false inputs with similar consequences. An attacker might also try to generate false reports purportedly from legitimate sensors.

If the cognitive engine can be prevented from receiving any sensor information then it will limit the communication options for the CR as many policies will require sensor measurements in order for them to be invoked. Sensor information exchanged via a common control channel provides a single and perhaps easy to jam channel.

In some CR designs, the sensor and radio share the same front end. Even when they are separate, the sensor sensitivity can be impaired by a nearby transmitter. As a result, sensing and transmission cannot occur at the same time. The radio can operate only for some fraction of the time, f, with the remaining time being used for sensing. In this case, any jamming becomes leveraged by a factor of $1/f$. For instance, if, because of sensing, the radio can only operate for $f = 70\%$ of the time. Then jamming 35% of the time will reduce the time for communication by $35\%/f = 50\%$.

4.5 Transmitter/Receiver Failures

The receiver of a cognitive radio is often designed to work at a wider range of frequencies than typical radios. The antenna and receiver front end are therefore less selective. The receiver front end is potentially more susceptible to direct physical jamming that does not jam the signals directly, but instead seeks to overload (desensitize) the front-end.

Different frequencies have different propagation characteristics. Jamming only lower frequencies may be sufficient to prevent communication. The CR may have available white spaces at higher frequencies, but the propagation losses at these frequencies are too high to be useful.

Receiver errors may be perceived as evidence of licensed operation in the same band. In this case, jamming a receiver can cause the CR to abandon the band.

A key CR operation is for a transmitter and re-

ceiver to find each other to initiate communication. In a CR, the available frequencies depend on time and place so that some type of spectrum initiation protocol is needed. Once initiated, communication may need to change the frequency of operation because of the appearance of a licensed user or CR mobility. These times are vulnerable because a failed initiation or handoff may require a long time for the radio to resume communication. An attacker can either induce a spectrum handoff via means described above, or recognize the CR signaling of a spectrum initiation/handoff and then start more aggressive jamming to cause a communication failure. By jamming only at these critical moments, the attacker has the potential to achieve a large jamming gain.

In a networked CR an attacker that can gain control of the transceiver can prevent its use. Such an attack would be possible with any networked radio. However, with a CR the attacker could cause the radio to transmit and interfere with licensed users. It also opens the possibility of so-called Sybil attacks where the radio transmits using multiple identities, some of which behave while others misbehave [NSS04].

A CR operating as an underlay will attempt to transmit so that its transmission does not cause interference to the licensed user. An attacker could add additional transmit power to the CR, which might collectively cause interference.

4.6 Operating System Disconnect

This attack can be made only if the cognitive radio is remote from the end user applications. Attacking this link would be the same whether the radio is cognitive or not and so is outside the scope of this paper. However, if the location information is to be provided via user input, then this disconnect does represent a new vulnerability, especially if this information can be selectively targeted.

In a distributed cooperative model the CRs may form an ad hoc or mesh network to distribute sensing and other information. Such networking is beyond simple physical or link layer access and so may require operating system support. A CR with disconnected or compromised operating system can inhibit or corrupt information dissemination and in general is subject to the well-known attacks on ad hoc networking [HBC01].

Throughout these vulnerabilities is a theme of proximity and whether the transmitter or receiver is jammed. This theme is summarized in the next section.

5. Transmitter jamming and attacker proximity

Traditional jamming occurs at the communication receiver. An attacker that is closer to the receiver can jam the communication, potentially with less power than transmitted by the transmitter. An attacker close to the transmitter has no special advantage when jamming the receiver. Knowing when a transmitter is on can be useful information in jamming [BJS06]. But all attacker locations that can sense the transmission are equally effective. With a cognitive radio, the transmitter must also sense, and so the attacker can prevent the receiver from receiving by jamming the transmitter's sensing. Put another way, an attacker near a traditional node can effectively interfere only with reception. An attacker near a CR can interfere with reception or prevent transmission.

DoS attacks become easier as the attacker's distance to the CR device under attack decreases. At great distances enough power must be used for the attacker even to be detectible by the CR. Greater power is needed to create false signals. Still greater power is needed for outright jamming of CR signals. These powers decrease as the attacker comes closer. As they decrease the attacker's energy use can be reduced and simpler, lower cost, and smaller RF front ends may be used. Antennas can go from large high gain dishes to compact integrated antennas. As a result, the attacker becomes harder to detect at shorter distances. It is conceivable that the attacking radio might become attached to the CR radio near its antenna from which detection by anyone but the victim CR itself would be very difficult. At the worst extreme, the attacker may gain access to the CR device's user interface and be able to deliberately misconfigure the device or gain access to security passwords.

6. Security Countermeasures

In general there are six areas of security; confidentiality, privacy, integrity, authentication, authorization, and non-repudiation [Sta06]. Confidentiality protects messages from being read by anyone but the intended recipient. Privacy protects the identity of the sender or receiver. Integrity prevents messages from being modified. Authentication validates the purported sender of a message to the receiver. Authorization controls access to services of authenticated users. Non-repudiation allows a receiver to prove that a message originated from its sender. These areas as they relate to CR user traffic will not directly be considered. However, these techniques will be useful in preventing DoS attacks to the extent that they protect the signaling and communication between networked CR elements. Many mechanisms exist for these different techniques which we will assume in our discussion.

The standard approach to DoS is protection, detection, and reaction [HMP01]. We focus here on protection techniques and leave the other techniques for future work.

The attacks in Section 4 can be divided into broad areas that affect multiple vulnerabilities—such as a compromised cooperative CR—and attacks on specific vulnerabilities.

We should acknowledge here that security is fraught with pitfalls that multiply with system complexity and require extensive system validation. The inherent complexity of CRs and the evolving system designs limit our discussion to general guidance rather than a complete solution.

6.1 Compromised cooperative CR

In a cooperative CR system, compromised nodes can be particularly insidious. They can produce false sensor information, false geolocation information, and invalid policies. They can also inhibit the forwarding and dissemination of valid information among CR nodes in a cooperative network. Authentication and integrity checks can mitigate the corruption of one user's data by others. In a centralized architecture, the central authority should require a public-key authentication and digital signature mechanism so that client CR can validate the source and integrity of the information. In the other direction, the central authority needs also to authenticate the source and integrity of the information. In some CR service models (e.g. if the secondary spectrum use is licensed), the client CR would be known subscribers and, as in cellular, secret keys for each subscriber could be maintained by a central authority. Distributed cooperative users are more difficult to verify. Tamper-proof packet ID's would help identify interfaces.

A compromised user could still originate corrupted data. One possibility is to have "tamper-proof" sensors (or geolocators) that report measurements with their own authentication and integrity check. A public-key scheme could allow any user to recover the measurements from a known class of sensors and prevent any intermediaries, including a compromised CR associated with the sensor from modifying the data without detection. If time stamps are included with the data, then replay attacks would be avoided. Public keys could be distributed by certified authorities.

A compromised user can avoid forwarding sensor information. This falls in the realm of ad hoc network security issues, which have been dealt with elsewhere [HBC01]. In general the approach is for nearby nodes to identify a misbehaving node and then isolate it, for instance refusing to accept messages or otherwise interact with the isolated node. An inherent tradeoff is that a CR has more capable sensing to identify the compromised and misbehaving nodes. However, a compromised CR node has a more capable transmitter for masking its activities.

We note that when CRs are non-cooperating, the value of a compromised CR is minimized to its local activity, which can not be leveraged to more widespread disruption: i.e., any attack with the compromised CR could have been performed with other radio types.

6.2 Common control channel attacks

A common control channel is a target for DoS attacks since successful jamming of this one channel may prevent or hinder communication across a large frequency range. For this reason, the channel should use a robust spread spectrum coding. The media access scheme should be robust and provide fair access. This fairness has to be thought through across multiple layers and the simplest access scheme focused on the control channel need is preferable. One complex media access protocol is 802.11. In 802.11 a number of unintended interactions between different elements and different layers have emerged over time [HRB03, PRR03]. Furthermore, complex protocols provide additional opportunities for attack [BJS06].

6.3 Spectrum occupancy failures

Attacks where the attacker spoofs or masks a licensed transmitter are best dealt with from a cooperative architecture. With cooperating users, the attacker would need to appear as a licensed user to multiple CR that may be widely distributed, which reduces the effectiveness of the attack. Alternatively, if licensed user occupancy is well documented in a database or in information distributed via a broadcast beacon, then a CR can use its location information and this database to have a reliable model of what white space is available. A non-cooperating user is more susceptible to this attack. Randomized detection intervals will force the attacker to continuously generate false signals rather than at predictable detection times. It could also rely on a licensed user data base. In the case that a good database is not available and only partial information is available, it has been shown that underlay-based schemes are more reliable than overlay schemes at avoiding interference to licensed users [MBR05]. The effectiveness of these attacks is predicated on the often long periods of times that the CR must avoid a licensed channel once it detects a licensed user. These periods should be minimized. Further, a CR that can use several small bands simultaneously in order to achieve its communication needs will be able to exploit smaller spectrum segments with less loss in communication continuity. If one segment is loss, the CR can continue on the remaining segments.

6.4 Policy failures

False policies can be prevented by having authentication and integrity certificates traceable to a trusted authority associated with each policy. These policies would have a lifetime associated with them that is preferably as long as possible. In this way policies can be freely exchanged among cooperative nodes, and for non-cooperative nodes they would require only infrequent policy updates and renewals. If valid policies can be exchanged freely and with confidence and stored for

long periods of time, it is unlikely that an attacker can prevent a CR from having at least some policies available. Policy time stamps would prevent replay attacks.

Policy information is ideally available for long periods or broadcast so that individual CR would not need to reveal imminent activity through policy requests.

6.5 Location failures

The key to having at least some location information available is for the CR to have multiple strategies for determining its location, especially if the CR is mobile. If it is cooperating it can share information with other users. In a centralized scheme with a subscriber base, subscriber nodes may be slaves to a trusted central authority and will transmit only under the permission and guidance of the central authority.

6.6 Sensor failures

Compromised sensors have been discussed in Section 6.1. False or blocked sensing information is not an issue if the sensor is collocated with the cognitive engine. The key to avoiding leveraged jamming is to make the fraction of time devoted to transmission, *f*, as close to one as possible. Good sensing strategies are needed for this.

6.7 Transmitter/Receiver Failures

The physical RF front end of a CR receiver needs to be designed for potentially large interfering signals. Use of multiple antennas or steerable antennas can enable the receiver to focus on the intended transmitter (and vice versa). Multiple antennas designed for different frequencies can also help mitigate the variable influence of frequency. Each antenna can be frequency matched with an RF front end to provide better frequency selectivity. The receiver also needs to be careful in how it interprets errors and uses error information as only one piece of evidence that there is a licensed user. As with the common control channel, the channel used for spectrum initiation/handoff has to be very robust and simple. An attacker which attempts to add its signal to an underlay user is unlikely to be effective since underlay signals are typically close to the noise floor.

Table 1 summarizes the vulnerabilities and poten-

Table 1: Cognitive Radio Vulnerabilities and Potential Countermeasures

Vulnerability	Countermeasure
Attacker emulates licensed user. Exploits long time before licensed channel can be reused	Cooperative detection. Accurate database of licensed users. Underlay schemes. Shorten licensed channel avoidance periods. More efficient spectrum handoff algorithms. Communicate over multiple disjoint bands.
Attacker masks licensed user	Cooperative detection. Accurate database of licensed users. Underlay schemes. Randomized detection intervals.
Attacker blocks access to policies	Diversity of policy sources. Long policy valid periods. Spread spectrum common control channel robust to jamming
Attacker injects false policies	Certificates traceable to a trusted authority. Time stamps on policies.
Attacker intercepts policy information to predict CR activity.	Minimize need for policy requests
Attacker blocks access to location information	Spread spectrum signals robust to jamming. Multiple sources of location information. Only communicate with trusted nodes known to have accurate location information.
Attacker injects false location information	Tamper-proof location devices that can be authenticated. Non-cooperative architectures.
Attacker blocks access to sensor information	Spread spectrum signals robust to jamming. Non-cooperative architectures. Sensors are collocated with cognitive engine.
Attacker injects false location information	Tamper-proof sensors that can be authenticated. Non-cooperative architectures. Sensors collocated with cognitive engine. Time stamps on sensor data.
Attacker leverages jamming against fraction of time transmitting versus sensing	Minimize the time devoted to sensing.
CR has more open front end	Multiple front ends and antennas for different bands. Steerable antennas.
Attacker exploits frequency differences	Multiple antennas for different bands.
Attacker induces receiver errors as if from a licensed device	Corroborate these errors with other evidence.
Attacker jams at spectrum handoff or initiation	Spread spectrum common channel robust to jamming.
Otherwise valid CR misbehaves	Use sensors to localize and identify misbehaving nodes. Have tamper-proof transmitter ID added to every packet.
Attacker causes underlay to exceed allowed power in licensed band.	Underlay signal is typically at or near the noise floor already.
Attacker blocks user input	Co-locate operating system and cognitive engine. Spread spectrum common control channel robust to jamming.
Attacker misbehaves forwarding information between networked CR	Ad Hoc network security techniques. Non-cooperating architectures.

tial countermeasures.

7. Conclusion

A naïve cognitive radio design will be vulnerable to multiple modes of failure from intentional and unintentional attacks. Any radio is subject to direct jamming. The cognitive-radio-specific attacks differ in that they have high jamming gain: they can induce large performance degradation for relatively little effort in terms of average transmission power. However, with modest effort on the part of the cognitive radio design, these jamming gains can be significantly reduced. Cognitive radio designers are encouraged to consider these vulnerabilities and remedies as they continue to develop cognitive radios.

Acknowledgements

This work was supported by NSF award CNS 0428887.

References

[ALV06] Akyildiz, I.F., Lee, W.-Y., Vuran, M.C., Mohanty, S., NeXt generation/dynamic spectrum access/cognitive radio wireless networks: A survey, Computer Networks, 50, 2006 pp. 2127-2159.

[Bro05] Brown, T.X. An analysis of licensed channel avoidance strategies for unlicensed devices, in *Proc. IEEE DySPAN*, Nov. 8-11, 2005.

[BJS06] Brown, T.X, James, J.E., Sethi, A., Jamming and sensing of encrypted wireless ad hoc networks," in *Proc. Seventh ACM International Symposium on Mobile Ad Hoc Networking and Computing* (MobiHoc)}, Florence, 22-25 May 2006.

[BrS07] Brown, T.X, Sicker, D., Can cognitive radio support broadband wireless access? submitted to IEEE DySPAN, 2007.

[DXG03a] DARPA XG Working Group, *The XG vision*. Request for Comments, version 1.0. Prepared by: BBN Technologies, Cambridge, Mass., USA. July 2003.

[DXG03b] DARPA XG Working Group, *The XG architectural framework*. Request for Comments, version 1.0. Prepared by: BBN Technologies, Cambridge, Mass., USA. July 2003.

[E2R06] End-to-End Reconfigurability (E2R) Phase II website (e2r2.motlabs.com)

[FCC02] FCC ET Docket No. 02-135. *Spectrum Policy Task Force Report*, Nov. 2002. (http://hraunfoss.fcc.gov/edocs_public/attachmatch/DOC-228542A1.pdf)

[FCC05] FCC, ET Docket No. 03-108, Facilitating Opportunities for Flexible, Efficient, and Reliable Spectrum Use Employing Cognitive Radio Technologies, *FCC Report and Order* adopted on March 10, 2005, (gullfoss2.fcc.gov/prod/ecfs/retrieve.cgi?native_or_pdf=pdf&id_document=6517509341)

[HRB03] Heusse, M.; Rousseau, F.; Berger-Sabbatel, G.; Duda, A.; Performance anomaly of 802.11b, *Proc.* of *INFOCOM* 2003. v. 2, 30 Mar. - 3 Apr. 2003 pp. 836-843

[HMP01] A. Householder, A. Manion, L Pesante and G. M. Weaver, *Managing the threat of denial-of-service attacks*, CERT Coordination Center, v10.0, October 2001.

[HBC01] J. Hubaux, L. Buttyán and S. Čapkun, *The Quest for Security in Mobile Ad Hoc Networks*, ACM press, New York, NY, 2001.

[MHS05] Ma, L., Han, X., Shen, C.-C., Dynamic open spectrum sharing MAC protocol for wireless ad hoc network, in *Proc. IEEE DySpan*, Nov. 8-11, 2005, pp. 203-213.

[MBR05] Menon, R. Buehrer, R.M., Reed, J.H., Outage probability based comparison of underlay and overlay spectrum sharing techniques, in *Proc. IEEE DySpan*, Nov. 8-11, 2005, pp. 101-109.

[NSS04] Newsome, J.; Shi, E.; Song, D.; Perrig, A.; The Sybil attack in sensor networks: analysis & defenses, in *Proc. of Third International Symposium on Information Processing in Sensor Networks.* IPSN. 26-27 Apr. 2004 pp. 259-268

[PeS05] Petrin, A. Steffes, P.G., Analysis and comparison of spectrum measurements performed in urban and rural areas to determine the total amount of spectrum usage, in *Proc. of the International Symposium on Advanced Radio Technologies* (ISART), March 1-3, 2005.

[PRR03] Pilosof, S., Ramjee, R., Raz, D., Shavitt, Y., Sinha, P., Understanding TCP fairness over a wireless LAN, *Proc.* of *INFOCOM* 2003. v. 2, 30 Mar. - 3 Apr. 2003, pp. 863-872

[SPM05] Sankaranarayanan, S., Papadimitratos, P., Mishra, A., Hershey, S., A bandwidth sharing approach to improve licensed spectrum utilization, in *Proc. IEEE DySPAN*, Nov. 8-11, 2005, pp. 279-288.

[Sta06] Stallings, W., *Network Security Essentials: Applications and Standards* 3rd Ed., Prentice Hall, 2006, 432 p.

[Vol01] Volpe, J.A., *Vulnerability assessment of the transportation infrastructure relying on the Global Positioning System*, Final Report for the National Transportation Systems Center, U.S. Dept. of Trans. Aug. 29, 2001. www.navcen.uscg.gov/gps/geninfo/pressrelease.htm

Combining Cognitive Radio and Software Radio Approach for Low Complexity Receiver Architecture

Edmund Coersmeier, Klaus Hueske, Marc Hoffmann, Felix Leder, Peter Martini, Harald Bothe

Nokia Research Center, Meesmannstrasse 103, 44807 Bochum, Germany
Edmund.Coersmeier@nokia.com, Marc.Hoffmann@nokia.com, Harald.Bothe@nokia.com
University of Dortmund, Information Processing Lab, Klaus.Hueske@uni-dortmund.de
University of Bonn, Institute of Computer Science IV, Peter.Martini@cs.uni-bonn.de,
leder@informatik.uni-bonn.de

Abstract *– Cognitive Radio techniques will be the next step towards efficient wireless bandwidth utilization. The Cognitive Radio approach is intended to investigate the spectrum allocation and to select an appropriate frequency for the corresponding wireless technology while guaranteeing a highly reliable wireless link. If one extends this approach by balancing between desired high capacity channel and corresponding receiver complexity one can introduce a method for optimum mobile receiver complexity. The support of Cognitive Radio for optimum receiver complexity can only be realized if Software Radio is applied. This paper describes the interaction between Cognitive Radio and Software Radio approach and presents an Artificial Neural Network channel decoder to demonstrate the algorithm complexity flexibility.*

Index Terms *– Cognitive Radio, Software Radio, Multi-Processors, Channel Decoding, Viterbi, Recurrent Neural Networks*

I. Introduction

Cognitive Radio approach is intensively discussed in [1] and intends to efficiently utilize the limited wireless spectrum. Therefore Cognitive Radio scans the spectrum and decides which spectrum or channel, respectively, is the best applicable for the corresponding wireless technology and user application. In [1] Cognitive Radio approach is based on three cognitive tasks, which have been defined as follows: Radio-scene analysis, channel-state estimation and predictive modelling, and finally transmit-power control and dynamic spectrum management. Radio-scene analysis handles interference temperature estimation and detection of spectrum holes on the receiver side. These tasks are not considered in this paper. Instead of channel-state analysis and transmit-power control are important items with regard to potentially optimum receiver complexity.

To realize a good spectrum allocation a high flexibility in the receiver architecture is required. An advantageous approach for such receiver architecture is to implement a Software Radio receiver [2], which is able to choose on the fly one algorithm from a set of different algorithms to solve a specific receiver task like synchronization, channel estimation, demodulation or channel decoding. This new Software Radio approach differs significantly from traditional receiver hardware implementation, because one or several Software Radio processors can run different algorithms based on the same hardware implementation. Instead of traditional pure hardware receiver implementation is realized as an optimal implementation in terms of gate count, silicon costs or power consumption for one or very limited amount of algorithms per receiver task. The drawback of that approach is the missing flexibility to redefine the functionality after implementation has been finalized. Thus pure hardware realization is not supporting Cognitive Radio approach very well. To achieve high data rates with Software Radio the most promising approach is actually to implement a multi-processor platform, which achieves the required processing power and speed by parallel execution of many operations and several algorithms.

Based on multi-processor Software Radio approach this paper investigates how multi-processor platforms can interact with Cognitive Radio to achieve optimum receiver complexity. Optimum means in this context balancing between receiver algorithm processing amount and required receiver performance. Typically pure hardware implementations are designed for worst case transmission scenarios by always applying high

performance receiver algorithms, which fulfil at all times the required receiver performance. This approach is far from optimum in terms of low receiver complexity because the receiver always processes data as it is required for worst case scenarios.

Now this paper proposes to design algorithms in a different way, optimally fitting on parallel-processor platforms to achieve exactly the required algorithm performance, which has been requested from Cognitive Radio. When operating with the exact matching receiver performance then the receiver complexity will be optimally as well.

The paper first summarizes important Cognitive Radio features. This is followed by a description about interaction between Cognitive Radio and Software Radio. After that an overview about potentially multi-processor Software Radio platform principles is given. Finally the new Cognitive Radio approach is analyzed by an example for channel decoding. Channel decoding algorithm and corresponding simulation results are based on Recurrent Neural Network (RNN) seen as alternative to Viterbi decoder.

II. Important Cognitive Radio features

In this section a short summary about channel-state estimation and transmit-power control, as proposed in [1], is given. These two items build the base to develop new meaningful interaction between Cognitive and Software Radio.

A. Channel-State Estimation

Channel-state estimation is an important activity within the Cognitive Radio approach to be able to judge whether a specific channel is able to provide enough channel capacity for the desired transmission technology or user application, respectively. For Cognitive Radio technology a continuous pilot transmission is not seen as reasonable way to analyze the channel conditions because it is wasteful in both, transmit power and channel bandwidth [1]. Instead of [1], [3] propose the use of semi-blind training which first employs a supervised training mode and finally tracks the initial channel state estimation to detect changes in the channel properties, Figure 1.

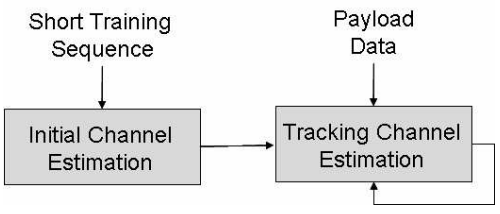

Figure 1 Combining supervised training and tracking mode.

After channel-state information is available in the receiver a so called rate-feedback [1] is provided from the receiver to the transmitter for setting up the data rate as well as the transmit-power control.

B. Transmit-Power Control

Cognitive Radio transmitter gets from the corresponding receiver a rate-feedback. The rate feedback is used to start planning the required transmit-power per transmitter. In a multi-transmitter scenario each data transmission needs to achieve its target data rate and therefore the corresponding transmission power needs to be regulated. In [1] a two-loop setup is proposed, Figure 2.

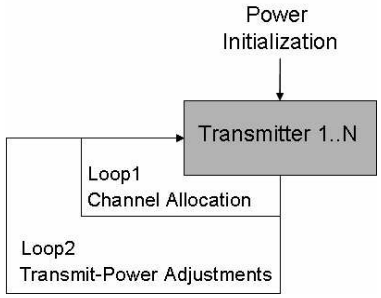

Figure 2 Two-loop setup for bandwidth allocation and transmit-power control.

After initial, equal power setup for all transmitters, a first inner loop, here called Loop1, see Figure 2, iterates from one transmitter to the next, where each transmitter allocates a number of channels based on Water-Filling approach [1]. After bandwidth allocation has been finalized, all transmission systems are investigated in the outer loop, here called Loop2, see Figure 2, whether their actual data rates are exceeding, matching or undershooting the target data rates. In case of exceeding or undershooting the target data rates, Loop2 adjusts the transmit-power of each transmitter so that the actual data rates are matching with the desired target data rates.

After summarizing in this section the proposal for Cognitive Radio from [1] the next section introduces an enhancement to Cognitive Radio approach for optimal mobile receiver complexity.

III. Optimal Receiver Complexity

The actual idea of Cognitive Radio is the optimal utilization of the available wireless spectrum by employing a highly flexible system, which adjusts bandwidth allocation as well as transmit-power to the corresponding requirements to achieve the desired target data rates. From the high-level wireless system perspective this approach is looking comprehensive and

is a significant step forward compared to the actual wireless transmission systems. From the wireless, mobile receiver perspective this approach can still be enhanced by additionally introducing a cognitive complexity regulation for mobile receivers. This section will first describe how to optimally utilize Software Radio for the required receiver flexibility and after that introduces an extension to the Cogntive Radio approach.

A. Software Radio

Figure 3 describes an analysis of Software Radio processor load for an OFDM receiver, completely running on a floating-point DSP processor [4], [5], [6].

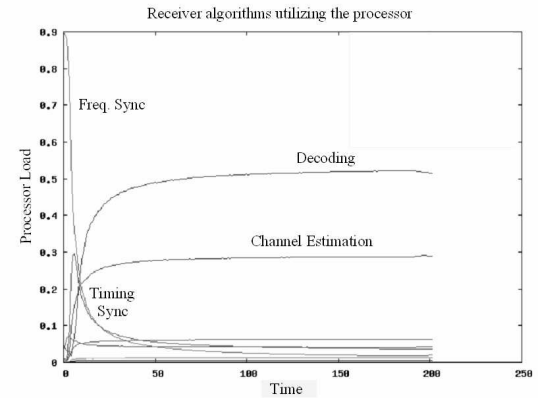

Figure 3 Example for Software Radio processor load for one Digital Radio Mondiale OFDM receiver.

There are a few algorithms which require significant amount of processor load during signal reception whereas several other algorithms individually do not add further large amount of processor load. For example, at the beginning of the receiver activities in Figure 3 synchronization algorithms for frequency and time synchronization require most processing amount whereas during tracking mode channel estimation as well as decoding algorithms significantly contribute to the overall processor load.

Transferring these results to the Cognitive Radio approach it is valuable to enhance the cognitive approach to support the employment of low complexity algorithms for special set of receiver tasks if possible. In some cases the support could be long-lasting in other scenarios one can assume temporary support from the Cognitive Radio approach to allow the mobile receiver to employ low complexity algorithms.

The motivation for low complexity algorithms can be described with the following items:

- Software Radio processor overload
- Receiver power consumption reduction

1) Software Radio Processor Overload

Software Radio processor overload can be the case if one runs more than one radio receiver at a time on a single or multi-processor field. Depending on each receiver complexity there might be temporary shortage of available processor power.

2) Receiver Power Consumption Reduction

Receiver power consumption reduction could be introduced as an option for the mobile user. If the user selects to run a very low power device, the handheld should be smart and understand how to reduce power consumption as much as possible. This could be done by informing the radio receiver to be as power efficient as possible.

Typically traditional receiver designs balance algorithm complexity and algorithm performance before implementation. Hardware implementations target high algorithm performance to handle worst case transmission scenarios, e.g. bad channel conditions. In case of good channel conditions, the hardware receiver is over-specified from the performance perspective. Unnecessary receiver battery power is wasted. This problem can be circumvented when employing a Software Radio receiver to find a compromise between algorithm performance and power consumption.

3) Software Radio Flexibility

Software Radio flexibility offers the chance to load different algorithm complexities for the same receiver task, depending on the channel conditions. In case of difficult channel conditions, high performance algorithms, requiring high processor load, can be applied. If channel conditions are not that worse, Software Radio receiver can reload an algorithm set with lower performance and less processor load. An example is shown in Figure 4 by introducing three algorithms sets.

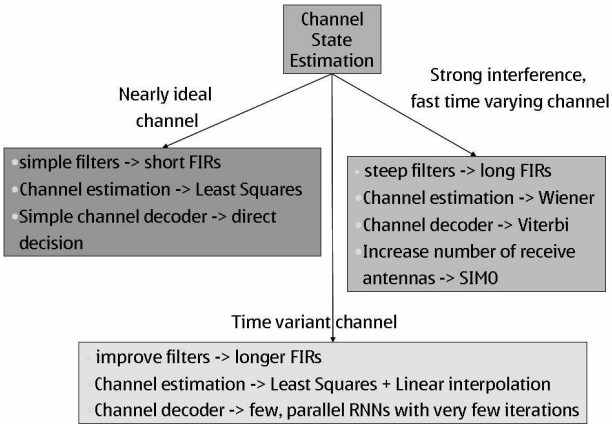

Figure 4 Software Radio approach to load receiver algorithms with different processing complexity.

The channel state estimation selects one of three sets of receiver algorithms, depending on the properties of the channel conditions, identified in the channel state estimation process. Nearly ideal channel conditions lead to simple receiver algorithms, which do not fully load single or multi-processor platform. When channel conditions get more critical, in Figure 4 defined as time variant channel, more complex algorithms have to be employed. This setup will require already significantly more load than the first algorithm set. Finally the worst case scenario considers strong interference and fast time varying channel conditions and the channel state estimation process selects the algorithms for highest receiver performance.

Figure 4 acts as Single-Input-Single-Output (SISO) channel example, which could be expanded for Multiple-Input-Multiple-Output (MIMO) cases. It is imaginable to select a subgroup from each algorithm set instead of selecting always a complete new set of algorithms as function of channel conditions.

After introduction how Software Radio can react on different channel conditions, the next section introduces the extension to the Cognitive Radio to enable selection of corresponding algorithm sets.

B. Cognitive Radio Enhancement

Cognitive Radio approach from [1] can be enhanced to a three-loop approach to introduce receiver complexity optimization. Figure 5 presents the modified drawing from Figure 2 by adding one additional outer loop, called Loop3.

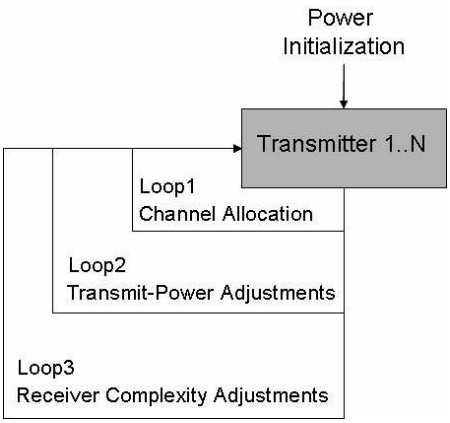

Figure 5 Three-loop extension for Cognitive Radio to support receiver algorithm set selection.

Figure 5 shows that after power initialization for all transmitters the channel allocation process starts and is lead over to transmit-power control. After Loop1 and Loop2 have been finalized, all transmitters run from data-rate perspective with optimal transmit-power. Now a third loop can be activated, which checks from all receivers an optional request for low complexity receiver algorithms. For all receivers, which indicate the wish for low complexity algorithms, a selection, based on Figure 4, starts. Selection process incorporates both previous loops, Loop1 and Loop2, respectively. Two system properties need to be investigated to enable the requested reduction of receiver complexity for selected radios:

- Transmit-Power Increase
- High Quality Channel Selection

1) Transmit-Power Increase

If within Loop2 the transmit-power of the corresponding transmitter is increased, less complex receiver architecture can be installed for that corresponding radio. At the same moment other radio receivers might need to increase a little bit the own receiver complexity because their transmitters might reduce the transmit power. But all those transmit-power reductions should be very small amount for each transmitter because absolute required power reduction will be distributed as a fraction over all transceivers. Thus receiver complexity reduction through transmit-power increase should be only considered as one minor possible option. If all radio receivers would always request power reduction, the system finally might not come to an improvement for any receiver when regulation is done via transmit-power increase.

2) High Quality Channel Selection

As a better alternative to transmit-power increase the channel selection process within Loop1 can be reactivated. If the Cognitive Radio manages to find another, better fitting, free high quality channel for the corresponding receiver, the low complexity request can be solved without transmit-power changes for any transmitter. If no further free channels are available it might be possible to exchange the already allocated channels of two radios, one radio with low complexity request, the other radio without activating this request option. Thus Loop1 channel re-allocation procedure might be the better option from the overall system perspective, because less action is required from all Cognitive Radios.

3) Low Complexity Parameter for Loop1 and Loop2

Another alternative is to leave out Loop3 at all and to consider already during first run of Loop1 and Loop2 the low complexity option. Each channel selection process and each transmit-power adjustment would be informed beforehand whether the corresponding receiver asks for low complexity support. If the low complexity option is enabled by one or more receivers, Loop1 and Loop2 take one more parameter into account

for the overall selection process. Thus the selection process is more complex during each run of Loop1 and Loop2, respectively, but this principle removes the need for Loop3 at all.

After investigation of the new Cognitive and Software Radio approach has been finalized, next sections introduce practical example how flexible channel decoder approach can implement the new idea. Therefore, first a short overview about possible Software Radio platforms will be given. After that Recurrent Neural Network channel decoder will be described and simulation results will be presented.

IV. Multi-Processor Software Radio Architecture

To successfully replace in future some pure hardware radio implementations by establishing new Software Radio designs, it is required to implement a high performance processor platform, which runs one or more radios in parallel at the same time. Power consumption is an important parameter for embedded systems hence it is not possible to speed up processors until the required processing power is available. Instead of multi-processor platforms seem to be a more realistic approach to address Software Radio requirements. Basically one can differentiate between heterogeneous and homogeneous multi-processor platforms, as shown in Figure 6.

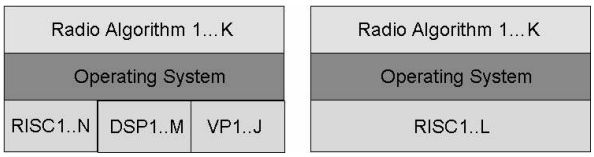

Figure 6 Heterogeneous and homogeneous multi-processor platform for Software Radio.

The left drawing in Figure 6 shows a heterogeneous platform, including different types of processors, e.g. RISC, DSP and Vector-processors [7]. The right drawing consists out of L processors, whereas only one processor type, e.g. RISC processor, has been implemented, see [8]. The Operating System (OS) bridges between hardware and radio algorithms. The algorithms are implemented processor independent, except for word length limitations, because C-Code instead of Assembler implementation is favoured. This approach makes software implementations better reusable without completely re-writing code in case of changes in hardware. New compilation run updates the object codes and executables. On the other hand abstract C-coding might be less efficient from performance perspective than implementing Assembler.

The OS scheduler assigns algorithms at runt-time to the corresponding processors. This task is in case of heterogeneous platforms more difficult than for homogeneous platform. When new algorithms need to be activated for the next radio task, both platform types need to identify and select an actually free processor. In case of heterogeneous platform an additional decision about best fitting processor type needs to be made. This additional selection process assumes that for one algorithm different executables, corresponding to the different processor types, are available.

If utilizing a multi-processor platform for Software Radio approach it is important to implement the radio algorithms in such way, that parallel processing is supported by the algorithm architecture. High performance Software Radio algorithm architectures might significantly differ from parallel hardware implementations because implementation bottlenecks like memory access, BUS bandwidth as well as available processing power are different for ASIC / FPGA designs and processor systems. When planning parallelization of algorithm parts, it needs to be considered that granularity of each algorithm segment should be high for Software Radio algorithms. The reason for that can be found in the limit of possible data transfers in the Software Radio platform. The longer one algorithm segment can work on a set of data the more efficient is the Software Radio platform utilization. For pure hardware implementations this statement needs not to be true, because data exchange can be speed up by direct wiring.

The next section investigates a channel decoder algorithm, which provides good decoding performance and can be parallelized on high abstraction C-code level.

V. Parallelization of Channel Decoder

Typically channel decoding of convolutional codes is done via Viterbi algorithm [9], [10] but can also be done by Recurrent Neural Networks (RNN) [11], [12]. The advantage of RNN is the flexible adaptation of algorithm parameters to adjust processing speed, algorithm performance as well as parallelization on high abstract level. Thus RNN channel decoder is a good candidate to fit on multi-processor Software Radio platform.

The encoding of information bit vector $\mathbf{a}$ to code word $\mathbf{c}$ is done by multiplication with generator matrix $\mathbf{G}$.

$$\mathbf{c} = \mathbf{G}^T \cdot \mathbf{a} \tag{1}$$

Interpreting the channel decoding process at the receiver as minimum search procedure, one can

compare the RNN approach with well known Least-Squares approach from adaptive filter theory [12], whereas error e is build from receive matrix $\mathbf{X}$, adaptive filter vector $\mathbf{w}$ and reference signal $\tilde{y}$. Variable n denotes time instances.

$$\min_{\mathbf{w}(n)} \left\| e(n) \right\|_2^2 = \min_{\mathbf{w}(n)} \left\| \mathbf{X}(n)\mathbf{w}(n) - \tilde{y}(n) \right\|_2^2 \tag{2}$$

The corresponding channel decoding problem is based on error $\mathbf{e}$, receive vector $\mathbf{r}$, code word $\mathbf{c}$, generator matrix $\mathbf{G}$ and information bits $\mathbf{a}$.

$$\min_{\mathbf{c}} \left\| \mathbf{e} \right\|_2^2 = \min_{\mathbf{c}} \left\| \mathbf{r} - \mathbf{c} \right\|_2^2 = \min_{\mathbf{a}} \left\| \mathbf{r} - \mathbf{G}^T \mathbf{a} \right\|_2^2 \tag{3}$$

Equation (1) can be modified to

$$c_k^{(j)} = -\prod_{i=1}^{K} \left(- a_{k+1-i} \right)^{g_i^{(j)}} \tag{4}$$

In equation (4) $c_k^{(j)}$ describes the kth coded bit at jth encoder output. The exponent $g_k^{(j)}$ is the ith component of the impulse response from the jth output. With an example of code rate $1/n = 1/2$ and constraint length $K = 3$ the error function can be described as

$$\min_{\mathbf{a}} f(\mathbf{a}) = \min_{\mathbf{a}} \sum_{k=0}^{l-1} \left| r_k^{(1)} + a_k a_{k-2} \right|^2 + \sum_{k=0}^{l-1} \left| r_k^{(2)} + a_k a_{k-1} a_{k-2} \right|^2 \tag{5}$$

Variable l denotes the length of the information bit vector. The characteristic of the error surface depends on the noisy input vector $\mathbf{r}$ and is assumed to be constant. Vector $\mathbf{a}$ needs to be defined by the minimization process in that way that the error-function will be as small as possible. The minimization process can be arranged by gradient approach.

$$grad(f(\mathbf{a})) = \nabla f(\mathbf{a}) \tag{6}$$

Parallelization of the network can be done by starting different decoders in parallel, each with another initialization starting point for the gradient. After all decoder gradients have finalized their iterations, a final selection process evaluates the most probable winner candidate. The setup is shown in Figure 7.

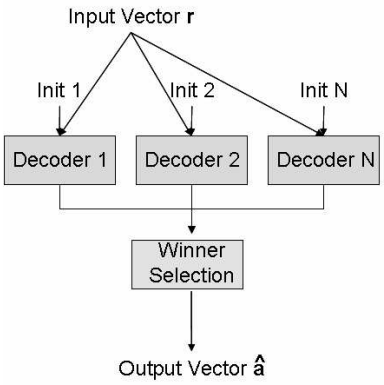

Figure 7 Winner selection from N parallel decoders.

Each of the N parallel channel decoders iterates on the same receiver data set. Thus no data transfer between the neural networks during gradient search process is required and consequently each decoder can be executed on an own processor from the multi-processor Software Radio environment.

Based on that RNN approach the next section presents simulation results to show how well the RNN performance of parallel decoders is compared to traditional Viterbi decoder and direct decision approach.

VI. Simulation Results of Parallel RNN Decoders

First starting point is traditional decoder analysis. Working point of 1e-4 BER is assumed. In Figure 8 Viterbi and direct decision decoders have a significant difference of 6.5dB performance.

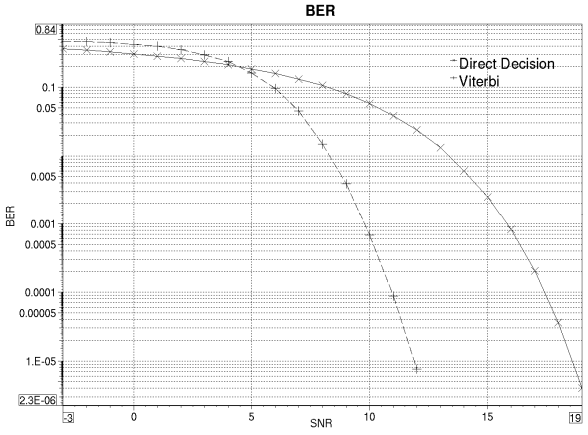

Figure 8 Comparing traditional Viterbi and direct decision decoders.

The huge performance discrepancy is based on significant difference in complexity for both algorithms. Thus employing both algorithms in a receiver design gives not much freedom when trying to

reduce complexity with performance degradation in small steps.

When introducing RNN approach from previous chapter as an alternative to Viterbi decoder, it is important to investigate how much differences in performance appear between Viterbi and RNN solutions.

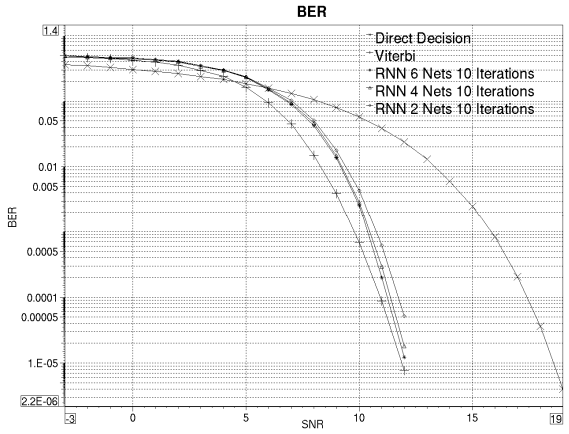

Figure 9 Six, four and two parallel RNNs.

Figure 9 shows three additional RNN decoders running 6, 4 and 2 RNN subnets in parallel, respectively. Each network's gradient makes 10 iterations until it decides the most probable received bit. At working point 1e-4 four parallel RNN subnets (RNN 4) gain 0.35dB over two parallel subnets (RNN 2), six subnets (RNN 6) gain 0.15dB over four subnets (RNN 4). Finally the Viterbi algorithm gains 0.3dB over six subnets (RNN 6). This can be seen in detail from Figure 10.

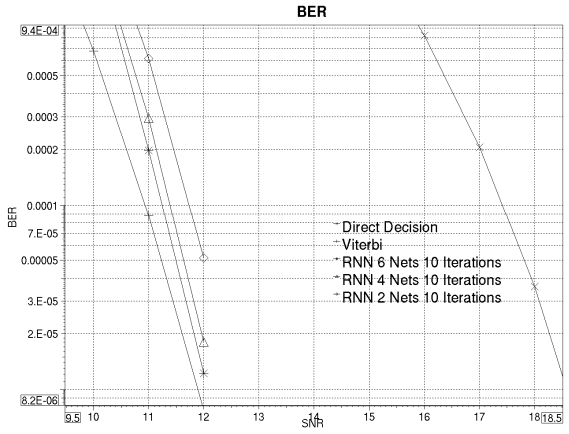

Figure 10 Zooming into working point 1e-04 BER.

Although Viterbi cannot be passed by RNN approach from performance perspective, it is obvious that RNN provides an important alternative for configurable complexity receivers. The RNN setup provides a highly parallel architecture, where any number of networks reaches significant better performance than direct decision decoding.

VII. Conclusion

This paper introduces a novel extension to Cognitive Radio approach by combining optimal channel selection as well as transmit-power control with flexible receiver architecture definition for Software Radio implementation. Balancing between receiver complexity and receiver performance can be achieved in excellent way when employing Recurrent-Neural-Networks for convolutional channel decoding. The RNN architecture can be implemented with parallel subnets, which can nicely fit into a multi-processor Software Radio platform. When reducing the number of RNN subnets and with that the receiver complexity, the radio performance degradation is small compared to direct decision algorithm.

References

[1] Haykin S., Cognitive Radio: Brain-Empowered Wireless Communications, IEEE Journal on Selected Areas in Communications, Vol. 23, No. 2, February 2005

[2] Jondral Friedrich K., Software-Defined Radio—Basics and Evolution to Cognitive Radio, EURASIP Journal on Wireless Communications and Networking 2005:3, 275–283

[3] Haykin S., Huber K., Chen Z., Bayesian sequential state estimation for MIMO wireless communication, Proc. IEEE, vol 92, no. 3, pp439-454, March 2004

[4] Coersmeier E., Bauer A., Kosakowski M., Pfuhl N., Spahl B., Tolksdorf D., Xu Y., Gerharz M., Hansmann W., Leder F., Evaluation Architecture for Digital Radio Mondiale Multimedia Applications, CSA2005, Banff, Canada, July 2005

[5] Coersmeier E., Bauer A., Saez C., Hotz A., Hoffmann M., Kosakowski M., Xu Y., Dynamic Wiener Filter Coefficient Update for Software Radio, Workshop on Software Radio, Karlsruhe, Germany, 2006

[6] Coersmeier E., Bauer A., Saez C., Hotz A., Hoffmann M., Kosakowski M., Xu Y., Improving Channel Estimation for Software Radios, CSA 2006, Banff, Canada, July 2006

[7] Schwoerer L., Moermann K., Benchmarking MIMO OFDM Algorithms on the EVP, GSPx – the 4th International Global Signal Processing Conference, Santa Clara, California, October 2006

[8] Goodacre, J.; Sloss, A.N., Parallelism and the ARM instruction set architecture, IEEE Computer Society, Volume 38, Issue 7, July 2005 Page(s):42 - 50

[9] Viterbi A.J., Error Bounds for Convolutional Codes and an Asymptotically Optimum Decoding Algorithm, IEEE Transactions on Information Technology, 13:260-269, April 1967

[10] Forney G.D., The Viterbi Algorithm, Proc. IEEE, 61: 268-278, March 1973

[11] Hämäläinen A., Henriksson J., Convolutional Decoding Using Recurrent Neural Networks, Procededings of Inter. Joint Conf. on Neural Networks, 5:3323-3327, San Diego, 1999

[12] Hueske K., Reduzierung der Komplexität von Verfahren zur Kanaldecodierung, Diplomarbeit D2-06, University of Dortmund, Feb. 2006

[13] Haykin S., Adaptive Filter Theory, Prentice Hall, Third Edition, 1996

A Study on the Impact of UWB Sensor on the Mobile station of Next Generation mobile System in Korea

Young-Keun Yoon
Radio Resource Research Team, Radio Technology Research Group
Electronics and Telecommunications Research Institute
161 Gajeong-dong,Yuseong-gu, Daejeon, 305-700, KOREA
Tel. +82-42-860-4897
Fax. +82-42-860-5199
Email. ykyoon@etri.re.kr
Heon-Jin Hong
Radio Resource Research Team, Radio Technology Research Group
Electronics and Telecommunications Research Institute
161 Gajeong-dong,Yuseong-gu, Daejeon, 305-700, KOREA
Tel. +82-42-860-4860
Fax. +82-42-860-4860
Email. hjhong@etri.re.kr
Yan-Ming Cheng
Division of information & Communication Engineering Department,
Kongju National University, Korea
Tel. +82-41-850-8620
Fax. +82-41-850-0062
Email. mycheng@kongju.ac.kr
Il-Kyoo Lee
Division of information & Communication Engineering Department,
Kongju National University, Korea
Tel. +82-41-850-8620
Fax. +82-41-850-0062
Email. leeik@kongju.ac.kr

Abstract

This paper presents the impact of Ultra Wide-Band (UWB) sensor using frequency of 4.5 GHz on Next generation mobile system in Korea. The Minimum Coupling Loss (MCL) method and Spectrum Engineering Advanced Monte Carlo Analysis Tool (SEAMCAT) were used to evaluate the interference impacts of UWB sensor on Next generation mobile system. The minimum allowable distance between UWB interferer and the victim receiver is required 0.02 m in indoor environment; in the case of multiple UWB interferers in outdoor environment, the maximum allowable UWB transmitting Power Spectral Density (PSD) should be -81 dBm/MHz below to guarantee co-existence with Next generation mobile system.

I. Introduction

The Ultra Wide-band (UWB) has changed dramatically in very recent history, the importance of

UWB technology has been increased with the advent of communication services including low-cost, high speed and wireless network as well as radar and safety applications. In addition, as the frequency resources become limit, the technology has been highly attracted in order to share the frequencies between UWB systems and other existing services such as mobile communications, satellite communications and broadcasting systems.

As the UWB spreads from DC to several GHz, it is appropriate for short-range communication networks requiring high rate and large capacity of data transmission. The Federal Communications Commission (FCC) defined the UWB system as 20 % above Fractional Bandwidth of center frequency or the system with 500 MHz above RF bandwidth [1].

There are two main potential UWB applications areas: communication systems and non-communication systems. Communication systems include indoor, outdoor and hand-held communication systems; non-communications systems include ground penetrating radar systems, medical imaging systems, wall imaging systems, through-wall imaging systems, vehicular radar systems and surveillance systems [2].

Although Multiband Orthogonal Frequency Division Multiplexing (MB-OFDM) and Direct Sequence-CDMA (DS-CDMA) have been discussed actively in IEEE because they have advantages of implementation feasibility and flexible frequency bandwidth [3], and also, spectrum masks proposed by FCC for all kinds of UWB systems, the potential interference due to the very large bandwidth occupied by the UWB signal have to be reevaluated for the successful operation of the existing and coming systems.

Recently, UWB sensor has been proposed in Korea. The spectral emission power of UWB sensor is summarized in Table 1. However, the UWB sensor will have impact on the next generation mobile system. In this paper, the impact of UWB sensor on Next generation mobile system is analyzed through Minimum Coupling Loss (MCL) method [4] and Spectrum Engineering Advanced Monte Carlo Analysis Tool (SEAMCAT) [5].

Generally the MCL is calculated and then converted to an interference distance using an appropriate propagation model. MCL between interfering transmitter (It) and a victim receiver (Vr) is defined as follow [6]:

MCL = It power (dBm/Ref.BW) +It antenna gain (dBi) +Vr antenna gain (dBi) -Vr interference threshold (dBm/Ref.BW)

In case of calculating minimum separation distance (Dmin): MCL=Propagation model (Dmin) [7], and then, using Free-space path loss equation [8]:

$$Lp=20\log10(F)+20\log10(D)-27.5$$

Where:
Lp = free-space propagation path loss, in dB;
F = frequency, in MHz;
D = propagation path length, in meters.

SEAMCAT is a new statistical simulation model has been developed based on the Monte-Carlo method,. This model and its supporting software implementation allow quick yet reliable consideration of spatial and temporal distributions of the received signals and the resulting statistical probability of interference in a wide variety of scenarios. It therefore enables more precise mutual positioning of those considered systems, hence more efficient use of the radio spectrum [5].

The simulation results showed the minimum allowable distance between UWB sensor and Next generation mobile system and also, the allowable transmitting power spectral density (PSD) of UWB sensor for the compatibility.

Table1. Spectral emission power level of UWB sensor in Korea

Frequency band	Indoor UWB sensor	Outdoor UWB sensor
	EIRP (dBm)	EIRP (dBm)
824MHz~849MHz	-81.2	-81.0
849MHz~894MHz	-81.2	-81.0
1.75GHz~1.78GHz	-85.7	-85.3
1.84GHz~1.87GHz	-85.6	-85.1
1.85GHz~1.91GHz	-84.8	-85.1
1.93GHz~1.99GHz	-85.6	-85.5
2.11GHz~2.17GHz	-85.9	-85.7
2.3GHz~2.4GHz	-86.4	-86.4
2.4GHz~2.5GHz	-86.2	-86.0
2.6GHz~2.7GHz	-86.8	-86.6
0GHz~1GHz	-77.7	-77.6
1GHz~2GHz	-82.9	-84.0
2GHz~3GHz	-86.0	-86.0
3GHz~4GHz	-87.2	-86.9
4GHz~5GHz	-87.2	-68.5
5GHz~6GHz	-85.4	-82.7
6GHz~7GHz	-84.8	-84.9
7GHz~8GHz	-84.9	-84.9
8GHz~9GHz	-65.6	-76.4
9GHz~10GHz	-69.8	-76.5
10GHz~11GHz	-76.6	-76.4
11GHz~12GHz	-76.4	-76.2

II. Analysis on the Impact of Single UWB Sensor on the Mobile Station of Next Generation Mobile System in Indoor Environment Using MCL Method

The impact of single UWB sensor on mobile station of Next generation mobile system was analyzed in terms of MCL method. The system parameters for MCL method and analysis scenario for worst case were considered. The minimum allowable distance between interferer and victim system was obtained.

The scenario for the interference analysis was established as follows, Service environment: Indoor environment, Victim system: Next generation mobile system, Interferer: Single UWB sensor, UWB sensor transmitting PSD: -87.2 dBm/MHz @4.5 GHz provided by Korea in indoor, In Bands: 4~5 GHz, Reference Bandwidth: 1 MHz.

The specifications of Next generation mobile system were defined as follows. Operating frequency: 4500 MHz, Channel bandwidth: 10 MHz, Noise Figure: 8 dB, Noise Floor: -96 dBm, Antenna characteristic: Omni directional Antenna, Path loss model: free space path loss.

When the Interference criteria which is the ratio of Interference over Noise Floor(I/N) was defined as –6 dB by considering worst case scenario[9], the minimum allowable distance is obtained as 0.14 m through using MCL method in Table 2.

Table2. Calculating the minimum allowable distance using systems parameters and MCL method

Parameter	Value	Units	Equation
Frequency	4500	MHz	F
Thermal noise density	-174	dBm/Hz	KT
Reference bandwidth	1	MHz	Bref
Victim bandwidth	10	MHz	B
Victim noise figure	8	dB	NF
Noise floor	-96	dBm	N = KT + B + NF
Interference criteria	-6	dB	I/Nth
Allowed interference level in victim bandwidth	-102	dBm	I = N- [I/Nth]

UWB EIRP In 10 MHz	-77.2	dBm	P=-87.2+ 10log(10)
Victim receiver antenna gain	0	dBi	GR
Victim receiver line loss	2	dB	LR
Path loss required	22.8	dB	Lp= P +GR-LR-I
Minimum allowable distance	0.14	m	20 log(D)=Lp - 20 log(F) + 27.5

III. Analysis on the Impacts of multiple UWB Sensors on the Mobile Station of Next Generation Mobile System in Outdoor Environment Using SEAMCAT

The SEAMCAT was used for the analysis of the impact of multiple UWB sensors on mobile station of Next generation mobile system in Outdoor environment. The maximum allowable UWB transmitting PSD was considered so as to keep minimum interference probability so much as no occurring in mobile station of Next generation mobile system.

The analysis scenario was assumed as follows Figure 1, Service environment: Outdoor environment, Interfering system: Multiple UWB Sensors, Interfering transmitter (It) is UWB Sensor, UWB sensor transmitting PSD: - 68.5 dBm/MHz@4.5 GHz provided by Korea in outdoor. In Bands: 4~5 GHz; the sensing distance is within 40 m of UWB , the space between sensors is 40 m, the fixing height on fence pillar is 2.2 m, the beam width : Horizontal is 150°, perpendicular is 35°. The number of active transmitters is 25. Unwanted emission power level of UWB senor for SEAMCAT simulation is summarized in Table 3. And then the unwanted emission mask of UWB sensor is shown as in Figure 2. Main parameters of UWB sensor were summarized in Table 4.

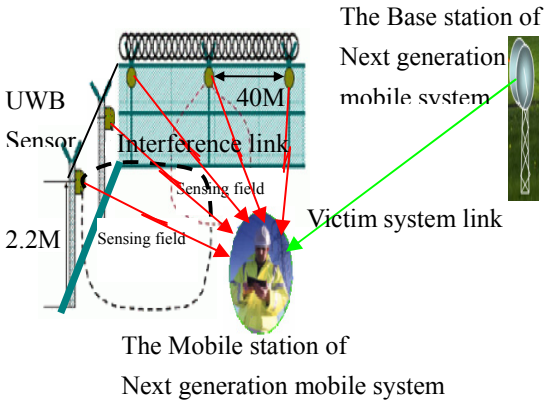

Figure1. Multiple UWB sensors and Next generation mobile system

Table3. Unwanted emission power level of UWB sensor in SEAMCAT

Frequency offset (MHz)	-68.5 dBm/MHz UWB Power	Attenuation in dBc in SEAMCAT
-4500~ -3500	-77.6	-9.1
-3500~ -2500	-84.0	-15.5
-2500~ -1500	-86.0	-17.5
-1500~ -500	-86.9	-18.4
-500~ 500	-68.5	0
500~ 1500	-82.7	-14.2
1500~ 2500	-84.9	-16.4
2500~ 3500	-84.9	-16.4
3500~ 4500	-76.4	-7.9
4500~ 5500	-76.5	-8

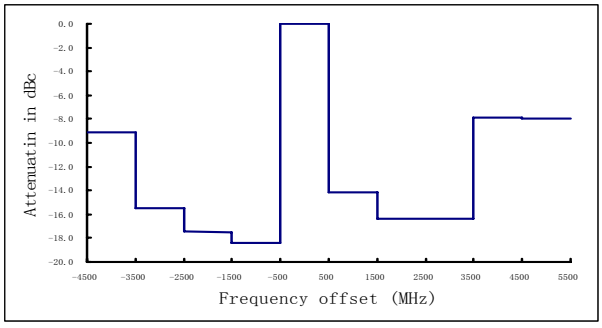

Figure2. Unwanted emissions mask of UWB sensor

Table4. Main parameters of UWB sensor

Parameter	Value	Units
Frequency	4500	MHz
UWB EIRP (Korea limit Outdoor)	-68.5	dBm/MHz
Transceiver Antenna Height	2.2	m
Antenna Gain	0	dBi
Sensing distance	40	m
Simulation radius	0.6	km
Number of active transmitters	25	
It->Vr propagation model	Free space (considering the worst case)	

Victim system: Next generation mobile system, Victim receiver (Vr) is the Mobile station (MS) of Next generation mobile system, Wanted transmitter (Wt) is the Base station (BS) of Next generation mobile system system; System parameters for Next generation mobile system were taken as follows. Operating frequency: 4500 MHz, channel Bandwidth: 10 MHz, Noise Figure: 8 dB, Noise Floor: -96 dBm, Antenna height: 15 m for base station and 1.5 m for mobile station, I/N of -6 dB is chosen as interference criteria considering the worst condition, propagation model; Free space considering the worst scenario. Main parameters of Next generation mobile system were summarized in Table 5.

Table5. Main parameters of Next generation mobile system

Parameter	Value	Units	Equation
Frequency	4500	MHz	F
Thermal noise density	-174	dBm/Hz	KT
Reference bandwidth	1	MHz	Bref
Victim bandwidth	10	MHz	B
Victim noise figure	8	dB	NF
Interference criteria	-6	dB	I/Nth
Noise floor	-96	dBm	N = KT + B + NF
SNR (QPSK 1/2)	9.4	dB	SNR
Victim receiver (Vr)Sensitivity	-86.6	dBm	RS=KT+B+NF +SNR
Victim receiver antenna gain	0	dBi	GR
Victim receiver line loss	2	dB	LR
Wanted transmitter (Wt) power	30	dBm	P_{Wt}
Wanted transmitter gain	10	dBi	GT
Path loss required	124.6	dB	Lp= P_{Wt} +GR+ GT -LR-RS
Wt->Vr Coverage radius	9	km	20lg(D)=LP-20lg(F)+27.5
Base station height	15	m	
Mobile station height	1.5	m	
Wt->Vr propagation model	Free space		

After setting up scenario with above parameters of UWB sensor and Next generation mobile system, the simulation has been done with the SEAMCAT [5]-[10]. For obtaining interference probability, first step is to select interference calculation parameters as following:

Calculation mode: Translation, Signal Type: Unwanted, Interference criterion: I/N, Algorithm: Quick, Samples: 50000, Translation parameter: Power supplied/Interfering link 1.

Second step is to start calculating, and then referring to SEAMCAT report, the interference probability Vs UWB sensor transmitter power supplied are obtained in Figure 3.

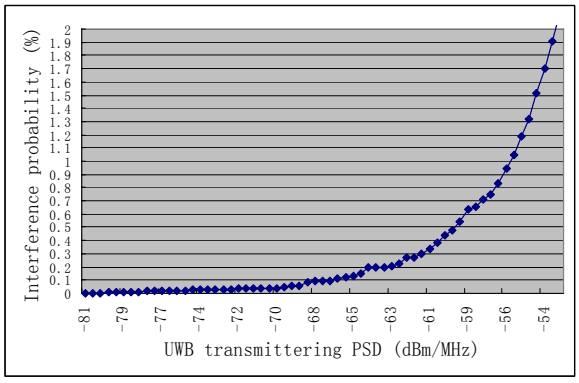

Figure3. Interference probability Vs transmitter power supplied

According to Figure 3, when UWB transmitting PSD=-68.5 dBm/MHz (Korea limit outdoor), the interference probability is 0.04%.

If interference probability of zero is required, the UWB transmitting PSD should be -80 dBm/MHz below.

IV. Conclusions

The impacts of single and multiple UWB sensors on Next generation mobile system were analyzed through MCL method and SEAMCAT.

As a result, when I/N of –6 dB is chosen as protection criteria, the required minimum allowable distance should be around 0.14 m when UWB transmitting PSD is -87.2 dBm/MHz (Korea limit indoor) in the case of single interferer in indoor environment. For multiple interferers case in outdoor environment, UWB transmitting PSD of around –80 dBm/MHz below should be required to avoid the interference probability occurring in mobile station of Next generation mobile system.

References

[1] Revision of Part 15 of the Commission's Rules Regarding Ultra-Wideband Transmission Systems: FCC 02-48 First Report and Order(R&O), FCC, Feb. 2002.

[2] Paul Hansell CEng FIEE, Dr Selcuk Kirtay AMIEE, Aegis Systems Ltd, "Ultra Wide Band (UWB) compatibility, Final Report to the Radio communications Agency" 1405/AE/UWB/R/2, 30th January 2002.

[3] M. Ghavami, L.B. Michael and R. Kohno, "Ultra Wideband Signals and Systems in Communication Engineering", John Wiely & Sons, 2004.

[4] "Methodologies for impact analysis of systems using UWB technology with systems operating under Radiocommunication Services" in "Ultra-wideband, Report of the Fifth Meeting of ITU-R Task Group 1/8", San Diego, 18-27 May 2005.

[5] "SEAMCAT SoftwareVersion2.1 User Manual", European Radiocommunications Office, 23 February 2004.

[6] Task Group 1 of the European Radio communications Committee, ERC REPORT [TG1/02], "adjacent band compatibility between UWMTS AND other services in the 2GHz band" Output from Edinburgh, 22-24 February 1999.

[7] Electronic Communications Committee (ECC) within the European Conference of Postal and Telecommunications Administrations (CEPT), "Share and adjacent band compatibility between UMTS/ IMT - 2000 in the band 2500-2690 MHz and other services", Granada, February 2004.

[8] Task Group 1/8, Document 1/88-E, Draft NEW

RECOMMENDATION ITU-R SM. [UWB.COMP], "Impact of devices using ultra-wideband technology on systems operating within radiocommunication services", 21 October 2005.
[9] 1-8/347(Annex 2)-E in "Ultra-wideband, Report of the Fifth Meeting of ITU-R Task Group 1/8", San Diego, 18-27 May 2005.
[10] Karl low, T-Nova, Deutsche Telekom, SEAMCAT Training (phase 1), "Analysis on Tetra MS interferes the BS of the analogue FM PMR using SEAMCAT", ERO, Copenhagen, 7-June-2001.

"This research was supported by University IT Research Center Project (INHA UWB-ITRC), Korea."

Standards Development for Wireless Communications for Urban Search and Rescue Robots*

Kate A. Remley [1], Galen Koepke, Elena Messina, Adam Jacoff
National Institute of Standards and Technology
1. Corresponding author: ph. (303) 497 3652, email: remley@boulder.nist.gov
and
George Hough, Lieutenant
New York City Fire Department (FDNY),
Urban Search and Rescue (US&R) NY-TF1

In order to gather data in support of standards development for urban search and rescue robots, NIST is conducting a series of field tests to quantify the functionality and performance of various candidate robots. During these tests, manufacturers bring robots that may be appropriate for various urban search and rescue applications, and emergency responders put the robots through NIST-derived tests designed to measure their performance in key areas. During a set of field tests at the Montgomery County Fire Academy in Maryland in August 2006, members of the Electromagnetics Division and Intelligent Systems Division of NIST developed and carried out a uniform series of spectral analysis tests on each of the robots that participated in the event. We report here on results of this initial set of field tests of the wireless link.

1. Introduction

Robots have been employed with great success in a wide variety of settings where precise, repetitive, or dangerous tasks need to be carried out. For example, they are commonly found in heavy manufacturing facilities on the production floor where they weld, assemble, and even deliver parts.

A relatively new use of robots is in the urban search and rescue (US&R) environment. The majority of robots utilized in dangerous environments such as explosive ordinance disposal and search and rescue may be considered as extensions of one's eyes, ears, nose, and hands. In this manner, robots have the potential to provide enormous utility for responders that perform vital search and rescue missions at sites of disasters. Robotic sensing devices can access dangerous areas more efficiently in many instances, and can provide information on trapped or missing people while minimizing the danger to which responders expose themselves at such events.

Robots for the foreseeable future will be controlled either with a physical tether wire or a wireless communications link. In most US&R applications, a wireless link is preferable since it offers the robot increased range and flexibility in navigation. However, as we discuss below, the wireless link may be subject to interference and/or signal loss, either of which can degrade reliable performance of US&R robots. We report here on results of initial field tests of the wireless link during an exercise designed to promote standards development for US&R robots.

2. Performance-Based Standards Development

The nature of emergency response is one that covers a wide variety of potential scenarios – from building collapses, to earthquakes, to terrorist employment of weapons of mass destruction. Equally daunting are the diverse variety of technologies that need to work in unison in order for a robot to work properly. When looked at concurrently, one can imagine the potential difficulty in creating a set of well-understood performance goals and means of measuring whether systems actually meet them. Presently, no standards or performance metrics exist [1].

In order to address this need, the Department of Homeland Security (DHS) Science and Technology (S&T) Directorate initiated an effort in fiscal year 2004 with NIST to develop comprehensive standards to support development, testing, and certification of effective robotic technologies for US&R applications. From their initial efforts, the NIST/US&R Responder consortium was able to define over 100 initial performance requirements, and generate 13 deployment categories. The performance requirements were grouped into categories such as human-system interaction, mobility, logistics, sensing, power, and communications. For each requirement, the responders defined how they would measure performance [2].

In the area of communications, the performance requirements specified by the responders included

(1) Expandable Bandwidth: *Will support additional operational components without loss of data transmission rate sufficient to allow each component to perform its function.*

(2) Range—Beyond Line of Sight: *Must be able to ingress specified number of feet in worst-case collapse. Worst case is a reinforced steel structure.*
(3) Security: *System must be shielded from jamming interference and encrypted.*
(4) Range—Line of Sight *[no notes]*
(5) Data Logging—Status and Notes: *Ability to pick up and leave notes.*

Items (2) and (4) were designated as critical in the initial standards development effort, scheduled for preliminary draft by the end of the calendar year 2006. These items depend on the technical specifications of the robot's radio link, as well as the radio environment in which the robots are deployed.

By assisting in the process of creating such standards, DHS seeks to provide guidance to local, state, and federal homeland security organizations regarding the purchase, deployment, and use of robotic systems for US&R applications.

NIST has since organized the standards effort through American Society for Testing and Materials (ASTM) E54.08 – Homeland Security Standards. In this effort, industry representatives and US&R responders have endeavored to slice the problem into manageable categories. The head of each working group is responsible for producing his or her standard test method that objectively measures a robot's performance in a particular area. Ultimately, the response organization will be able to determine which robots best suit their requirements. Robot researchers and manufacturers will benefit from the definition of test methods and operational criteria, enabling them to provide innovative solutions to meet the universal requirements.

3. Performance testing in representative radio environment

One key step in this performance-based standards creation process has entailed testing robots utilizing specially designed test-beds; i.e., standardized obstacle courses. In these tests, commercially available robots have been put through a series of real US&R training scenarios with responders operating the robots. Tests have been carried out at facilities in Nevada, Texas, and Maryland. During the testing done in Texas and Maryland, wireless communications were sometimes found to be problematic when several robots attempted to communicate simultaneously. At the last event, in August 2006 at the Montgomery County Fire Academy in Maryland, members of the Electromagnetics Division of NIST developed and

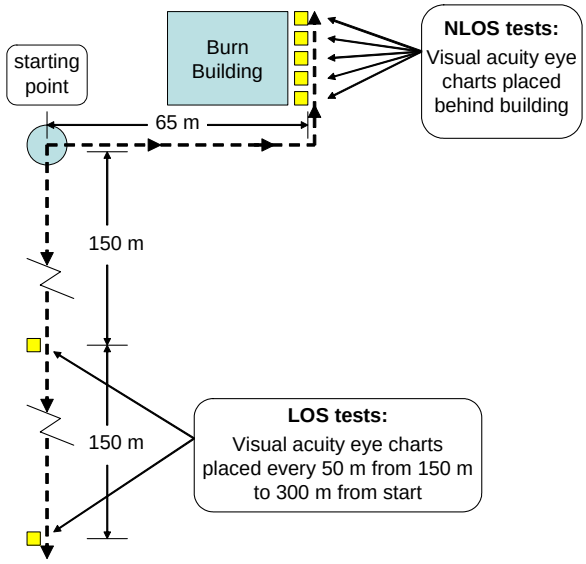

Figure 1: Diagram of the Montgomery County Fire Rescue Academy tests for wireless communications showing the communications LOS and NLOS tests.

carried out a uniform series of spectral analysis tests on each of the robots that participated in the event.

3.1 Wireless communications test logistics: During the Montgomery County tests, we gathered a substantial amount of data on the technical specifications of various US&R robots and on the typical radio-interference environment when several robots were deployed simultaneously. In both line-of-sight (LOS) and non-line-of-sight (NLOS) tests the operator and a NIST engineer were stationed in a fixed location (see the dot labeled "starting point" in Figure 1) while the robot moved away.

In the LOS test, the robot moved away from the operator down a long driveway as shown in Figs. 1 and 2. Markers that included visual acuity eye charts were placed every 50 m between 150 m and 300 m from the starting point. Control of the robot was monitored continuously, while video data transfer from the robot was checked at each marker.

For the NLOS tests, the robot moved about 65 m away from the operator in an LOS condition, then turned the corner behind a five-story building, which provided the NLOS condition. See Figs. 1 and 3(a). Markers were placed every three meters behind the building, as shown in Figs. 1 and 3(b), to test whether and when the robot lost data and control capabilities.

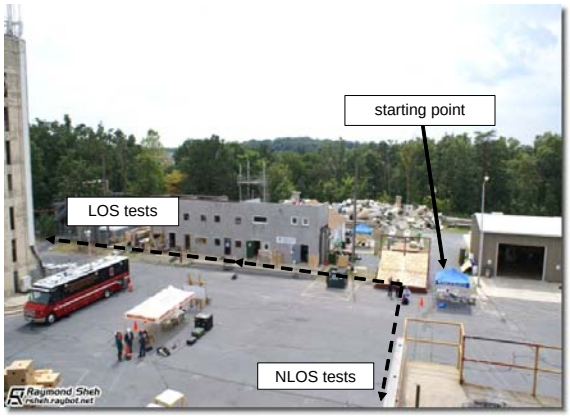

Figure 2: Location of the wireless communication tests. For the LOS tests, robots start at the blue tent shown by the arrow, and proceed down a long driveway to the left. For the NLOS tests, robots leave the tent and proceed down a path perpendicular to the first one, to the rear of a tall building. Photo courtesy of Raymond Sheh.

3.2 Physical environment: The environment was relatively open with only a few large structures in the area. One was a five-story tall concrete building known as the "burn building" (shown in Fig. 3(a)), where our NLOS tests were carried out. The ground was covered with a concrete or asphalt surface throughout the test area.

3.3 Radio interference environment: As can be seen in the data below, most of the robots operate in the "industrial, scientific, and medical," or "ISM" frequency bands. There is no regulation for licensing or frequency coordination in these frequency bands; thus, the spectrum is readily available for use in commercial applications. While protocols that minimize interference between systems in these bands were often used by the robot designers, when the ISM frequency bands get crowded or when one user has a much higher output power than the others, interference can occur—even on frequencies quite removed from the robot under test. We saw cases where transmitters in the 1760 MHz band knocked out video links in the 2.4 GHz frequency band.

4. Test results

We collected several types of data relevant to understanding the wireless environment and characterizing robot performance including

- frequency of operation
- type of data transmitted (i.e., video or control)
- output power level
- hardware placement for items such as antennas

(a)

(b)

Figure 3: For the NLOS tests, the robots moved away from their operators (a) along the right side of the burn building then (b) around the back side of the building. At each orange cone, the robot stopped and attempted to send data from an eye chart back to the operator. Photos courtesy of Raymond Sheh.

- radio-interference environment
- physical environment

These data are summarized in Table 1. Several of these items may interact with and influence the performance of others. As a result, we saw a range of success in transmissions for the various robots deployed in the tests, depending on their set-ups and which robots were nearby.

In particular, the radio interference environment had a significant effect on the robots' ability to successfully complete the tests. Several of the robots used similar frequency bands and wireless access schemes, such as

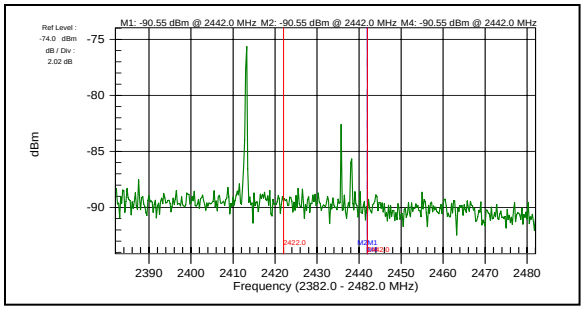

(a)

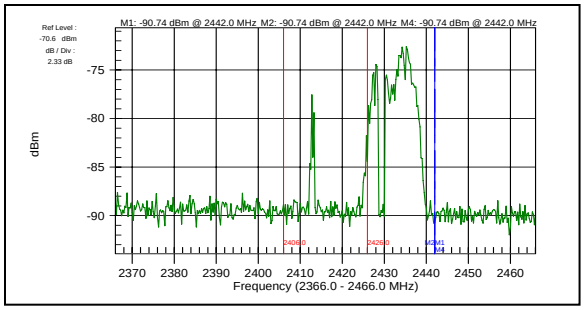

(b)

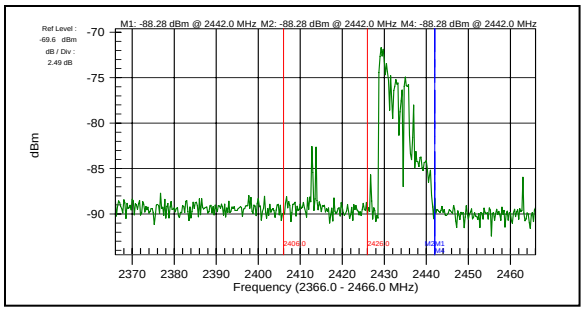

(c)

Figure 4: Example of radio interference on an analog video link transmitting at 2.414 GHz from a nearby robot. In (a) the 2.414 GHz robot is approximately 65 m away from the operator and the signal level is high enough for good reception. In (b), the robot is 100 m away and its video signal becomes choppy. In (c) at just under 150 m separation between robot and operator, the 2.414 GHz signal level becomes significantly weaker than a neighboring 802.11b signal, and the video link is broken.

802.11b. Robots utilizing higher power levels often overwhelmed those with lower power levels. An example of this is shown in Fig. 4 for a robot that utilized an analog video link centered at 2.414 GHz. As the robot moved away from the operator, its signal became weaker than those from nearby robots. After a separation of just under 150 m, the link was lost, even though the robot was using an analog modulation scheme that is normally quite robust in weak-signal conditions. Interference—both in-band and out-of-band—was the most significant impediment to radio communication success and had a negative impact on 10 out of the 14 robots we tested.

The issue of radio interference clearly needs to be addressed because it degrades the reliability of US&R robot performance in situations such as those where multiple robots using the same frequency bands are deployed. Interference from nearby robots during field tests may also impact our ability to develop meaningful standards for radio communications.

5. Improving wireless communications for US&R robots

A wide range of options exist for mitigating the interference results experienced during this initial set of radio tests. Some are currently being investigated by robot manufacturers. Some of these options include

5.1 Frequency coordination: In this scenario, robots are assigned specific control and telemetry frequency bands. Frequency coordination would be relatively straightforward for narrowband control and telemetry channels because they may fall into the existing licensed land mobile radio channels already utilized by emergency responders.

It would be difficult to assign frequencies for US&R robot use in the ISM bands since these bands are unlicensed and open to noncommercial users. However, use of the new 4.95 GHz spectrum allocated for licensed public safety use may enable transmission of broadband data such as video in US&R robot applications.

5.2 Transmission protocols: Several modulation formats and access schemes have been developed to mitigate interference from collocated wireless systems. Already mentioned are the 802.11 protocols that utilize encoding and error correction to minimize interference. Systems with even more robust error correction such as 802.16 will be available in the near future [3].

Another option for minimizing interference to broadband data that would normally be transmitted in the ISM bands would be to reformat them into narrowband data and send them over existing licensed frequency bands. For example, sending still photographs instead of streaming video would drastically reduce the bandwidth needed and may enable use of licensed bands with frequency coordination.

5.3 Output Power: Increasing the radiated output power level is one method of increasing the potential for maintaining a wireless link. However with this option there is also the potential for increased interference to other systems and, at high output power levels, a potential

health risk for human exposure. The U.S. Federal Communications Commission (FCC) specifies safe limits of human exposure to radio-frequency energy and these are reflected in legal output power levels. A higher output power level also correspondingly decreases battery life, a particular problem for US&R robots, which are battery powered.

5.4 Priority access: Priority access protocols could be adopted that would ensure coordination of assets such as US&R robots. This coordination would need to take place among public safety agencies, and also between all response agencies and commercial enterprises that may share a given band of spectrum. One approach would be to create hardware and software that would sense users in a particular area and grant priority access to public safety agencies during times of emergency. Because of the large amount of equipment already in use in the ISM band, the 4.95 GHz and potentially new public-safety frequencies in the 700 MHz spectrum may be the best candidates for this approach. These bands have sufficient bandwidth, and standards and hardware are still being determined at this time.

5.5 Multi-hop Communications

One strategy for increasing the range of wireless systems such as US&R robots is with multi-hop communications employing relay transceivers that receive, amplify, and retransmit a signal. Digital repeaters are currently being used in a variety of applications by military and industry. However, research is underway to use deployed robots or first responder radios as repeaters in multi-hop systems.

6. Summary

Emergency responders may one day be able to leverage the use of robots for US&R missions. However, to efficiently deploy robot technology, a set of performance-based standards and associated test methods need to be developed. NIST, through the Department of Homeland Security, is working to develop standards that will ensure secure and robust wireless communications.

While standards and test methods specify a minimum level of radio performance for US&R robots, for successful communications a many-faceted approach may need to be taken. Part of the answer may come in the form of technological advancement, such as new access schemes or software-defined radios that allow interoperable communication schemes for the different entities that seek to utilize them. Part of the answer may also come from coordination of access among civilian and public safety in a particular frequency band, and also among public safety agencies as the gravity of an incident escalates.

Through continued participation in the standards development process, US&R and public safety agencies can help ensure that the needs of their communities are heard and incorporated into the standards development process.

Acknowledgement

This work was funded in part by the Department of Homeland Security Science and Technology Directorate through the NIST Office of Law Enforcement Standards.

References

[1] Elena Messina, “Performance Standards for Urban Search and Rescue Robots,” *ASTM Standardization News*, August 2006, http://www.astm.org/cgi-bin/SoftCart.exe/SNEWS/AUGUST_2006/messina_aug06.html .

[2] National Institute of Standards and Technology, “Statement of Requirements for Urban Search and Rescue Robot Performance Standards-Preliminary Report” http://www.isd.mel.nist.gov/US&R_Robot_Standards/Requirements%20Report%20(prelim).pdf .

[3] TIA Roadmap 2006.

Table 1: Summary of Data Collected August 19-20 at the Montgomery County Fire Rescue Training Academy

Robot	Video (MHz)	Control (MHz)	Output Power (W)	Success	Failure Due to Interference	Issues with Interference
1	2400	900	0.5	--	NLOS	yes
2	2432	2432	0.2	LOS, NLOS	--	no
3	2437	2437	0.2	LOS, NLOS	--	no
4	2414	2414	?	--	LOS, NLOS	yes
5	2400 (analog)	900	?	--	LOS, NLOS	yes
6	2400	2400	1	LOS, NLOS	--	yes
7	1760	900	1 control, 2, video	LOS, NLOS	--	no
8	1756	900	?	--	LOS, NLOS	yes
9	2400	35	0.1?	--	LOS, NLOS	yes
10	1400	35	0.1?	LOS, NLOS	--	no
11	5200	5200	?	NLOS	--	yes
12	2400	2400	?	LOS, NLOS	LOS, NLOS	yes
13	2400	?	0.1	--	LOS, NLOS	yes
14	2400	2400	?	LOS	NLOS	yes
15	900	75	?	--	--	--

Spectrum Sharing and Potential Interference to Radars

Brent Bedford and Frank Sanders
NTIA Institute for Telecommunication Sciences, Boulder, CO USA

Voice: +1-303-497-5288/7600; fax: +1-303-497-3680
bbedford@its.bldrdoc.gov, fsanders@its.bldrdoc.gov

This paper describes the results of interference tests and measurements that have been performed on a wide variety of radar receivers. Radar target losses have been measured under controlled conditions in the presence of radio frequency (RF) interference. Radar types that have been examined include short range and long range air traffic control; weather surveillance; and maritime navigation and surface search. Radar receivers experience loss of desired targets when interference from high duty cycle (more than about 1-3%) communication-type signals is as low as -10 dB to -6 dB relative to radar receiver inherent noise levels. Conversely, radars perform robustly in the presence of low duty cycle (less than 1-3%) signals such as those emitted by other radars. Target losses at low levels are insidious because they do not cause overt indications such as strobes on displays. Therefore operators are usually unaware that they are losing targets due to low-level interference. Interference can cause the loss of targets at any range. Low interference thresholds for communication-type signals, insidious behavior of target losses, and potential loss of targets at any range all combine to make low-level interference to radar receivers a very serious problem. The results indicate that radar receivers are potentially very vulnerable to interference from communication signals if such systems share spectrum with radars.

1. Introduction

Radars play critical roles in national security, air traffic control, weather observation and warning, scientific applications, mapping, search and rescue operations, and other safety-of-life missions. Radar transmitter and receiver characteristics are engineered to successfully accomplish their missions in these areas. The technical characteristics of radars (such as high peak power levels emitted by the transmitters and very sensitive designs for the receivers) have usually resulted in exclusive, or at least primary, spectrum allocations for their operations.

In recent years, spectrum crowding has led to proposals for reduction of available spectrum for exclusive or primary radar operations, as well as for co-channel (or nearly co-channel) spectrum sharing between radars and non-radar radio signals. It has been proposed in various forums, for example, that communication signals can (and should) sometimes share spectrum bands with radar systems. Such proposals typically presume that radar receivers will not suffer undue loss of technical performance due to such sharing so long as the interference levels are relatively low. Some sharing analyses assume that radar receivers are relatively robust against radio frequency (RF) interference effects from low levels of non-radar signals.

These proposals raise critical technical questions. These include: At what power levels do interfering signals cause adverse effects on the performance of these receivers? How are interference effects manifested in these radar receivers? Specifically, what are the interference levels at which radar receivers lose desired targets, and do low-level interference effects create observable manifestations on radar receiver displays?

NTIA, in cooperation with other US Government agencies and the United Kingdom (UK)[1], has performed a series of tests and measurements of the response of microwave radars to low levels of RF interference from a variety of communication and non-communication signals. This paper describes the results of interference tests and measurements on several representative radar receivers. Interference data have been collected on radars performing various missions in several different spectrum bands. Radar types that have been examined include short range air traffic control; long range air traffic control; fixed weather surveillance; airborne weather surveillance; and maritime navigation and surface search. These radars have been operational in the spectrum bands 1200-1400 MHz; 2700-2900 MHz; 2900-3700 MHz; and 8500-10500 MHz.

[1] Including the National Oceanic and Atmospheric Administration (NOAA), U.S. Coast Guard (USCG), Federal Aviation Administration (FAA), and the United Kingdom's (UK) Fraser Test Range at Portsmouth.

2. Limiting Factors in Radar Performance

Microwave radar receiver performance is limited by internal receiver noise and external clutter. Figure 1 shows an example of clutter on a radar display.

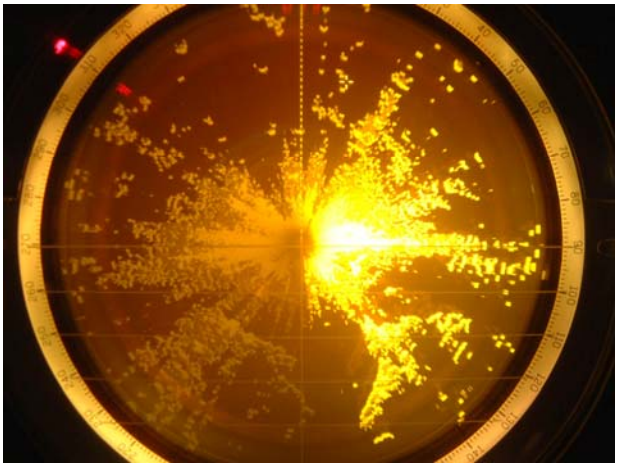

Figure 1. An example of clutter on a 9-GHz maritime radionavigation radar display. The clutter includes local buildings, terrain, and vegetation. No intentional interference or test targets are present on this display.

Radars often detect target echoes that are at a lower power level than the receiver noise floor. Radio interference sources that raise the radar noise floor will degrade overall radar performance and exacerbate existing degradation from such factors as clutter.

3. Radar Interference Rejection (IR) Capabilities

Some radars incorporate interference rejection (IR) features. IR circuits work on the principle of pulse-to-pulse correlation so as to accept echo energy from targets that have been exposed to a radar's transmitted pulses, and to reject pulsed energy from other sources, as shown in Figure 2. An example of a radar screen with and without activation of the IR feature is shown in Figure 3.

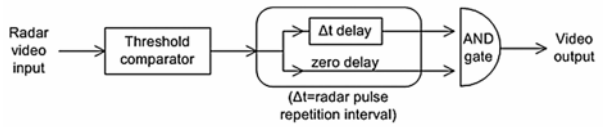

Figure 2. Example of a radar IR circuit.

IR circuits are somewhat effective against pulsed interference but not against high duty cycle interference. Use of IR comes at a cost: some desired targets are lost when IR is used.

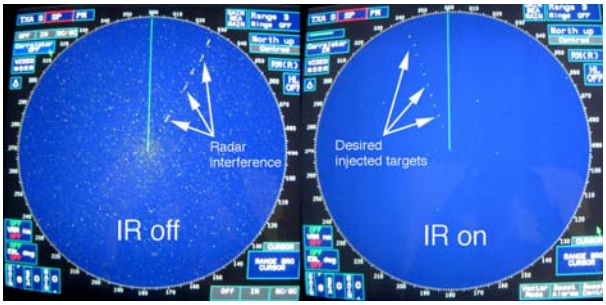

Figure 3. A radar display without IR (left) and with IR activated (right), demonstrating effectiveness of IR against some types of pulsed interference.

4. Other Radar Receiver Mitigation Techniques

There are additional radar processing techniques that improve radar performanc. Two of the most important are instantaneous automatic gain control (AGC) and constant false alarm rate (CFAR). AGC works through a negative-feedback loop between the IF amplifier output and the gain control of that circuit. The time constant of the AGC is set to a long interval, so that extended clutter effects are reduced, while the short-response time responses due to echoes from discrete targets are not affected. AGC is commonly implemented in some aircraft-tracking radars. AGC causes reduction in receiver sensitivity in the presence of strong signals and thus mitigates radar display overload, but it also decreases the probability of detection of undesired targets. It is therefore not an interference mitigation technique.

CFAR is a technology that helps to distinguish targets from noise and clutter on radar displays. It is an optional feature for many simple, analog radars, but its implementation is often essential for digitally processed radar signals. The reason for the discrepancy is the intelligence that human operators bring to the problem of interpreting radar displays, versus the inherent limitations of digital processing algorithms relative to human intelligence. Human operators can become skilful at distinguishing true targets from noise and clutter artifacts on such displays, and if too many false targets (false alarms) are occurring, then the operator can reduce the gain setting of the—in effect providing an approximation of automatic CFAR.

But in automated detection and tracking systems, where the design goal is to automatically designate targets and display them, the processing algorithm can be overwhelmed by too many false targets. (A change of only 1–dB in the threshold-to-noise or threshold-to-clutter ratio can change the false alarm rate by 2 orders of magnitude. Thus an automatically adaptive CFAR technique is therefore essential for such radars.

In a typical CFAR, a test cell is designated. Around that cell, a group of delay lines are used to estimate the average level of noise or clutter. The tap outputs (usually 16 to 20) are summed, the sum is multiplied by an appropriate constant, and the result is used to set the detection threshold for the test cell. The output of the test cell is the radar output. Additional variations of CFAR exist.

CFAR processing has a number of drawbacks. It causes losses relative to optimum detection, and the number of pulses that are required for processing must be large to minimize this loss. CFAR inevitably reduces the overall probability of detection of desired targets, and thus will cause some targets to be lost. These losses can be insidious because operators will often be unaware that CFAR-controlled detection thresholds are gradually creeping upward as noise, clutter, or interference increase in some environment.

CFAR processing is a necessary evil. It suppresses clutter and noise effects at the cost of losing some desired targets. Like IR, CFAR will suppress interference from low duty-cycle (less than a few percent), asynchronously pulsed sources (i.e., other radar transmitters). But CFAR does not function as an anti-interference technique for higher duty-cycle (i.e., non-radar) signals. In fact CFAR can make the effects of high duty-cycle interference worse by insidiously suppressing desired targets in the presence of such interference without any awareness of the problem on the part of radar operators.

5. Radar Interference Tests and Measurements

If spectrum is to be shared between radars and communication signals, then the effects of relatively high duty cycle interference signals need to be assessed for a variety of radar receivers. At such duty cycles, conventional radar interference mitigation technologies will not be expected to be effective.

NTIA engineers, working in conjunction with radar engineers in other Federal agencies (including the Federal Aviation Administration (FAA), the National Weather Service (NWS), the U.S. Coast Guard (USCG), and the United Kingdom's Maritime and Coast Guard Agency (MCA), have performed such tests and measurements over the past six years on the following types of radars: Long range air search, short range air search, ground-based meteorological, airborne meteorological, and maritime radionavigation and surface search. The radio bands used by these radars have included: 1200-1400 MHz, 2700-2900 MHz, 2900-3700 MHz, and 8500-10500 MHz.

The test and measurement protocol has been to inject desired targets into the radars via hardline connections while simultaneously injecting varying types and levels of interference into the receivers. (Desired targets for the meteorological radars have been ambient weather returns.) Targets and interference signals are always injected at the RF front-end of the radar receiver, as shown in Figure 4.

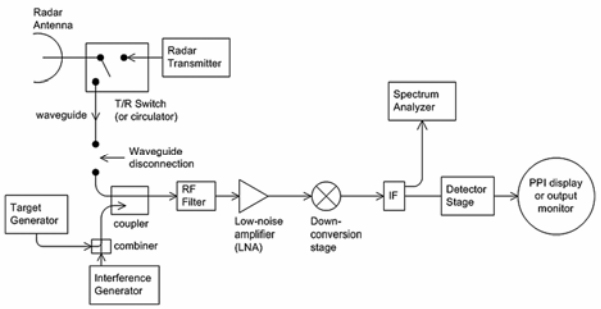

Figure 4. Block diagram of a typical test configuration in this interference study. Interference and desired targets were generated at radio frequencies and were injected at the radar receiver RF front-end ahead of the first RF filter and LNA. The spectrum analyzer is an external, diagnostic test and measurement accessory that is tapped from the IF via a directional coupler.

Interference effects are assessed by counting targets (for non-meteorological radars) or by assessing changes in radar receiver noise floor (for meteorological radars). As target counts decrease and noise floor rises, radar performance degradation is quantified.

6. Results

A typical degradation curve is shown in Figure 5.

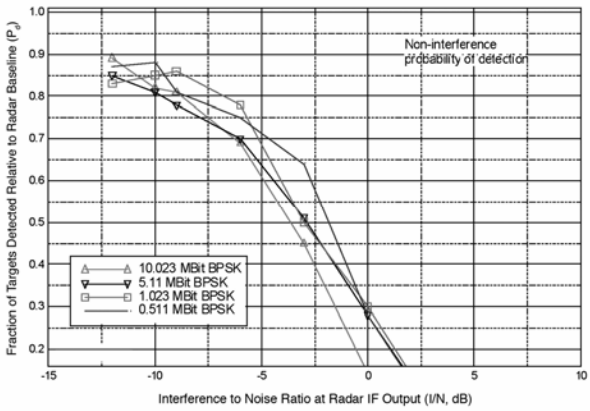

Figure 5. Effects of interference on the probability of detection of targets by an air-search radar. Interference effects begin to occur at an *I/N* level of -10 dB.

Effects are assessed as a function of the ratio of the level of the interference energy, *I*, to the level of the radar internal noise, *N*, the *I/N* ratio, as shown in Figure 5.

Communication interference signal modulations included: CW, CDMA, QAM, GMSK, BPSK, QPSK, UWB, and OFDM. Radar-like pulsed signals were also tested. The results of interference tests with these signal modulations are summarized in Table 1.

Table 1. *I/N* levels of Communication Signal Modulations at which Performance Decreased for All Radars Tested

Radar Tested	*I/N* Threshold for Decreased P_d
Long Range Air Search Radiolocation Radar 1 (installation 1)	-9 dB
Long Range Air Search Radiolocation Radar 1 (installation 2)	-9 dB
Long Range Air Search Radiolocation Radar 2	-6 dB
Short Range Air Search Radionavigation Radar	-9 dB
Fixed Ground-Based Meteorological Radar	-9 dB*
Maritime Radionavigation Radar A	-7 dB
Maritime Radionavigation Radar B	-10 dB
Maritime Radionavigation Radar C	-6 dB to -9 dB
Maritime Radionavigation Radar D	-9 dB
Maritime Radionavigation Radar E	-6 dB
Maritime Radionavigation Radar F	-6 dB
Airborne Meteorological Radar	-6 to -2 dB

* -14 dB is the predicted threshold for an upgraded version of the fixed meteorological radar.

Conversely, all of the tested radars have performed with little or no degradation when exposed to radar-like pulsed interference signals at duty cycles less than 1-3% and *I/N* levels of +30 dB or more.

Of special concern is the observation that, at low *I/N* levels (at or below -3 dB), desired targets fade away without any additional features on the display that might indicate the interference is occurring. An example if shown in Figure 6. This phenomenon indicates that such interference causes targets to be lost by operational radars without any indication to radar operators that interference is occurring.

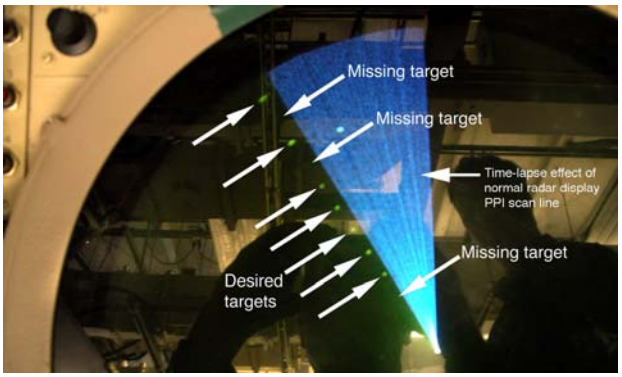

Figure 6. Target losses due to low-level interference effects (occurring here at an *I/N* level of about -3 dB in an air search radar) are insidious; *there is no indication on the display that interference is occurring*. The bright wedge in this image is not interference; it is merely a time-lapse effect of the electron beam that generates the radar display.

7. Conclusions for Interference that May Occur Due to Spectrum Sharing Between Radars and Other Systems

We draw the following four conclusions: 1) Radars are vulnerable to communication signal interference at *I/N* levels on the order of -9 dB to -6 dB; 2) radars perform robustly in the presence of interference from other radars, up to *I/N* levels of +30 dB and higher; 3) low-level interference effects in radar receivers are insidious; and 4) low-level interference can cause loss of radar targets at any range. These conclusions are discussed below, and at more length in [1].

Interference with communication-type modulations caused degradation in radar performance at *I/N* levels between -9 dB to -2 dB (at duty cycles in excess of 3%), well below the noise floor of each radar receiver. One radar lost targets at an *I/N* level of -10 dB, and *I/N* = -6 dB caused most of the radars to lose targets. Future improvements to meteorological radars are predicted to render them vulnerable at *I/N* levels as low as -14 dB.

In contrast to the effects of interference from communication signal modulations, pulsed interference at low duty cycles (less than about 1-3%) was tolerated at *I/N* ratios as high as +30 dB to +63 dB. The radar receivers that were tested performed robustly in the presence of signals transmitted by other radars.

We have observed during our tests and measurements that the loss of desired radar targets at low interference

levels is insidious; there is no overt indication to radar operators or even to sophisticated radar software that losses are occurring. No dramatic indications such as flashing strobes on radar screens are observed. This insidiousness can make low-level interference more dangerous than higher levels that will generate strobes and other obvious warning indications for operators or processing software.

Even when radars experience serious performance degradation due to low-level interference, it is very unlikely that such interference will be identifiable as such. It is therefore unlikely that such interference will ever result in reports to spectrum management authorities even when it causes loss of desired targets. Since low-level interference is not expected to be identified or to generate reports when it occurs, lack of such reports *cannot* be taken to mean that such interference does not occur.

Interference can (and will) cause loss of targets at any distance from any radar station; loss of targets due to radio interference is not directly related to distance of targets from radar stations. When radar performance is reduced by some number of decibels, *X*, then all targets that were within *X* decibels of disappearing from coverage will be lost. Range from the radar is not a factor in this equation. Interference can cause loss of desired, large cross section targets (such as commercial airliners, oil tankers, and cargo ships) at long distances, as well as small cross section targets at close distances. Low-observable targets that could be lost include, for example, light aircraft; business jets; incoming missiles; missile warheads; floating debris including partially submerged (and extremely dangerous) shipping containers; life boats; kayaks, canoes, dinghies; periscopes; and swimmers in life jackets.

Because any radar target can potentially be lost at any distance in the presence of radio interference, radio interference does not translate directly into an equivalent radar range reduction. “Range reduction” should therefore *not* be used as a metric in discussions of adverse effects of interference on radars, unless such range reduction is qualified with a reference to a (unrealistic) condition of fixed, constant cross sections for all desired targets.

Any scheme for sharing spectrum between radars and non-radar, communication-type signals needs to take these results into account. For example, the low *I/N* levels at which radar receivers lose targets, and the insidiousness of such losses, means that coordination distances between radars and non-radar systems that might try to share spectrum may easily extend to the radio horizons of the radar receivers at altitudes of 35,000 to 60,00 feet. Such distances are on the order of 200 miles.

8. Future Work

During radar interference measurements, the interference signals should be standardized to include: broadband noise; CW; impulse UWB (dithered and non-dithered); direct sequence UWB, multiband OFDM UWB; CDMA; TDMA; BPSK; QPSK; QAM; GMSK; OFDM; and pulsed signals (both linear FM-modulated (chirped) and unmodulated).

Plots of P_d versus *I/N* are a useful and effective method of displaying interference data and should be adopted as a standard for future radar interference measurements.

There exists a gray zone in interference effects versus duty cycle, where interference duty cycles are between 1-3%. This area needs to be investigated further. For pulsed signals, the parameters of pulse width and pulse repetition interval which comprise the duty cycle should be varied to determine the point at which interference effects transition from pulse-like to noise-like or CW-like. For linear-FM pulsed interference signals, the chirp rate and chirp bandwidth should be varied to observe the onset of the same effects.

9. References

[1] F.H. Sanders, R. Sole, B. Bedford, D. Franc, and T. Pawlowitz, “Effects of RF Interference on Radar Receivers,” NTIA Technical Report TR-06-444, Sep. 2006.

Acknowledgments

The body of work presented in this paper is the result of a long-term, dedicated, and cooperative work effort. It would have been impossible to accomplish without critical contributions from the following governments, organizations, and individuals: the Administration of the United Kingdom (including critically important guidance and assistance from Mr. Peter Griffith; Mr. Kim Fisher of Maritime and Coast Guard Agency; and the staff of the Fraser Range facility at Portsmouth); the Sperry Marine radar company; the Kelvin Hughes radar company; the Federal Aviation Administration (including critical assistance from Mr. Greg Barker and Mr. Mitch Hughes and the rest of the staff of the long range radars of the FAA Technical Center in Oklahoma City, OK; the staff of the airport surveillance radars at that facility; Mr. Michael Biggs; and the FAA radar staff at Kirksville, MO); the U.S. Coast Guard radar staff at Curtis Bay, MD, who assisted us well beyond ordinary limits in their already-busy schedule; the

National Weather Service (including Mr. Dan Friedman and the radar staff at Norman, OK); the US Air Force, including especially Darrell McFarland and Ricardo Medilavilla of the 84th Radar Evaluation Squadron (RADES) from Hill AFB, UT; staff of the NTIA Office of Spectrum Management (OSM), especially Mr. Robert Hinkle and Mr. Mike Doolan, and also Matt Barlow and Larry Brunson; and finally Ms. Kristen Davis of the NTIA/ITS laboratory, who drafted the technical drawings. Photographic images in this report were taken by one of the authors (Sanders).

Spectrum Management Support for Developing Countries:
Critique and Recommendations

John Murray
Applied Spectrum Research
1509 Linden Lake Road
Fort Collins, Colorado, 80524

970 407 7988

jmurray@asrworld.com

Spectrum's role in any economy, and especially in developing countries, is broadly recognized. Unfortunately but understandably, many developing countries are not well prepared to manage the spectrum. Numerous agencies attempt to assist and advise in widely varying ways. Many of these assistance projects have been marginally helpful at best. Some of these problems are reviewed here as the basis for recommendations for more productive (cost-effective) efforts in the future. The paper is based on the author's largely disappointing experience assisting developing and transitioning countries in South Asia, Africa, and Eastern Europe

This paper has been prompted by some hands-on , but largely disappointing, experience attempting to help some of these countries develop their national spectrum management capabilities. Here we present a brief look at the shortcomings, especially as they apply to the Least Developed Countries (LDCs) and suggest some modest steps toward improvement to serve as the basis for planning future projects

The opinions presented here are based on a limited sample, although others have reported similar experience. And of course, things can change – sometimes rapidly. Comments on any aspect of this issue are invited – especially about examples and improvements in place or in prospect.

1 The Need

The need for better spectrum management (SM) infrastructure in Developing Countries seems widely recognized and accepted, at least in broad and general terms. Specifics are a little harder to come by. One ITU document[1] lists 7 needs (as identified within the ITU community.).. Among them are

- training in ITU matters
- Assistance with computerized frequency assignment and monitoring
- Assistance with the economic and financial aspects of S.M.
- Assistance with preparations for World Radio Conferences
- Assistance with participation in ITU Study Groups

[1] ITU World Telecommunications Development Conference, Doha, 2006, Annex 1 to Resolution 9

Implicit in this list is the assumption that a viable spectrum management infrastructure already exists. – a questionable assumption in some cases, and that suggests a pre-emptive set of more fundamental requirements. The list places an understandable emphasis on ITU matters, but in the LDC case, other issues deserve comparable attention – perhaps even higher priority. One such local consideration is the ability to answer Mischa's question.

Mischa's Question

Mischa was the head of the technical department at a telecommunications regulator. Late one Friday afternoon, faced with a priority need to find temporary assignments for the security officers of two visiting delegations, he asked me "What frequency should I assign next?" The classical approach to the question is pretty well known, relying on some knowledge of what frequencies are already in use and some fundamental planning tools. But the first of these was not available and I wasn't able to help much, at least not with his immediate problem. Since that simple, direct, very relevant, awkward

query, I argue strongly that addressing this question is a fundamental consideration in developing basic SM capabilities, and in many cases, we're not doing a very good job of it.

When the many forms of Mischa's question are answered (including the case where "It doesn't matter." applies) a major share of fundamental spectrum management operations has been covered. Here is planning from the "bottom up".

Note that the ITU needs listed above don't help much either, except possibly the "computerized" question, and even that deals with a tiny part of the general issue.

The United Nations identifies 50 "Least Developed" countries. All of them suffer, in varying degree, from limited landline telephone service and they are seeing growing demand for cellular service to fill that void. And, of course they present needs for many other spectrum dependent services, although not necessarily to the same degree and with the same priorities that obtain in the industrialized countries.

The LDC Profile

The 50 LDCs identified by the ITU define the constraints the serve as the basis for this paper – most prominently budget and human resources..

Table 1
Profile for the 50
Least Developed Countries

Average Population	13 000 000
Average GDP	$5.5B 15 countries with less than $1B
Smallest GDP	$ 76 M
Largest GDP	$ 63 B
Average GDP per Capita	< $500
Total Population	650 000 000
Source: CIA World Fact Book, ITU	

GDP and per capita GDP serve as a rough indicator of potential telecom market size, spectrum demand, and the potential for regulatory agency funding via license fees. (However, there is no guarantee the fee revenue will flow to the regulator.)

Telecommunications technology is changing at light speed and, while regulation is struggling to keep up globally, some major changes in spectrum management are in prospect, especially greater reliance on marketplace mechanisms. These changes hold promise of reducing and perhaps simplifying the spectrum management process. Responding to these changes will take some special expertise that is not considered in the discussion here. Here the focus is on traditional process and procedures, but the policy makers among you are reminded to look to the future and the opportunity that spectrum reform has to offer.

2 Spectrum Support to Developing Countries – Unhappy results from past investments – and why

In the past, the US has made frequent (and sometimes substantial) investments in reform of the telecommunications regulatory process (with spectrum as a component) in many developing countries, either directly via AID, or less directly via the World Bank and even more indirectly through the ITU. There is every reason to expect this support to continue and probably to expand, especially given the growing awareness of the advantage of wireless telephony (cellular, etc.) in developing countries and the consequent explosive growth in demand.

In some cases this investment has been unnecessarily lost, sometimes as it was being made, for several largely inter-related reasons. Here are some:

a) Inadequate Planning

Planning for support in some cases has been (understandably, I think) based on a set of inappropriate expectations. (The scope of this specialized subject is both broader and deeper than is evident even to professional observers one step removed from the subject.) And those preparing plans are often from another part of the telecom world.

b) Advisors have specialized experience

Professionals who advise on this subject usually gain their experience in the relatively well developed countries and well established spectrum management institutions. And experience rarely deals with all of the factors that can become prominent in the development context (like lack of transparency, inadequate or non-existent banking systems. Projects that are broadly defined at the outset rapidly present

challenges new to even the most broadly experienced advisor. Good advisors can improvise, but usually at the cost of more effective work that could be done on other issues.

For large enough projects, multiple experts can respond with their various specialties, but in the context we consider here, assignments are often solitary. Evaluating practical requirements and providing for preparation and coordination prior to on-site arrival provides for better expectations and results that are more likely to serve the client.

Advisors also bring expertise in depth to some particular aspect of this complex subject. But frequently, what's needed is reasonable understanding of the entire process and the many essential interfaces to other aspects of spectrum and telecommunications.

c) Local Context Considerations

What happens in industrialized countries does not convert well, or at least not directly, to most of the developing countries of concern here. (Providing United States regulations with another country's name substituted does not serve.) Current processes can't be scaled down indefinitely and, where it is practical in some measure, still may not fit the local circumstance.

d) Limited and Fractured Infrastructure

In some cases, there is no effective SM organization in place, If not spectral anarchy, local management is the result of one person and an ad-hoc solution to each new requirement. This condition serves as a substantial justification for some projects and demands even more basic planning and implementation than usual. The extent to which it expands, extends, and delays even simple tasks does not seem to be very well recognized in setting up support projects.

e) Absence of Appropriate Training Resources

Training (especially long term training) is essential in any enterprise and has been in very short supply , especially in such a specialized subject as spectrum management. Training in some of the important supporting subjects like radio engineering (propagation, modulation, antennas, etc.) is more accessible, but even these topics are often neglected because of limited budgets and unbalanced priorities. Perhaps the most ubiquitous training opportunities are in the use of computers – an increasingly important part of spectrum management operations (but this is a support skill, rather than a part of the spectrum planning, analysis and licensing skill set.)

There are some encouraging signs.

A limited number of universities are offering courses in Spectrum Management.

There are short, usually introductory or survey courses offered by the ITU, national governments, and industry. These provide important awareness, but usually don't provide depth necessary for application to detailed operational needs. (The USTTI continuing program is one example. The CISCO Corporation has established a number of training centers world wide, although these teach Information Technology course rather than spectrum management.)

The ITU has offered an on-line course in Spectrum Management that appears appropriately detailed. Unfortunately, it has been offered only once and has not been rescheduled. The efficacy of distance learning still remains to be demonstrated, especially in this context.

f) Absence of Appropriate Long-term Support

Effective reform of telecom regulatory process (and its spectrum management component) is most effectively accomplished when an advisor is regularly available to consult and advise in day-to-day matters as well as in the big issues that form the core of the assignment.. Available aid funding and the paucity of experienced advisors make this unfeasible, I think.

g) Absence of Appropriate Software products

Computers and their software seem to rule every facet of our lives - sometimes ludicrously so. In this case, there are two fundamental functions that cry for some elemental computer capability: the need to keep large lists (of licenses and related information) and the need to perform some calculations (to permit reasonably efficient use of scarce frequencies). Computer support of these two functions requires software that provides the unusual features that this

job imposes. At the same time, the software needs to be simple to use, easy to maintain, and supportable over its operational life.. These are idealistic requirements if every aspect of spectrum management is to be pursued in even the smallest of organizations. They are attainable if requirements focus first on the basics.

But one more requirement imposes a serious constraint. The product must be affordable. The market for this specialized product is small enough (especially for the bare-bones versions for developing countries and smaller applications) that economies of scale are not realized.

The ITU has attempted to support these requirements for over a decade. Several projects offer promising steps to help with this issue.

The latest project provides a multi-purpose spectrum management tool (SMS4DC) [2] which is provided to developing countries at no cost. Short training workshops are provided, but operational support may prove difficult.

There is commercial software available and some support, but quality and capability is not generally known to the community at large (and to prospective buyers.) (Vendors are, understandably, very proprietary, and users are reluctant to discuss any shortcomings in their ability to use such systems once they have made the investment.) Initial cost is understandably high and budgets or support projects don't provide the kind of funding use of such software usually requires. It would be helpful to have knowledgeable, objective reviews of how the several systems are being used and how well they satisfy operational needs.

h) Equipment is (NOT) the total solution

Even considering comments in the preceding section, there is an undue reliance on equipment as the solution to many problems (especially radio monitoring equipment) that is ill founded and is often unproductive. Some basic office computer systems are necessary (but they must be supportable). The specialized, costly, and complex equipment for radio spectrum monitoring does not offer a comprehensive solution under the best of circumstances and often quickly falls into disuse. The important monitoring function needs to be matched to the stage of development of the complete spectrum management organization and operation.

3 Assistance – Problems and Barriers

Table 2: Example Task Statement: Spectrum Management Support for a Developing Country
1 adviser for *3 weeks*

TOPIC	Extracts from a Work Statement
Master Plan	Evaluate and apply a national frequency management plan
Policy Options	Explore various policy options for spectrum management
Evaluate Proposed Assistance Projects	Evaluate offers of assistance and investment from multilateral agencies and the private sector.
Spectrum Monitoring	Examine in detail the monitoring equipment needs of the Ministry, and propose different options that can be adopted.
Evaluate existing equipment and procedures	
Propose Practical Alternatives	
Evaluate a Proposed Alternative	
Licensing Procedure	Develop a mechanism to issue licenses for spectrum use; and the follow-on work for monitoring the fair use of assigned frequencies
Comprehensive Training	Provide on-site training for staff on the above issues
-- all technical staff – in all subjects	
Support as Assigned and Requested	
Reports	Task Planning
	Work Accomplished

The disappointing return on SM support investment is the result of overly optimistic (and unrealistic) planning and the lack of matching resources, especially funding and staffing. And the staffing limitations occur both in the time available to the project and the suitability of the advisor(s).

Requirements for assistance are, in some cases, drawn up by personnel with little or no experience in the field and the results can be preposterous. Often requirements are an amalgam of input from the recipient and an intermediate contractor, and in both cases spectrum management may be one small task among many.

[2] Spectrum Management System for Developing Countries.

In some cases, the aid recipient may not have a good understanding of the practical requirements.

The lack of realistic planning also denies realistic accountability for the support project.

Table 2 provides an example drawn from one task statement.

Except for the time constraint, this is not an unreasonable list of requirements. If anything, it's missing some important pieces. But time (and, of course, budget) make this a very unrealistic set of tasks. Expectations are high and results must inevitably be extremely disappointing.

As a footnote, the three weeks makes no allowance for debilitating discomforts that are inevitable even with the most careful attention to diet.

A comprehensive spectrum management capability includes a broad range of functional capabilities and the ITU Spectrum Monitoring Handbook provides a recommended list, including:

Table 3
Some Frequency Management Functions

Frequency Assignment
Border Coordination
International Coordination
Organization
Staffing and Human Development
Stakeholder Coordination
Licensing
Billing
Legislation
Monitoring
Enforcement
Inspection
International Policy Coordination
Spectrum Planning
Frequency Allocation Planning
Automation
Engineering Analysis
Economic Analysis
Policy Planning
Equipment Type Approval

,

In some cases, all the functions of an ideal SM organization are beyond the budget, capability and sometimes needs. And there is very little guidance as to how to prioritize and scale down requirements to manageable levels.

One consequence of this condition is that important basic issues are not considered adequately, if at all.

It is also hard to find experts who can provide working level guidance on all these subjects and their interrelationships.

In most aid cases, a skeleton SM organization is in place and the support project has been preceded by others. Local practice and experience, along with lessons learned from previous aid support are often ignored because of the time constraints on a project. And yet, new advice conflicting with existing experience needs to be explained if it is not to be counter productive.

Most support projects are one-time events, often short. To be effective, consistent support needs to be available on a continuing m(but not necessarily full-time) basis. Advisors that are on-site on a part-time, recurring basis can be very effective be reinforcing earlier work and concentrating on priority issues defined and refined in the interim. And interim on-line/telephonic support provides a valuable supplement (although not nearly as effective when translation is required.)

The ITU provides handbooks for Spectrum Management, Spectrum Monitoring, and other related subjects. While the handbooks provide a comprehensive overview of their respective subjects, they fail to recognize the limitations that face the LDCs. Fulfilling all of the requirements identified in the handbooks is well beyond the budget, abilities, (and sometimes needs) of the LDCs.

Language and culture constraints: Effective support needs to be provided in the recipient's working language. Doing so involves planning and budget considerations that are sometimes neglected, or viewed as an unacceptable dilution of the technical project.

Donors have emphasized equipment (and, to a lesser degree, software) when project performance is judged on delivery of a tangible that has a relatively predictable life. Unfortunately, hardware delivery is not the same as hardware use and long term utility. The human element is subordinated, with some justification when considering the human resources dilemma.

Lack of a long term, continuing source of training and support for comprehensive frequency management dealing with the special issues faced by

developing countries is also a barrier to efficient support.

4 PROSPECTS

There are a number of activities can improve on the problems described here. Here are some examples and some suggestions.

1. Cultural Issues: There is a need for understanding, diplomacy, respect for culture, tradition, and personal, professional and national pride. This can be a non-trivial element of the planning and budgeting process, especially in matters of translation.

2. Handbooks: Updated handbooks for Spectrum Management, Spectrum Monitoring and other related topics have been prepared by the ITU. These handbooks provide excellent guidance for broad planning.

   The handbooks do not address issues at the operational level (but some software products may help in this regard.)

   The handbooks are expensive and time consuming to produce. Maintaining currency is a continuing struggle.

   The handbooks do not address the special problems of small scale spectrum managers on very restrictive budgets. A "Small Scale National Spectrum Management" is needed.

3. Diagnostic Assessment: All support projects (with two exceptions noted below) should be based on a careful review of recipient status and needs, including the progress and impact of any prior training and support. This raises the cost of the project. It also raises the cost-effectiveness.

   Exception 1. Support is directed to the solution of a single clearly defined problem or issue

   Exception 2. Support is to provide an "advisor in residence" to offer hands on assistance with day-to-day issues as they arise.

4. Development Tools. Several tools will help both advisors and aid recipients.

   Planning, Allocation and Licensing (PAL) tools.

   These three SM functions are highly interrelated. Individually and collectively they lend themselves to the use of automated systems (if they are appropriately designed with the LDCs in mind.)

   PAL software is available from commercial sources, but it is costly, as is the support required. In addition, PAL software has been available to developing countries for the past decade and new, enhanced versions have been recently introduced. Spectrum advisors should have a good working knowledge of these systems and their capabilities and limitations as they apply to LDCs.

   Allocation Planning – Guidance, Examples, and Data and software. Some of this material is logically contained in the handbooks. In addition, a standard format allocation table template (computer file) provides an effective assist both to the planning process and to operations.

   Example spectrum allocation tables are available on many national SM websites to serve as examples, although these can be misleading. A prototype file specifically designed for this purpose and appropriately annotated insmuch to be preferred.

   Automated PAL systems must be designed to interface with other SM tools, most notably the spectrum monitoring process and billing and administrative services.

   Frequency Assignment; This is a central part of traditional SM operations and involves a wide range of approaches, procedures and techniques. Most available guidance seeks to optimize spectrum use, where optimum means maximize capacity. In some situations, times, and places, maximum spectrum capacity is not needed and inefficient assignments can be made in favor of economy and simplicity. In such case, however, it is important that reliable provision be made for changes to accommodate growing future demand. Handbooks, reports, and software from the ITU and industry provide guidance and

operational capability. Further experience in the LDC application is needed to know how effective these can be.

Network Planning.: In many places, planning or evaluating a spectrally dependent telecommunications network is the responsibility of organizations and agencies other than the telecommunications regulator. Even in those cases, the spectrum manager can benefit from a comprehensive overview of how radio systems are deployed and how effectively they use the spectrum. As with frequency assignment, commercial source and the ITU provide this part of PAL software. Using even the best engineered software, however, requires special skills that may be beyond the LDC spectrum manager. Plans to utilize these tools should consider carefully the required skills, training, data resources, and long term operations and maintenance that such systems entail.

Legislation: Enabling legislation is an important part of SM organization. Guidance, including best or recommended practices appropriately considering the LDC circumstance would be useful. The ITU Spectrum Management Handbook contains a list of "Best Practices" that should be considered her. A further development of that list for covering legislative practices is needed.

Regulation; "Best Practices" guidance is important here as in Legislation and distinctions will necessarily depend very much on local circumstances. More refined guidance is needed.

Organization and Operations: Organize to provide efficiency and transparency. Especially in any effort affecting fees and revenues, transparency considerations are important. Further development tools are needed.

Human Resources: The lynch pin of SM operations and one that presents serious barriers to effective operations (and serious concerns for aid donors.) One symptom of the general problem is the turnover that occurs as staff become trained and experienced. The results, obviously, are loss of training investment, long term corporate memory, and operational capability. (This is a problem shared by spectrum managers globally.) The resolution of this problem is well known – and hard to implement: better training and better pay, and more interesting work.. The changing face of SM offers some opportunity for the last of these.

5 Considerations for the Future

Spectrum Management support for developing countries will continue to be an important part of our spectrum planning for many reasons. Experience so far has been instructive with respect to future operations, but it's not clear whether the lessons have been learned.

In general, future support projects need to and can bbe better planned and evaluated . A more fundamental understanding of the character of the spectrum management process and the special needs of the Least Developed Countries will be critical..

Plans need to be more pragmatic, starting with a realistic understanding of the current and potential abilities of the recipient organization. Initial focus should be on the basics that are essential to current and near term operations. That means that some things in a classic organization must be left out (set realistic priorities). There is a generic approach to this issue that can serve well as the basis for such planning – including the preparation of Terms of Reference for Advisors and setting goals by which the success of support projects can be assessed. There are surely some who doubt this assertion, and for them I would hope this paper would serve to stimulate a little more thoughtful review and discussion.

REFERENCES

ITU Spectrum Management Handbook, 2002, Geneva

ITU Spectrum Monitoring Handbook, 2005, Geneva

SMS4DC Brochure describing the Spectrum Management Software for Developing Countries, ITU, Geneva.
www.itu.int/ITU-R/conferences/seminars/porto-seguro-2005/docs/E/10-**SMS4DC**.doc

Spectrum Management System for Developing Countries (SMS4DC) – Version 1.0
http://www.itu.int/opb/publications.aspx?lang=en&parent=D-STG-SPEC&folder=D-STG-SPEC-2006

Spectrum Management, Online Internet Distance Learning Course, ITU Bureau of Telecommunications Development.
http://www.itu.int/ITU-D/hrd/tc/tcdetails.asp?course=7825

(This is a detailed course that has been offered once and is yet to be rescheduled.)

ITU World Telecommunications Development Conference, Doha, 2006, Annex 1 to Resolution 9

Propagation Model Development Considerations for Short-Range and Low-Antenna Height Applications

Nicholas DeMinco
Institute for Telecommunication Sciences
National Telecommunications and Information Administration
Phone # : 303-497-3660
Fax # : 303-497-3680
ndeminco@its.bldrdoc.gov

Abstract: *This paper describes an analysis effort for determining the technical considerations for developing radio-wave propagation models to assist electromagnetic compatibility analysis and spectrum management efforts of mobile wireless devices. After performing an exhaustive review and evaluation of currently available radio-wave propagation models, ITS determined that none of the currently available models were suitable for performing radio-wave propagation loss computations to facilitate electromagnetic compatibility analyses of mobile wireless devices. ITS initiated an analysis effort to determine how to develop alternative models that would be valid in this parameter range. This analysis effort involved investigating various propagation loss prediction methods that would be valid for close separation distances (one meter to two kilometers), low antenna heights (one to three meters), and frequencies of 150-3000 MHz. This paper describes the preliminary analysis and investigation that will later be used to develop the radio-wave propagation models that would meet the requirements of the short range mobile-to-mobile (MTOM) propagation model. It was determined that a combination of the complex two-ray method and a method that computes mutual coupling would meet the requirements.*

1. Introduction

With the tremendous growth in demand for licensed and unlicensed mobile wireless devices, it is necessary to perform electromagnetic compatibility analyses to address the problems of interference between users of the electromagnetic spectrum to accommodate the increasing number and type of these new mobile devices. The evolution of our communications infrastructure depends heavily on the use of licensed and unlicensed mobile wireless communication devices. The growth and prosperity of our economy depends on the successful operation and compatible coexistence of these wireless devices in a crowded electromagnetic spectrum. It will be necessary for regulatory agencies to perform electromagnetic compatibility analyses to address the problems of interference between users of the electromagnetic spectrum to accomodate the increasing number and type of these new mobile devices. An accurate and flexible radio-wave propagation model is essential for meeting the needs of both spectrum management and the electromagnetic compatibility analysis process.

In an Executive Memorandum from the President dated November 30, 2004, the Department of Commerce was requested to submit a plan to implement recommendations that would ensure that our spectrum management policies are capable of harnessing the potential of rapidly changing technologies. These recommendations include providing a modernized and improved spectrum management system for more efficient and beneficial use of the spectrum. In addition, these recommendations include developing engineering analysis tools to facilitate the deployment of new and expanded services and technologies, while preserving national security and public safety, and encouraging scientific research and development of new technologies. In meeting these recommendations in the area of engineering analyses and technology assessments, it will be necessary to determine the best practices in engineering related to spectrum management, and also address the electromagnetic compatibility analysis process.

In response to this Executive Memorandum, the National Telecommunications and Information Administration's (NTIA) Office of Spectrum Management (OSM) tasked the Institute for Telecommunication Sciences (ITS) to determine what radio-wave propagation models currently existed and whether or not they could be used reliably for electromagnetic compatibility analyses and for spectrum management of mobile wireless devices that were very close to each other (distances of one meter to two kilometers)and located at very low antenna heights (one to three meters). ITS reviewed all currently available propagation models in the literature and also those described in the International Telecommunication Union-Radiocommunication Sector (ITU-R) Recommendations to determine their applicability. Even though the models that were examined have their own regions of validity, they were all found to be inadequate to simultaneously meet all of the requirements for the short-range mobile-to-mobile (MTOM) model: one

meter to two kilometer separation distances, one to three meter antenna heights, and a frequency range of 150-3000 MHz. Existing radio-wave propagation models are valid only for much higher antenna heights (four meters or greater) and larger separation distances (between 10 meters and one kilometer). It was therefore necessary to initiate an analysis effort to develop new radio-wave propagation models that would be valid in the required parameter range. ITS initiated an analysis effort for developing new propagation models that would perform predictions that would be valid for the frequencies, separation distances, and antenna heights typical of the new generations of short-range MTOM communication devices. The preliminary analysis effort has determined what technical considerations need to be included in a propagation loss prediction model for short-distances and low-antenna heights. Existing radio-wave propagation models separate the antenna from the propagation loss, and calculate a basic transmission loss that is independent from the antennas. At short ranges and low antenna heights it is necessary to develop propagation models that include the interaction of the antennas and the radio-wave propagation loss. Investigations were made of various propagation computation methods and mutual-coupling calculations. This information will be used in future efforts to develop radio-wave propagation models for the short-range MTOM environment.

2. Discussion

Initially, when a literature search was performed, only a small percentage of the references were found to be even partially applicable for use in our short-range MTOM propagation model development. None of the models and measured data in the existing literature or ITU-R Recommendations can provide an accurate analysis and meet all of these requirements simultaneously. Each of these requirements provides conditions and constraints that have to be provided for to make accurate propagation loss predictions. Satisfying all three of these requirements simultaneously increases the complexity needed for a model or group of models to meet our objectives. These existing models can be used for analyses on a limited basis, providing only part of the needed frequency band, a portion of the required distance range, and higher antenna heights.

An environment description must also be included to provide a model that will accurately predict radio-wave propagation loss. The environments considered for model development will be similar to those of Recommendation ITU-R P.1411-2 [1] (urban high-rise, urban/suburban low-rise, residential, and rural) with the addition of a fifth environment to include the short-range indoor environment as described in Recommendation ITU-R P.1238 [2]. The models used in these two ITU-R recommendations will require extensive modifications and additions to the applicable antenna heights, distances, and frequency ranges to meet the short-range MTOM propagation model requirements.

There is a hierarchy of approaches that could be used to develop the short-range MTOM model, ranging from the simple slope and breakpoint methods to a more complex site-specific approach that uses ray-tracing methods with actual scenario geometries. The simple slope and breakpoint methods use regression fits to measured data which are site-general and provide a rough approximation of the propagation loss. The site-specific approach is more accurate, but requires more information about the scenario and environment. An approach in between the simple site-general and site-specific approaches would include algebraic formulas derived from the site-specific rigorous analysis, but simplified for easy use for specific but different scenarios.

In the survey of the current literature, it was found that many of these analyses, model development efforts, and measurements were conducted at around 900 and 1900 MHz for cellular and PCS communications. There is little data available for urban environments above and below these frequencies. New analytical models will need to be developed, and new measurements will have to be performed for frequencies in the 150-300 MHz and 1900-3000 MHz bands. The ITU-R Recommendation 1411-2 will cover 300-3000 MHz, but the minimum base station antenna height of four meters for ITU-R P. 1411-2 is just outside of the required range, so new models need to be developed for the 300-3000 MHz range for lower antenna heights. A minimum distance is not specified for the line-of-sight (LOS) model, but the maximum distance is one kilometer, which falls short of the two-kilometer requirement. The minimum distance needs to be determined and is a function of mutual coupling, surface wave effects, and a distance in the far-field region. The antenna heights for the LOS model are not specified in this recommendation. The non-LOS distance range is specified as 20-5000 meters, and a frequency range of 800-2000 MHz. The receiver antenna height is for low antennas held by a pedestrian or in a vehicle, but the base-station antenna height ranges from 4-50 meters. Reference [3] uses the identical LOS model with transmitter heights of 6.6 and 3.3 meters, and a receiver antenna height of 1.5 meters, and a minimum distance of 10 meters at a frequency of 1956 MHz. The measured data in this reference validates the LOS model of ITU-R P. 1411, but not the non-LOS model. A model for attenuation in foliage needs to be developed, since ITU-R P. 833-4 has one antenna height that is too high for the short-range MTOM model.

For indoor propagation ITU Recommendation ITU-R P. 1238 can be used for frequencies above 900 MHz, but a model will have to be developed for frequencies below 900 MHz. The minimum useable distance for the ITU indoor model of slightly greater than one meter is greater than the distance that specifies the far-field region at 900 MHz, but the distance to the far-field region will increase with decreasing frequency and the model will not be valid below 900 MHz. Reference [4] can provide additional measured data at 433, 869, and 2450 MHz. Reference [5] can provide indoor models in the form of power law equations with statistics, and measured data at 900, 1300, and 1900 MHz at low antenna heights. Reference [6] contains data and similar models for the indoor environment at frequencies from 850 to over 4000 MHz. Reference [6] is also a recent survey of all existing indoor and outdoor propagation models. Reference [7] is similar to the previous references [5,6], but contains added shadowing considerations created by objects in the indoor environment. In addition to having to develop models at lower frequencies, investigations will have to be made for very close-in distances, since the near-field considerations and mutual coupling considerations become more critical and will have to be taken into account at the lower frequencies.

The models and measured data in References [8-13] are for the frequencies of 900 and 1900 MHz with a transmitter height of 3.3 meters and a receiver height of 1.6 meters. Both LOS and non-LOS scenarios are considered. These models are the results of theoretical derivations and regression fits to measured data. The shortest distance for the models and measured data is 30 meters. Models at other frequencies, antenna heights, and shorter ranges will need to be developed. Reference [14] contains similar measured data at 1900 MHz with single and double regression fits to measured data at low antenna heights of 3.7 and 1.7 meters, but the shortest transmitter/receiver separation distance is 10 meters. Reference [15] contains measurements and prediction models at 1800 MHz using low antenna heights where both antennas are at 1.7 meters. Reference [16] describes much of the work that appeared in references [8-13] with some additional material on the various aspects of model development for 900 and 1900 MHz. Reference [17] is a recent paper describing the prediction of radio channel behavior for wireless systems beyond the second generation for 900 and 1900 MHz. The radio channel parameters are described in statistical terms, but third and later generation wireless systems require additional statistical information about the delay spread and angle-of-arrival of the multipath signals. This paper describes the use of ray-tracing codes to predict channel statistics. Angle-of-arrival and delay spread are also available from these ray-tracing codes. New models need to be developed for the shorter ranges and low antenna heights at frequencies other than 900 and 1900 MHz.

3. Modeling Effects to Consider

ITS performed an initial analysis effort and has determined that the development of a model that will provide propagation loss predictions at frequencies of 150-3000 MHz, for close-in distances as short as one meter and low antenna heights, requires the use of mutual coupling predictions and also should include the effects of the surface wave and the near-field effects of the antennas. The surface wave must be included in propagation loss predictions for frequencies below 450 MHz. The antenna patterns or gains of the antennas may not be valid at close separation distances, since they may not be in the far-field region of the antennas. In addition, the analysis determined that for low antenna heights, the effects of the close proximity of the Earth to the antenna produces a strong interaction of the antenna with ground, changing its impedance and radiation patterns and thus affecting the efficiency and gain of the antennas.

When the separation distances are great enough, other propagation methods can be used. When the separation distances are not great enough, then it is necessary to develop computation methods that will take into account the factors that need to be considered for close-in antenna separations and low-antenna heights. As mentioned previously, the computation of radio-wave propagation loss must include the interaction between the antenna and the propagation model, since they are not separable for close-in distances and low-antenna heights, making the usual assumptions of being in the far-field region of the antenna and being away from Earth invalid. Other effects need to be considered, which are described in this paper.

3.1 Near-Field and Far-Field Regions of an Antenna

There are three field regions surrounding an antenna: the radiating far-field region also known as the Fraunhofer region, the radiating near-field region also known as the Fresnel region, and the non-radiating reactive near-field region closest to the antenna. The distances from the antenna at which these regions occur are based not only on aperture size and frequency, but also on phase error, amplitude error, and the reduction of the higher order terms of near-field reactive and near-field radiated field terms. In the far-field region of an antenna, the electromagnetic fields exhibit plane wave behavior. The radiating far-field region of an antenna is also characterized as having an angular field distribution that is independent of the radial distance from the antenna. When the transmitter and the receiver

are at a separation distance such that the far-field region conditions are satisfied for both of the antennas, then antenna parameters such as gain and radiation patterns can be used to make performance and interference analyses. When the far-field region conditions are not met, then the gain and radiation patterns are not valid. The radiation pattern of an antenna in the far-field region is independent of distance, r, and hence the angular field distribution of the fields from the antenna will not depend on distance. The electromagnetic fields in the far-field region of an antenna have a 1/r dependence and only the transverse components of the electric and magnetic field are present. The ratio of the electric to magnetic field in free space is 377 ohms in the far-field region, but over real ground this ratio can be different from 377 ohms in the far-field and near-field regions of the antenna. For these reasons it is informative to know where the reactive near-field region, the radiating near-field region, and the far-field region of the antenna occur. The radiating near-field region of an antenna occurs in a distance range that lies between the reactive near-field region and the radiating far-field region of the antenna. It is characterized as having an angular field distribution that is dependent on the radial distance from the antenna. Close to the antenna, the reactive near-field dominates over the radiated near field.

3.2 The Surface Wave

Since the short-range MTOM model must include very short distances and very low antenna heights, propagation is predominantly via the ground wave in this situation. The ground-wave signal includes the direct LOS wave, the ground-reflected wave, and the Norton surface wave that diffracts around the curved Earth or propagates along the surface of a flat Earth. The direct LOS and reflected waves add together to form the space wave component of the ground wave. The Earth can be considered flat for all practical purposes in the short-range MTOM model. The Norton surface wave will be referred to as simply the surface wave in this paper. Propagation of the ground wave depends on the relative geometry of the transmitter and the receiver location and the antenna heights. The radio wave propagates primarily as a surface wave when both the transmitter and receiver antennas are near the Earth in terms of wavelengths, because the direct and ground-reflected waves in the space wave can cancel each other to varying amounts and the surface wave can then be significant. The surface wave is predominantly vertically polarized since the ground conductivity effectively shorts out most of the horizontal electric field component. What is left of the horizontal field component of the surface wave is attenuated at a rate many times the vertical component of the electric field of the surface wave. When one or both of the antennas are elevated above the ground to a height comparable to a wavelength, the space wave predominates. Propagation loss computations were made with and without the surface wave to show its effect on the magnitude of propagation loss. Extensive computations performed for this analysis have shown that for short distances the surface wave was still of significant amplitude at frequencies less than 450 MHz, and should be considered for accurate computations of propagation loss.

3.3 Antenna to Ground Interaction

For low antenna heights the effects of the close proximity of the Earth to the antenna produce a strong interaction of the antenna patterns with the ground. The antenna pattern performance is vastly different than if the antenna were in free space. If the antenna is within a half wavelength of the ground, the antenna input impedance is also affected, and will affect the efficiency and gain of the antennas. Elevation coverage plots of the radiation patterns of antennas over real Earth are different due to the presence of ground. The main beam is generally scanned up in elevation from the horizontal position that it would have had in free space. This causes the antenna to have less low elevation angle coverage. The antenna patterns over ground are quite different from the free-space antenna patterns and have an increased lobing effect as the frequency increases and the antenna height increases. In addition, the antenna radiation pattern in the far-field region of the antenna is not valid at these short distances above Earth, so the normal far-field region parameters of radiation pattern and gain cannot be used.

3.4 Mutual Coupling

Two antennas will always have a mutual coupling present between them, which becomes quite strong when the antenna separation distances are small. In addition, when the antennas are in close proximity to Earth or a large ground plane, there also will be a strong interaction with the antenna images created by the Earth or ground plane. This can have a major influence on the antenna gain, impedance, and radiation patterns. The fields from one antenna will induce currents in the other antenna, which will in turn cause radiation from the other antenna and induce currents in the original antenna. A mutual coupling will exist between the two antennas and the images formed by the presence of a ground plane or the Earth. In many cases involving close antenna separations, the mutual coupling between the antennas must be considered when computing propagation loss between the antennas. However, there are scenarios where this effect can be neglected, which will be discussed in the next sections.

4. Methods of Computing Propagation Loss for the Short-Range MTOM Model

Several approaches were compared in an effort to determine how accurately these simplified methods can predict propagation loss. Two sophisticated methods were the mutual-coupling method and the undisturbed-field method. A mutual-coupling method was the most accurate means for computing propagation loss, but it was also the most difficult to implement. Therefore, the loss prediction method that performs mutual-coupling computations between closely spaced antennas over real ground was used as a reference and compared to other methods. It was necessary to investigate other methods that could accurately predict propagation loss and compare their results to the mutual-coupling method to determine when the simpler methods could replace the mutual-coupling method. One alternative method was the undisturbed-field method which was much easier to implement than the mutual-coupling method and could still maintain a high degree of accuracy for propagation loss prediction. The complex two-ray method was compared to both the mutual-coupling and undisturbed-field methods to determine under what conditions it could be used, but it was found to not be accurate for close-in distances and low-antenna heights. The undisturbed-field computation is easier to implement for a large number of computations of different antenna heights, distances, frequencies, and ground constants. These methods will be described in this section.

4.1 Two-Ray Methods

A simple two-ray method for wave propagation where antenna patterns are not taken into account and the reflection coefficient is set equal to -1.0 does not represent the real-world physical scenario. This method will predict an unrealistic propagation loss versus frequency with very deep nulls and a lot of lobing structure. A better two-ray method is one that factors in the far-field region radiation patterns of the antennas and uses the actual reflection coefficient as a function of frequency, incidence angle and ground constants, even though the gains are not valid in the near-field region of the antenna for close-in distance separations. This will be referred to here as the complex two-ray method. The simple two-ray and the complex two-ray methods can be shown to be informative, but they are inadequate to determine electric fields and propagation loss at close-in distances and low-antenna heights, though the complex two-ray method can be used at longer distances with low-antenna heights. Even though the complex two-ray method can make a better prediction of propagation loss than the simple two-ray method, it still does not take into account necessary effects for the short ranges and low antenna heights simultaneously. Comparisons between the complex two-ray method and the more sophisticated methods (based on mutual-coupling and undisturbed-field methods) will show where the complex two-ray method is not adequate at short distances, but can be used at longer distances for LOS scenarios as a simpler and computationally faster method.

4.2 The Undisturbed Field and Mutual Coupling Methods

For an even more accurate propagation model, sophisticated prediction methods would factor in a near-field antenna response or a far-field region antenna response when appropriate. Two sophisticated methods for propagation loss prediction that factor in these effects were investigated. One involves a mutual-coupling computation between two antennas; the other involves computation of the undisturbed electric field and the loss based on the amplitude of the electric field as a function of distance. The undisturbed-field method includes near-field effects, the complex two-ray method, near-field and far-field antenna response, and the surface wave. This method involves computing the electric field produced at different distances and heights above average ground from a transmitting antenna at different heights using the Numerical Electromagnetics Code (NEC). This electric field is then used in the equation that relates electric field to propagation loss as a function of frequency. These computations and results can then be used to generate a set of equations for building a propagation model.

The mutual-coupling method includes all of the effects of the undisturbed-field method, but also factors in the mutual-coupling effects between the transmitter and receiver antennas and their antenna images with the ground. This method uses the NEC code for computation of mutual coupling between two antennas. Many iterative runs of the NEC code are required for implementing the mutual-coupling method for each scenario and configuration at all separation distances, antenna heights, and frequencies. It is an intensive computation method requiring lots of computation and setup time to produce the results. The impedances of the antennas must be rematched at each distance and each set of antenna heights for each frequency. The input files representing each scenario are run in NEC to determine the input impedances of the antennas for all configurations so that the antennas can be conjugate matched for accurate predictions of the mutual coupling loss. When all scenarios and configurations have been run, then the input files with matched impedances are all rerun to determine the induced current in the receiver antenna for a specific input power at the transmitter

antenna. The induced current, input power, and the real part of the receiver antenna input impedance are then used to compute the mutual coupling loss.

4.3 Comparison of Prediction Methods

The undisturbed-field method was compared to the complex two-ray method and free-space loss method to show why the latter two methods are not adequate to predict propagation loss for the desired scenarios when the distances are small (<10 meters). The undisturbed-field method includes more significant effects and is therefore more accurate than all of the methods except the mutual-coupling method. The undisturbed-field method can predict the propagation loss within one dB of the mutual-coupling method for distances greater than two meters.

The undisturbed-field method should be the method of choice whenever possible for best accuracy and fast computation time. However, it would be convenient to use the complex two-ray method for larger distances instead of the undisturbed-field method where possible to simplify the propagation model. The complex two-ray method gives adequate results for longer distances.

For vertical polarization involving a variety of antenna heights, distances, frequencies, and ground constants, the undisturbed-field method is almost equivalent to the method using mutual coupling except for very short distances where mutual coupling has a strong effect. Even at very short distances where the difference in the prediction of propagation loss is a maximum, the propagation losses computed by the two methods differ by less than two dB and are typically less than one dB for distances greater than two meters. The greatest difference in the two predictions occurs when there is a difference in transmitter and receiver antenna heights, and is approximately two dB when the antenna heights differ by two meters and the transmitter to receiver separations are small (<2 meters). The propagation loss predicted by these two methods for six combinations of antenna heights and five frequencies across the desired frequency range of 150-3000 MHz indicated that the differences in the two computation methods are small and can be neglected in most scenarios. As a result, the undisturbed-field method will be preferred for the final propagation model derivation over the mutual-coupling method, and the propagation loss will be compensated for in those limited scenarios where the difference approaches the maximum of two dB. The undisturbed-field method was chosen over the mutual-coupling method because of its simplicity and reduced computation time for many combinations of frequencies, antenna heights, distances, and ground constants. In the analysis, comparisons were made between the undisturbed-field method and the mutual-coupling method to determine the magnitude of the error. The errors for different scenarios of antenna heights, distances, and frequencies are available for reference to the user of the model. If the error between the two methods is considered to be too large for a particular application, then the mutual-coupling method can be used for these short distances.

Figure 1 shows a comparison of propagation loss versus distance predicted by three methods of increasing complexity and accuracy at 900 MHz for vertical polarization. Free-space loss is the least complex and least accurate method, while the mutual-coupling method including all effects is the most complex and most accurate method. The complex two-ray theory, including complex reflection coefficient and antenna effects, is of intermediate complexity.

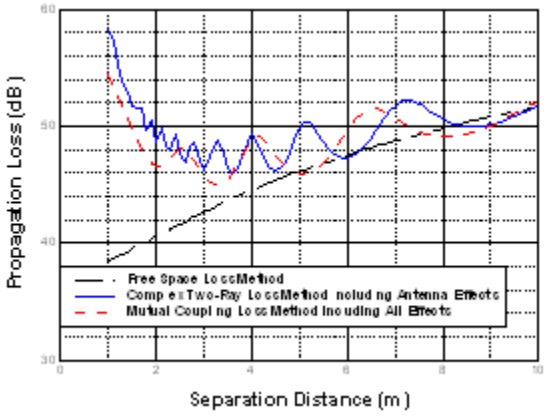

Figure 1. Three propagation loss prediction methods at 900 MHz for a transmitter height of 3 meters and a receiver height of 1 meter with vertical polarization.

5. Conclusions and Recommendations

Investigations of different propagation modeling methods and the special considerations of a short-range propagation model with low antenna heights have resulted in the development of alternative approaches to be taken to accurately model propagation loss in a MTOM environment. This initial analysis addressed the LOS propagation environment in an open scenario for vertical polarization. Non line-of-sight propagation will be addressed in future efforts, as will horizontal polarization. Other analysis efforts to be performed will address the urban/suburban canyon (LOS and nonLOS), the parking lot canyon (LOS and nonLOS), the general

nonLOS propagation environment, the suburban residential environment, the rural environment, and an indoor environment.

A hierarchy of approaches will be utilized to develop the short-range MTOM model that would account for different levels of complexity, from very simplistic methods where not much information about the scenario was known, to increasingly more sophisticated methods that include all of the above mentioned effects for scenarios where more site-specific information would be available.

None of the models and measured data in the existing literature or ITU-R Recommendations can provide an accurate analysis and meet all of the requirements simultaneously. During the analysis it was discovered that models using the free-space loss term in the power-law propagation formula at distances that are too close for the lower frequencies will result in inaccurate predictions. These models were all found to be inadequate for the short-range MTOM model requirements of one meter to two kilometer separation distances, one to three meter antenna heights, and a frequency range of 150-3000 MHz. It has been determined by analysis that alternate methods must be used in the development of radio-wave propagation models that can be used to assess the electromagnetic compatibility between the new generation of mobile wireless devices because of the challenging scenarios of very close separation distances and very low antenna heights. A loss-computation method that performs mutual-coupling computations between closely spaced antennas over real ground was used for the initial analysis and compared to other methods. This mutual-coupling method included the effects of the near- and far-field regions of the antennas as well as a mutual-coupling interaction between the antennas and the antenna images with ground. It was considered the most accurate method for prediction of propagation loss, but is rather difficult to implement for a wide variety of antenna heights, antenna separations, frequencies and ground constants. Therefore, an alternative method, the undisturbed-field method, also was investigated. The propagation model to be implemented for distances in the range of 1-20 meters will be based on this undisturbed-field method that includes compensation for the antenna near-field and far-field responses, ground constants, close-antenna spacing, and geometries created by the different antenna heights. For distances less than two meters, the mutual-coupling method can be used if the accuracy of the undisturbed-field method is not considered accurate enough. For longer distances (greater than 20 meters), a complex two-ray method that includes antenna parameters and the complex reflection coefficient could be used. In future propagation modeling efforts, mathematical algorithms will be developed from the results of the current analysis and measurement effort.

6. References

[1] ITU-R (International Telecommunication Union-Radiocommunication Sector), “Propagation Data and Prediction Methods for the Planning of Short-Range Outdoor Radiocommunication Systems and Radio Local Area Networks in the Frequency Range 300 MHz to 100 GHz,” Recommendation ITU-R P. 1411-2, International Telecommunication Union, Geneva, Switzerland, 2003.

[2] ITU-R, “Propagation Data and Prediction Methods for the Planning of Indoor Radiocommunication Systems and Radial Local Area Networks in the Frequency Range 900 MHz to 100 GHz,” Recommendation ITU-R P. 1238-3, International Telecommunication Union, Geneva, Switzerland, 2003.

[3] V. Erceg et al., “Urban/suburban out-of-sight propagation modeling,” *IEEE Communications Magazine*, June 1972, pp 56-61.

[4] L.J.W. van Loon, “Mobile in-home UHF radio propagation for short-range devices,” *IEEE Ant. and Prop. Magazine*, Vol. 41, No. 2, April 1999, pp. 37-40.

[5] T.S. Rappaport and S. Sanhu, “Radio-wave propagation for emerging wireless personal-communication systems,” *IEEE Ant. and Prop. Magazine*, Vol. 36, No. 5, October 1994, pp 14-24.[8].

[6] T. Sarkar et al., “A survey of various propagation models for mobile communication,” *IEEE Ant. and Prop. Magazine*, Vol. 45, No. 3, Junee 2003, pp. 51-82.

[7] T.S. Rappaport, “Factory radio communications,” *RF Design Magazine*, Januaury 1989, pp 67-73.

[8] H.H. Xia et. al., “Radio propagation characteristics for line-of-sight microcellular and personal Communications,” *IEEE Trans. Ant. Prop.*, AP-41, No. 10, October 1993, pp. 1439-1447.

[9] H.H. Xia, et. al., “Microcellular propagation characteristics for personal communications in urban and suburban environments,” *IEEE Trans. Vehic. Technol.*, Vol 43, No. 3, August 1994, pp. 743-752.

[10] D. Har, H.H. Xia, and H.L. Bertoni, “Path-loss prediction model for microcells, *IEEE Trans. Vehic. Technol.*, Vol. 48, No. 5, September 1999, pp. 1453-1462.

[11] L.R. Maciel, H.L. Bertoni, and H.H. Xia, “Unified approach to prediction of propagation over buildings for all ranges of base station antenna height,” *IEEE Trans. Vehic. Technol.*, Vol. 42, No. 1, February 1993, pp. 41-45.

[12] H.H. Xia, “A simplified analytical model for predicting path loss in urban and suburban environments,” *IEEE Trans. Vehic. Technol.*, Vol. 46, No. 4, November 1997, pp. 1040-1046.

[13] D. Har and H.L. Bertoni, “Effect of anisotropic propagation modeling on microcellular system design,” *IEEE Trans. Vehic. Technol.*, Vol. 49, No. 3, May 2000, pp. 1303-1313.

[14] M.J. Feuerstein, et. al., “Path loss, delay spread, and outage models as functions of antenna height for microcellular system design,” *IEEE Trans. Vehic. Technol.*, Vol. 43, No. 3, August 1994, pp. 487-498.

[15] N. Patwari et. al., “Peer-to-peer low antenna outdoor radio wave propagation at 1.8 GHz,” *IEEE Vehicular Technology Conference*, May 16-20, 1999, Houston, TX, Vol. 1, pp. 371-375.

[16] H.L. Bertoni, *Radio Propagation for Modern Wireless Systems*, New Jersey, Prentice Hall, 1999.

[17] H.L. Bertoni, S.A. Torrico, and G. Liang, “Predicting the radio channel beyond second-generation wireless systems,” *IEEE Ant. and Prop. Magazine*, Vol. 47, No.4, August 2005, pp. 28-40.

Short Range Propagation Measurements for Interference Model Development

Peter Papazian[1], Paul McKenna

National Telecommunications and Information Administration
Institute for Telecommunication Sciences
Boulder, CO USA 80305
1. Corresponding author phone: (303) 497.5369
Fax: (303) 497-3680
Email: ppapazian@its.bldrdoc.gov

This paper summarizes preliminary work on a short range propagation measurement program. The objective of this program is to create a measurement data base which can be used to develop an empirical short range propagation model which can be used in inference studies of proposed short range wireless systems operating in existing communication bands. This paper describes the impulse response measurement, the propagation environments to be studied, and the frequency ranges proposed for measurements.

1. Introduction

Recently there has been growing interest in spectrum allocation schemes which do not rely on separate frequency allocation bands for different services or systems. A typical application for this type of spectrum allocation is short range mobile to mobile communications in urban areas. To determine the feasibility of such schemes, the NTIA Office of Spectrum Management (OSM) has begun a propagation study to support the development and validation of short range propagation models. These models would then be used to determine interference between existing allocations and the proposed systems. The propagation program is utilizing an Institute for Telecommunication Sciences (ITS) wideband impulse response measurement system. The measurement system currently is configured to operate at multiple frequencies between 450 MHz and 5.8 GHz. A preliminary data set has been collected between 450 MHz and 5.8 GHz using 4 frequencies using measurement bandwidth of 20 MHz. Currently three more impulse response channels are being added at 183 MHz, 915 MHz and 1602.5 MHz with bandwidths of 4, 20 and 10 MHz respectively. This paper describes the measurement system in Section II, shows measurement locations and methods in Section III and presents preliminary results in Section IV.

2. Measurement System

The transmitter and receiver system is based upon the ITS channel sounder that measures the radio channel impulse response. The system can be configured for multi-frequency or multi-code operation. For these tests the system is configured for multi-frequency operation as well as variable code rate operation. The block diagram of a wideband sounder transmitter is shown in Figure 1. The transmitter utilizes a pseudo-random m-sequence generator clocked by a 10-MHz rubidium frequency standard. The sequence generator is a self-controlled field programmable gate array (FPGA) and uses a maximal length shift register pseudo-noise (P/N) code of length 511 chips clocked nominally at 10 mega chips per second for the preliminary measurements. For follow-on measurements a multi-rate code generator as well as more frequencies of operation will be added. The frequencies and code rate will be matched to existing channelization and frequency allocations to allow testing over specific bands of interest to OSM. By varying the code rate the bandwidth of operation can be varied to fit in existing channels. The bandwidth determines the time resolution of the impulse and with a fixed code length also the maximum measured signal delay.

The P/N sequences are level shifted by a wideband limiter to have precise ±1 outputs which are then low-pass filtered for pulse shaping. The 10-MHz clock is also used to synchronize the local oscillator and a timing generation to synchronize sampling at different frequencies operation and code rates. Output RF filters eliminate unwanted sidebands.

Figure 1 shows a block diagram of a four-channel receiver. When chipped at 10 MHz an impulse measurement is accomplished in 51.1 microseconds. The delay between impulses is set to 5 ms to allow adequate sampling and averaging of the signals over the large frequency range of operation. To average random signals in a mobile channel signals are usually averaged over 10-50 wavelengths. Using an FPGA timing circuit, bursts of 256 impulses are collected on 4 channels simultaneously. The

signals received by the antenna array are filtered with pre-selection filters to eliminate out of band interference before amplification by low noise amplifiers. After down conversion using signal generators for LO generation and a second rubidium clock, each channel of the receiver is output to a 14-bit digitizer, sampling at 40 mega-samples per second. The receiver then waits 5 seconds as the measurement van is moving and another random burst of channel data is collected. The van position and velocity is recorded using a GPS receiver at the start of each data burst. This information is used during data processing to determine the appropriate number of averages for each frequency to meet the sampling requirements for recording Doppler frequencies and averaging.

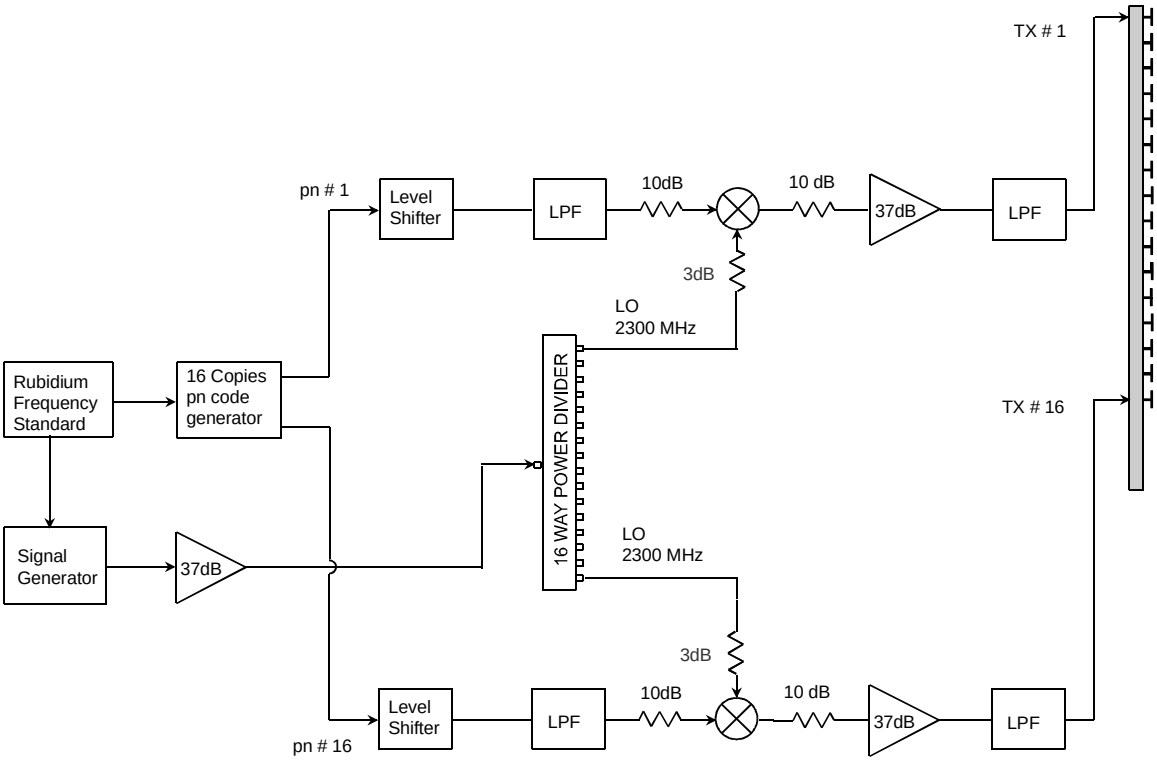

Figure 1. Typical transmitter block diagram.

3. Measurement Sites and Procedures

Figure 2 shows the measurement van configured with an 8 channel measurement system. Four channels of the system were utilized during the initial measurements. The transmit frequencies of this system were set to 450 MHz, 1360 MHz, 2250 MHz and 5750 MHz. The chip rate for all these channels was 10 MHz.

Figure 2. The measurement van configured with an 8 channel receiver.

During the next phase of testing additional channels will be added at 183 MHz, 915 MHz, and 1602.5 MHz. The chip rates for these channels will be 2 MHz, 10 MHz and 5 MHz.

Figure 3. The 5.8 GHz and 2260 MHz transmitter antennas that were used in mall parking lot measurements.

Since close range mobile to mobile measurements are desired the transmit antennas a located between 4 to 6 feet elevation. To speed up measurements the transmitters remained fixed and only the receiver was moved. This allows larger number of sites to be surveyed and hopefully a statistical data base with lower variance to be created for model development. Figure 3 shows a typical arrangement of transmit antennas.

The first measurement sites were in a mall parking lot and a sports complex parking lot. The mall lot allowed easy access and variable conditions as cars moved around the lot. The sports complex was a more urban environment and allowed measurements when the lot was empty and also again when the lot was full. GPS data for both sites are shown overlain on aerial photographs in Figures 4 and 5.

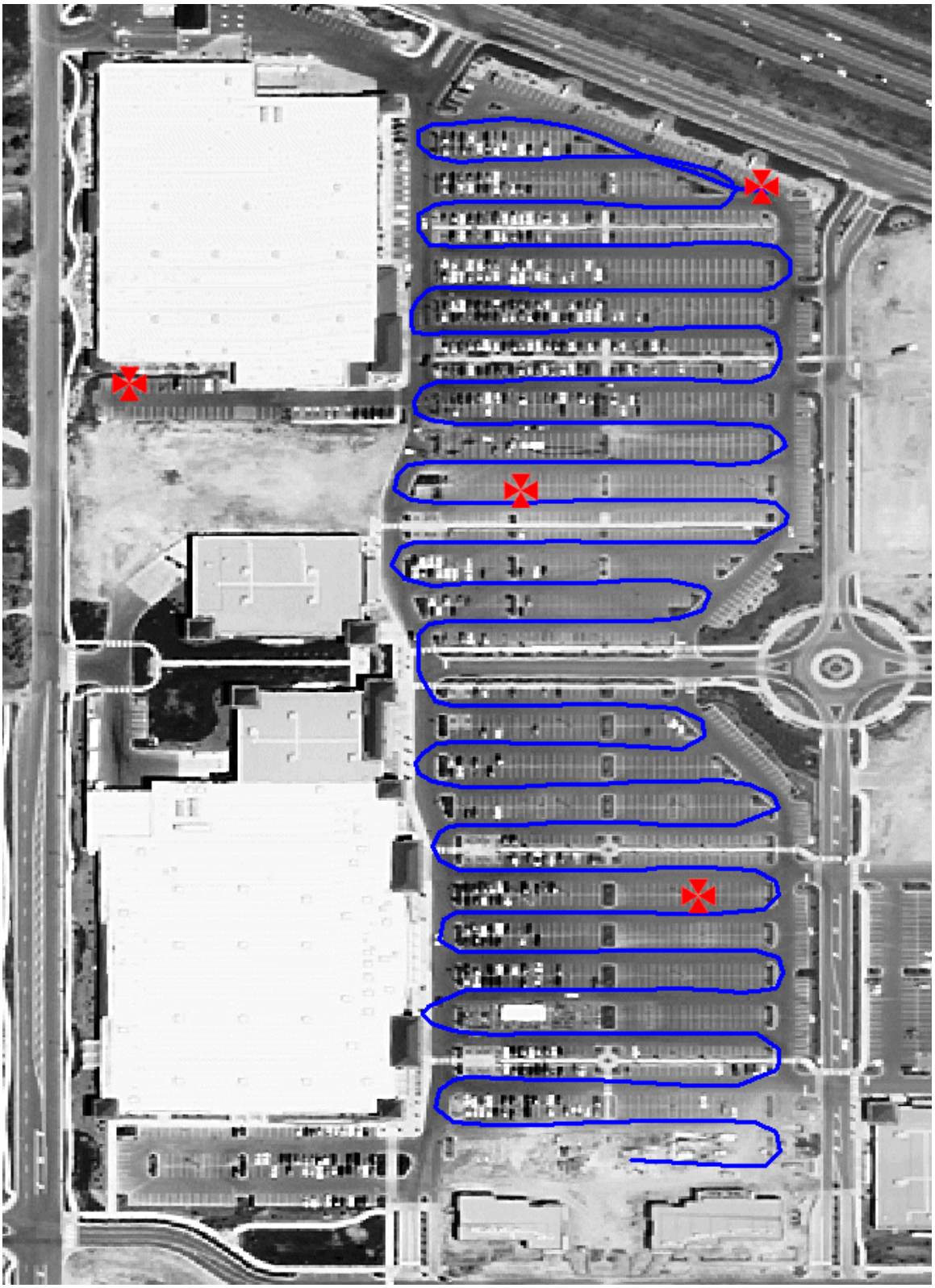

Figure 4. The measurement route and transmitter locations used at a mall near Superior, CO.

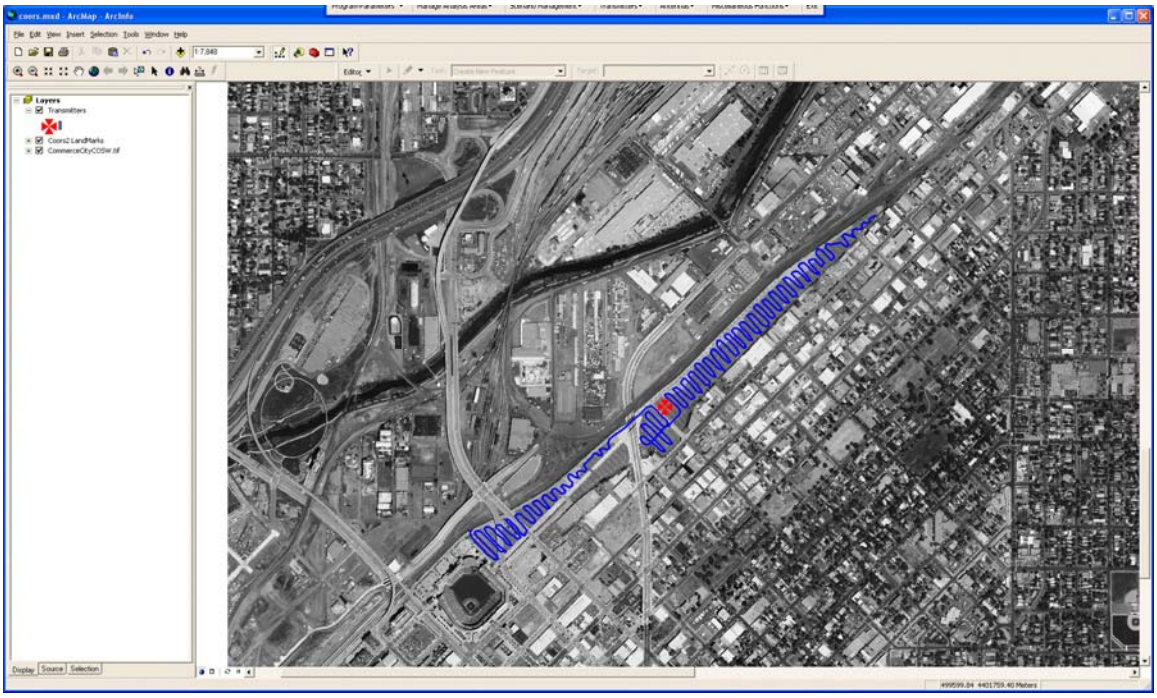

Figure 5. The measurement route and transmitter location used in the sports complex parking lot.

4. Conclusions

Currently measurement work for short range model development is ongoing. Several preliminary data sets have been collected and are being analyzed. Several additional frequency channels are being fabricated. These channels are at 183, 915 and 1602.5 MHz. Interference requirements at these frequencies are of particular interest to OSM. The preliminary results will be analyzed to determine if measurement parameters are sufficient for interference model development over frequencies of interest.

5. Appendix

Table 1. Data Collection Log.

Site	Transmitter	Latitude	Longitude	Relative Power*, Lot Status*	Data Files
Mall	1	39.959675	-105.172203	L, P	881-910
	1			H, P	911-940
	2	39.958392	-105.173217	H, P	941-970
	2			L, P	971-1000
	3	39.958843	-105.174872	H, P	1001-1030
	4	39.956681	-105.172470	H, P	1031-1060
				L, P	1062-1091
Sports complex	1	39.761819	-104.986672	L, E	1093-1102
	1			H, E	1103-1167
	1			H, F	1168-1234
	1			L, F	1235-1244

High Accuracy Nationwide Differential Global Positioning System
Merging Concepts and Techniques from the Past and Present

James Arnold
Federal Highway Administration
(202)493-3265
(202)493-3419
James.a.arnold@fhwa.dot.gov

This paper describes the development and of the High Accuracy Nationwide Differential Global Positioning System (NDGPS), which augments GPS, providing a 10 centimeter positioning accuracy in real time. As a low frequency broadcast using the groundwave technique to broadcast corrections to users on the surface, the broadcast overcomes obstructions commonly limiting use of satellite based services. It was developed to meet the demands of surface based safety related transportation services in both the maritime and land based modes including the Intelligent Transportation System. HA-NDGPS is intended to support a wide range of current and future positioning and navigation requirements for federal, state and local government agencies. Some of the current and future needs of the private sector may also be satisfied, but this is not the primary purpose of the system. Dual coverage will improve system availability from 99.7%-99.9%, meeting the accuracy, integrity, and availability requirements of many safety applications.

1. Introduction.

The High Accuracy Nationwide Differential Global Positioning System (HA-NDGPS) project was established to assess the implementation feasibility for improving the accuracy of the NDGPS service, using the existing infrastructure, to meet the requirements of additional applications without decreasing availability and integrity and still meeting the needs of existing users. Partner agencies include:

Federal Highway Administration
US Coast Guard
Federal Railroad Administration
US Army Corps of Engineers
National Geodetic Survey
Forecast Systems Laboratory
Interagency GPS Executive Board

1.1. Goals.

The project had three major goals. These were to examine ways to enable 3-D dynamic positioning at the centimeter level throughout the US, coexist with existing infrastructure, and minimize deployment costs.

1.2. Project Development.

The project was divided into three broad phases. The first phase emphasized development and integration. Some of the milestones addressed included:

- Develop Modulator and Data Link Receivers
- Interface System Modules
- Broadcast Characterization and Optimization
- Single Site Concept Demonstration

Phase II emphasized pushing the limits and trying applications that could be enabled with the greater accuracy and integrity provided by HA-NDGPS. It emphasized:

- Pre-Broadcast Integrity Algorithm Development
- Multiple Site/Baseline Concept Demonstration
- Ionosphere/Troposphere Prediction
- Application Development

In Phase III, project development into a fielded system is the focus. Some of the areas addressed include:

- Development of Agency Responsibilities
- Integrate Into Existing and Future NDGPS Sites and Control Stations
- Finalize Site Software
- Integrity
- Compression
- Troposphere and Ionosphere Models
- Finalize and Validate
- Develop Compression

2. System Description.

The HA-NDGPS concept broadcasts all code and carrier phase observables for L1 and L2, for up to 12 GPS satellites each second. The system has the capability to include L2C, L5, and other satellite constellations (i.e. Galileo) as they become available, also each second.

2.1. Broadcast Description

The modulation is raised cosine minimum shift keyed, synchronized to GPS. This makes for a very efficient broadcast that can support a multitude of uses.

2.1.1. Data.

The data to be broadcast includes GPS Satellite observables (both code and carrier), data for a tropospheric model, data for an ionospheric model, precise orbit data, and integrity. It can also accommodate observables for other navigation satellite constellations (Galileo, GLONASS, etc), and augmentation systems if they are deemed capable of providing sufficient data to make them useful.

2.1.2. Data Rate

The data rate used to date is 1000 bits per second. This allows for the transmission of all GPS observables in 1-second epochs from 12 GPS satellites. As additional data is added, this is reduced. For example, adding Galileo to the data set would reduce the GPS observables to once every two seconds. Since there is no reason to provide Galileo data every other second, it could be provided every fifth second with GPS observables four out of five seconds. When Galileo becomes available or decisions made on the use of GLONASS, appropriate analysis will be completed to identify the appropriate amount of data that is needed for these other navigation constellations. It may also be possible to increase the data rate at some broadcast locations due to extended coverage and increase signal reliability at longer ranges.

2.1.3. Synchronization.

Both the data and the carrier are synchronized to GPS. In the event GPS fails, synchronization will be maintained with an internal facility atomic clock. Synchronization was done initially to improve the data link reliability at the edge of the coverage area. It provides a moderate processing gain. While this is still the primary goal, it is important to note that carrier synchronization of both the HA-NDGPS and the NDGPS creates a new capability. The dual broadcast from the facility can serve as a ranging signal independent of GPS. The accuracy has not been determined but, depending on the modulator and the transmitter characterization and the distance to the broadcast facilities, the accuracy, in free space, could be better than 1 meter.

2.1.4. Frequency.

The frequency band identified for the broadcast is 435 kHz to 495 kHz. This is a relatively little used portion of the spectrum and is currently allocated for Maritime Mobile on a primary basis and Aeronautical Radionavigation on a Secondary basis. There is no Maritime Mobile operations in the US and little Aeronautical Radionavigation usage. There are certain frequencies that should not be used. 455 kHz is a prime intermediate frequency (IF) used by many inexpensive radios. By there very nature, they are susceptible to interference. While the HA-NDGPS service can legally use this frequency, staying away from it reduces the potential for interference to these devices. Additionally, NAVTEX uses 490 kHz for local broadcast in other than English and, while not used in the US, broadcast on 490 KHz has the potential to impact foreign users. Thus, we will not use 490 kHz. This leaves more than 50kHz available across the US. By reusing frequencies and spacing adjacent facilities no closer than 3 kHz, sufficient spectrum will be available.

2.2. Proof of Concept Deployments.

Thee prototype systems have been deployed to date. These are located at Hagerstown, MD, Hawk Run, PA, and Topeka KS. Plans are to install one more at St. Mary's WV as soon as the site is established. The site locations are highlighted in Figure 1.

Figure 1. Site locations

2.2.1. Broadcast Configuration.

Figure 2 shows the configuration for the broadcast of the HA-NDGPS data. The existing GPS Reference Station (RS) is connected to the rack mount personal computer (PC) via an unused bi-directional RS-232 port. The RS is instructed to generate observables at 1-second epochs and this data is then analyzed in the PC to ensure it meets specific criteria for integrity. The data is then compressed and modulated in the PC and sent to the transmitter where the signal power is increased up to 3 KW and fed to the antenna for broadcast. Note that the data is stored within the PC for later use if needed.

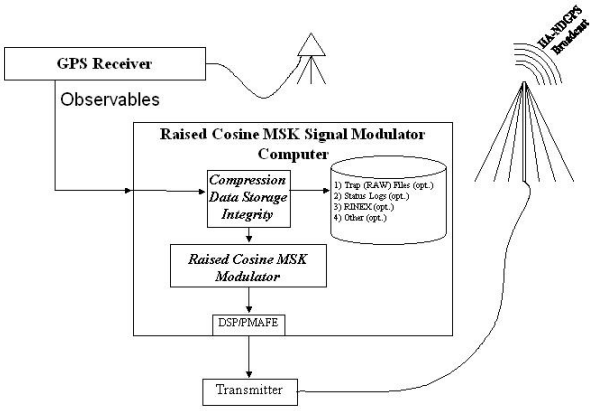

Figure 2. Site Configuration

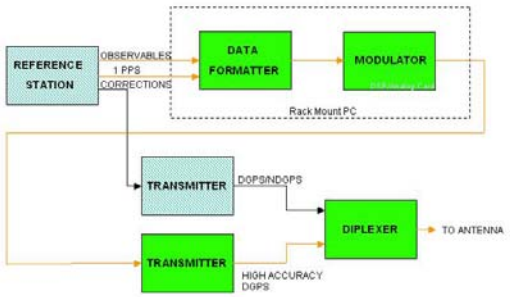

Figure 3. Site Block Diagram

2.2.2. Site Modifications.

Figure 3 is a block diagram of what equipment was added to the NDGPS facility to support the prototype HA-NDGPS broadcast. The equipment added includes a rack mount PC, a transmitter, and a diplexer. The rack mount PC includes a data formatter and modulator card (Figure 4) as well as the data compression and modulation software. Additional cabling includes the RS-232 connection between the RS and the PC, a cable taking the 1 PPS signal from the receiver to the PC, the low power RF cable between the PC and the transmitter, and some 400 feet of LDF-450 between the transmitter and the diplexer.

Two different transmitters have been used. The first was a 1500W unit from Nautel, Inc. This was chosen to meet signal stability and power output requirements. The additional transmitters are 3000W units, again from Nautel, Inc.

The diplexer was designed by Morgan Burroughs and Associates and built by the Saxton Highway Electronics Lab. Figure 5 shows three of the six panels of the diplexer after it was mounted inside the ATU hut at the base of the broadcast tower. Note that the large inductor is approximately 4 feet tall. This gives some idea of the size of the unit.

Figure 4. Data Formatter and Modulator Cards

Figure 5. Diplexer

2.3. End User Prototype Configuration.

The end user configuration is just as straight forward as the broadcast configuration. The signal is received and demodulated. The demodulator supplies a

data stream to the laptop PC. Within the PC, the data is decompressed, stored, and provided to an application residing on the same PC. The example shown combines the demodulated and decompressed observables with GPS data to calculate a solution. In the test configurations we use, all data is stored to the hard drive in the computers so that it can be played back later.

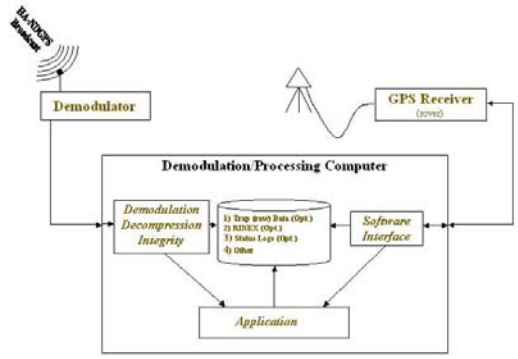

Figure 6. End User Equipment Block Diagram

3.0 Deployment Configuration.

3.1. Broadcast Facility

3.1.1. Hardware Configuration.

Figure 7 is a block diagram of the proposed broadcast facility as it would be in a fully updated and recapitalized NDGPS broadcast facility. Note that the additions to the baseline provided by the Coast Guard include a PC, atomic clock, transmitter, RS232 Ethernet converter, coupler, diplexer, computers and low power RF cables, and a roughly 400 foot long RF cable from the amplifier to the coupler. It is important to note that the diplexer design did not take into account that a coupler would be installed and vice versa. Thus, it is possible to design portions of the diplexer into the couplers, reducing costs, space, and potential equipment failures.

3.1.1.1 Transmitter.

During discussions with transmitter manufactures, it has been determined that it may be possible to combine the two amplifiers into a single unit with common modules. There are questions concerning the cost and reliability of such a unit. The additional cost, if any, may be offset by the reduced cost of shelters for established broadcast sites.

3.1.1.2. Atomic Clocks

The atomic clocks that assist in maintaining a backup navigation capability are directly linking one GPS receiver with two reference stations. This is not likely to be the final configuration but is provided here for simplification. When the final design is complete, it may be possible to provide the time synchronization through the network devices, but care must be taken to ensure no unknown delays occur.

3.1.1.3. GPS Receivers

The GPS receivers identified in the block diagram are L1/L2 units. It is expected that this will be upgraded to include L5 and Galileo as these signals and systems become available. If at all possible, these should be procured early in the deployment program in order to maximize the usefulness of the system. Since much of the control of these receivers is performed in software, the software can be upgraded via the frame relay network connection.

3.1.1.4. Computer

The PC contains not only software to interface to the various GPS receivers, but also the modulator card and its associated software. The modulator card for HA-NDGPS could, potentially, reside in the same computer as the legacy modulator. In the diagram shown here it was drawn as a separate computer due to the limited space within the currently identified computer. The Coast Guard has already procured several of these computers and, unfortunately, they do not have sufficient space to support two modulator cards. Two potential configurations could be employed. The first would have four computers for each site, using the supplies already procured. The second could have two computers per site, using a newly procured computer with sufficient space for two modulators.

3.1.1.5. MSK Receiver

The MSK receiver is a multi-channel device use to monitor the local broadcast, both legacy and HA-NDGPS. It could be used to monitor adjacent sites as well, providing status information to the Network Control Station if communication with the adjacent site is lost.

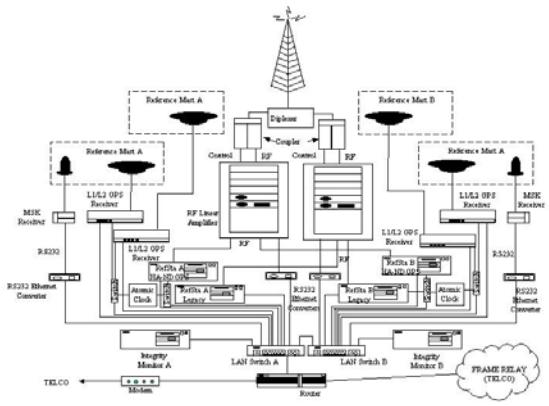

Figure 7. Proposed Broadcast Facility Block Diagram

3.1.2. Software.

There are three main software programs within the HA-NDGPS systems; (1) a program to interface with the GPS receiver and compress the observables, (2) a program to modulate the compressed observables onto the 450kHz carrier, and (3) an overall control program.

3.1.2.1. GPS Receiver and Reference Station.

Communications between the GPS receiver and the Reference Station PC, be it HA-NDGPS or legacy, is over the Ethernet link. In the existing configuration interface software from Trimble is used to pull data from the GPS receiver and format it for the modulator. This software, GPS Receiver Interface Module (GRIM), is available off-the-shelf and can be used for both the HA-NDGPS system and the legacy system. GRIM offers several compression schemes as well as data storage options, each selectable by the user.

3.1.2.2. Modulator

The software for the modulator has gone through several iterations from the initial development program. It is now finalized and an easy to use graphical user interface (GUI) has been developed. It can be used to select the modulation frequency and data rates, among other options.

3.1.2.3. Control Software

Both GRIM and the modulator program can be controlled, or initiated, by the High Accuracy Control Program (HACP). In the event power is lost to the computer, HACP provides the initiation routine to enable both GRIM and the modulator program without a control operator needing to intervene.

3.1.3. Additional Information to the End User

3.1.3.1. Integrity.

Integrity has not been fully defined at this point. Currently we examine the residuals and if they fall outside a predetermined bound, the data from the satellite that causes that out of bound condition is eliminated from the data stream to the modulator before it is broadcast. This provides a near instantaneous integrity function. Further work will be completed to define what the user is told about the removed data and to demodulate the data after it leaves the modulator to ensure its accuracy. The capability will also be added to monitor the actual broadcast to look for gross failures. This information will be provided to the user at the next epoch. Additionally, a panel will be convened to examine the software to ensure it adequately addresses all the concerns a safety of life system should address.

3.1.3.2. Atmospheric Models

The Forecast System Laboratory (FSL) has been under contract to develop predictive models for the ionosphere and the troposphere. The tropospheric model is undergoing validation testing and the ionospheric model should be entering that phase shortly. Trimble has been contracted to add these to the existing HA-NDGPS data stream. It is intended to trickle this data out over several minutes, but provide enough data every few seconds to allow users to improve their navigation solution.

The method for supplying this data to the broadcast site has not been determined and is the subject of further work. Currently, it is envisioned the tropospheric and ionospheric data will be provided to the National Control Station (NCS) and the model will be run there. The output from the model will then be parsed to the individual broadcasts sites. Once received at the sites, it will be encoded, compressed, and provided to the end user through the broadcast.

3.1.3.3. Precise Orbits.

The usefulness of precise orbits broadcast from the reference stations has been debated for some time. With the Improved Clock and Ephemeris from the GPS constellation there has been some doubt that it is necessary. It is expected that the precise orbits, broadcast from the reference stations, will be useful and current plans call for including it in the data stream. The source of the precise orbits will be determined in the near future.

3.2. End User Equipment

The current demodulator used for test scenarios is a single channel modified DNAV-212 from Raven Industries. While these units are adequate for testing, additional capability will be needed to make full use of the broadcast. The end goal for the

development and engineering phase demodulator/receiver is to have at least four independent channels (six will provide additional capability long term, but four is sufficient to prove the current concepts) that can be tuned to either the legacy service or the HA-NDGPS service in such a way as to select all legacy channels, all HA-NDGPS channels, or some combination of the two. The demodulators will also be capable of synchronizing to GPS in order to pull the weaker signals out of the noise at the edge of the coverage area, effectively increasing the range of the broadcast.

The output of the demodulator can be selectable at this time. Vendors will be able to create their own data since they will have access to either the observables (in the case of the HA-NDGPS broadcast) or the data routinely sent over the NDGPS service. Thus, the output can be a RTCM type 9 message, RTCM type 18/19, or a vendor proprietary format. The test units will provide either the observables or the RTCM type 18/19 messages, along with integrity and troposphere and ionosphere model data as they become available.

4. Work To Be Completed.

Several efforts need to be completed in the near term. Several of these were identified above include integrity, atmospheric modeling, and precise orbits. During this same time frame, development of a standardization package for the end user data shall be developed for coordination with RTCM or another standards organization, implementation designs, and identification of NCS upgrades.

4.1. Phased Approach.

One of the strengths of the approach used in the development of the HA-NDGPS program has been the addition of capabilities over time. For example, inclusion of a rack mount PC running GRIM in the reference station allows the collection and dissemination of the GPS observables to NGS immediately. With slight modifications, this will also allow the site to collect site status information and hold it if commercial communications are lost. The data can then be provided to the NCS once communications are restored. This approach allows us to incrementally field HA-NDGPS where site conditions will not allow a full implementation immediately, but also allow the implementation of additional capability (i.e. ephemeris) as the data becomes available.

4.2. Additional Work to be Completed

4.2.1. Requirements Definition

This is the first item that will be completed since much of the additional work depends on the basic requirements placed on the system. The top-level requirements have been identified and built to in the prototype systems. Additional descriptive language will be used to provide guidance to implementers and identify functional requirements. It is important to note here that how something is done is very different from what capability needs to be included. Thus, the requirements definition will focus on capability first and address how as a derived requirement.

4.2.2. Signal Specification

Many aspects of this have been defined, tested, and documented, but needs to be placed in a signal specification document. Since this is one of the earliest products needed, it will also be one of the earliest deliverables.

4.2.3. Automatic Control and Data Logging

The USCG has discussed this over the years and the recent events along the Gulf of Mexico have heightened the need for a quick solution. A multi-pronged approach is proposed here.

First, collect all the observables at 1-second epochs and send them to NGS, along with integrity data is it becomes available. There appear to be two ways of doing this.

One way, which we shall call approach 1, appears easiest, would convert the data from RS232 to Ethernet and monitor/control it with a separate PC in the equipment hut running GRIM. GRIM would be there to ensure that after a reset the particular port we are interested in is reset to the appropriate data rate as well as store the data and forward it at a later time if communications to the site are last.

The other way, which we shall call approach 2, while more complicated, may offer a longer-term solution. This can be accomplished quickly by, again, installing a rack mount PC and adding a second virtual data link to the site to provide data back to NAVCEN and NGS. During times when commercial communications are lost, the data can be stored locally at the site and forwarded once communications are restored.

The second part of this is to tap into the existing RSIM data and log it at the end of each epoch of GPS data. If communications is lost, the data can be stored until communications is restored or, in the case of a HA-NDGPS modification, it may be possible to include it at the end of the broadcast.

The third and final prong of this work would provide two-way communications to the NDGPS facility. In the event of commercial communications loss, the data can be sent, by exception, to one of the control stations by an alternate communications link, perhaps satellite. The station can also be controlled and

if additional data is needed that has been recorded, the site can be instructed to provide that data.

4.2.4. Equipment Specification

Much of the equipment that has gone into the HA-NDGPS prototype installations has had specifications developed for it. Much of this work should be transferable to the deployable installations. Thus, this work will focus on documenting equipment specifications that have already been developed and identifying equipment and documenting its specifications prior to full-scale deployment.

4.2.5. Receive Data Standard.

The approach decided upon was to use an off the shelf compression, modulation, and control program. This package is collectively called the broadcast software. Each of these can be purchased or licensed in sufficient quantity and at a low enough price that it does not appear to be reasonable for the Government to develop one independently. Add in the cost of maintaining the code, and the benefits to purchasing off the shelf software increases substantially. Since this will be a safety system, care must be exercised to ensure it meets the required level of acceptability. Thus, portions of the software have been negotiated to be opened to review by a panel established by the Federal Government.

Given that the broadcast software is proprietary, concerns about the decompression/demodulation software (referred to as the user software) could arise. This raises the concern that the user software would be proprietary. The developer has agreed to make the user software available as an open standard and assist with providing it to a standards group.

4.2.6. Atmospheric Models

The two models that are being developed, one for the troposphere and one for the ionosphere, have been in development for several years. Much of the work that remains is speeding up their prediction capability (in the case of the ionosphere model) and validating them. Incorporation of both models into the broadcast software has begun. Techniques to move information on both the troposphere and ionosphere to and from the reference stations need to be detailed and their impact on the overall system need to be defined.

4.2.7. Integrity

The current integrity function examines the residuals in the carrier data and, if they are outside a predefined envelope, the data from the satellite is removed from the data steam prior to modulation. Additional integrity will be added including using the observables with a second receiver to verify solutions are where they are supposed to be.

As the integrity function develops, an Integrity Panel made up of Government and Private Sector experts will be convened to ensure the integrity defined meets the requirements established by potential users.

5. Summary

Combining old concepts with new technology, we have created a service that exceeds the expectations of most users. Accuracy is better than 10 cm horizontal 95%, integrity is instantaneous, and availability is above 99.9% in the defined coverage area.

The prototype systems have been functioning for several years and have provided a test bed for controlled development. Users are being defined and their requirements built into the system. Some work remains to be completed to document the system and finalize it for full deployment, but that is straight forward and can be accomplished quickly.

BPL Update: 2007

Ed Hare, ARRL Laboratory Manager
225 Main St
Newington, CT 06111
Phone: (860) 594-0318
Email: W1RFI@arrl.org

This paper provides a brief tutorial on BPL; a short explanation of the regulatory history that has led to the present set of FCC rules governing BPL; a brief overview of the FCC regulations and a summary of the electromagnetic compatibility (EMC) issues and problems associated with BPL. It also looks to the common ground that does exist between the players in this field (preventing and resolving interference, for example). The paper describes how some in the BPL industry have been improving their designs past the limitations of the present BPL regulations and communicating cooperatively with ARRL to help design BPL systems to avoid major interference problems.

1. Introduction

Broadband over Power Lines has been touted as a "disruptive technology," a complementary term generally applied to new technologies that are expected to result in major changes to our social environment and have a major impact on other technologies. Others have noted that the radio noise levels, frequency use, and time and geographical distribution factors will result in BPL having a disruptive effect on nearby radiocommunications. These two views have, to some extent, separated into camps that don't at first glance appear to have a lot of common ground.

Although there is no doubt from the record that BPL can and does have major interference issues to address, recent history shows that if BPL carefully follows good EMC engineering practice and avoids locally used spectrum sufficiently well, the industry can address EMC problems and ultimately enjoy installations that are successful from an EMC perspective.

2. About ARRL and Amateur Radio

Many of the BPL EMC issues have been focused on the Amateur Radio Service. Amateur Radio is a licensed radio service governed by international treaty and local government rules. Its licensees are pursuing a personal interest in radio communications, without pecuniary interest. Amateurs, often known as "hams," must pass a rigorous technical and operating examination in order to become licensed. Amateurs have access to small segments of spectrum starting at 1.8 MHz and extending past 300 GHz. Amateurs are perhaps best known for their organized role in emergency and public-service communications. But its licensees also contribute to technology and international goodwill.

Worldwide, there are approximately 3 million Amateurs. In the US, there are, at this time, there are over 650,000 licensees. Recent changes to the FCC rules governing Amateur Radio have removed the Morse-code-testing requirement, so it is expected that the number of licensees will increase somewhat over the coming months and years.

ARRL is the National Association for Amateur Radio in the United States. Its administrative headquarters is located in Newington, CT. It has about 150,000 licensed Amateurs as members, many of whom serve in a volunteer capacity within the organization. ARRL represents the interests of Amateur Radio in regulatory proceedings, on industry committees and in media public relations, to name a few areas. It provides information about Amateur Radio to its licensed members and the public. Naturally, ARRL's interest in BPL has stemmed from the EMC potential and experience in BPL systems.

ARRL's interest in BPL extends only to its interference aspects. Other than interference issues, ARRL would see and treat BPL no differently than any other technology. Amateurs are interested in technology, and are often early adopters of new technology.

ARRL's web page at http://www.arrl.org has more information about ARRL, Amateur Radio and BPL. The BPL page can be accessed at http://www.arrl.org/bpl.

3. BPL Tutorial

BPL uses electrical power-line wiring to send high-speed digital signals from point to point and to network those signals to the Internet. It comes in two flavors. The first is known as access BPL. This uses the electrical distribution system to provide Internet access to homes and businesses, and to provide a broadband communications channel for certain electric-utility applications. Because much of

the electrical distribution system uses overhead wiring that has the propensity to radiate any noise that may be present on the lines, access BPL has been the focus of most of the EMC concerns associated with BPL. Access BPL has also been involved in all of the EMC problems that have cropped up from BPL deployments.

In-premise BPL uses building wiring to send high-speed digital signals within a building. It can be used to connect computers to a router or to form a network of computers within that building. Uses can range from creating a local-area network using the building's wiring to providing Internet access to rooms in hotels. The attractiveness of in-premise BPL is that it is often possible to network a building quickly without the expense of adding new wires. The downside is that in some cases, one part of the building does not seem to network well to other parts of the building, as outlets on opposite phases may not be connected well to each other.

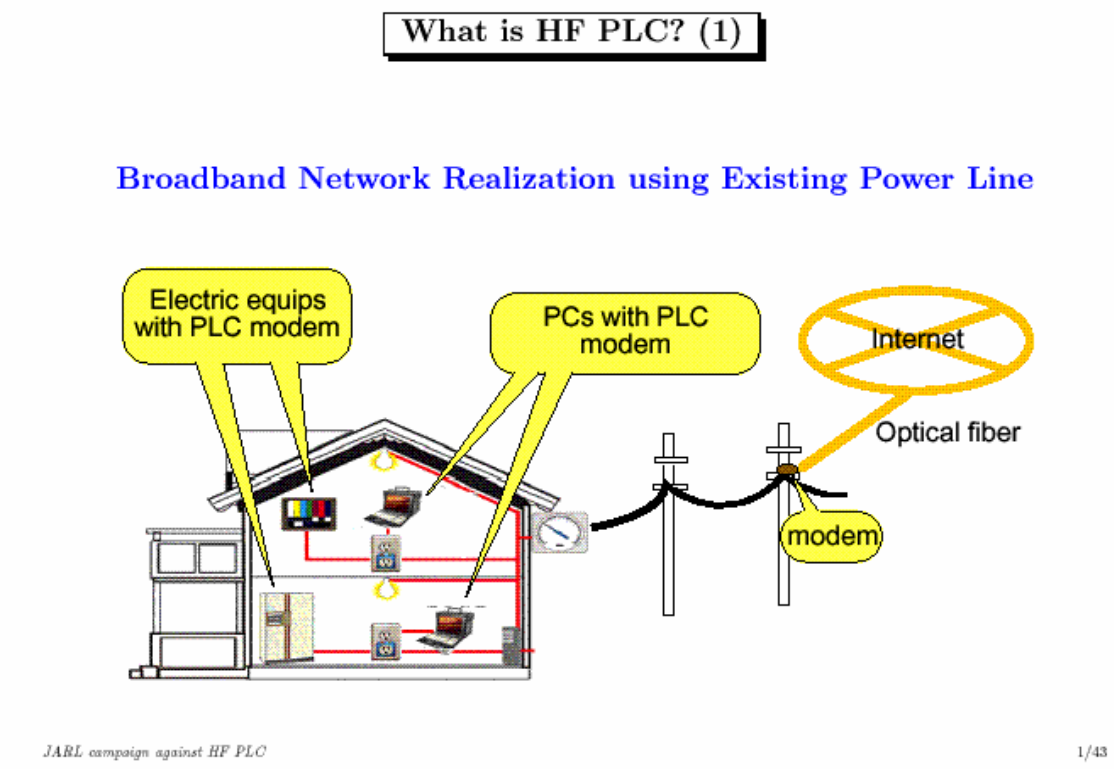

Figure 1 -- BPL, also known as Power Line Communications in some parts of the world can be used on electrical distribution lines (overhead and underground) for access BPL or within a building for in-premise BPL. Electric utilities may use a combination of access and in-premise BPL for utility applications.

Utility applications can cross into both areas. Utilities may use BPL within a substation or building, or may extend that into the distribution network. At this time, access BPL is becoming less attractive, as competing technologies such as cable or DSL become more entrenched. Utility applications, however, are becoming more important. This can include things like remote meter reading; time-of-day or rate-based pricing; equipment control; video monitoring. These concepts are gradually evolving into various "smart-grid" concepts, where the ability to monitor, communicate with and control the electric power grid are intended to improve the reliability of the system; control costs and perhaps even in the long run, have a positive effect on things like reduced emissions of greenhouse gasses. All in all, everyone agrees that these are all good things to do. It remains to be seen what role BPL should play in that, as the balance between the cost and performance issues of BPL vs other technologies that can accomplish the same thing are better understood.

Power lines are also a noisy environment, and devices like electric motors or relatively minor failures on primary distribution equipment (such as an insulator on a power pole becoming noisy) can and does have a negative impact on BPL, sometimes to the point of causing it not to work. BPL systems can and do interfere with each other, as the different

types of BPL are neither interoperable nor compatible. The industry has been trying hard to address this through standardization, primarily through various IEEE committees, with little success to date.

4. Regulatory History - A Brief Overview

A discussion of the complex and sometimes convoluted history of BPL regulations could be a paper in and of itself. In April, 2003, the FCC opened a Notice of Inquiry (NOI) (ET 03-104). The NOI asked a series of questions about BPL, most related to the EMC aspects of the technology. ARRL, BPL manufacturers and others responded, answering the questions and providing information to represent their positions. In general, radiocommunications users outlined the EMC issues and concerns, while the BPL and electric-utility industries generally dismissed the EMC issues, focusing on the value of BPL as a technology. All told, over 6000 comments were received in this proceeding, many from Amateur licensees.

In February, 2004, the FCC issued a Notice of Proposed Rulemaking for BPL. The 1800 comments received repeated many of the arguments raised in the NOI, adding new information about interference and the value of BPL. This culminated in an FCC Report and Order in October, 2004, announcing new rules. Soon thereafter, ARRL and BPL-industry proponents filed various Petitions for Reconsideration; Opposition to Petitions for Reconsideration and new Petitions for Rulemaking.

In August of 2006, the FCC issued a Memorandum Opinion and Order, dismissing most of the new petitions, and making some changes to the rules. In August of 2006, ARRL filed the necessary paperwork in federal court and with the FCC to institute an appeal in federal court with respect to certain procedural and technical issues with the rulemaking.

5. Final Rules

It should be noted that prior to the enactment of these new rules, BPL was governed by the other provisions on CFR47, Part 15, of the FCC's rules. The new rules added significant new restrictions to BPL that are intended to address the EMC issues raised during the proceedings.

The major technical components to the rules that govern BPL are:

- The new rules govern BPL that operates between 1.7 and 80 MHz. This range includes a number of licensed uses, from commercial HF to VHF television broadcast. In residential neighborhoods, spectrum use includes the reception of international shortwave broadcast; Amateur Radio and CB.
- BPL is an unintentional emitter of RF energy. BPL is also a carrier-current device. As such, it needs to meet the FCC emissions limits for intentional emitters. As a carrier-current device, it is exempt from the conducted-emissions limits that govern most unintentional emitters.
- Under the rules, access BPL equipment must be certificated by the FCC before it can be marketed. Certification is a process where the applicant must test the product extensively and submit test results to the FCC. In the case of BPL, Certification can be done only by the Commission, not the Technical Certification Bodies that authorize most products.
- The FCC outlined a complex test procedure for BPL systems that require testing at three typical overhead and three typical underground installations; testing at maximum power levels and data rates; testing across the entire frequency range used by BPL; testing at multiple points along overhead lines and at multiple angles around buildings.
- BPL must not generate intentional signals in 12 bands of spectrum deemed to be of critical importance. (Although the FCC indicated that BPL has a minimal interference potential, it carved out these 12 bands of spectrum that BPL cannot use.)
- BPL must not operate in certain locations near critical installations, as outlined in the rules.
- The ZIP-code locations; frequencies used and contact information for BPL operators must be included in an industry BPL-interference database.
- BPL systems must be designed with the ability to remotely configure frequency use, power levels and have a remote shut-off mechanism.
- As an unlicensed, unintentional emitter, BPL must not cause any harmful interference to licensed users of spectrum and must accept any interference caused to it.
- The rules specify that for mobile stations only, a level of less than 20 dB lower than the FCC emission limits will not be considered to be harmful interference. Because this still represents a strong noise level that degrades the mobile environment by tens of dB, this is one of the issues being challenged by ARRL and others in the Federal Court of Appeals.
- Under the rules, the responsibilities of the BPL manufacturer (certification) and the BPL operator (not cause harmful interference) must

both be met if BPL is to address its regulatory EMC responsibilities.

An important point: Meeting the FCC emission limits is not enough to avoid harmful interference to local radiocommunications.

6. How BPL is Different from Other Types of Unlicensed Emitters

Under the rules, BPL is governed by the same rules that apply to most other types of unlicensed emitters. However, BPL is different in many ways from most other noise sources:

- Most noise sources emit strongly on only specific, spot frequencies. BPL emissions completely occupy tens of MHz of spectrum.
- Many noise sources are intermittent in nature. Generally, access BPL systems operate continuously.
- Most noise sources are localized to areas only near the building they are located in. Access BPL that uses overhead wiring emits at strong levels for as much as a kilometer or two along the line.

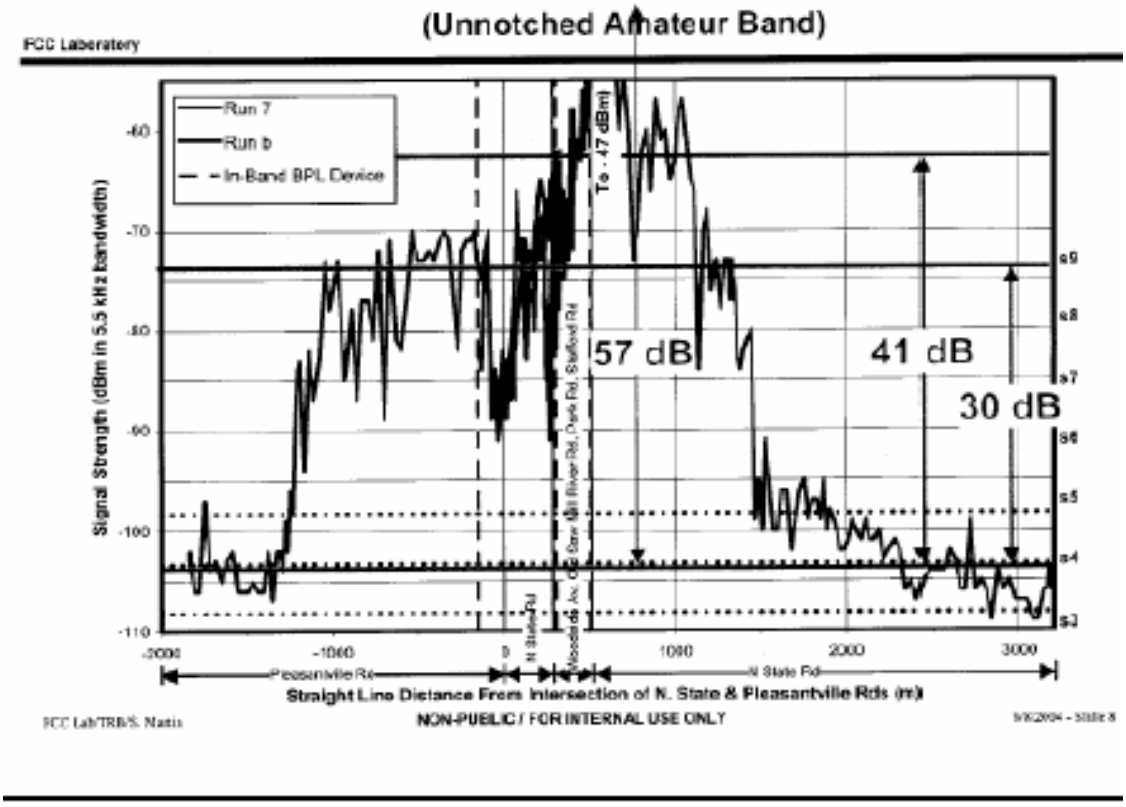

Figure 2 -- This graph from an FCC report shows the measured noise levels from a BPL system (generation 1) located near New York City. The noise was measured at 57 dB greater than the noise up or down the line a kilometer away from the source. It is typical for BPL noise operating at the FCC emissions limits to be strong for as much as two or three kilometers along an overhead power line.

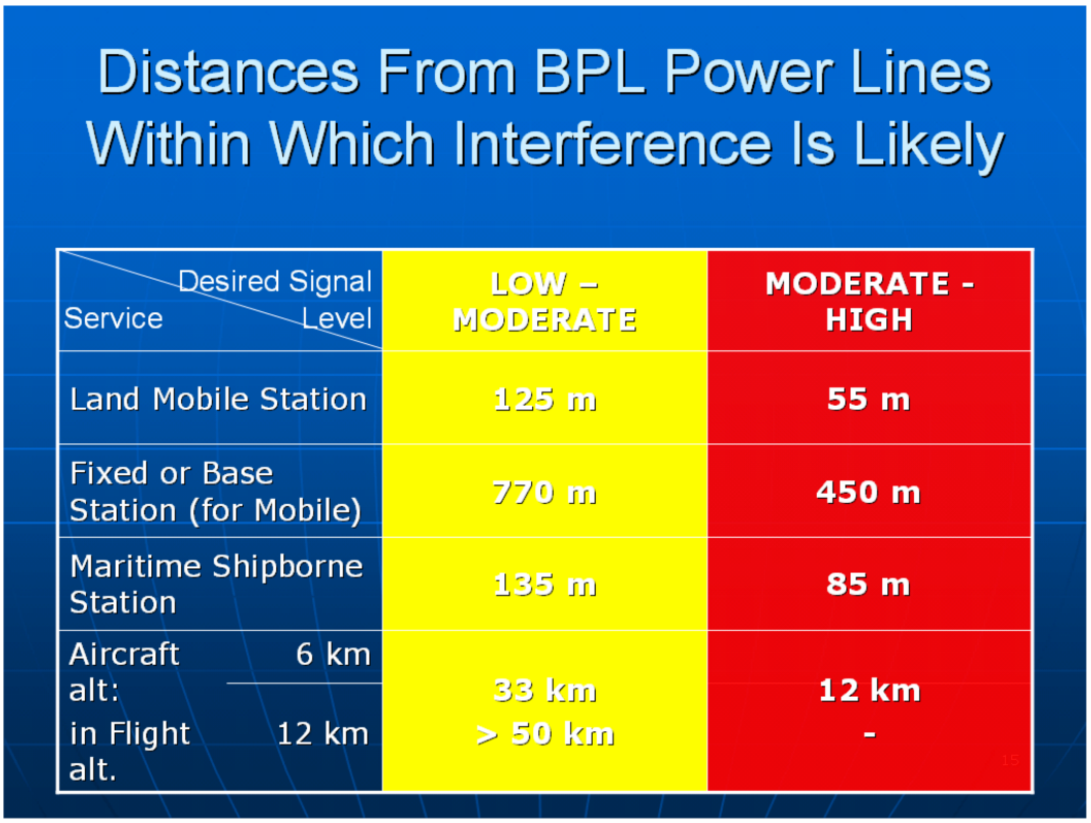

Figure 3 -- This chart, taken from the NTIA Phase I report on BPL, shows that the likelihood of interference from BPL is moderate to high for distances of 450 meters from BPL sources for fixed stations, as an example. Most fixed stations are located closer than 450 meters from overhead power lines or neighboring homes.

7. Emissions limits

It has been ARRL's position that a device that exhibits these significant difference from other types of devices should not be permitted to operate at the relatively high noise levels permitted to devices whose interference potential is smaller than BPL.

The emissions levels permitted to BPL over the HF and VHF range are:

Frequency	Limits and distance	Measurement bandwidth	Detector
1.7-30 MHz	30 uV/m at 30 m	9 kHz	Quasi-peak
30-88 MHz	90 uV/m at 10 m	120 kHz	Quasi-peak
88-216 MHz	150 uV at 10 m	120 kHz	Quasi-peak
216-960 MHz	210 uV at 10 m	120 kHz	Quasi-peak
960-1000 MHz	300 uV at 10 m	120 kHz	Quasi-peak
> 1000 MHz	300 uV at 10 m	1 MHz	Average

8. Locally, the FCC Emissions Limits Result in Strong Signals

Below 30 MHz, for example, a signal of 30 uV/m is many tens of dB greater than typical, local ambient noise levels.

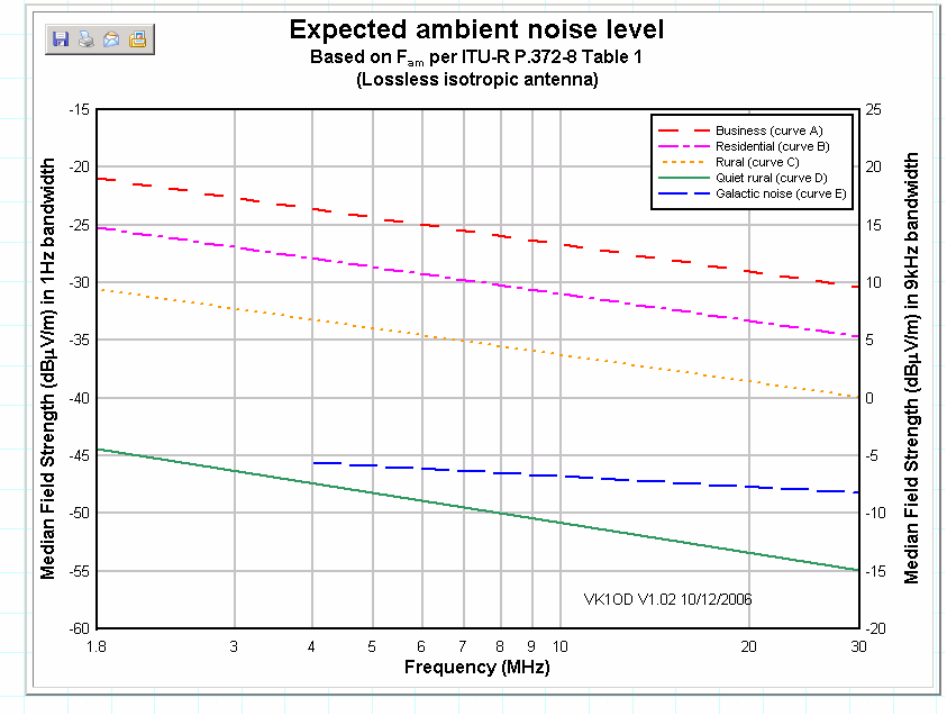

Figure 4 -- This shows the expected levels of the median values of man-made noise in various environments, based on the ITU-R Recommendation P-378.2. The minimum levels on quiet parts of an Amateur band and at quiet times can be as low as the minimum levels shown on the graph.

From an HF radiocommunications perspective, the FCC limits represent strong signals. Stations in the Amateur Radio Service often operate at or below the levels shown in Figure 4 above. The levels shown as the median values of man-made noise are described in ITU-R Recommendation P-378.2. In this context, the term "median" means that half of the measurements were above the values shown, while half were lower. The minimum values of man-made noise as measured can be tens of dB lower the median values. Most noise is not constant with time or frequency. Even when man-made noise is relatively high, there are frequencies or times when the noise level is much lower. Licensed radio services, such as the Amateur Radio Service, that have frequency agility will make use of the quieter part of the band and times.

So a constant noise source such as BPL can degrade that Service even more than the levels shown in Figure 4. As an example, on 28 MHz at night, it is likely that distant noise will not propagate to the area by skywave. In that case, the minimum levels of noise shown on the graph in Figure 3 will likely represent the ambient noise levels in a quiet location. Stations operating in the Amateur Service will often make use of the local non-skywave communications paths. Broadband emitters will in that case, degrade local communications by 50 dB or more.

As a practical example of the strength of Part-15 level signals locally, let's look at a "legal" signal on 3.5 MHz. Under the FCC rules, this could be at a level of 29.5 dBuV/m at 30 meters distance (30 uV) and a level of 49.5 dBuV/m to a typical mobile antenna located 10 meters slant-range (hypotenuse) from overhead power lines. This would result in a calculated noise level of -86.4 dBW as received on a 3.5 MHz dipole located 30 meters from the source. To translate this into terms better understood by most licensed operators using a radiocommunications receiver, this is S9+15 dB on most receiver signal-strength meters. Locally, this is a very strong signal.

BPL operating at the FCC emissions limits is much stronger than the ambient noise levels typically found in residential environments. In fact, it is also stronger than most of the signals routinely used for communications by licensed users below 30 MHz. In areas where BPL is operating, on the spectrum it is using, only the strongest of signals are typically above the BPL levels, and even those are almost always going to be somewhat noisy.

9. EMC - The Bottom Line

It is pretty clear that near power lines carrying BPL, if BPL systems are operating at or near

the FCC limits, interference is almost inevitable if there are receivers nearby trying to use the same spectrum that BPL is using. The permitted levels are clearly stronger than most of the signals used for communications.

The bottom line is that if BPL is going to avoid causing harmful interference -- and the rules say that the operators of BPL systems must -- it must not use spectrum that is use locally. In residential neighborhoods, this includes Amateur Radio, Citizens Band, International Shortwave Broadcast and broadcast television.

10. Harmful Interference

The issue can boil down to "harmful interference." There has been some disagreement between the players in this arena as to what constitutes harmful interference.

Harmful interference is defined in the rules as any disruption of emergency communications or the repeated disruption of other radiocommunications services. Merely hearing a noise on a particular frequency does not constitute harmful interference. For example, if that noise is at or below the emissions limits and is occurring on a frequency that no one is using locally, then harmful interference may not happen. Even within the Amateur Radio Service, not all noise constitutes harmful interference. For example, a noise that occurs on only one narrowband frequency may not cause harmful interference if the licensed operator can easily choose to use a different frequency for the same communication. A noise that is present only for a very short time period, and not very often, also many not be overly disruptive.

For those reasons, the FCC limits can work -- to a degree -- for isolated, local sources. However, as discussed earlier, BPL that operates over a wide swatch of spectrum, all of the time, along kilometers of overhead power lines, or in entire neighbor hoods or communities, has a dramatically different interference potential.

The converse is true -- if BPL at the FCC limits operates on spectrum that no one is using locally, locally, it will not cause harmful interference.

This is part of the reasons that BPL operators and licensed spectrum users see the EMC issues differently, however. To a BPL operator, the majority of a BPL system will not be located near a licensed station at any particular time, so interference will be rare. To that licensed station, however, if BPL is operating on nearby overhead power lines, or the station operator is mobile in the BPL area, BPL interference will not be rare at all -- it will probably be occurring nearly all of the time.

11. This is NOT Just and Amateur Radio Problem

BPL and EMC is *not* just a problem involving Amateur Radio. During the FCC rulemaking, a number of users, from the US military to law-enforcement agencies to broadcasters and their organizations filed comments with strong concerns about BPL interference issues. In most BPL areas, for example, even those systems that do a good job protecting Amateur Radio, international shortwave broadcast and WWV time signals are strongly affected.

12. Cooperation

So far, this paper has presented a rather unenthusiastic picture of BPL and its interference potential. It should leave little doubt that there are ways to do BPL "wrong" that will result in harmful interference to nearby users. This interference is not theoretical -- it has been observed and reported in a number of BPL systems installed to date.

ARRL has a long track record of working cooperatively with industry to help it prevent major interference problems and to resolve them if they occur. For example, it maintains regular contact with the cable and DSL industries, to help ensure that any interference issues involving their technologies can be managed effectively.

This cooperation has extended to the BPL industry, long before access BPL was envisioned. For example, in the 1990s, ARRL worked effectively with HomePlug (http://www.homeplug.org), to help its member companies decide to implement an industry specification that did not use the licensed Amateur bands.

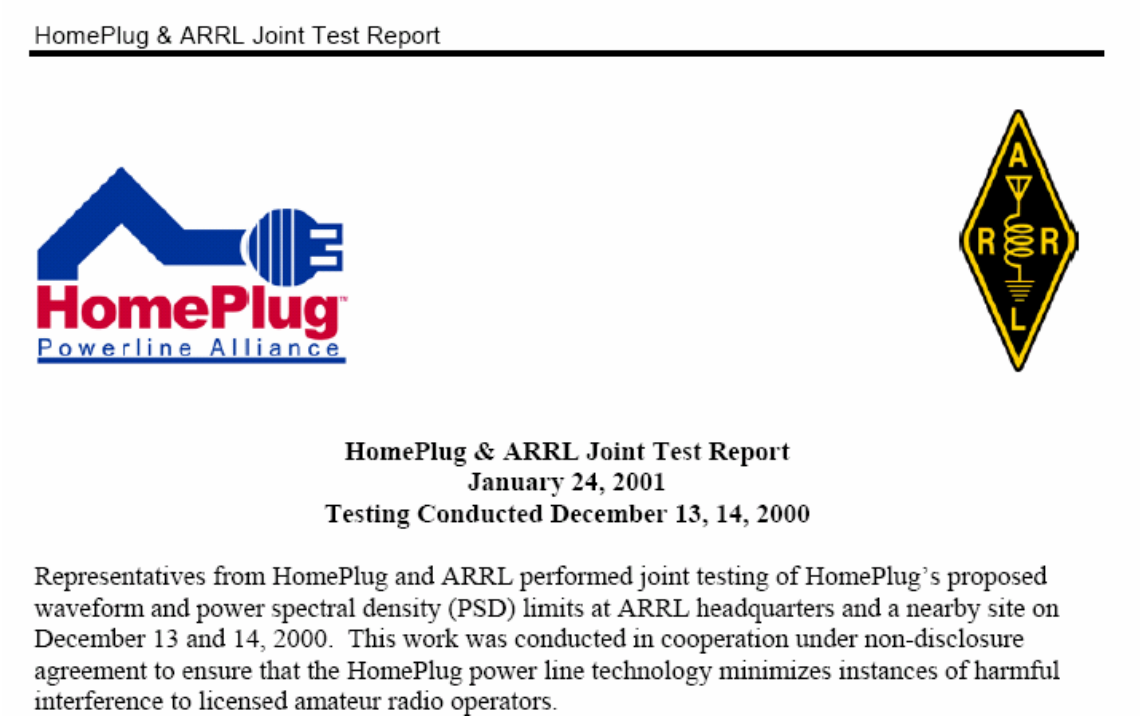

HomePlug & ARRL Joint Test Report

HomePlug & ARRL Joint Test Report
January 24, 2001
Testing Conducted December 13, 14, 2000

Representatives from HomePlug and ARRL performed joint testing of HomePlug's proposed waveform and power spectral density (PSD) limits at ARRL headquarters and a nearby site on December 13 and 14, 2000. This work was conducted in cooperation under non-disclosure agreement to ensure that the HomePlug power line technology minimizes instances of harmful interference to licensed amateur radio operators.

Figure 5- ARRL and HomePlug worked cooperatively together to help design an industry specification for in-premise BPL that has deployed without major interference problems.

This approach was successful for the HomePlug industry and for licensed Amateur Radio. At this point, with over 6 million HomePlug BPL companies deployed, ARRL does not have a single report of interference to Amateur Radio from HomePlug devices.

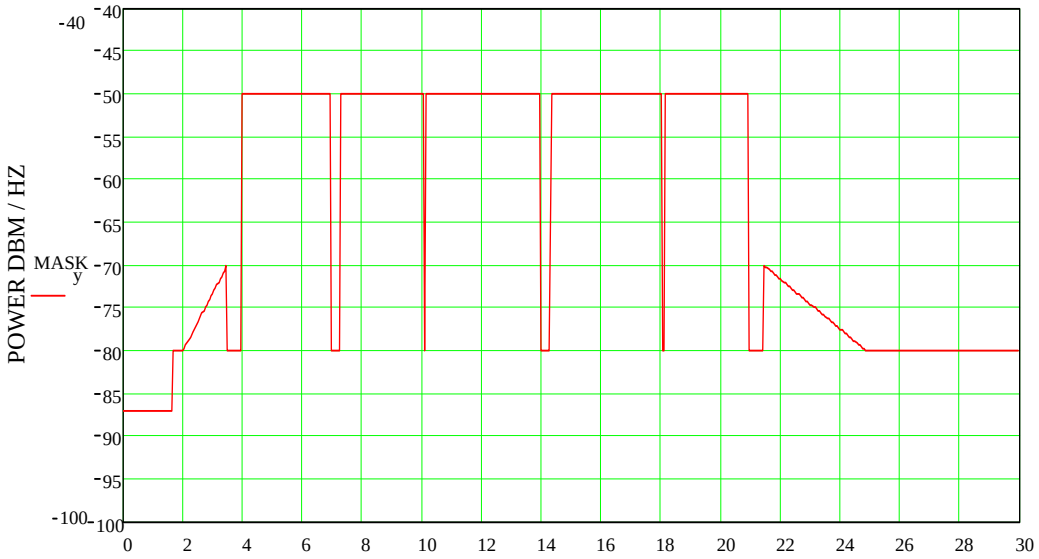

Figure 6 -- This is the specification for the HomePlug first generation specification. Note that it does not use the Amateur bands. This has helped HomePlug manufacturers to avoid interference problems involving the Amateur Radio Service.

HomePlug is also being used successfully by the access BPL industry. The Current Technologies system in Cincinatti, OH passes about 60,000 homes. To date, it has deployed without major interference

problems involving Amateur Radio. Current is also planning to complete the installation of BPL in the Dallas, TX area, ultimately passing about 2 million homes. (This system is primarily focused on utility applications.) With the size of these installations, Current is arguably the most successful BPL company to date. It should be noted that this success is building on work ARRL helped to get done.

13. DS2 and Notching

As successful as HomePlug has been, its approach can be applied to other BPL technology. For example, at this point, many of the BPL companies are choosing not to use the Amateur bands in their deployments, at least within any areas where Amateur Radio operation is likely. As can be seen in Figure 6 above, thus technique is appropriately called "notching." BPL systems must have the ability to notch any spectrum as needed.

However, no notching or filtering is perfect, and there will always be some noise in the notched spectrum. If this noise is below the ambient noise levels in the area, there will be no interference, but if the notching is inadequate, residual noise will result and nearby communications will be degraded.

Early implementations of BPL often resulted in 15 dB or more of degradation to Amateur Radio in the "notched" spectrum. Naturally, at the strong BPL levels seen in some systems, complaints about interference in the notched spectrum were filed.

Many of these systems with early complaints used technology employing the DS2 chipsets. (DS2 is an integrated-circuit manufacturer). ARRL had suggested to DS2 that they improve their notching by 15 dB to eliminate many of the interference problems. To everyone's benefit, DS2 responded to this in the release of their 2nd-generation, 200 Mb/s chipsets. At an industry event attended by ARRL, a DS2 presentation mentioned the improvement in their notching. This got ARRL's attention, and, by happenstance, ARRL was going to Houston, TX the next day to look at a new DS2-based system.

In its tests, ARRL noted that there were improvements in the performance of the DS2 notching. It provided DS2 with feedback and further refinements were made. This culminated in a visit to ARRL HQ by DS2 engineers, a pair of modems in tow. The results of this are shown o Figure 7 below.

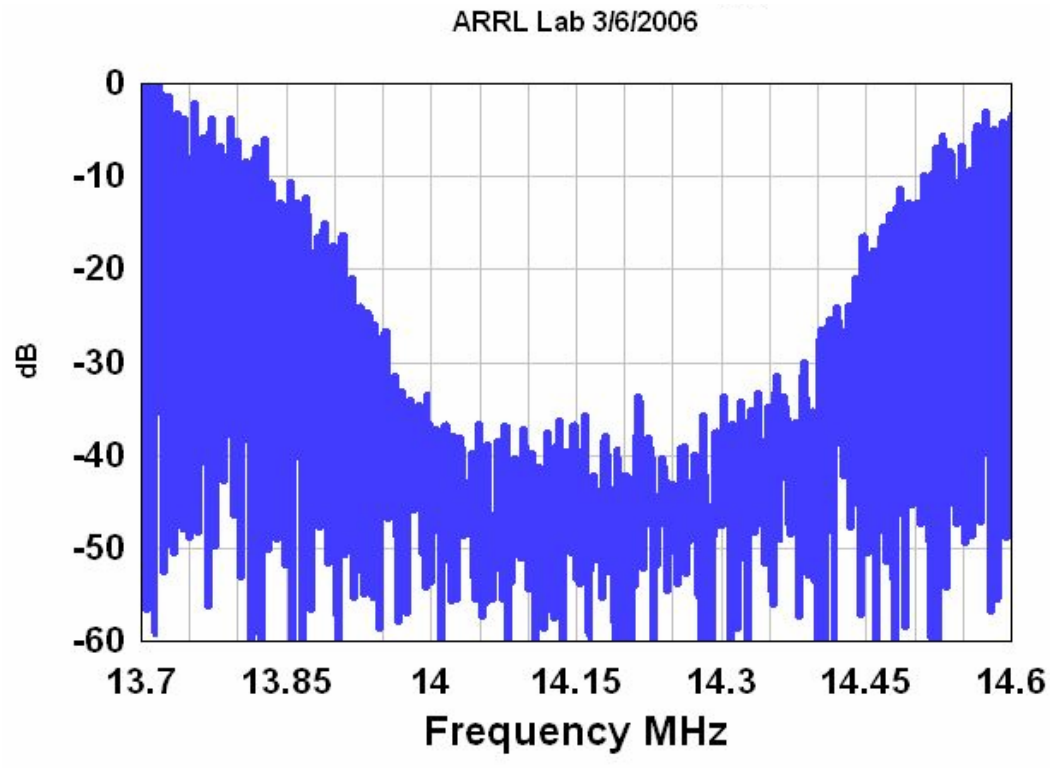

Figure 7 -- In this test of a DS2 modem in the ARRL Laboratory, a notch depth of 40 dB was achieved across the entire 14 MHz Amateur band.

Several months later, CenterPoint, the electric utility in Houston, had wired a larger area of the city with DS2-based modems made by Corinex. ARRL staff again went to Houston and assessed the system there. ARRL Laboratory Manager Ed Hare had a few observations to report:

"I found that most of the Corinex BPL nodes I tested were at or under the FCC emissions limits. In this system, all of the nodes are reported to be notched in the ham bands, and from what I saw, that appears to be the case. In the majority of the system that was "FCC-legal," the BPL noise was loud and clear outside the ham bands, but when I parked a mobile station right under the injector on the pole, in the ham bands, the noise was inaudible or just barely audible (and inaudible 100 feet up the road). A fixed station had filed a formal complaint with the FCC. Thanks to the good work of the CenterPoint utility engineer, the utility response was fast and, after a couple of weeks of trying different things, effective. I went to the Amateur station, and had him point his Yagi at the power lines 150 feet away. The BPL system was not audible in the ham bands. I am reporting the emissions-limits violations to CenterPoint, with the expectation that they will take a close look at the issue and correct any problems. We are fortunate that we have a good electric utility working on this issue, as it is likely that if they were not solidly behind not causing interference, the usual round of denials probably would have happened."

Communication

It is clear that communication is important to preventing and resolving BPL issues. The technique of avoiding locally used spectrum has worked acceptably for the Amateur Radio Service, if done well enough. These successes represent what should be mandated by good regulations and recommended by good industry practice and standards. Resolving EMC issues with systems that have the characteristics of BPL is not easy, and must include good communication and meticulous attention to technical detail.

About Your Presenter

Ed Hare is the department manager for the ARRL Laboratory. He has been employed by ARRL since 1986. He holds an Amateur Radio license with a call sign, W1RFI, which represents his life's work, helping Amateur Radio address radio-frequency-interference problems and issues. He is also well known in the EMC community, serving on a number of industry standards committees such as the IEEE EMC Society's Standards Development Committee (as Secretary) and the ANSI accredited C63™ EMC committee, as the Chair of its Subcommittee 5, Immunity.

An Overview of the Institute's Role in Determining Effects of the Radio Channel on Radio System Performance

Robert J. Achatz
Institute for Telecommunication Sciences
(303) 497-3498
rjachatz@its.bldrdoc.gov

Abstract

This paper provides a brief overview of the Institute for Telecommunication Sciences' role in understanding and predicting the effects of the channel on radio system performance. The overview describes relevant deleterious channel conditions, channel measurement equipment, and channel measurements made by the Institute. It then discusses how measurement data is used for channel characterization, channel modeling, and radio system performance prediction. It concludes with a description of current work in the design of a tool that will quantify the effect of deleterious channel conditions on receiver signal processing algorithms.

1. Introduction

Telecommunications play a vital role in providing services essential for modern life. Many of the systems providing these services use radios operating over unreliable radio links composed of a transmitter, receiver, and channel separating the two. The channel is often the foremost impediment to fast and reliable radio system performance.

Such channels can be found in high-frequency ionospheric, troposcatter, fixed line-of-sight, land mobile radio, cellular, wireless local area network, broadcast television, satellite, air-to-ground, and local multipoint distribution radio systems. Parameters that differentiate the channels include frequency, bandwidth, antenna directivity, antenna platform (handheld, automobile, aircraft, tower, etc.), and environment (rural, residential, urban, indoor, etc.).

An important goal of the Institute is to help designers and regulators understand and predict the effects of the channel on radio system performance. It does this by measuring, characterizing, and modeling the channel and using these results to quantify the effect the channel has on radio system performance. This paper provides a brief overview of the Institute's contributions in these areas. References pointing to major publications by the Institute under various U.S. Department of Commerce offices are provided, i.e. National Bureau of Standards (NBS), Environment Sciences Service Administration (ESSA), Office of Telecommunications (OT), and National Telecommunications and Information Administration (NTIA). It concludes with a description of current work in the design of a tool that will quantify the effect of deleterious channel conditions on receiver signal processing algorithms.

2. Deleterious Channel Conditions

Radio system performance is degraded by a number of radio channel phenomena which can broadly be classified into either multipath or noise. Multipath is caused by reflection, diffraction, and scattering propagation-phenomena which create additional signal paths between the transmitter and receiver [1]. Summation of the signals from these paths by the receiver causes undesirable filtering that distorts the transmitted signal. Multipath causes bit errors by introducing inter-symbol-interference in digitally modulated wideband systems and power fading. Time-variation of these effects is introduced by movement of transmitter or receiver.

Noise is introduced by natural sources such as atmospheric lightning and man-made sources such as power lines, electrical devices, and other radio links [2]. Summation of the noise with the signal by the receiver produces a distorted version of the transmitted signal and corresponding bit errors. Receiver filtering can significantly change the characteristics of noise in the receiver as compared to the channel. For example, filtering can transform a short impulse into a long pulse or a periodic pulse into a continuous wave signal. These changes can have profound impact on the performance of a radio system.

3. Channel Measurement Equipment

The Institute measures multipath with a channel probe which transmits a binary phase shift keyed signal that

has been modulated by a pseudo-noise codeword. An estimate of the channel impulse response is derived from the cross-correlation of the received signal with the same codeword. Early impulse response channel probes used an analog signal correlator [3]. More recently the Institute has designed an impulse response channel probe based on digital signal processing techniques [4]. This probe offers significant advantages, including more precise filtering and quadrature demodulation.

Early noise measurement equipment collected average power, average voltage, and average logarithmic voltage statistical moments [5]. The amplitude probability distribution was estimated from these moments. This approach was improved upon by the development of the amplitude probability meter which measured the amplitude probability distribution directly [6].

Currently, noise measurements are performed with spectrum and vector signal analyzers. Older spectrum analyzers provide noise amplitude samples from analog envelope detection circuitry. Modern spectrum analyzers and vector signal analyzers provide complex samples, i.e., amplitude and phase samples, from digital signal processing algorithms. The complex samples are preferred because they allow post-measurement filtering and computation of noise autocorrelation functions and corresponding power spectral densities from the same data used to compute amplitude statistics.

4. Channel Measurement

Early multipath measurements made by the Institute were at microwave frequencies in an airport environment [7]. These same techniques were then applied to measuring multipath at microwave frequencies for mobile radio [8] [9], line of sight microwave [10], and troposcatter [11] radio systems. They were also used to measure multipath at millimeter wave frequencies for local multipoint distribution radio systems [12] and unspecified radio systems operating in urban and suburban [13] and pecan orchard [14] environments. More recently this expertise has been applied to measuring multipath for land mobile radio [15] [16], cellular [17], broadcast television [18], and wireless local area network [19] [20] [21] radio systems.

In its earlier years, the Institute measured atmospheric radio noise [22]. These data became the basis for the International Telecommunication Union (ITU) atmospheric noise model [23]. This expertise was later translated to the measurement of man-made noise in urban, residential, and rural areas [24]. Similarly, these data became the basis for the ITU man-made noise model [25].

More recently measurements at very high frequencies [26] and ultra high frequencies [27] were made to determine whether technological change had made the ITU man-made noise model outdated. The Institute has also measured ultrawideband signals which will share spectrum with a number of legacy radio systems [28].

5. Channel Characterization and Modeling

Channel measurement data is typically reported in terms of its channel characteristics. Multipath measurement characteristics include the impulse response correlation function or "power delay profile," frequency response correlation function, narrowband correlation function, narrowband power spectral density, root mean square delay spread, coherence bandwidth, coherence time, and Doppler bandwidth. Noise measurement characteristics include the amplitude probability distribution, autocorrelation function, power spectral density, repetition period, level crossing rate, peak power, average power, skew, and excess.

Some characteristics are more important than others because of their relationship to radio system performance. For example, under specific deleterious channel conditions the coherence bandwidth or root mean square delay spread of a multipath channel [29] and the ratio of average voltage to root mean square voltage of a noise channel [30] are well correlated to the bit error rate of a demodulator.

Measurement data is also used to create a model of the channel. Such models can be in the form of computer programs, hardware, i.e., circuits or instruments, or mathematical functions. The quality of the model is determined by how well it recreates channel characteristics. The Institute has developed models for ionospheric multipath [31] [32], ionospheric noise [33] [34], cellular multipath [17], broadcast television multipath [18], and man-made noise [26] channels.

6. Effect of the Channel on Radio System Performance

Our primary interest is to determine the effects of the channel on radio system performance. This has been done at the Institute in a number of ways. The most straightforward way is to measure performance with the radio system operating through the actual channel. This approach was used at the Institute to measure channel impulse response and bit error rate in multipath impaired line-of-sight [35] and troposcatter [36] radio systems.

Another way is to measure performance with the radio system operating through a hardware model of the channel in the laboratory. This approach provides repeatable test conditions. It has been used to quantify the effects of multipath on ionospheric [37] radio systems. It has also been used to quantify the effects of ultrawideband signals on global positioning satellite [38] [39], land mobile radio [40], and satellite broadcast [41] [42] [43] receivers.

Another approach is to measure performance with computer models of the transmitter, channel, and receiver. This approach is more flexible but often requires simplification of transmitter and receiver functions. This method was used by the Institute to collect bit error statistics for a number of demodulators and noise channels [44], speech and video quality measures for a number of demodulators and noise channels [45], and bit error statistics for trellis coded quadrature amplitude modulation in multipath channels [46].

Finally, a mathematical function which models the channel can be incorporated into an analytic expression which can determine performance. This was done to determine the bit error rate of a quadrature phase shift keyed radio link operating in multipath [47]. If the analytic expression is intractable, performance may be determined with numerical computing methods. This approach was used at the Institute to compute bit error rate for a number of demodulators in noise channels [48].

7. Current Work

Currently the Institute is creating a tool that will help us understand and predict the effects of the channel on signal processing algorithms within the receiver that perform such diverse functions as antenna optimization, equalization, interleaving, and error correction.

The need for such a tool was made evident during previously mentioned projects which quantified the effects of ultrawideband signals on global positioning satellite, land mobile radio, and satellite broadcast systems. Inaccessibility of key performance metrics within the receiver prevented us from understanding how deleterious channel conditions affected demodulation and the various post-demodulation signal processing algorithms individually.

Our new tool will address this shortcoming with the flexibility and accessibility of software simulation in a popular scientific programming environment. The tool will be divided into two parts. The first will focus on the effects of the deleterious channel on signal demodulation while the second will concentrate on the effects of the deleterious channel on the various signal processing stages which operate on the demodulated bits. This division provides faster computer processing since bits use far fewer samples than signals. Previous research using demodulated bit processes can be found in [45], [49], and [50].

A significant portion of the development of the tool will be devoted to the mathematical analysis of the characteristics of signal, noise, and bit random processes at all stages of receiver signal processing [51]. Uncertainty analysis methods will also be applied [52] [53] and developed as necessary [54] to assure that the results are accurately quantified.

8. Conclusions

This paper has briefly described the Institute's long history of studying the radio channel and its effects on radio system performance. We have also provided an overview of current research efforts that involves creating a tool that quantifies the effect of the channel on signal processing algorithms within the receiver. The Institute is continuing in its important role as a leader in advancing the design and regulation of modern radio systems.

9. References

[1] W.J. Hartman, Ed., "Multipath in air traffic control frequency bands. Vol. I: Classification of multipath, effects of multipath on systems, and causes of multipath. Vol. II: Causes of multipath (continued), methods for reducing the effects of multipath, and specific system considerations," Department of Transportation Report FAA-74-75, I and II. (NTIA sponsor report)

[2] R. Dalke, "Radio noise," in *The Wiley Encyclopedia of Electrical and Electronic Engineering*, J.G. Webster, Ed., New York: John Wiley & Sons, Inc., 1999, Vol. 18, pp. 128-140.

[3] R.W. Hubbard, "Characteristics and applications of the PN channel probe," OT Technical Memorandum 76-218, 1976.

[4] K.C. Allen and W.A. Lindsey-Stewart, "Method and apparatus for measuring the impulse response of a radio channel," United States Patent 5,371,760, Dec. 6, 1994.

[5] W.Q. Crichlow, C.J. Roubique, A.D. Spaulding, and W.M. Beery, "Determination of the amplitude probability distribution of atmospheric radio noise from statistical moments," *Journal of Research NBS*, Vol. 64D, No. 1, Jan.-Feb. 1960.

[6] R.J. Matheson, "DM-4 operation and maintenance manual," NTIA Technical Memorandum 80-50, Nov. 1980.

[7] R.W. Hubbard, L.E. Pratt, and W.J. Hartman, "The measurement of microwave multipath in an airport environment," Department of Transportation Report FAA-RD-76-163, Jan. 1977. (NTIA sponsor report)

[8] R.W. Hubbard, R.F. Linfield, and W.J. Hartman, "Measuring characteristics of microwave mobile channels," NTIA Report 78-5, Jun. 1978.

[9] G.A. Hufford, R.W. Hubbard, L.E. Pratt, J.E. Adams, and S.J. Paulson, "Wideband propagation measurements in the presence of forests," U.S. Army Communications-Electronics Command Research and Development Technical Report CECOM 82-CS029-F, 1982. (NTIA sponsor report)

[10] R.W. Hubbard, "Atmospheric multipath measured in LOS microwave circuits," NTIA Technical Memorandum 82-81, Dec. 1982.

[11] R.W. Hubbard, "Delay-spread measurements over troposcatter links," NTIA Technical Memorandum 83-84, Mar. 1983.

[12] P.B. Papazian, M. Roadifer, and G.A. Hufford, "Initial Study of the Local Multipoint Distribution System Radio Channel," NTIA Report 94-315, Aug. 1994.

[13] E. Violette, R. Espeland, and K.C. Allen, "Millimeter-wave propagation characteristics and performance for urban-suburban environments," NTIA Report 88-239, Dec. 1988.

[14] P.B. Papazian, D.L. Jones, and R.H. Espeland, "Wideband propagation measurements at 30.3 GHz through a pecan orchard in Texas," NTIA Report 92-287, Sep. 1992.

[15] P. Papazian, P. Wilson, M. Cotton, and Y. Lo, "Flexible interoperable transceiver (FIT) program test range. Part I: Radio propagation measurements at 440, 1360, and 1920 MHz, Edwards Air Force Base, CA," NTIA Report 00-380, Oct. 2000.

[16] P. Papazian and M. Cotton, "Relative propagation impairments between 430 MHz and 5750 MHz for mobile communication systems in urban environments," NTIA Report TR-04-407, Dec. 2003.

[17] J.A. Wepman, J.R. Hoffman, and L.H. Loew, "Impulse Response Measurments in the 1850-1990 MHz Band in Large Outdoor Cells," NTIA Report 94-309, Jun. 1994.

[18] G.A. Hufford, J.R. Godwin, R.J. Matheson, V.S. Lawrence, and L.E. Pratt, "Characterization of the HDTV channel in the Denver Area," NTIA Report 90-271, Dec. 1991.

[19] P.B. Papazian, Y. Lo, E.E. Pol, M.P. Roadifer, T.G. Hoople, and R.J. Achatz, "Wideband propagation measurements for wireless indoor communication," NTIA Report 93-292, Jan. 1993.

[20] R.J. Achatz, Y. Lo, E.E. Pol, "Indoor direction diversity at 5.8 GHz," NTIA Report 98-351, Jul. 1998.

[21] M.G. Cotton, R.J. Achatz, Y. Lo, and C.L. Holloway, "Indoor polarization and directivity measurements at 5.8 GHz," NTIA Report 00-372, Nov. 1999.

[22] National Bureau of Standards, "Quarterly radio noise data," NBS Technical Note 18 (1-32) , U.S. Dept. of Commerce, Washington, D.C., 1959-1966.

[23] CCIR, "*Characteristics and applications of atmospheric radio noise data*," Rep. 332-3, Geneva, Switzerland: International Telecommunications Union, 1986.

[24] A.D. Spaulding and R.T. Disney, "Man-made radio noise. Part 1: Estimates for business, residential, and rural areas," OT Report 75-67, Jun. 1975.

[25] CCIR, "*Man-made radio noise*," Rep. 258-5, Geneva, Switzerland: International Telecommunications Union, 1990.

[26] R.J. Achatz, Y.Lo, P.B. Papazian, R.A. Dalke, and G.A. Hufford, "Man-made noise in the 136 to 138-MHz VHF meteorological satellite band," NTIA Report 98-355, Sep. 1998.

[27] R.J. Achatz and R.A. Dalke, "Man-made noise power measurements at VHF and UHF frequencies," NTIA Report 02-390, Dec. 2001.

[28] W.A. Kissick, Ed., "The temporal and spectral characteristics of ultrawideband signals," NTIA Report 01-383, Jan. 2001.

[29] P.A. Bello and B.D. Nelin, "The effect of frequency selective fading on the binary error probabilities of incoherent and differentially coherent matched filter receivers," *IEEE*

Trans. on Commun. Syst., Vol. CS-11, pp. 170-186, Jun. 1963.

[30] J.H. Halton and A.D. Spaulding, "Error rates in differentially coherent phase systems in non-Gaussian noise," *IEEE Trans. on Commun. Technology*, Vol. COM-14, No. 5, Oct. 1966, pp. 594-601.

[31] C.C. Waterson, J.R. Juroshek, and W.D. Bensema, "Experimental verification of an ionospheric channel model," ESSA Technical Report ERL 112-ITS 80, Jul. 1969.

[32] J.A. Hoffmeyer and M. Nesenbergs, "Wideband HF Modeling and Simulation," NTIA Report 87-221, Jul. 1987.

[33] J.J. Lemmon and C.J. Behm, "Wideband HF noise/interference modeling Part I: First order statistics," NTIA Report 91-277, May 1991.

[34] J.J. Lemmon and C.J. Behm, "Wideband HF noise/interference modeling Part II: Higher order statistics," NTIA Report 93-293, Jan. 1993.

[35] J.A. Hoffmeyer and T.J. Riley, "Long-term performance and propagation measurements on single and tandem digital microwave transmission links, Vols. I, II, and III," NTIA Report 265, Jun. 1990.

[36] J.J. Lemmon and T.J. Riley, "Propagation and performance measurements over the Berlin-Bocksberg digital troposcatter communications link," NTIA Report 88-232, Mar. 1988.

[37] C.C. Watterson and C.M. Minister, "HF channel simulator measurements and performance analyses of the USC-10, ACQ-6, and MX-190 modems," OT Report 75-56, Jul. 1975.

[38] J.R. Hoffman, M.G. Cotton, R.J. Achatz, R.N. Statz, and R.A. Dalke, "Measurements to determine potential interference to GPS receivers from ultrawideband transmission systems," NTIA Report 01-384, Feb. 2001.

[39] J.R. Hoffman, M.G. Cotton, R.J. Achatz, and R.N. Statz, "Addendum to NTIA Report 01-384: Measurements to determine potential interference to GPS receivers from ultrawideband transmission systems," NTIA Report 01-384, Feb. 2001.

[40] J.R. Hoffman, E.J. Haakinson, and Y. Lo, "Measurements to determine potential interference to public safety radio receivers from ultrawideband transmission systems," NTIA Report TR-03-402, Jun. 2003.

[41] M. Cotton, R. Achatz, J. Wepman, and B. Bedford, "Interference potential of ultrawideband signals. Part I: Procedures to characterize ultrawideband emissions and measure interference susceptibility of C-band satellite digital television receivers," NTIA Report TR-05-419, Feb. 2005.

[42] M. Cotton, R. Achatz, J. Wepman, and P. Runkle, "Interference potential of ultrawideband signals. Part II: Measurement of gated-noise interference to C-band satellite digital television receivers," NTIA Report TR-05-429, Aug. 2005.

[43] M. Cotton, R. Achatz, J. Wepman, and R. Dalke, "Interference potential of ultrawideband signals. Part III: Measurement of ultrawideband interference to C-band satellite digital television receivers," NTIA Report TR-06-437, Feb. 2006.

[44] H. Akima and A.D. Spaulding, "Development of a computer simulation model for analyzing performance of some simple communication systems on a digital computer," Department of Transportation Report FAA-RD-76-181, Nov. 1976. (NTIA sponsor report)

[45] E.A. Quincy, R.J. Achatz, M.G. Cotton, M.P. Roadifer, and J.M. Ratzloff, "Radio link performance prediction via software simulation," NTIA Report 00-371, Oct. 1999.

[46] R.A. Dalke, G.A. Hufford, and R.L. Ketchum, "A digital simulation model for local multipoint and multichannel multipoint distribution services," NTIA Report 97-340, Jul. 1997.

[47] R.H. Ott, M.C. Thompson, Jr., E.J. Violette, and K.C. Allen, "Experimental and theoretical assessment of multipath effects on QPSK," *IEEE Trans. on Commun.*, Vol. 26, No. 10, Oct. 1978, pp. 1475-1477.

[48] A.D. Spaulding, "Digital system performance software utilizing noise measurement data," NTIA Report 82-95, Feb. 1982.

[49] L.E. Vogler, "An extended single-error-state model for bit error statistics," NTIA Report 86-195, Jul. 1986.

[50] J.J. Lemmon, "Wireless link statistical bit error model," NTIA Report 02-394, Jun. 2002.

[51] R.J. Achatz and R.A. Dalke, “Receiver model for study of the effects of the radio channel on radio system performance. Part 1. Analytic model,” NTIA Report, to be published.

[52] E.L. Crow and M.J. Miles, “Confidence limits for digital error rates from dependent transmissions,” OT Report 77-118, Mar. 1977.

[53] M.J. Miles, “Sample size and precision in communications performance measurements,” NTIA Report 84-153, Aug. 1984.

[54] R.A. Dalke, “Statistical considerations for noise and interference measurements,” NTIA Report, to be published.

HD RADIO COVERAGE MEASUREMENT AND PREDICTION

John Kean
NPR Labs, National Public Radio
Washington DC

ABSTRACT

Because of its unique digital transmission, HD Radio® requires new methods and standards to measure and predict signal coverage, relative to analog FM. Because analog FM reception quality is known to decline gradually with degraded RF signal quality, analog FM service may be quantified in simple terms of signal strength. With digital audio broadcasting, reception quality remains 'perfect' until signal quality degrades below threshold requirements, at which point reception ends. This "cliff effect" as it is commonly known in digital television, required NPR to use new techniques to measure HD Radio reception and predict coverage.

No model for measurement and prediction has been developed for this new service. Since real coverage is an oft-mentioned concern of station engineering and management, NPR Labs embarked on a year-long project to collect data from stations transmitting HD Radio and form a propagation model for this digital radio service. The following report summarizes our study, discusses current conclusions, and addresses future work that should be done to improve the coverage analysis process.

HD RADIO LOGGER DESIGN

Concurrent with the rollout of HD Radio, numerous questions have arisen about the coverage offered by the digital signal. For examples: What field strength is required to provide reliable HD Radio reception, and what does "reliable" mean? To resolve those questions, NPR Labs' HD Radio Coverage Measurement Initiative set out to collect data from NPR member stations across the country broadcasting HD Radio. We obtained the RF signal prediction tools to estimate field strength, but we also needed data about real signal reception to calibrate our prediction model of HD Radio signal coverage. To collect these data we needed a suitable measuring device with these capabilities and features:

- Collect calibrated field strength data (from the analog host) in a log file with GPS location and time stamps;
- Easy to ship to the field, easy to set up and operate, and capable of providing best-available receiver performance;
- Log HD Radio reception information in a mobile or portable (battery operated) environment;
- Support Supplemental Program Service ("multicast") reception;
- Provide high-quality audio outputs for HD Radio demonstration.

After examining a variety of industry solutions (none of which completely met our needs at the time) we decided to design and build our own unit for receiving, measuring and logging the HD Radio reception, as shown in Figure 1. Our 'homemade' approach resulted in substantial savings in capital monies for the project over the purchase of commercial units.

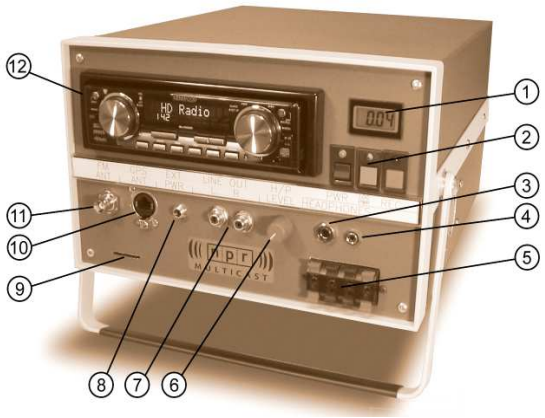

Key Features of the HD Radio Logger

1. Digital Volt Meter - Provides real-time RSL (Received Signal Level) and power supply conditions
2. Instrument Controls and Indicators - (from left to right) Main Power Switch (with blue LED), Logger On/Off Button (with green LED), Logger Start/Stop Button (with red LED)
3. 1/4" Headphone Out
4. 1/8" Headphone Out
5. Terminal Block for External Loudspeakers (4 x 20W)
6. Headphone Level Control
7. Preamp-Level Stereo Output Jacks
8. Power Input Jack
9. MMC Card Slot
10. Global Positioning System (GPS) Jack
11. FM Antenna Input Jack
12. Kenwood EZ500 Receiver Head Unit (with internal KTC-HR100MC tuner)

Figure 1 HD Radio Logger designed and built by NPR Labs.

After extensive lab testing of available receivers, we chose a Kenwood KTC-HR100MC, an FM/AM tuner for after-market car radio systems, as the HD Radio receiver. This "black box" is controlled by a Kenwood EZ500 'head unit' for tuning, display and audio amplification. NPR Labs modified the tuner to output an accurate signal level over a 70 dB dynamic range as well as provide HD Radio status measurements.

The tuner and control unit are housed in an instrumentation case with a rechargeable 12-volt battery to permit portable operation and to maintain radio memory functions when not powered externally. The unit has internal stereo loudspeakers, terminals for up to four external loudspeakers, headphone jacks and preamp-level audio output.

A suitable microcomputer-controlled data logger, providing multiple channels of analog and digital input was found. This unit, originally designed for logging race car parameters, includes the essential GPS receiver and software to log data with location and time stamps. The data is logged on a MMC memory card (similar in size to SD cards) and requires no computer to operate.

A 32" vertically polarized magnetic-mount antenna was selected for signal reception. NPR conducted field measurements with a calibrated dipole antenna at 30 feet and 7 feet above ground to characterize the reference antenna's performance on the Engineering Department's Toyota Sienna van. This provided data to convert the unit's received signal voltage readings into field strengths in microvolts/meter (or dBuV).

All functions are displayed and controlled on the front panel. Users simply lay the logger on a car floor or seat, connect the GPS unit and FM antenna (placed on the vehicle roof), tune in the desired station and press the record button.

After the logging unit had been designed and constructed, we presented it in April at the Public Radio Engineering Conference at NAB-2005. We were warmly received by engineers keen to understand their new digital coverage, and collected a long list of station engineers eager to collect data in their markets. From this list, we selected candidate stations that represented as broad of a cross-section of public radio stations as possible - we were interested in getting variety, and the final stations ended up running the gamut in terms of class, morphology, and overall market size.

Drive-Test Data Collection Requirements

To meet the demand for station measurements, and to collect a larger database of HD Radio coverage, NPR built three more HD Radio Logger units for a total of four. Over the remainder of the year the logging units were shipped to nearly 30 stations. Each station drove their broadcast area, paying attention to a few particular concerns:

- Diversity of road types – highways allowed the coverage area to be driven quickly, but often provided inflated data, as they are elevated and generally free from obstruction. We requested data be collected on a variety of roads, from city streets to small state roads.

- Driving in and out of the HD Radio reception area – the most useful information for our statistical model is gathered by crossing the boundary of a staiton's reliable HD reception, as illustrated in Figure 2. A hypothetical station's HD coverage is shown in yellow. Examples of "good" drive testing routes are displayed in green; these routes yield the most information about HD reception because they repeatedly explore the threshold of HD service, providing information about the field strengths when HD Radio reception . The route in red is not as useful to our model, as signal levels are so high that HD service is received nearly 100% of the time.

- Diversity of existing conditions – data from known problem-areas was encouraged, especially areas with adjacency concerns.

Figure 2 Drive test routes that are preferred (green) and not preferred (red) for measurement of a station's HD Radio signal coverage area (yellow).

Post-Processing Logger Data

The MMC cards containing each station's data were mailed to NPR at the conclusion of testing. Upon receipt of the memory cards, each separate data file was offloaded and concatenated into a master file for each station. Analog received signal strength (RSL) was logged as a voltage measurement (0-5V). A calibration table for each logging unit was prepared by NPR Labs and was used to convert the voltages in estimated field strength in dBµV/m. (Field strength measurements correspond to an antenna height of 2 meters, as constrasted to 9.1 meters for FCC field strength contours. This height represents the average height of the measurement antenna when affixed to a standard size car roof.)

The chart in Figure 3 shows an example of the measurement data collected on a drive-test of WAMU, Washington DC along Interstate 95 from the DC city limits through Baltimore. This sample route covers approximately 70 miles and 1½ hours of driving. The HD Radio signal (as represented by the analog FM signal measurement) declines as the distance increases from WAMU. The temporary signal drop within the Baltimore Harbor Tunnel is clearly visible.

The HD Radio reception status is logged concurrently, as displayed in red at the bottom of the chart. As the field strength drops below approximately 60 dBµ interruption of the HD Radio signal is evident. (Note that field strengths measured at a height of 2 meters differ from FCC field strengths. Also that because I-95 is a wide open roadway extending radially away from WAMU's transmitter, signal reception in this case may be better than on arterial cross streets.)

As the data arrived from stations, we gradually developed theories about how a large variety of factors were affecting the digital signal. We anticipated that the Longley-Rice propagation model would tend to overestimate signal strengths compared to measured signal levels, even when matched to a receiver antenna height of 2 meters above ground. This is because the terrain elevation data used in the predictions represent "bare earth" conditions that lack local clutter (buildings, trees, etc.) that can scatter and absorb the signal.

It is common to incorporate US Geological Survey Land Use and Land Cover (LULC) adjustment factors to minimize these prediction errors. US Geodetic Survey Land Use-Land Cover data identifies general surface characteristics, such as mixed urban, residential, rangeland, evergreen forest, water, etc., within small grid blocks. There are 21 possible categories of land cover type; these we grouped into seven primary designations for signal loss matching. Spatial resolution of the data used in NPR's study is 15 arc-seconds (approximately 500 meters). Figure 4 shows classifications in an area of the central California coast with an enlargement for the City of San Francisco.

Despite the common use of LULC with Longley-Rice predictions, we felt that fixed adjustment factors could

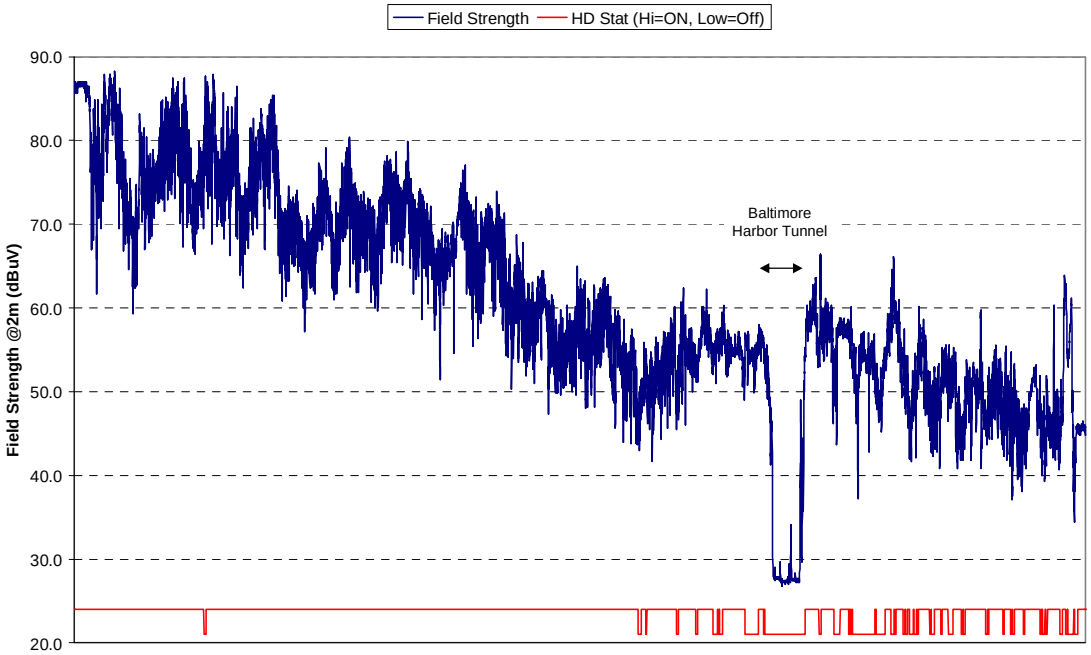

Figure 3 Timeline graph of approximately 70 minutes of raw HD Radio Logger data of WAMU(FM), on a drive from downtown Washington DC to near the Maryland-Delaware border. Field strength is blue, while corresponding HD Radio receive status is shown in the red at the bottom (high/low represents HD Radio received/not received).

increase rather than decrease errors, which required us to develop a new computational technique to generate LULC adjustments for each market drive-test.

To improve accuracy, we computed adjustments by comparing the local mean of drive-test field measurements to the underlying bare-earth predicted signal, noting the difference between measured and predicted fields. Then, the differences between measured and received signal level were averaged for each LULC type. These delta values were then used as adjustments to the Longley-Rice predictions, in a sense, a closed-loop correction at the grid-block level. This allows the signal predictions to be optimized for each market context, which substantially improved the resulting accuracy.

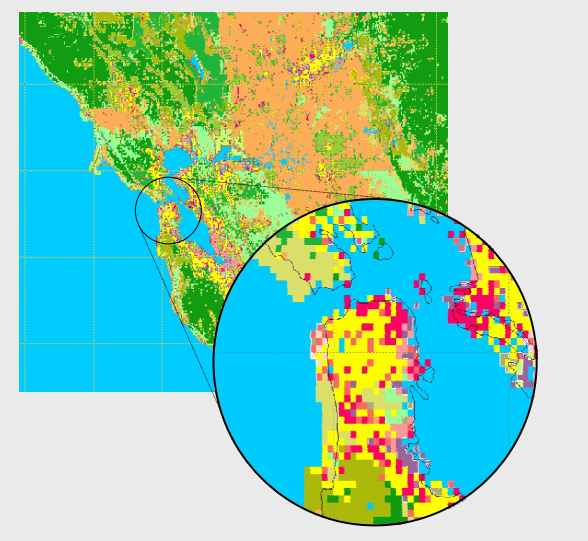

Figure 4 Illustration of Land Use-Land Cover data used in the signal propagation modeling. Enlargement in circle shows LULC bin classifications in San Francisco.

Signal Requirements for HD Radio

An important finding from the HD Radio measurement program is: How much signal is required to produce reliable reception? To answer this question, NPR studied the statistics of signal reception for the stations as a function of received signal level.

Figure 5 shows the availability of reception as a function of field strength for three stations: KXJZ, a Class C2 in Sacramento, California, WUOT, a Class C in Tampa, Florida, and KQEI a Class A in North Highlands, California. It is apparent that the reception availability falls off differently for the three stations, particularly for KQEI, even though these stations serve similar areas across Sacramento. The differences may arise from a combination of factors, including amounts of Rayleigh fading and multipath from each station, differences in environmental noise and station interference on each frequency. (KQEI shares a tight contour protection with first-adjacent channel station KVMR, a Class B1 in Nevada City, California.)

Differences in measurement techniques at each station may affect individual results. Although a standard antenna was used throughout the measurements, different vehicles were used by each station. (Minivans were recommended because of their relatively wide and level roof, providing more consistency in antenna gain.) Nevertheless, distortions of the horizontal plane pattern will occur, affecting gain at various orientations of the vehicle. Extensive driving was encouraged to help even out these directional gain variations. Vehicles may exhibit excessive RF noise from the ignition or electrical system, which could pollute the reception and degrade measured sensitivity. Also, the terrain varies from smooth and flat to hilly. Population density of the areas measured range from rural to dense urban. However, considering the measurements include 26 operating stations it can be said that the overall results represent real-world experience that may resemble the consumer's results.

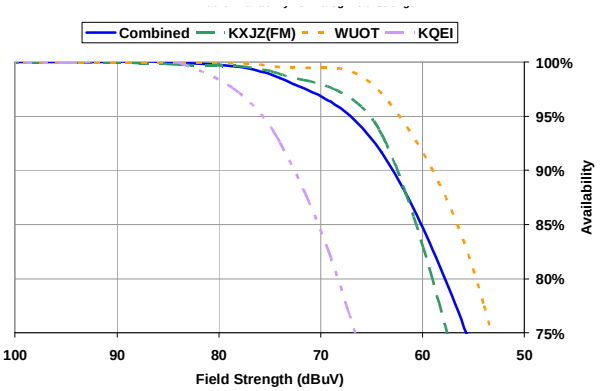

Figure 5 Availability vs. field strength for three HD Radio stations KXJZ, WUOT and KQEI (dashed lines) plus combined results for 26 stations (solid line).

Considering the variability that may result from vehicle to vehicle, it is appropriate to look at HD Radio coverage performance for all 26 stations in the current statistical database. This list contains a wide variety of transmitting facilities, from smaller Class A stations to large Class C stations. Figure 5 presents two histograms showing the numbers of stations with minimum field strengths to achieve reception availabilities of 90% and 97% (blue and gold, respectively). The stations are grouped in 5 dB ranges. As expected, the higher availability of 97% requires higher field strengths than does 90%.

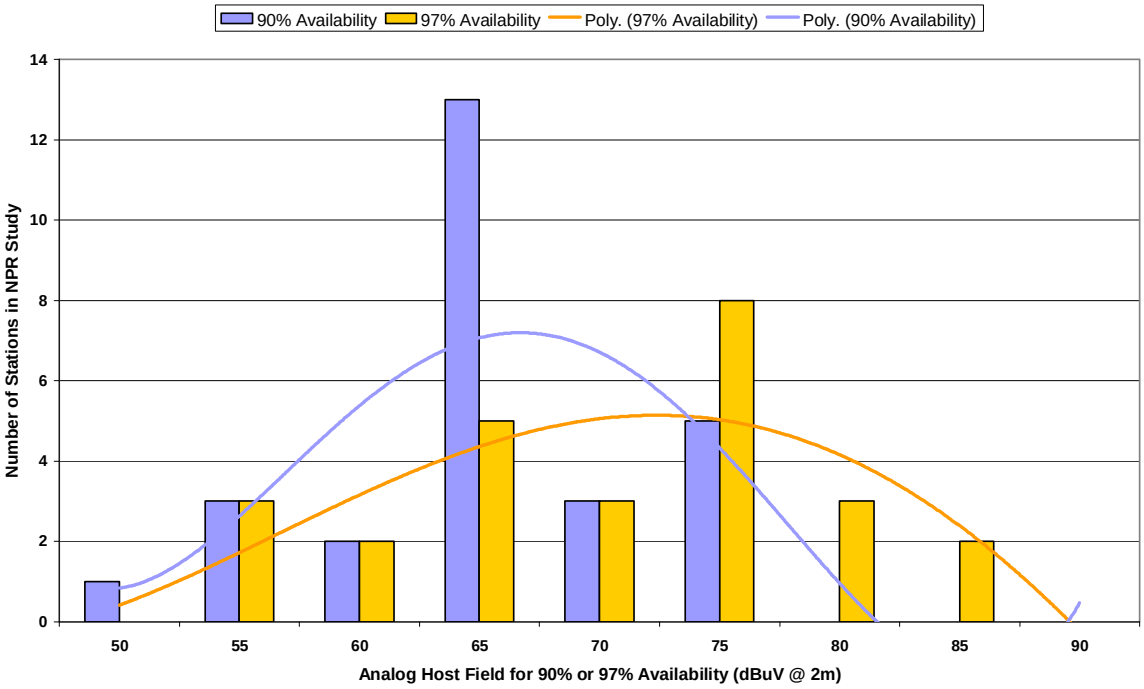

Figure 6 - Field strength requirements for 26 HD Radio stations, based on NPR Logger and measurement analysis.

The range of the field strength distribution is notable. Eight stations required at least 70 to 75 dBuV to achieve 97% availability, but two stations required between 80 and 85 dBuV and three required between 75 and 80 dBuV. On the other hand, three stations required as little as 50 to 55 dBu and two stations required 55 to 60 dBuV. The distribution for 90% is much narrower, with 13 stations requiring 60 to 65 dBuV. To help identify these trends, the chart includes 3rd-order polynomial curves in colors matching the distributions. Median field strength for the 97th percentile availability is 70 dBuV, and for the 90th percentile is 63 dBuV, referred to a receive height of 2 meters above ground.

The roof-mount whip antenna supplied with NPR's HD Radio Logger kit operates at greater heights than production antennas in automobiles and may produce higher signal levels. Also, built-in antennas are usually hidden in front, rear or side windows, or even bumpers, which may result in greater pattern distortion than the logger kit.

A study of the environment types and terrain conditions reveal some correlation with the field strength findings. There is a tendency for HD Radio to require higher signal in hilly or rough terrain and less in areas of smooth terrain. To date, the data indicate that lower class stations require the same levels of digital signal as higher class stations. However, Class A stations with minimal spacing to other first-adjacent channels may have more signal overlap than the FCC contours suggest. These may be conditions of digital interference that require further study.

Indoor Reception Projections

Indoor reception cannot be determined from these mobile measurements because signal penetration into buildings is case-specific. The FCC's early studies with television signal penetration in the lower VHF channels indicated a wide range of 5 dB to 15 dB in building penetration loss. To this variability one must add the potential inefficiency of indoor antennas, which include short wires (often provided with table model radios) having possibly 5 to 10 dB of loss relative to a dipole. These factors may combine to require greater field strength for indoor reception.

As mentioned earlier, HD Radio reception experiences a "cliff effect" when signal quality degrades below minimum requirements. For digital systems these requirements are governed primarily by the signal to noise ratio, or strictly speaking the bit energy relative to the power spectral density of the noise, expressed as Eb/No. Thus while it is convenient to predict reception by signal strength, HD Radio is effectively a noise- and interference-limited service. For mobile HD Radio, basic signal strength tends to determine system noise (unless one is in a vehicle with abnormal ignition noise or alternator hash), but in buildings, where the signal is already weakened by penetration loss sources of RF noise (computers, electric motors, etc.) may determine digital reception.

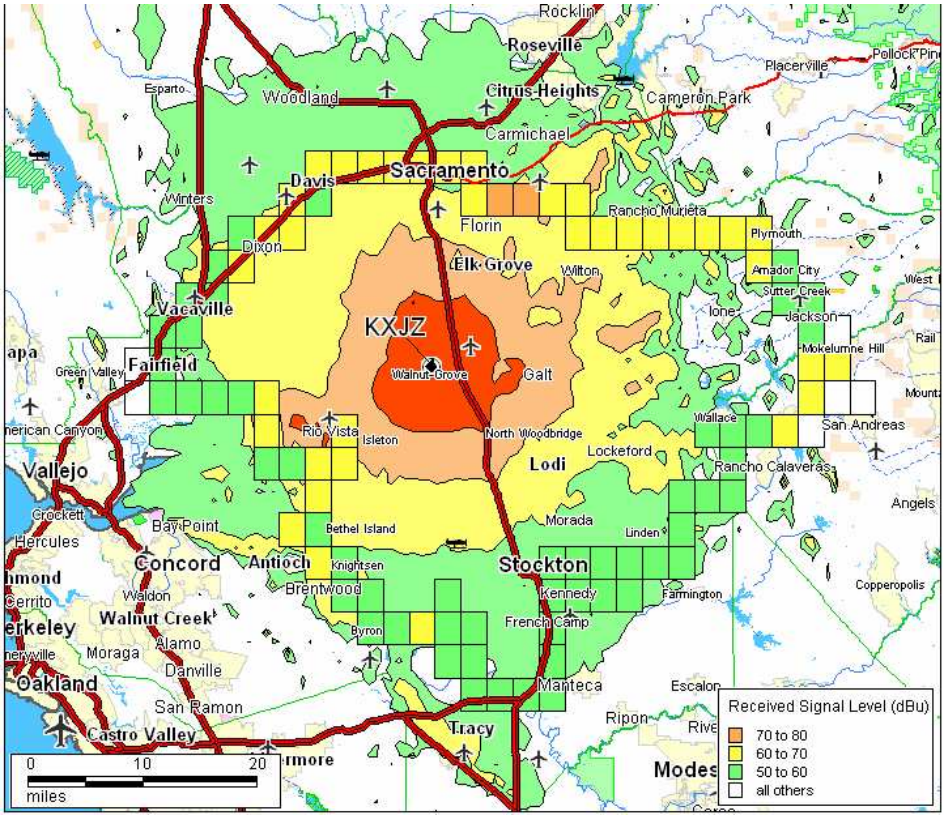

Figure 7 Drive-test map example of KXJZ, Sacramento, showing aggregated field strengths over Longley-Rice prediction.

The presence or absence of RF noise is beyond any deterministic model of HD Radio coverage. Fortunately, listeners with fixed receivers have the opportunity to adjust their radio's location and antenna position for best reception, which can contribute numerous dB to their link budget. NPR is currently engaged in a survey of early users of indoor HD Radios to gather coverage information on this important user group. These findings should provide valuable information on "best practices" for stations and radio manufacturers to achieve optimal reception of HD Radio.

Mapping Display

The optimized Longley-Rice predictions were imported into MapInfo®, a well-known Geographic Information System program used to manipulate and map multiple layers of geo-information. Using Vertical Mapper®, a suite of MapInfo tools, the Longley-Rice data were interpolated using an Inverse Distance Weighting and rendered in contour regions of 50-60dBu, 60-70dBu, 70-80dBu and 80-120dBu.

The core drive-test data were added to the maps over the optimized Longley-Rice predictions. Drive-test data was aggregated into grid blocks of typically 100-300 samples, representing the mean field strength or HD status of all drive-test samples within a specified distance of the grid block's center. This "binning" allowed large amounts of data collected by each station to be viewable on a large scale map, and offered viewers of the maps a better characterization of regional service. Figure 8 shows how the drive-test routes were converted and displayed in black, gray or white, according to reception availability. Availability refers to the percentage of time that HD Radio reception was present for the local area indicated by the grid block.

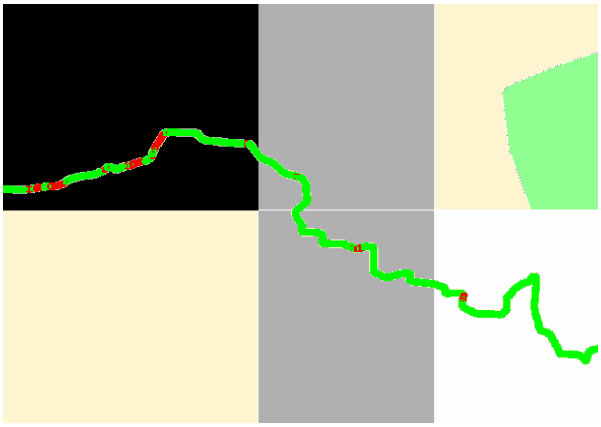

Figure 8 Highly-magnified portion of a drive-test route showing HD Receive status (green or red) overlaid on bin-aggregated results (white, gray, black).

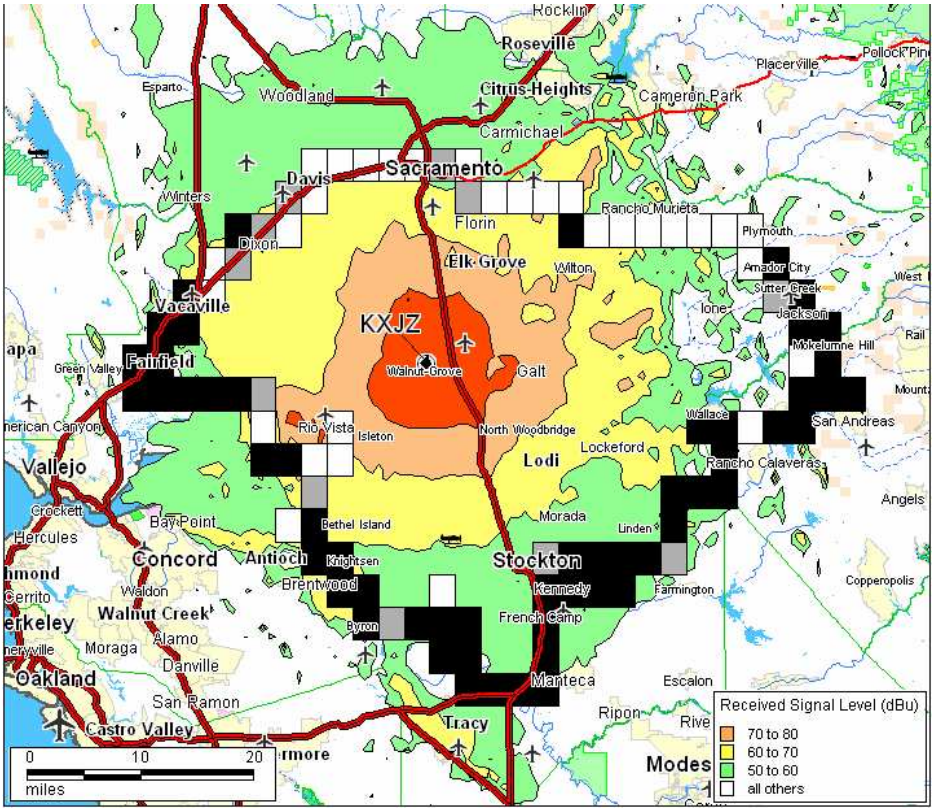

Figure 9 Example of a drive test route map for KXJZ. Aggregated data in white blocks is >97% availability of HD Radio reception; gray indicates 90%-97% availability and black indicates <90% availability.

The ranges selected for the HD Receive Status map are 0-90%, 90-97%, and 97-100%. These ranges relate to a general "annoyance factor" associated with dropout rates – the premise being that if the HD signal is not received a large amount of the time on a Supplemental Audio Channel (with no analog backup) it would quickly get annoying. Thus, a higher standard of 97% was chosen to represent availability that may be required for SAC reception. The 90% availability threshold is included more as a reference for a lower figure than to represent any specific perceived quality.

A similar method was used to aggregate received signal level for the drive-test RSL maps. Each bin was colored to correlate to the Longley-Rice contour intervals for a Received Signal Level map, and shaded to represent a percentage range of HD Reception for an HD Receive Status map

Three maps are created for each station supplying drive-test data. The first map shows a binned analog field strength along the station drive-test route over an optimized Longley Rice prediction. Figure 7 shows ans example of one station from the current group, KXJZ(FM), Channel 205B, Sacramento, California. The colors of the field strengths match so one may compare the accuracy of Longley-Rice predictions, as an underlay, to the analog field strength measurements.

The second map, Figure 9, shows aggregated and binned HD Radio Logger reception along the same route as the field strength, above. Bins that are shaded white received HD Radio at least 97% of the time, while gray bins received between 90% and 97% of the time and black bins show reception less than 90% of the time.

Evaluating the correlation between the underlying field strength and the availability of HD Radio reception is a difficult matter by eye. This problem becomes more evident if one is asked to chose what field strength represents HD service, even when it has been binned into ranges of percent availability along the route. As discussed earlier NPR Labs developed a statistical method whereby availability of reception is evaluated against measured field strength, as shown in Figure 5. From this distribution the engineer may determine the necessary field strength for specific availability targets.

Figure 10 shows the result of the KXJZ analysis, with HD Radio coverage predicted over the entire coverage

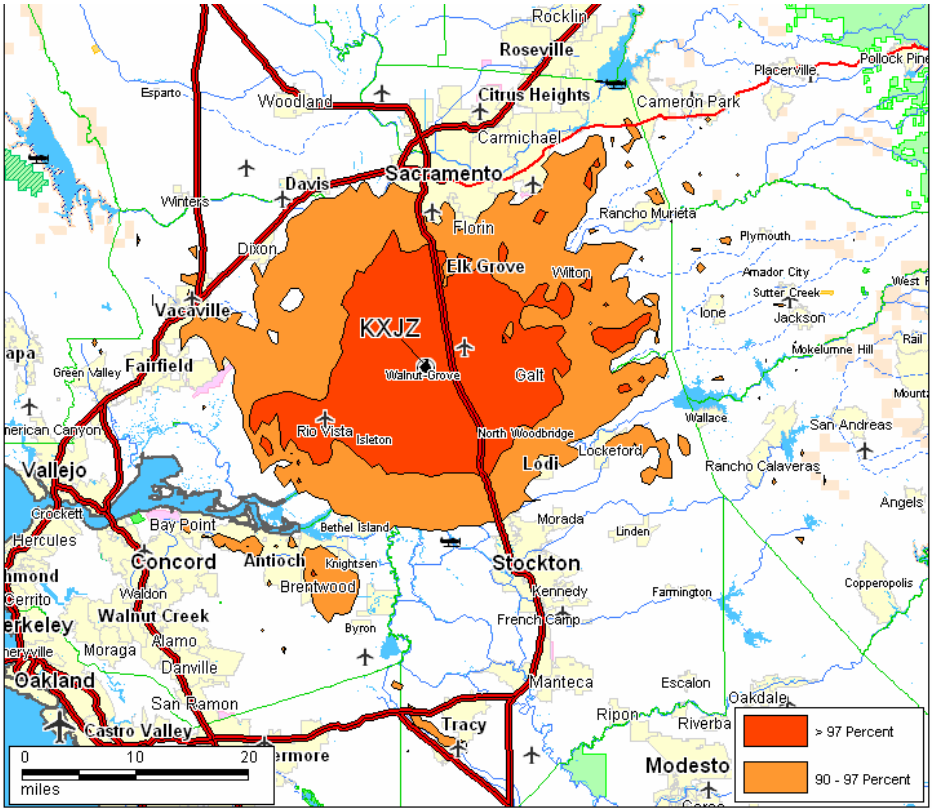

Figure 10 HD Radio availability map for KXJZ, showing geographic areas in which reception availability is expected to greater than 90% and 97%.

area to availabilities of 90% and 97%. This map results from the following steps:

- drive-test measurement collection,
- Longley-Rice signal prediction,
- optimization of the Longley-Rice predictions by using LULC corrections correlated to the measurement data,
- derivation of the statistical distribution of HD Radio availability versus measured field strength, and
- preparation of maps showing the area of predicted HD Radio service availability, as measured by the HD Radio Logger.

Methodology Issues and Future Work

As noted earlier, the predictions of HD Radio reception are based on results collected by the HD Radio Logger. Thus the results are representative of this receiving system only, and "your mileage may vary". Certainly, future work should include development of a standardized antenna system that is not influenced by the vehicle on which it is mounted. The variations from station to station should be explored and causes identified. A review of current data for adjacent channel interference is inconclusive, but futher study is needed. Rayheigh fading effects are suspected with stations having very rough terrain; the existing data can be "mined" further to investigate this effect. The statistical model was based on total service availability within discrete bins or locales, but the durations of individual outages should be considered. For example, listeners may respond differently to ten one-second outages in a minute than one ten-second outage, although the statistics register identically at present. We look forward to continued work with station engineers on these measurements and further research on the application of HD Radio.

Acknowledgements

The author wishes to thank Kyle Evans of NPR Labs for his tireless work on the geographic software and statistical work, Dave Harry of Potomac Instruments for supplying field strength calibration instruments, and Mike Bergman of Kenwood Corporation for lending his experience on past HD Radio studies with NPR and his company's receivers.

Hybrid Propagation Models for Broadcast Coverage Predictions and Spectrum Management

Emanoel Costa
CETUC-PUC/Rio
Rua Marquês de São Vicente 225
22453-900 Rio de Janeiro RJ Brasil
epoc@cetuc.puc-rio.br

Markus Liniger
Hochschule für Technik und Informatik
Biel, Switzerland
markus.liniger@bfh.ch

Thousands of path profiles incorporated into the ITU-R Correspondence Group 3K-1 (ITU-R CG3K-1) and the Institute for Telecommunication Sciences (ITS) databases will be described. Models that estimate diffraction effects on the propagation of radio waves over irregular terrain in the VHF and UHF bands available for digital broadcast applications (T-DAB and DVB-T) will be used to predict field strengths that will be compared with those from the corresponding measurements. The mean value and the standard deviation of the difference between predictions and measurements will be presented for each model, as functions of their number of main obstacles. A better basis for comparison between predictions and experimental data was obtained from a special measurement series performed by HTI to determine the height function of the received field strength. These measurements will be described, also compared with model predictions and statistically analyzed.

1. Introduction

Collective effort is in progress within ITU-R Working Party 3K to develop, test, and finally recommend path-specific propagation models for improved broadcast coverage and interference predictions. The present work has been developed as part of this effort.

Initially, thousands of VHF and UHF links selected from those incorporated into the ITU-R Correspondence Group 3K-1 (ITU-R CG3K-1) [1] and the Institute for Telecommunication Sciences (ITS) [2] databases will be described. It should be observed that the CG3K-1 and ITS databases received contributions from several sources and that its path profiles have been estimated using different survey techniques.

Many models are available to predict diffraction effects on the propagation of radio waves over irregular terrain in the VHF and UHF bands that are or will be used by digital TV applications. These effects will be estimated using: (i) the classical prediction models proposed by Bullington, Epstein-Peterson, and Deygout [3]-[7], with modifications; (ii) the ones described by the most recent versions of Recommendations ITU-R P.526 [8] and ITU-R P.1546 [9], that have been continually improved by work performed over decades and that may be key elements in the path-specific propagation models being developed; (iii) the Longley-Rice model [10]. The predicted field strengths will be compared with those from the corresponding measurements. The mean value and the standard deviation of the difference between predictions and measurements will be presented for each model, as functions of their number of main obstacles.

A better basis for comparison between predictions and experimental data was obtained from a special measurement series performed to determine the height function of the received field strength. From the height functions, the average received field strength value was determined [11],[12]. In the second part of this contribution, these measurements will be described, also compared with predicted data and statistically analyzed.

2. Experimental Data

2.1. ITU-R CG3K-1 and ITS Data

The total of 9633 radio links have been selected from the ITU-R CG3K-1 (EBU and HTI) [1] and ITS (Phase 1 and Phase 2) [2] databases of VHF/UHF measurements relating to terrestrial broadcasting. The data contains terrain profiles provided with non uniform resolutions (typically from 40 m to 300 m), combined frequencies, terminal heights, ERP, polarizations, measurement values and other information. Fundamental parameters of the links are observed in Figures 1 to 3. It is remarked that a few links with parameters outside the adopted horizontal and vertical scales (for example, approximately 10 links with path lengths longer than 150 km) are not represented in these Figures. Note that multiple links have been defined over some of the profiles by the used of different combinations of frequencies, antennas heights and polarizations. The links represent different conditions in the VHF and low UHF bands, as well as those for particular frequencies and path lengths in the high UHF band. High inclinations are observed for short links and, while the transmitter height covers a wide interval, the receiving antennas have been kept relatively close to the ground.

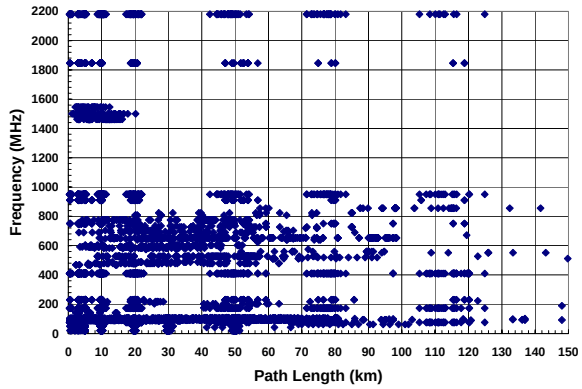

Figure 1. Scatter diagram for the path length and frequency of the links

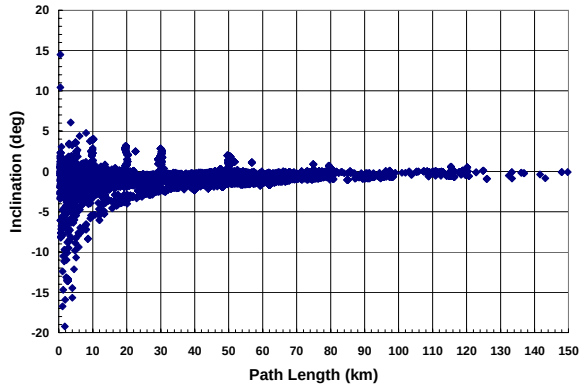

Figure 2. Scatter diagram for the path length and inclination of the links

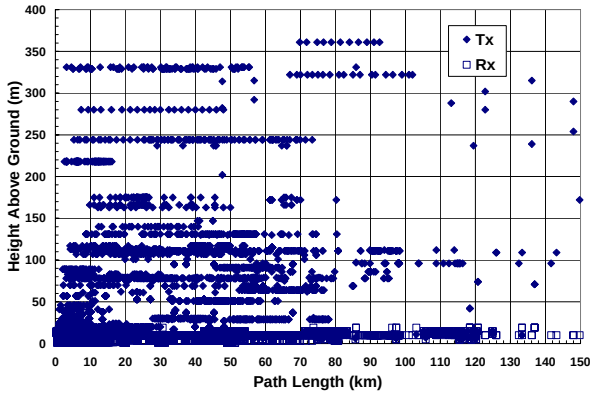

Figure 3. Scatter diagram for the path length and the heights of the transmitting and receiving antennas above the ground

For all cases to be described in the next sections, the heights of each terrain profile were initially corrected for the Earth curvature and for the standard refractivity. The number of main obstacles was then determined for each terrain profile, using the basic stretched-string analysis [3], with the following modifications: (i) all consecutive points of the terrain profile touching the string were merged into a single isolated obstacle; (ii) all continuously contiguous sections of the terrain profile between two consecutive obstacles that additionally intersect 60% of the first Fresnel ellipsoid characterized by them were also merged with the closest obstacle. These procedures are implemented in such a way as to keep the sections of the stretched string between the extreme points of the isolated obstacles unchanged. As a result, the position of the approximate center of the isolated obstacle and its equivalent height is determined by the intersection of the appropriate unchanged sections of the string. As a result from the above processing, from zero to nine main obstacles were identified for each of the 9633 links (respectively, 2930, 4789, 1057, 521, 186, 132, 20, 16, 7 and 2 ITU-R CG3K-1 and ITS link). The numbers of these links displaying line-of-sight, line-of-sight with sub-path diffraction or transhorizon conditions are 1187, 1716 and 6730, respectively.

2.2. HTI Data

To get more accurate information on the applicability of different propagation models, about 500 height function measurements have been carried out [11],[12]. Nineteen TV transmitters operating at twelve sites in bands 4 and 5 served as high power sources. The measurements have been performed using the OFCOM measurement car. This car is equipped with a height-adjustable telescopic mast (up to 11 m in height) that support a Yagi antenna, being able to automatically measure the field strength versus height or azimuth. The features of the antenna and cable are stored in calibration files, allowing exact conversion of the received signal into field strength. The transmitter data (frequency, coordinates, antenna radiation pattern and radiated power) were recorded by the measurement computer. The measurement files have been treated and the results calculated and plotted using the HTI propagation program implemented in MATLAB. As an example, Figure 5 shows the height function measured at the right end of the profile plotted in Figure 4. The theoretical height function was calculated using the nearest obstacle to the receiver. The height difference between the minima of theoretical and measured field strength (approximately 2 m) is due to an imprecision of height in terrain information.

The measurement sites have been chosen to avoid some effects that are not considered in prediction models, such as attenuation due to vegetation, or short and near obstacles. For obtaining only a dominant reflection, which produces a clear height function, sites with flat terrain near the receiver in direction of the transmitter

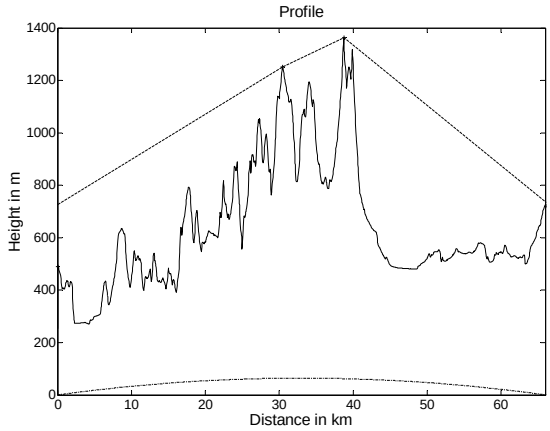

Figure 4. Profile between S. Chrischona (transmitter) and Frienisberg (receiver), showing two obstacles

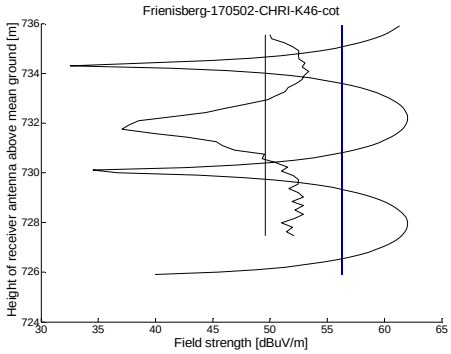

Figure 5. Height function measured at Frienisberg

have been chosen. From the height functions, the mean received field strength values were also determined and assigned to the fixed height of 10 m. These measurements will be compared with predicted results and statistically analyzed.

3. Propagation Models

The Bullington method [4] initially determines the position and height of an equivalent knife-edge obstacle from the intersection between the two straight lines defining the horizons from each terminal. The loss due to the equivalent knife-edge obstacle is taken as the additional path loss due to diffraction.

In the Epstein-Peterson method [5], the loss for each obstacle is calculated by assuming imaginary terminals placed at the top of the immediately adjacent obstacles to its left and right (or at the top of the real terminals, for the first and the last obstacles). The individual contributions are then added to determine the total path loss due to diffraction.

The Deygout method [6] involves the calculation of the loss due to each obstacle in the absence of all the others. The obstacle providing the highest loss subdivides the path into two, to which the procedure is recursively applied. The individual losses are again added to determine additional path loss due to diffraction. In the present implementation, the Deygout scheme is applied to the total path and then only once to each of the sub-paths defined by the terminals and the most important main obstacle.

For these three methods, the loss due to a single knife-edge obstacle is calculated according to section 4.1 of Annex 1 to Recommendation ITU-R P.526-9 [8]. Sub-paths were classified into the two cases displayed in Figure 6. If the obstruction of 60 % of the first Fresnel zone for a sub-path is fractionally small, it is treated as a knife-edge obstacle. On the other hand, an equivalent Plane Earth is adjusted to an extended obstruction by the least-squares method and the corresponding excess path loss is calculated using the well-known Norton theory [13]. Additional losses due to antennas which are imbedded in local ground clutter are also considered using the simple model of Recommendation ITU-R P. 452-12 [14] with a relatively favorable ground cover category.

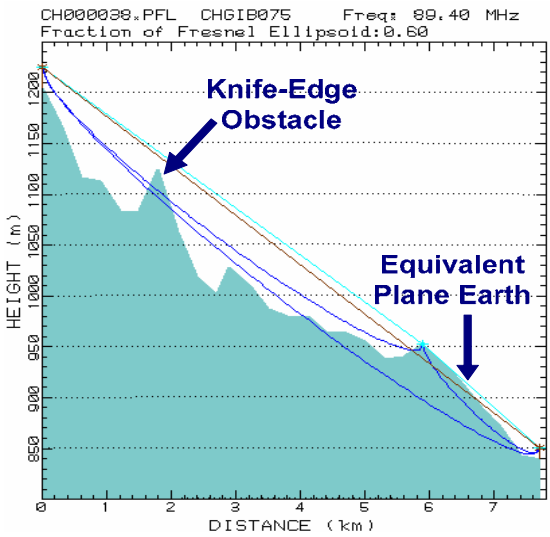

Figure 6. Classes of sub-paths considered by the Bullington, Epstein-Peterson and Deygout models

The knife-edge prediction model of Recommendation ITU-R P.526-9 [8] has also been implemented. It coincides with the classical ones when the terrain profile displays a single obstacle. For two obstacles, it initially applies the Epstein-Peterson algorithm when the contributions from the two obstacles to the path loss are approximately equal or the Deygout algorithm when the contribution from one of the obstacles is clearly dominant. In the absence of obstacles and for three or more obstacle, the Deygout algorithm is initially

prescribed. However, it is also applied only for the principal obstacle in the path and for the most important obstacle in each of the two sub-paths defined by the terminals and the principal obstacle. Specific correction procedures, different from the ones described in association with Figure 6, are applied in each case (except for a single obstacle).

Note that the effects of the radii of the obstacles have been neglected in all the above models.

In the prediction model described in Recommendation ITU-R P.1546 [9], the environment surrounding the transmitter up to a distance of 15 km is used to determine the effective antenna height. Obstacles located further away from the transmitter are not taken into consideration. As a result, predictions tend to be optimistic in cases with large obstacles. An attempt is made to overcome this situation by taking terrain features into account using a "clearance angle". In this case, the angle between the line connecting the transmitter to the receiver and the line from the receiver to the highest obstacle within a distance of up to 16 km is determined. A correction value is then calculated from this angle in Recommendation ITU-R P.1546-2. Even so, it has long been known that for mountainous terrain, the Recommendation ITU-R P.1546 method produces major deviations when its predictions are compared with measured values. This method has been applied only to the HTI data.

Finally, the ITS Irregular Terrain Model (Longley-Rice) has been downloaded [15] and incorporated into the present package after a limited number of input and output changes.

4. Comparison Between Prediction and Experimental Results

4.1. ITU-R CG3K-1 and ITS Data

The average values and the standard deviations of the errors between predictions from each of the methods discussed in the previous sections and measured results are displayed in Figures 7 to 10, using the number of obstacles in the profiles as a parameter. The results from the links without sub-path diffraction effects are shown in Figures 7 and 9 and from the links with sub-path diffraction effects are shown in Figures 8 and 10. It is important to initially note that optimistic methods predict field intensities that are greater than the corresponding measured values on average and yield positive values in Figures 7 and 8.

It is observed that:

- The Bullington method [4] yielded generally optimistic results, but with relatively small errors in the average values for the received field intensity, even as the number of obstacles increases. This may be due to the fact that the influence of intermediate obstacles located between the ones defining the horizon of the terminals is not taken into account. The average errors were accompanied by standard deviations in the intervals from 9 dB to 13 dB for the links without sub-path diffraction and from 10 dB to 16 dB for the links with sub-path diffraction;

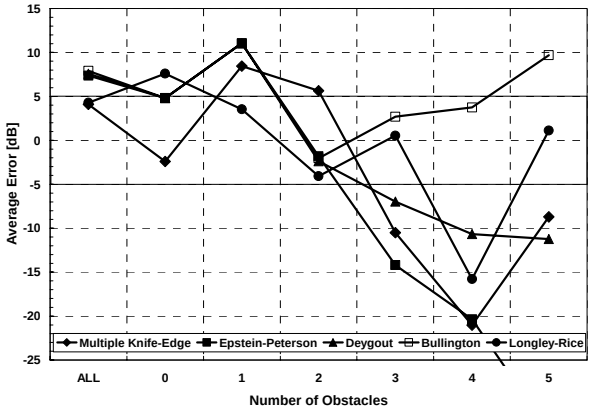

Figure 7. Average values of the errors between calculations and measured results for the links without sub-path diffraction

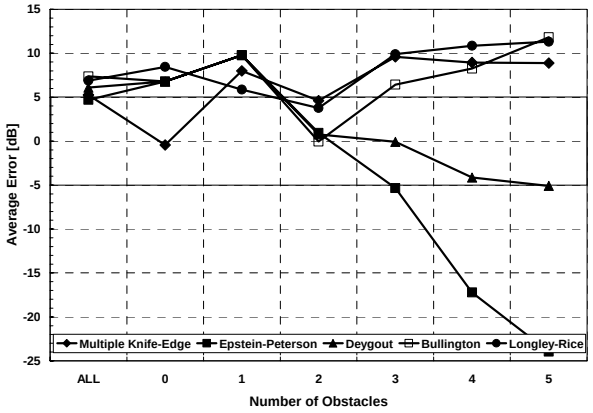

Figure 8. Average values of the errors between calculations and measured results for the links with sub-path diffraction

- the Epstein-Peterson [5] and the Deygout [6] methods provided increasingly pessimistic average values for the received field intensity as the number of obstacles increases. It is observed that the errors associated with the Deygout method are smaller in absolute value, as a result of the limitation in the number of obstacles considered in the calculations.

These average values are accompanied by standard deviations in the intervals from 10 dB to 14 dB for the Epstein-Peterson method and from 10 dB to 16 dB for the Deygout method;

- the method of Recommendation ITU-R P.526-9 [8] and the Longley-Rice model [10] provided increasingly pessimistic average error values for the links without sub-path diffraction and optimistic average error values for the links with sub-path diffraction. The standard deviations are in the interval from 12 dB to 18 dB or even higher. These observations may indicate the need for further adjustments in the correction procedures for the prediction of the diffraction effects in future revisions of Recommendation ITU-R P.526.

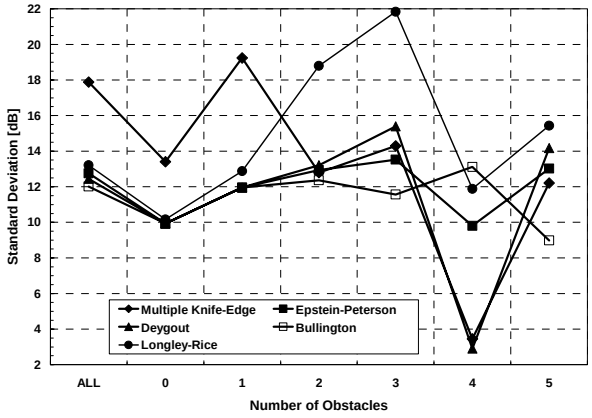

Figure 9. Standard deviations of the errors between calculations and measured results for the links without sub-path diffraction

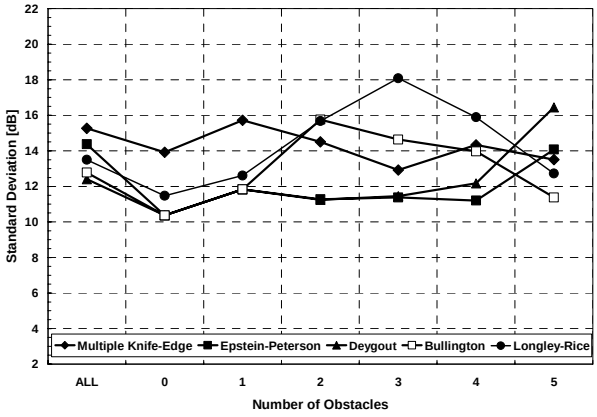

Figure 10. Standard deviations of the errors between calculations and measured results for the links with sub-path diffraction

4.2. HTI Data

The cumulative distribution function of the difference between predicted and measured value have been calculated. For the following statistics, we also used different variants of the classical models. The models with results displayed in Figure 11 were implemented by HTI Bienne. The ones in Figure 12 were implemented by L&S Telcom in their prediction tool. In particular, note that: (i) GEG-7, developed by Gemischte Experten Gruppe ARD/DBP, Germany, combines the Epstein-Peterson method with a modified free space model; and (ii) IRT-2D and IRT-3D, developed by Institut für Rundfunktechnik, Germany, are modified Deygout models. The models take the obstacle in the first Fresnel zone into account, to improve precision. It is observed that the Longley-Rice, Epstein-Peterson and Deygout models are pessimistic for more than 2 or 3 obstacles and earlier ITU models are too optimistic. The cumulative probabilities of differences between measurements and predictions from the models implemented by HTI and by L&S Telcom give similar results.

As an additional comparison between the models, we have calculated and plotted in Figures 13 to 16 the mean value and the standard deviation of the difference between predictions and measurements for different profile types (0, 1, 2 and 3 obstacles).

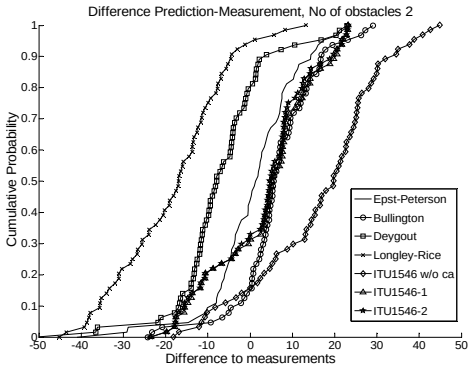

Figure 11. Cumulative probability of difference between values calculated with different models, implemented by HTI, and measured value, using profiles with two obstacles

The Bullington and the L&S Telcom models give the best results if one takes into account the mean value and the standard deviation.

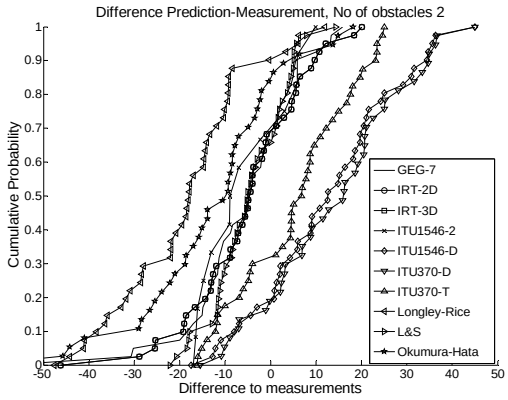

Figure 12. Cumulative probability of difference between values calculated with different models, implemented by L&S Telcom, and measured values, using profiles with two obstacles

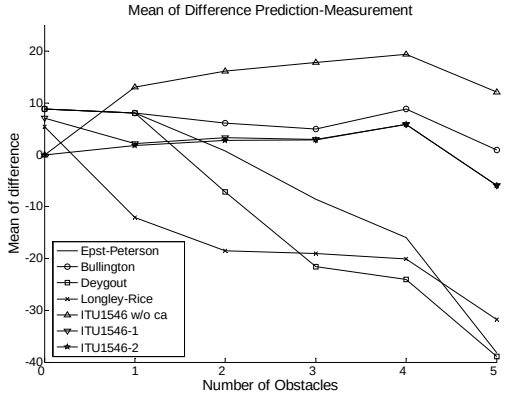

Figure 13. Average values of differences between measured and calculated values (HTI implementation).

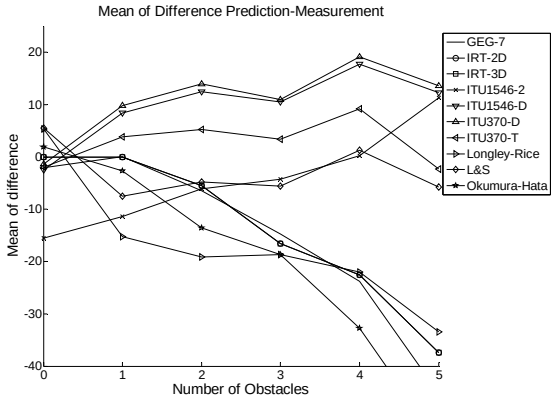

Figure 14. Average values of differences between measured and calculated values (L&S Telcom implementation)

The Recommendation ITU-R P.1546-2 model also has a small mean error but has a larger standard deviation. The weak point of this model became not important, because there are only few profiles with obstacles in the zone which is not taken into account by the procedure. One can see differences between the results of the two implementations of the same model, because the sets of investigated profiles are not totally equal.

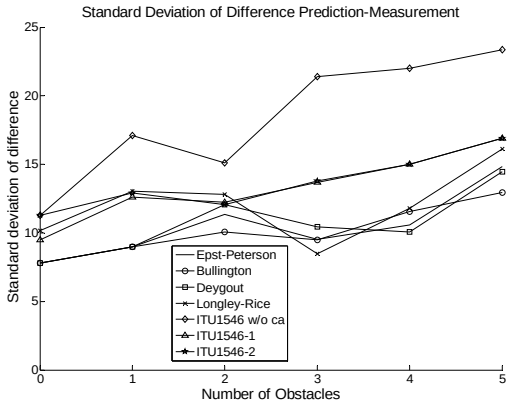

Figure 15. Standard deviations of differences between measured and calculated values (HTI implementation)

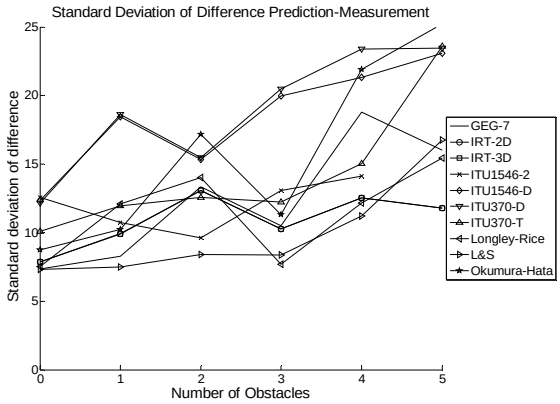

Figure 16. Standard deviations of differences between measured and calculated values (L&S Telcom implementation)

5. Conclusion

For many reasons, the task of comparing the performance of different prediction methods of diffraction effects is a difficult one. Most of the methods discussed in the present contribution possess several variants, each with its own set of input variables. It is even possible that independent implementations of the same algorithm could lead to different results. It is also important to remember that certain input parameters of each of the methods have been kept fixed during the calculations. Different results could have been obtained if different values had been used for these input parameters. A fundamental parameter for the present calculations is the resolution

adopted in the representation of terrain height profiles. The impact of fine resolutions on the performances of the different prediction methods has not yet been investigated. Additionally, it was assumed that the measurements were error-free.

With the cautionary remarks of the previous paragraph in mind, it can be said that the present implementations of several methods yielded average values for the received field intensity that were bounded within the interval from -10 dB to 10 dB. However, it has been observed that the standard deviations provided by these methods are generally large.

These preliminary results indicate that it is necessary to investigate the reasons why the application of several methods to relatively undemanding terrain profiles (with one or no obstacles) provided large average values for the received field intensity, together with also large standard deviations. Finally, efforts should be made to correct the observed average errors, o decrease the standard deviations of all the methods considered here and to extend this study to other frequency bands of interest.

Acknowledgements. EC acknowledges the support of Conselho Nacional de Desenvolvimento Científico e Tecnológico (CNPq), through Research Grant 301909/2003-2. The authors also wish to thank Mr. Mirko Marghitola, Biel School of Techniques and Informatics for the additional measurements, Mr. Michael Rohner, LS Telcom, Germany, for the calculations with their tool and the Federal Office of Communications (OFCOM) for the support with equipment and manpower for the measurements.

References

1. http://www.its.bldrdoc.gov/s-s_model.

2. http://flattop.its.bldrdoc.gov/propdata/.

3. ITU Handbook, *Terrestrial Land Mobile Radiowave Propagation in the VHF/UHF Bands*, International Telecommunication Union, Geneva, Switzerland, 2002.

4. Bullington K., Radio Propagation at Frequencies Above 30 Megacycles, *Proc. Inst. Radio Eng.*, *35*(10), pp. 1122-1136, October, 1947.

5. Epstein J., and Peterson D.W., An Experimental Study of Wave Propagation at 850 Mc/s, *Proc. Inst. Radio Eng.*, *41*(5), pp. 595-611, May, 1953.

6. Deygout J., Multiple Knife-edge Diffraction of Microwaves, *IEEE Trans. Antennas Propagat.*, *14*(4), pp. 480-489, July, 1966.

7. Assis M.S., A Simplified Solution to the Problem of Multiple Diffraction over Rounded Obstacles, *IEEE Trans. Antennas Propagat.*, *19*(2), pp. 292-295, March, 1971.

8. Recommendation ITU-R P.526-9, Propagation by Diffraction, International Telecommunication Union, Geneva, Switzerland, 2005.

9. Recommendation ITU-R P.1546-2, Method for Point-to-area Predictions for Terrestrial Services in the Frequency Range 30 MHz to 3000 MHz, International Telecommunication Union, Geneva, Switzerland, 2005.

10. Hufford G., The ITS Irregular Terrain Model, Institute for Telecommunication Sciences, National Telecommunications and Information Administration, Boulder, CO, U.S.A., 1995.

11. Liniger M., Baumberger A., Rohner M., and Cocco T., Application of Different Diffraction Models in Mountainous Terrain, Proceedings of URSI Commission F Meeting on Climatic Parameters and Diffraction Effects on Radiowave Propagation Prediction (ClimDiff 2003) [CD-ROM, paper Diff.32 (7 pags.)], Fortaleza, CE, Brazil, November, 2003.

12. Liniger M., and Rohner M., Planning Tool for Mountainous Terrain, Proceedings of URSI Commission F Meeting on Climatic Parameters and Diffraction Effects on Radiowave Propagation Prediction (ClimDiff 2005) [CD-ROM, paper Diff.25 (4 pags.)], Cleveland, OH, U. S. A., September, 2005.

13. Norton, K. A., The Propagation of Radio Waves over the Surface of the Earth and in the Upper Atmosphere, *Proc. Inst. Radio Engs.*, *24*, pp. 1203-1236, 1937.

14. Recommendation ITU-R P.452-12, Prediction Procedure for the Evaluation of Microwave Interference Between Stations on the Surface of the Earth at Frequencies Above About 0.7 GHz, International Telecommunication Union, Geneva, Switzerland, 2005.

15. http://www.its.bldrdoc.gov/software/

Results from a Long Term Propagation Measurement Campaign[1]

Mike Willis[2], Ken Craig[3]
Radio Communications Research Unit, CCLRC Rutherford Appleton Laboratory, UK

Abstract

This paper describes the measurement results from the first phase of a unique long-term microwave propagation experiment that is currently running in the United Kingdom. The experiment aims to improve the interference models used for channel assignment to allow more efficient packing of co-channel terrestrial microwave point-to-point links. The results form a database against which link joint attenuation models can be tested and improved. The deployment was completed in February 2005 and has been gathering data since then on 17 links. This paper presents an analysis of the data recorded over up to the time of preparation in December 2006.

Standard Cumulative distributions of the path loss for each link and the joint probability distributions of multiple entry interference are given. The cumulative distributions have been plotted to emphasise both ends of the distribution from 99.99% to 0.01%. This new data is required for developing 100% time models. Current models tend to favour either fading or enhancement but do not predict both. The measured single entry distributions are compared against the predictions from ITU-R P.452 and ITU-R P.530.

Keywords: Trans-horizon propagation, terrain diffraction, troposheric scatter, ducting/super-refraction ,joint statistics of fading and enhancement, area variability, measurement results, time series.

1. Introduction

The radio spectrum is a limited resource and it is necessary for fixed link radio systems to share spectrum. When a new link is required, a channel and power must be allocated that permits the system to meet the desired quality of service while not causing or suffering excess interference to and from links in the same and adjacent channels. Channel assignment algorithms aim to pack links into as few channels as possible while managing interference at an acceptable level. To do this, planners need to be able to calculate the instantaneous path loss between multiple co-channel transmitters and the receiver.

Current assignments made within the UK are based on predictions of signal strengths and using the relevant ITU-R recommendations (ITU-R P.530 [1] for the wanted signal and ITU-R P.452 [2] for unwanted interference paths). While the recommendations yield reliable predictions of the probability density function (PDF) of signal strength against percentage of time on a single path, they give no advice on the correlation of signal strength between different paths.

There is currently no model to produce joint wanted/unwanted PDFs for fixed links and the assignment procedures therefore have to make assumptions about the degree of likely correlation. The long term measurement campaign has been set up in order to assess what the true correlation is between fading and enhancements on typical paths used in the fixed link service.

2. System design

To simulate the situations that occur in practice, the configuration of test links shown in Figure 1 was developed to model links that only just passed the UK channel assignment criteria [3][4]. A wanted system availability of 99.99% was assumed.

The plan consists of a Hub station where the signal levels from 7 outstations are received and amplitude detected at a rate of 10 Hz. Antennas and link lengths are all compatible with current fixed link practice. A victim path T_w to R_{Hub} is used as the reference. This path, which is line of sight, is designed to achieve 99.99% availability. The distance from the Hub in Figure 1 is intended to represent the path loss; so the path loss from Tu2 to the Hub is less than the path loss from Tu1 to the hub. Two offset angles and the three radial co-linear paths are implemented to investigate how any correlation of enhancements is related to the offset angle.

[1] This work has been sponsored by Ofcom. The experimental team wish to thank Ofcom for their continued support. Further information on this project is available at the experiment web site http://www.ltmc.rl.ac.uk
[2] m.j.willis@rl.ac.uk Tel. +44 1235 445492
[3] k.h.craig@rl.ac.uk Tel. +44 1235 445134

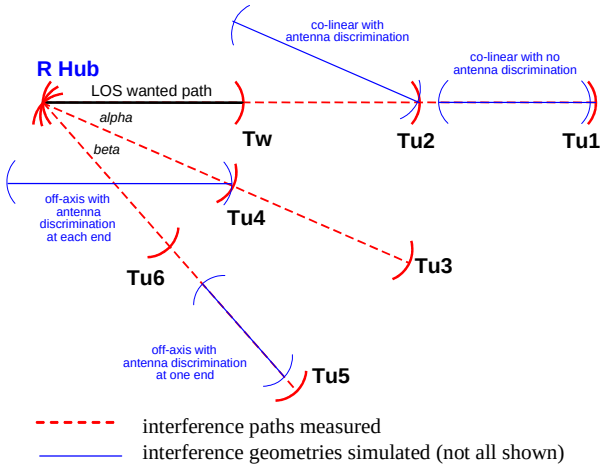

Figure 1 – Cluster configuration

To avoid interference at least a minimum amount of isolation must be provided between the victim receiver and the interfering transmitter. This isolation can be achieved purely through path loss or as the sum of the antenna discrimination and the path loss. Where the interference path is off axis at either the victim receiver site or the interfering transmitter site, the minimum loss needed to constrain interference will be less than when the antennas are aligned. The antenna discrimination for this experiment was assumed to be 20 dB when one antenna is off axis and 40 dB when both antennas are off axis.

At the test site developed to reflect the interference geometries shown in Figure 1, the degree of isolation needed dictates that all of the Tu paths are trans-horizon. The experimental aims required trans-horizon links with at least 99% availability in order to extend the validity of current interference models. In order to achieve a good measurement using practical link parameters of power and antenna gain, in the experimental configuration all antennas are aligned on axis. As well as providing the best possible margin for measuring signal level statistics this also ensures that link measurements are not made through antenna sidelobes as there is always some uncertainty over the sidelobe gain of an antenna, which is strongly influenced by the tower structure and nearby antennas. The choice of test frequencies of 1.4 GHz, 7.5 GHz and 18.6 GHz and the length of the reference link at around 60-80 km was made based on the current loading of the fixed service bands.

East Anglia, a region in the East of the United Kingdom was chosen as this area was already known to suffer fixed link reliability problems through anomalous propagation. Many clear air outages were known to be occurring in the Fenland region of East Anglia around the Wash. The land in this region is almost exclusively of a coastal category as defined in ITU-R P.452 and was therefore likely to suffer multipath fading on the reference link at the same time as ducting enhancement of the interfering links.

A NW-SE alignment of the reference path was chosen, as one of the commonly established weather patterns found over the UK is that of a ridge of continental high pressure in SE England being encroached upon by Atlantic low-pressure frontal systems from the NW. This can often lead to active cold fronts sweeping southeastwards across the UK and links that are aligned NW-SE might be expected to experience rain and ducting at opposite ends. The ITU-R P.530 path loss predictions for the reference path are given in Table 1.

Table 1 – 50% and 99.99% loss for reference path (dB)

	1.4 GHz	7.5 GHz	18.6 GHz
50%	132	147	158
99.99% Clear air	164	185	202
99.99% Rain	---	152	188

The cluster configuration determined the target trans-horizon path losses for each link in the system to meet current UK assignment criteria. The final configuration of the 6 Tu sites is shown in Figure 2 and the predicted path losses are presented in Table 2.

Figure 2 – Deployed Cluster

Links at 18.6 GHz are only deployed at Tw, Tu2 and Tu6. The system has been fully operational since early 2005 and data has been analysed between April 2005 and October 2006.

Table 2 – Path losses for interference paths (dB)

	Length (km)	1.4GHz 50%	1.4GHz 0.01%	7.5GHz 50%	7.5GHz 0.01%	18.6GHz 50%	18.6GHz 0.01%
Tu1	194.2	202.6	154.5	221.9	182.9	--	--
Tu2	142.0	193.3	132.5	212.6	150.1	225.0	167.1
Tu3	90.5	177.2	144.2	202.4	167.8	--	--
Tu4	53.1	130.5	130.2	145.0	135.5	--	--
Tu5	88.5	175.6	134.5	203.2	155.2	--	--
Tu6	43.7	150.5	132.8	166.5	152.6	176.9	165.4

Measurements were made of the total power in a 1.5 kHz bandwidth for each link at a rate of 10 Hz. The total power method was chosen in preference to coherent detection as although the latter would give a higher dynamic range, it is unreliable for trans-horizon paths when scattering is significant. The 10 Hz sampling rate was chosen to allow the detection of scintillation on the line of sight path and to determine if multipath fast fading was significant on the trans-horizon paths. Recording at 10 Hz has previously been seen as expensive in terms of data storage, the 50 Mbytes per day required is no longer a problem with modern hard disk capacities.

3. Single entry statistics

The plots of single entry Cumulative Density Functions (CDFs) have been plotted on an unusual type of graph paper which emphasises both the low and high time percentage ends. In all these plots signal levels are normalised such that 0 dB represents the free space level.

The line of sight links are compared with ITU-R P.530 in Figures 3-5. The agreement is very good. This gives us confidence in the quality of the measurements.

The attenuation of the 18.6 GHz link at high time percentages has been higher than expected. Examination of the data has shown that this was caused by several significant rain fade events. One of the most extreme examples is shown in Figure 6. Here the attenuation is in excess of 40 dB for over an hour. 0.01% of a year is ~52 minutes, so this event alone exceeds the ITU-R P.530 predicted 29.6 dB not exceeded for 0.01% of time.

Examination of the weather radar data for the period of Figure 6 shows that heavy rain was present over most of the path and it is most likely that the path reduction factor is causing the underestimation.

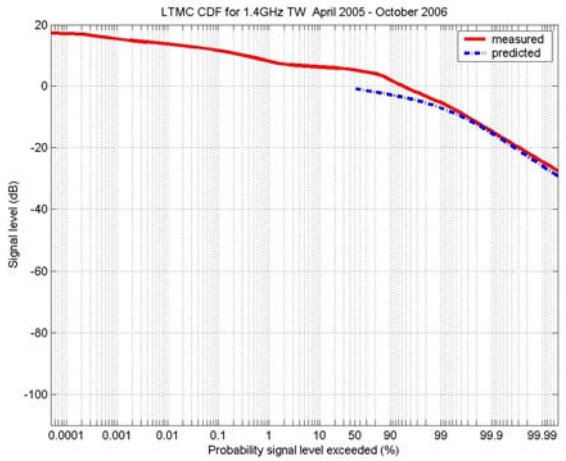

Figure 3 – Line of sight 1.4 GHz link

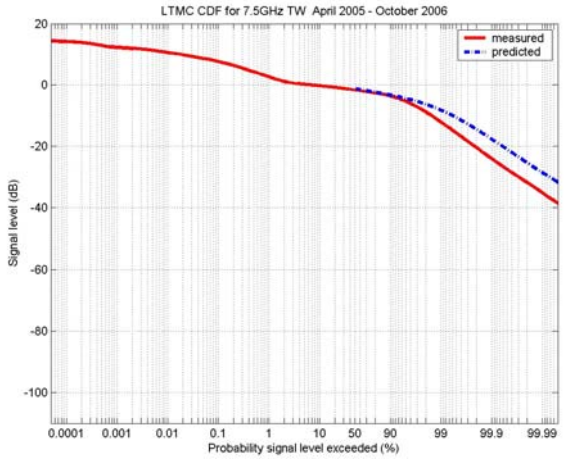

Figure 4 – Line of sight 7.5 GHz link

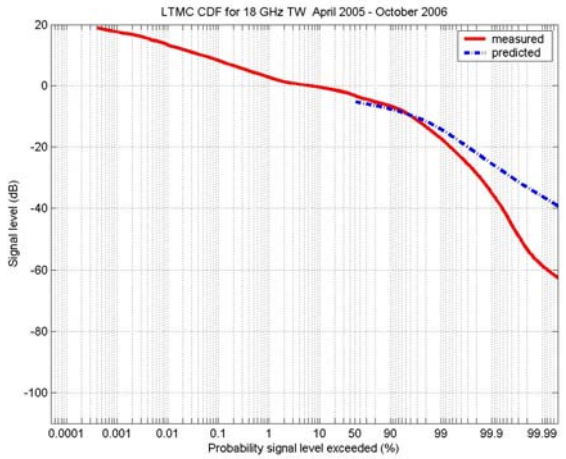

Figure 5 – Line of sight 18.6 GHz link

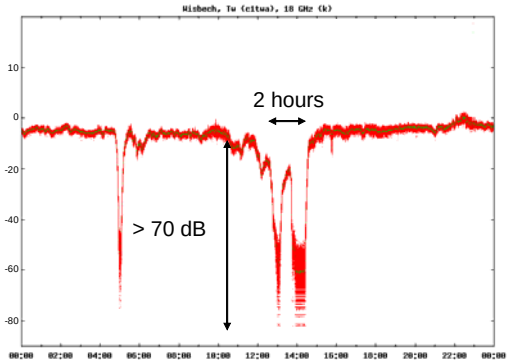

Figure 6 – Rain fades on Line of sight 18.6 GHz link

The trans-horizon links are compared with predictions from ITU-R P.452 in Figures 7-11. Here the agreement is also very good in many cases but not so good in others. The results above 99% should be treated with caution for the long distance links Tu1 and Tu2.

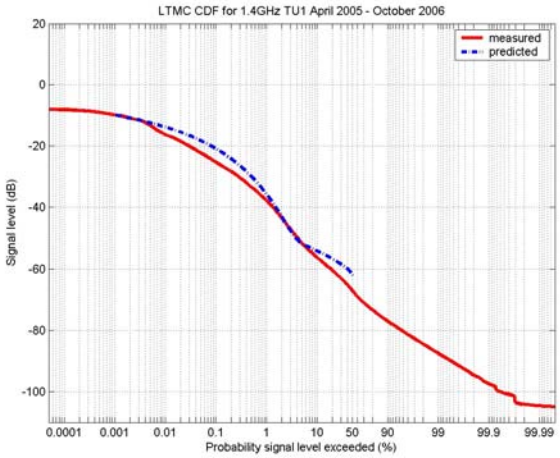

Figure 7 – Trans-horizon 1.4 GHz link

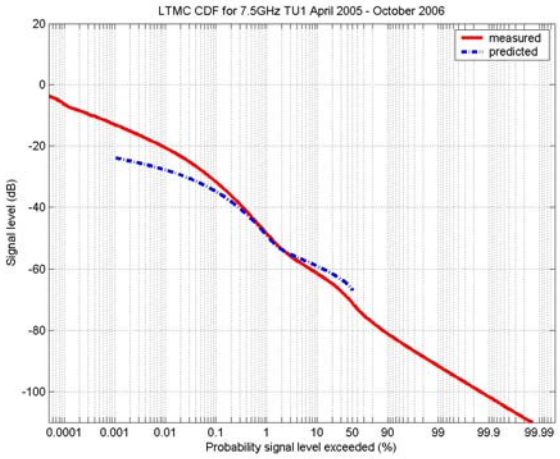

Figure 8 – Trans-horizon 7.5 GHz link

Figure 9 shows a case where the agreement is not so good. This link is almost line of sight. The reason for the prediction error was investigated and the most likely cause was found to be clutter arising from a line of trees along a ridge forming the first diffraction edge along the path. The ITU-R P.452 model uses a terrain database to extract the path profile but this does not contain vegetation data.

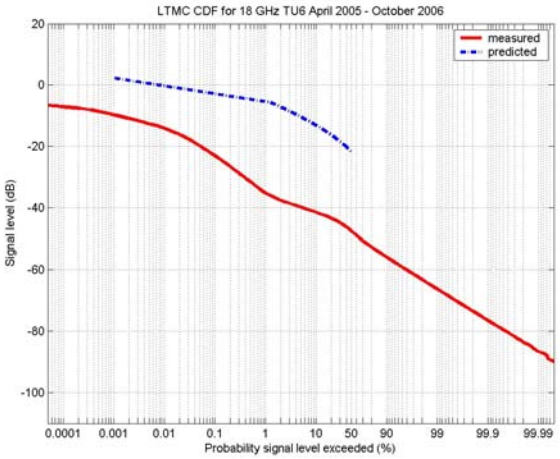

Figure 9 – Near-LOS 18.6 GHz link

The theory that the extra losses are due to vegetation losses is supported by the lower differences found on the 1.4 GHz and 7.5 GHz links which are also deployed along this path. Plots for these frequencies may be found in Figures 10 and 11. It is clear that the offset becomes progressively worse as the frequency increases.

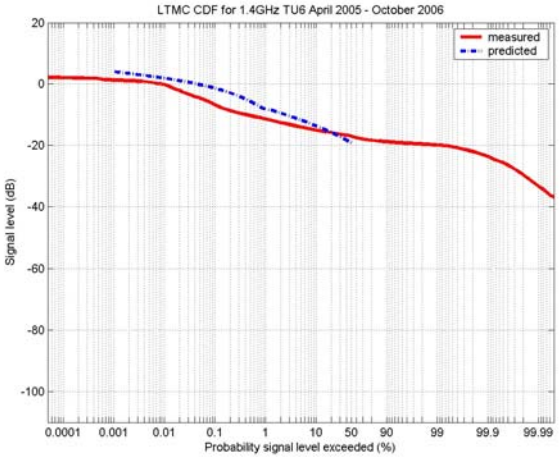

Figure 10 – Near-LOS 1.4 GHz link

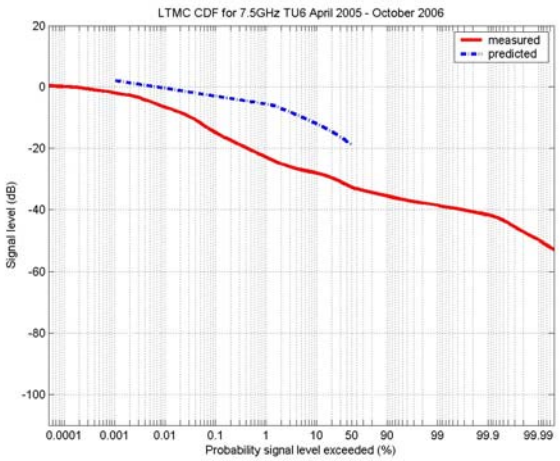

Figure 11 – Near-LOS 7.5 GHz link

The data from the trans-horizon links when compared with the models does show up some differences but these are considered to be within the errors expected from the model. The extension to time percentages above 50% is useful new data for developing models covering all time percentages which are needed for Monte Carlo simulation.

4. Time series

The relatively high temporal resolution of the trans-horizon measurements and the total power within bandwidth method of measurement has produced some interesting results. As expected, the trans-horizon paths show strong multipath for much of the time when the main propagation mechanism is diffraction with the signals becoming more coherent when ducting occurs. This behaviour is most strongly evident on the long Tu1 path and an example was presented previously in [3].

Detailed examination of the 10 Hz time series data indicated that most of the high variability outside enhancement events on trans-horizon path is most probably caused by multipath. With lower sampling rates, it becomes more difficult to distinguish this multipath from noise. Figure 12 demonstrates little would be lost by sampling slower on the line of sight links.

The main aim in deploying the experiment was to obtain simultaneous time series on several paths. Events similar to Figure 13 were found to be very common along the Tw, Tu2, Tu1 path, occurring before sunrise on nearly every day during August. This is an important result as current assignment procedures assume that simultaneous fading and enhancement is unlikely.

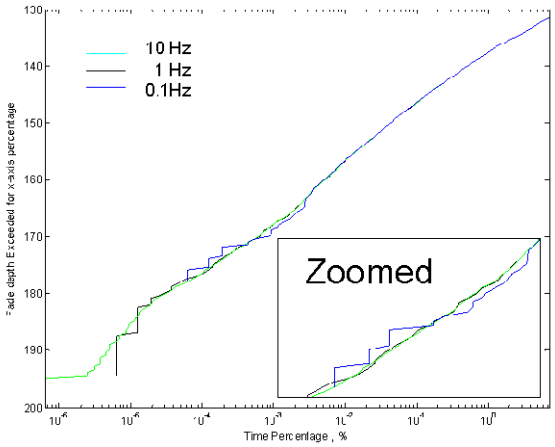

Figure 12 – Comparison of statistics from Tw 1.4 GHz when sampled at 10 Hz, 1 Hz and 0.1 Hz

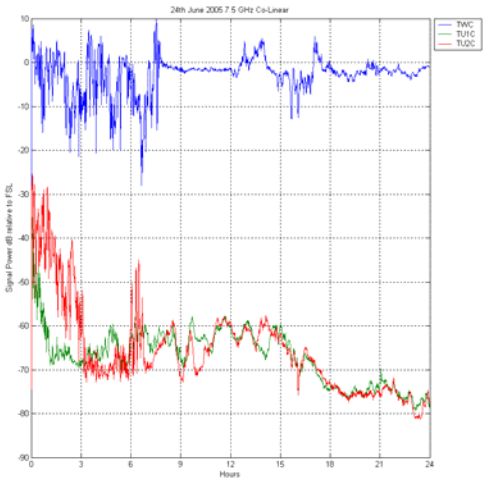

Figure 13 – Simultaneous fading and enhancement at 7.5 GHz

The results of a joint statistical analysis of the recorded time serries data will now be presented.

5. Joint statistics

A unique feature of this experiment is the availability of joint signal distributions. Some pair-wise examples are shown in this paper. Combinations of more than two signals are available but impossible to plot on paper.

There are 44 possible 2 way combinations of plots in the database, assuming all pairs are at the same frequency, a few examples will now be introduced.

Figures 14-17 show some sample combined signal PDFs. As these plots are unusual they require some explanation. The joint PDF is generated from time series data of two channels with one channel controlling

the X axis and the other the Y axis. The Z axis in these plots is the relative frequency of the associated combination of X and Y signal amplitudes. As in the previous single entry statistics, all levels are relative to free space. The Z axis is represented by a grey scale, the mapping shown in Figure 14 is applicable to all plots. A logarithmic scale of probability is used as fixed link interference planning requires knowledge of rare combinations.

Figure 14 shows the combination of two 1.4 GHz signals, one line of sight signal and the other via a co-linear long range trans-horizon path. The line of sight signal is clearly much more stable and there does not appear to be much correlation between the two signal levels.

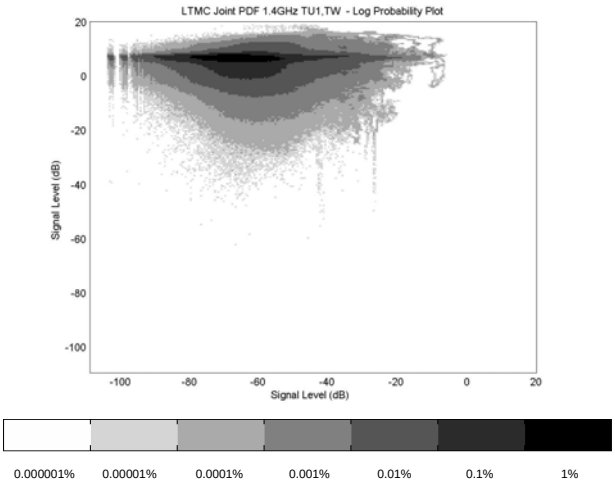

Figure 14 – A line of sight and a co-linear trans-horizon signal at 1.4 GHz

The trans-horizon signal in Figure 14 is highly variable which is a feature of this type of path where the median signal level is dominated by a troposcatter path and consequently strongly attenuated and exhibiting high levels of scintillation. Occasional signal enhancements up to the line of sight level are caused by ducting. The CDF of this signal predicts a 60 dB range between 50% and 0.01% was shown in Figure 7.

Figure 15 shows a combination of two signals at 7.5 GHz. Here one signal is line of sight and the other near line of sight and of a similar length but at a different azimuth. Again, there is no obvious correlation between the signals. The variability of the near line of sight signal is much less than the trans-horizon signal of Figure 14.

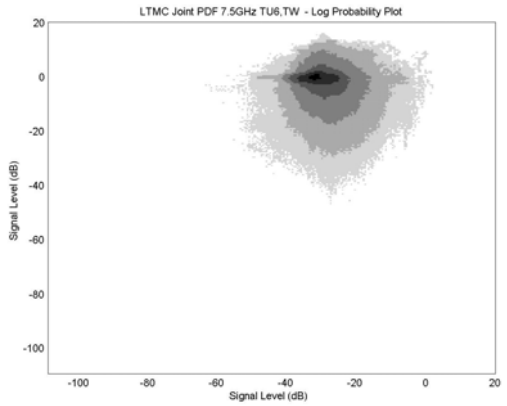

Figure 15 – A line of sight and an off-axis trans-horizon signal at 7.5 GHz

Figure 16 shows a case where two trans-horizon signals show a degree of correlation. This is evident in the 45^{o} slant to the plot. This correlation is expected as these two paths, Tu1 and Tu2 are co-linear. For these paths super-refraction and ducting are the most likely cause of significant enhancements.

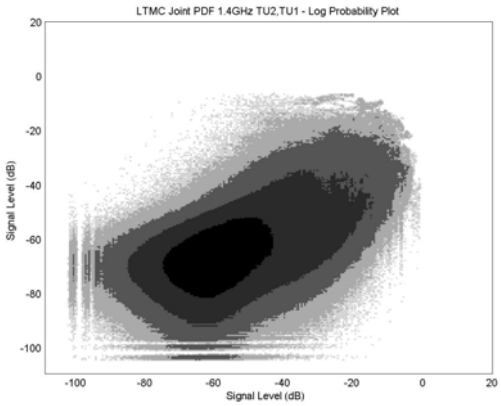

Figure 16 – Co-linear trans-horizon signals at 1.4 GHz

Figure 17 shows the same paths as Figure 16 but at 7.5 GHz. The shapes are the same demonstrating that the correlation holds with frequency, at least between 1.4 GHz and 7.5 GHz.

Figures 18 to 20 show the three medium range trans-horizon signals. All these paths were designed just meet assignment criteria when one antenna is off-axis. Within the limitations of the experiment they should have similar characteristics. Tu3 is approximately 30^{o} offset in azimuth from Tu2. Tu5 is 30^{o} offset from Tu3 and 60^{o} offset from Tu2. All these paths show some correlation and there does not appear to be a very strong dependence on offset angle.

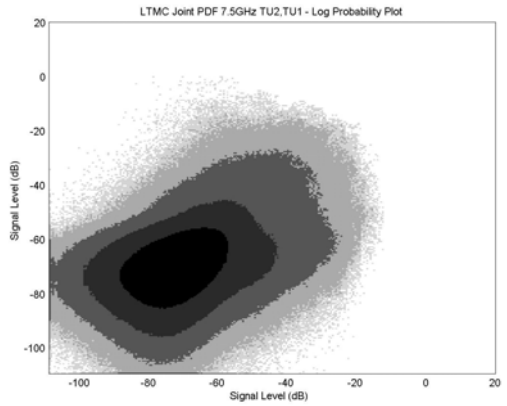

Figure 17 – Two co-linear trans-horizon signals at 7.5 GHz

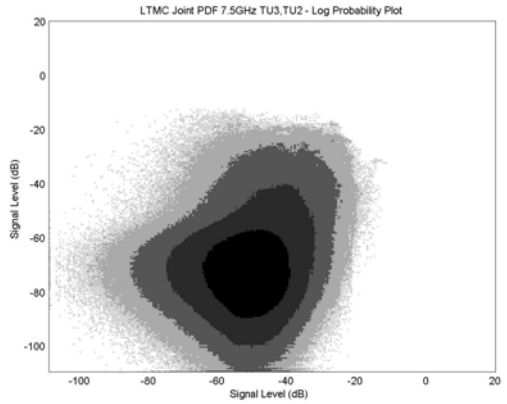

Figure 18 – The co-linear trans-horizon signal and an off-axis trans-horizon signal at 7.5 GHz

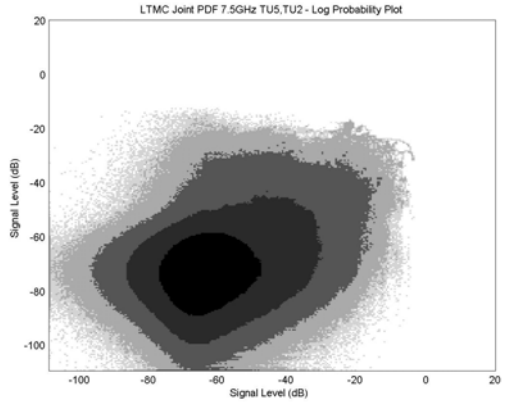

Figure 19 – The co-linear trans-horizon signal and the other off axis trans-horizon signal at 7.5 GHz

Tu3 and Tu5 appear to be very well correlated with each other. The correlation between these links at 1.4 GHz is lower. Figure 21 shows the relationship between Tu2 and Tu3 and Figure 22 shows the relationship between Tu3 and Tu5, both at 1.4 GHz.

This is an interesting result, although paths Tu3 and Tu5 are correlated with each other, unlike the result at 7.5 GHz neither is well correlated with Tu2. Tu2 is a much longer path and this may be the reason for this.

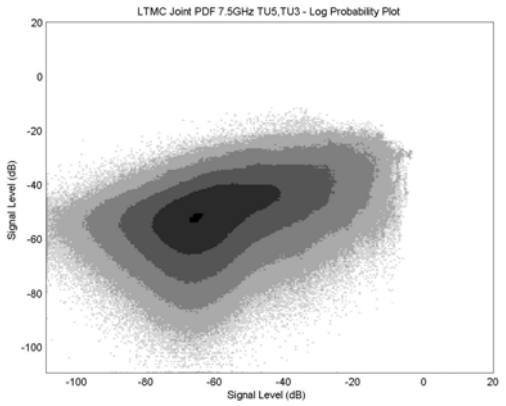

Figure 20 – Both off-axis trans-horizon signals at 7.5 GHz

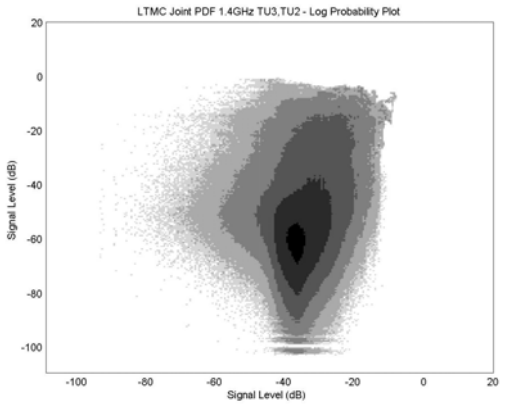

Figure 21 – The co-linear trans-horizon signal and an off-axis trans-horizon signal at 1.4 GHz

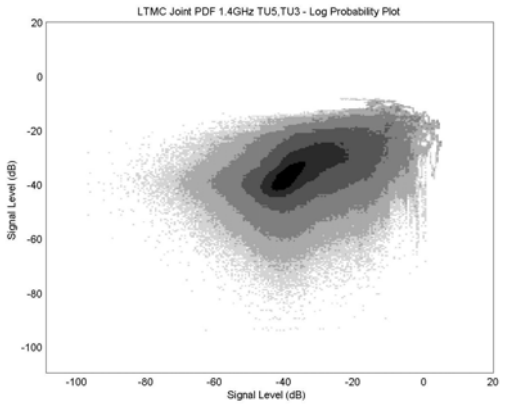

Figure 22 – Both off axis trans-horizon signals at 1.4 GHz

6. Conclusions and future steps

This paper has described some of the results from a long term measurement programme that has now gathered close to two years of high quality link data.

This data has been collected with sufficient dynamic range to provide input towards the goal of producing a propagation model covering 0% to 100% of the time. Work is currently progressing on this within ITU-R.

The time series data has yielded many interesting propagation events that are worthy of further study, including events demonstrating rain fading, rain scatter, atmospheric multipath and ducting. The sampling rate of 10 Hz has been found to be about right for this type of study, a rate of 1 Hz is statistically sufficient on the line of sight paths but the higher rate data makes it easier to separate propagation mechanisms on the trans-horizon paths.

The single path statistics have been compared with ITU-R models and have been found to agree within the expected error range of the models.

The joint statistical information gathered by the experiment now forms a valuable resource that is being used to develop a joint statistical model for interference. This model is progressing well and is reported in the companion paper [5]. The measurements are so far limited to a single site. That site is characterised by low lying flat coastal plains and is known to have a high incidence of ducting. It is hoped to repeat a similar experiments in another part of the UK with different terrain.

7. References

[1] ITU-R Recommendation P.530-11, “Propagation data and prediction methods required for the design of terrestrial line-of-sight systems”, Available from ITU http://www.itu.int

[2] ITU-R Recommendation P.452-12, “Prediction procedure for the evaluation of microwave interference between stations on the surface of the Earth at frequencies above about 0.7 GHz”, Available from ITU http://www.itu.int

[3] A long term propagation measurement campaign, Dr Mike Willis, Professor Ken Craig, Mr Malcolm Hamer, Mr Roger Stuckey, ClimDiff.11, ClimDiff 2005, URSI, 1, Cleveland, Ohio, USA.

[4] Terrestrial fixed link assignment criteria for Fixed Point-to-Point Radio Services with Digital Modulation, OfW46, OfW47 & OfW50, available from Ofcom http://www/ofcom.org.uk

[5] A Model for the Correlation of Fading and Enhancement on Radio Links, K.H. Craig, ISART 2007, Boulder Colorado

A Model for the Correlation of Fading and Enhancement on Radio Links

K.H. Craig
Radio Communications Research Unit, CCLRC Rutherford Appleton Laboratory, UK
Tel: +44 1235 445134; Fax: +44 1235 446140; Email: k.h.craig@rl.ac.uk

Abstract

A new approach to the modelling of correlation between fading and enhancement on radio links is proposed. The joint probability density function (PDF) is central to characterising the statistical dependence of the statistics of multiple paths. The proposed method makes use of statistical functions called copulas to generate families of joint PDFs from the single-path cumulative probability distribution functions (CDF). These CDFs are obtained directly from ITU-R Recommendations P.530 and P.452, and so the new model can be seen to extend the ITU-R models to multiple paths. The paper describes a prediction model for joint pair-wise PDFs. The choice of copula function and the parameters of the model are based on recent measurements in the UK.

1. Introduction

The planning of radio services often requires assumptions to be made about the correlations of fading and enhancements between radio links in a region. The current ITU-R models for fixed link (P.530 [1]) and interference (P.452 [2]) planning only consider the statistics of a single path, and give no guidance on the joint statistics of neighbouring paths. Two important applications are:

- Co-ordination of millimetric point-to-multipoint systems with "sensitive" services (such as radioastronomy) requires a calculation of the aggregate interference generated by a large number of user terminals in a service area. An assumption of either fully correlated or fully uncorrelated statistics between the paths is usually made. The two results can differ by tens of decibels (at both ends of the distribution) and neither assumption is realistic.
- Line-of-sight link planning is based on the fading statistics of the wanted path, and the enhanced interference signal statistics of the unwanted paths. Assumptions are made about the correlation between the multiple interference paths, and between the wanted and interference paths. Over-conservative assumptions could lead to inefficient use of the radio spectrum.

Improvements require a methodology for representing the joint fading statistics (in particular, the joint probability density function—PDF) between the radio paths. Joint PDFs can be derived directly from suitable measurements, such as those described in [3]. Developing a new prediction model requires more than this however. There needs to be some parameterisation of the joint PDFs in terms of physical quantities of the paths (frequency, path length, path separation, etc) *so that the results can be extended to different path geometries and climates than those specific to the measurements*.

The parameterisation of the joint PDFs should encapsulate the notion of dependence between the statistics of the two single paths, or in practical terms, how the fading and enhancements on the wanted and unwanted paths are related. A classical measure of dependence is the "correlation coefficient". However (a) a correlation coefficient between the wanted and unwanted PDFs does *not* by itself define a joint unique PDF; in fact there are infinitely many PDFs that have the same correlation coefficient; (b) a rigorous definition of dependence can only be made within the context of a mathematically sound basis for the joint PDF.

The paper describes a methodology based on functions called *copulas*. Copulas are mathematically rigorous functions for generating joint PDFs from *marginal* PDFs such as are given by P.452 and P.530. There are many suitable copulas that can give rise to a variety of shapes for the joint PDF. These provide a rigorous basis for a prediction method of "correlated" path statistics, parameterised by means of physical parameters. An advantage of this approach is that any new model will reduce to the P.530 and P.452 models for the single path statistics, and so will build on the generality and widespread acceptance of these models.

The necessary statistical background of multivariate statistics is given. This is followed by a description of the proposed approach to modelling joint PDFs. A tentative formulation of the complete model is then presented, based on recent measurements made in the UK [3].

2. Multiple path statistics

The output of propagation models such as P.530 and P.452 is expressed in terms of cumulative probability distribution functions (CDF). For example, Figure 1 shows the interference levels calculated by P.452 for two transhorizon paths. Conventionally basic transmission loss ("path loss") is plotted against time percentage (log axis). This graph is therefore strictly an *inverse* CDF, since a CDF is the probability (that is, time percentage divided by 100) of a given path loss level being exceeded or not exceeded. Formally the CDF $F(x)$ of a random variable X is defined as the probability that X is less than the value x:

$$F(x) = \text{Prob}(X \le x); \qquad f(x) = \frac{dF(x)}{dx}$$

$f(x)$ is the corresponding *probability density function* (PDF).

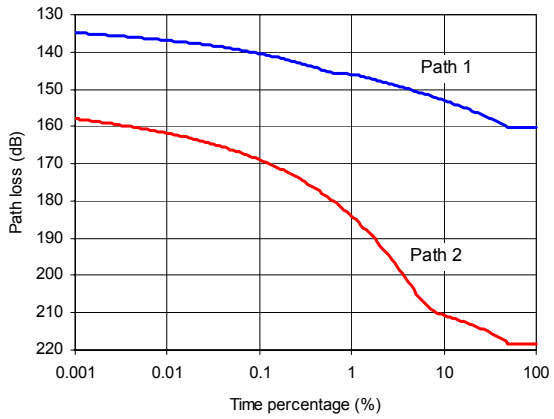

Figure 1: CDFs of two transhorizon paths

To describe the joint statistics of multiple paths we must consider *multivariate* probability distributions of more than one variable. In this paper we focus on two-path statistics, although the extension to N paths is conceptually straightforward. The *joint* cumulative distribution function for 2 random variables, X_1 and X_2, is defined by:

$$F_{X_1X_2}(x_1, x_2) = \text{Prob}(X_1 \le x_1 \text{ and } X_2 \le x_2)$$

and the joint PDF for this bivariate distribution is:

$$f_{X_1X_2}(x_1, x_2) = \frac{\partial^2 F_{X_1X_2}(x_1, x_2)}{\partial x_1 \partial x_2}$$

The difficulty for modelling the fading and interference problem is that neither P.530 nor P.452 consider the joint probability function at all. Instead, these models give the univariate *marginal* distribution for each single path. The marginal cumulative distribution for path 1 is:

$$F_{X_1}(x_1) = P(X_1 \le x_1 \text{ and } X_2 \in [-\infty, \infty])$$

This is obtained by integrating the bivariate PDF over all values of X_2 (giving the univariate marginal probability density function) and then integrating this univariate PDF to the value of x_1:

$$F_{X_1}(x_1) = \int_{-\infty}^{x_1} \int_{-\infty}^{\infty} f_{X_1X_2}(y, x_2) dx_2 \, dy$$

$F_{X_2}(x_2)$ is calculated similarly.

Figure 2 shows a joint PDF that has the two univariate distributions of Figure 1 as its marginal distributions. The way in which this PDF was generated is discussed in the following Sections. The PDF is shown as a contour plot of probability, with each contour representing a decade of probability. The upper curve labelled Path 1 in Figure 1 corresponds to the x-axis of Figure 2, while the lower curve labelled Path 2 corresponds to the y-axis.

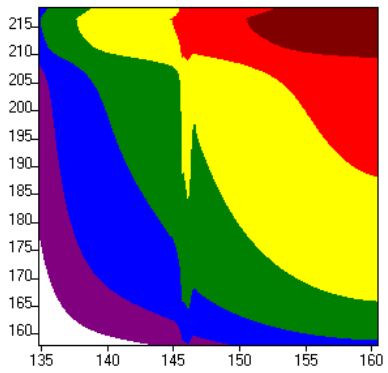

Figure 2: Joint PDF corresponding to Figure 1 (independent variables)

In this example, the statistics of the two paths have been assumed to be independent so that the joint PDF $f_{X_1X_2}(x_1, x_2)$ can be written as:

$$f_{X_1X_2}(x_1, x_2) = f_{X_1}(x_1) \, f_{X_2}(x_2)$$

In this case the joint PDF is fully defined by the two marginal distributions via the univariate PDFs $f_{X_1}(x_1)$ and $f_{X_2}(x_2)$.

However the situation is quite different when the two paths are not statistically independent. In this case

knowledge of the one-dimensional marginal distributions is not sufficient to construct the joint PDF. One classical measure of the degree of dependence between two random variables is the (Pearson product moment) correlation coefficient. Figure 3 shows two examples of PDFs that again have marginal distributions corresponding to the two one-dimensional distributions of Figure 1. Figure 3(a) in particular shows a "top-right to bottom-left" alignment that would be expected of two variables that are positively correlated (that is, both tend to fade together). So the degree of correlation is one parameter that can be used to differentiate between different 2D PDFs with given marginal distributions.

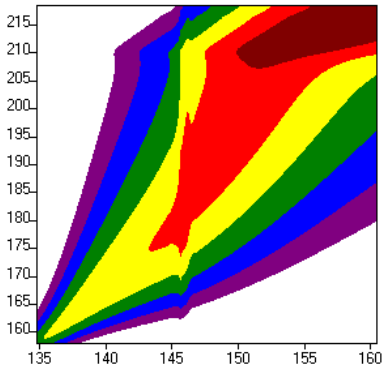

(a)

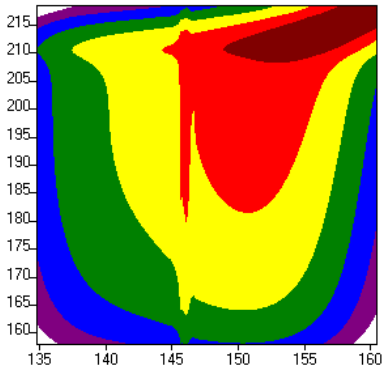

(b)

Figure 3: Joint PDFs corresponding to Figure 1 (dependent variables)

However Figure 3 illustrates another important fact: Figure 3(a) and (b) actually have the *same* correlation coefficient of 0.75. Thus even knowing the correlation coefficient is not sufficient to uniquely define the joint PDF.

The way in which we choose an appropriate joint PDF to represent the statistics of radio paths is given in the following Sections.

3. Modelling joint signal-level PDFs

The aim of this work is to develop a method for calculating the joint PDFs of the fading and enhancements on wanted and unwanted paths or enhancements on multiple interference paths. The mathematical basis is the theory of copulas. An explicit model has been developed that constructs the joint PDF from the single path statistics given by P.530 or P.452. The details and parameters of the new model are based on recent measurements.

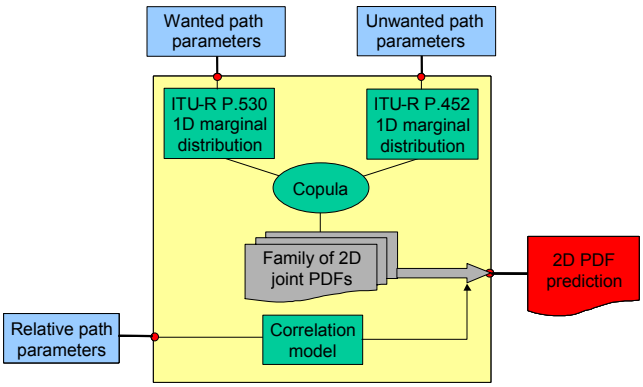

Figure 4: Proposed joint PDF prediction model

The model consists of 3 steps. Figure 4 shows a conceptual view of these steps for a wanted/unwanted path PDF:

1. For a wanted-unwanted path PDF, the single path statistics are generated from ITU-R P.530 and P.452 as usual. (For joint interference-interference PDFs, P.452 would be used for both paths.) These models actually give cumulative distribution functions (CDFs) rather than PDFs

2. The copula is a function that combines the two single path CDFs and produces a family of joint CDFs. Every member of the family has the *same* one-dimensional marginal distributions which are just the two single-path CDFs, but each has different joint properties. The joint PDF is simply obtained from the joint CDF by differentiation.

3. A model is required to select the correct joint PDF for two particular paths from the copula family. This is referred to as a "correlation model" since one of the main features of the different members of the copula family is that they have different correlation properties. In practice we do not need to calculate numerical correlation *coefficients*. Instead we use the copula parameter directly. We aim to make the correlation model depend only on

"relative path" parameters (such as path separation angle or path length ratios) rather than on the specifics of the individual paths (which are accounted for in the P.530 and P.452 models).

In statistics, copulas are functions that join multivariate distribution functions to their one dimensional marginal distributions A two-dimensional copula is a function from the unit square $[0,1]\times[0,1]$ to the unit interval $[0,1]$ with certain simple properties that make it suitable to represent a CDF. The existence of such a function is ensured by Sklar's theorem [4]. Given a pair of random variables X and Y on $[-\infty,\infty]$ with joint CDF $F_{XY}(x,y)$ and marginal CDFs $u = F(x)$ and $v = G(y)$, Sklar's theorem states that there exists a copula $C(u,v)$ such that $F_{XY}(x, y) = C(u, v)$.

Conversely, for any copula $C(.,.)$, the function $F_{XY}(x,y)$ defined by this equation is a joint CDF with marginal CDFs given by $F(x)$ and $G(y)$.

In fact there exist an infinite number of such copulas and so an infinite number of joint CDFs can be generated from a pair of marginal distributions. In practice there are many, relatively simple, analytical expressions for the copula $C(u,v)$. Commonly these expressions contain a parameter θ, the copulas thus falling into families. Members of each family produce 2D CDFs (and hence PDFs) of broadly similar "shape", with members of the same family distinguished by the value of θ and differing from each other in some property of the 2D distribution. In this case we seek to relate this property to the notion of correlation.

Three implicit, independent and non-trivial assumptions are being made: (a) single copula family is able to describe the statistical dependence between all pairs of paths, irrespective of the single path statistics; (b) the variety of joint PDFs represented by varying the copula parameter is sufficient to represent the range of correlation observed between the pairs of paths; and (c) a model can be devised for calculating the copula parameter from relative path parameters alone.

The work undertaken to test these assumptions, and to develop the necessary model, used the measurement data described in [3].

4. Derivation of the joint PDF model

The measurements described in [3] produce a total of 45 pair-wise joint PDFs as shown in Table 1.

Table 1: Number of pair-wise joint PDFs

Frequency	Wanted-unwanted	Unwanted-unwanted
1.4 GHz	6	15
7.5 GHz	6	15
18 GHz	2	1

As an example, two unwanted-unwanted PDFs are given in Figure 5. (These PDFs are plotted on axes of path loss relative to free space, as was done in [3]).

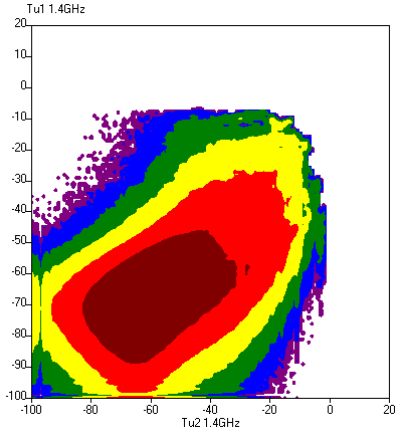

(a) Tu1-Tu2

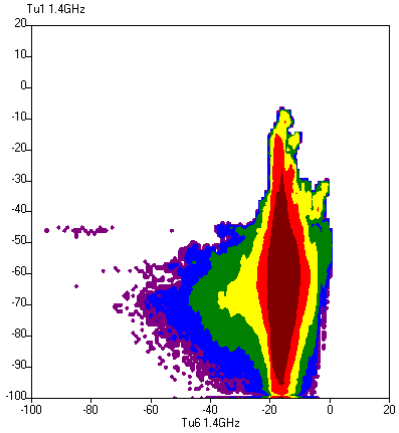

(b) Tu1-Tu6

Figure 5: Measured PDFs of two unwanted-unwanted path pairs

There are a number of things to note:

1. The PDFs cover a large "dynamic range" (hence the logarithmic probability contours).
2. The shapes of the different path pairs, and the wanted-unwanted and unwanted-unwanted path pairs are quite different.
3. There is evidence of correlation on some path pairs (that is, a higher probability of enhancements occurring at the same time on two interference paths, or of enhancement on an interference

occurring at the same time as fading on a wanted path, than vice versa.)

To develop a quantitative model, it is necessary to separate the correlation effects (point 3) from the (stronger) effects (points 1 and 2) caused by the statistics of the individual paths. This separation process is shown graphically in Figure 6. All the graphs, apart from the measured PDF, use linearly spaced contours of probability.

The most significant step is the transformation from "path loss" space to "probability" space. Each axis of the 2D CDF of path loss is transformed by converting every value of path loss to a value of probability via the corresponding 1D marginal CDF. This results in a joint CDF (bottom right in Figure 6) that maps the unit square [0,1]×[0,1] of 1D CDFs to the unit interval [0,1] of the joint CDF. Sklar's theorem proves that there is a copula that does precisely this.

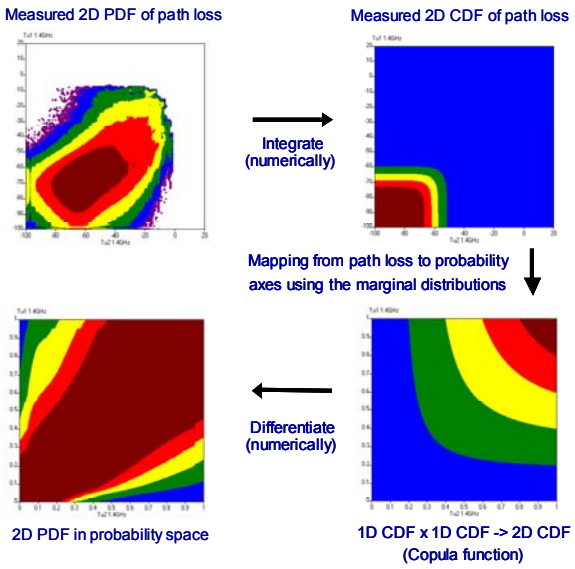

Figure 6: Extracting the "pure" joint statistics from a joint PDF of path loss

5. Choosing a copula

There are many and varied analytical representations of copulas in the literature. A particular class of copulas, known as Archimedean copulas, is favoured because of the ease with which they can be generated. They are also symmetric, which fits in with our assumption that the correlation model should depend only on "relative" path parameters. In the standard textbook on the subject of copulas [5], Nelsen provides a Table of 22 one-parameter families of Archimedean copulas, and these are conventionally referred to as Nelsen 1, Nelsen 2, etc. (Some of the families have alternative names associated with them in the literature.) Based on this, and an earlier study [6], we have focused on this class of copula.

Choosing an appropriate copula for this application is as much an art as a science. In the end numerical fitting is done to derive the model, but it is first necessary to choose a copula family with the correct "shape" to represent the measured data distributions. Differences in the shapes of copulas are more obvious in the joint probability PDFs than in the CDFs (copulas) themselves. Two examples are shown in Figure 7. Comparing these with the experimentally derived PDF shown in the bottom left graph of Figure 6, it should be obvious that the shape of the Clayton copula is more appropriate than the shape of the Gumbel copula. 14 copulas were considered, but only two (Clayton and Nelsen 13) had shapes that merited further quantitative investigation.

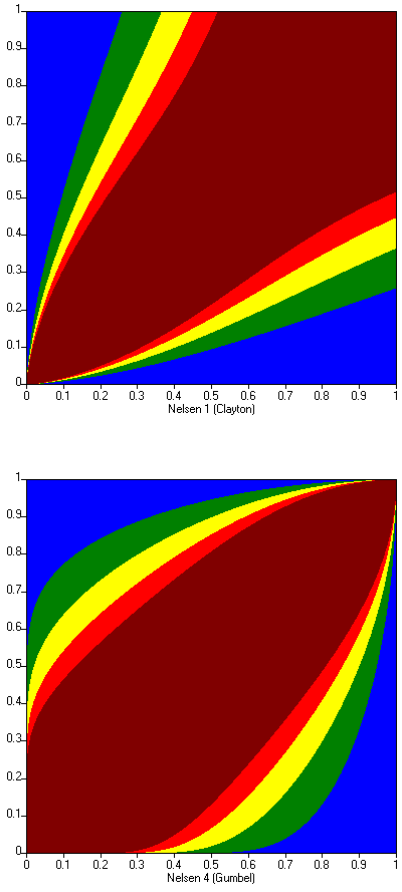

Figure 7: PDFs of Nelsen copulas 1 (Clayton) and 4 (Gumbel)

The definition of the Clayton copula is very simple:

$$C(u,v) = \left(u^{-\theta} + v^{-\theta} - 1\right)^{-1/\theta}$$

u and v are values of the single path marginal CDFs in the range [0,1] and θ is the copula parameter. For this copula, θ can take any value in the range [-1,∞) except for the value 0. Positive values of θ correspond to positive correlation (as illustrated in Figure 7) while negative values of θ correspond to negative correlation.

While it may be possible to find a copula that allows a uniform approach to both positive and negative correlations, the Clayton copula does not have the correct shape for negative values of θ to model the observed (negatively correlated) wanted-unwanted path statistics. At this stage of the work we are content to consider only positive correlations. The wanted-unwanted path PDFs are converted from negative to positive correlation simply by considering the percentage of time that a *fade level* is exceeded for the wanted path and the percentage of time that an *enhancement level* is exceeded for the unwanted path.

So for now we are only interested in values of θ in the range (0,∞). In the limit $\theta \to 0$ the variables are independent, while the "degree of correlation" increases as θ increases. In practice, the range of correlation in the data does not require a value of θ greater than 2.

So having accepted the Clayton copula as a possible candidate, the next step is to find the value of θ which gives the best match to each of the joint probability PDFs derived from the 42 path pairs at 1.4 and 7.5GHz.

The metric used for quantifying the match between model and measurements was the r.m.s. value of the difference between the copula and the measured CDFs. This was done with all 42 measured CDFs. In all cases where a degree of correlation was apparent in the data, a well-defined minimum in the graph of r.m.s. error against θ was obtained.

6. Derivation of the correlation model

The final step in deriving the model is to relate the values of the best-fit copula parameter to some simple "relative path" parameters. There are many choices available. Initial results are given, based on the simplest intuitive ideas.

Radio links on two fully coincident paths must be fully correlated (assuming identical system parameters). As two paths separate, the degree of correlation will decrease. It was found useful to describe the degree of separation in terms of both the angle between the paths, and the difference in path lengths involved. So probably the simplest "correlation" parameter is

$$\beta = \frac{d_{\min}}{d_{\max}}\left(1 - \phi/180\right)$$

where $d_{\min} = \min(d_1, d_2)$, $d_{\max} = \max(d_1, d_2)$, ϕ is given in degrees, and d_1,d_2 and ϕ are defined in Figure 8.

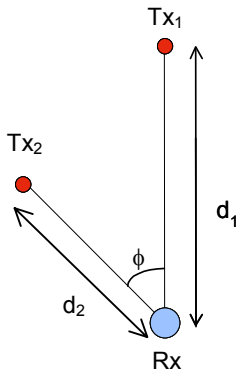

Figure 8: Definition of path parameters

The values of the best-fit copula parameter θ are plotted in Figure 9 against the quantity β for the 15 unwanted-unwanted paths (circles) and the 6 wanted-unwanted paths (squares) at 7.5 GHz. Considering that this is almost the simplest "correlation parameter" possible, a reasonable trend between the two parameters can be discerned, at least for the unwanted-unwanted paths, although there is a large scatter.

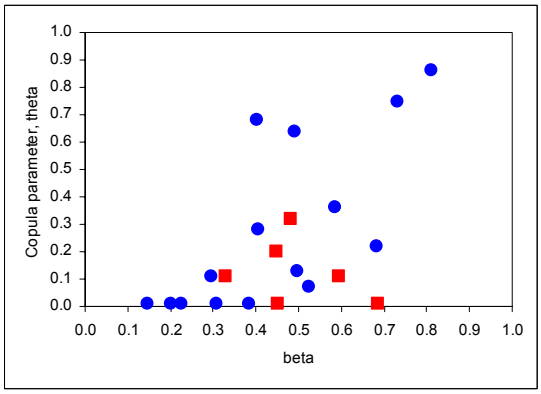

Figure 9: Copula parameter plotted against β for the 7.5GHz paths

A simple trend line of the form $\theta = a\,\beta^b$ was fitted. The values of a and b differed to some extent depending on which subset of paths were included. So for example, the 1.4GHz and 7.5GHz datasets gave somewhat different fits. Further work is obviously required to develop a more sophisticated correlation model to reduce the spread of points in Figure 9 (for example by taking account of the terrain between the paths). In the meantime, values of a and b based on all

30 unwanted-unwanted paths at 1.4 and 7.5GHz are $a = 1.67$, $b = 2.7$.

7. Using the model

Based on the methodology above, we now give an explicit step-by-step procedure for generating the joint, two-dimensional, probability density function (PDF) of basic transmission losses L_1 and L_2 for two paths paths, P_1 and P_2 converging to a common receiver. Call this $PDF(L_1, L_2)$.

The steps are:

1. From the path geometry (path lengths and path separation angle) defined in Figure 8, define the quantity β:

   $$\beta = \frac{d_{\min}}{d_{\max}}\left(1 - \phi/180\right)$$

   where $d_{\min} = \min(d_1, d_2)$ and $d_{\max} = \max(d_1, d_2)$ and ϕ is given in degrees.

2. Calculate the value θ:

   $$\theta = 1.67\,\beta^{2.7}$$

3. For a given pair of values L_1 and L_2, obtain the time percentage values p_1 and p_2:

   (a) For an unwanted (interference) path, the time percentage p_i for which transmission loss L_i is *not exceeded*, is obtained from P.452 (by iteration, since P.452 gives L_i as a function of p_i).

   (b) For a wanted (line-of-sight) path, the time percentage p_i for which transmission loss L_i *is exceeded*, is obtained from P.530.

   (c) Alternatively, the values of p_i can be obtained from L_i using the measured single path statistics, if available.

4. Calculate $CDF(L_1, L_2)$:

   $$CDF(L_1, L_2) = \left[(p_1/100)^{-\theta} + (p_2/100)^{-\theta} - 1\right]^{-1/\theta}$$

5. $PDF(L_1, L_2)$ is obtained from $CDF(L_1, L_2)$ by numerical differentiation

   $$PDF(L_1, L_2) = \frac{\partial^2 CDF(L_1, L_2)}{\partial L_1\, \partial L_2}$$

   for example, using two-variable central differences.

Steps 1 and 2 only need be performed once for each pair of paths, while steps 3–5 need to be repeated for each value of L_1 and L_2.

The function in step 4 is the Clayton copula. This was found to give the best fit of the copulas investigated, but is tentative. The ("correlation") model representing the path geometry in step 1 and the fit of the copula parameter θ in step 2 are also tentative.

Figure 10 compares this model against the measured data for a wanted-unwanted PDF and the unwanted-unwanted PDFs of Figure 5. The measured single path statistics have been used rather than P.452 and P.530, as this is a better test of the "correlation" part of the model. Mismatches between P.452/P.530 and the measurements will produce some shifting and stretching of the simulated PDFs.

8. Conclusions

It has been shown that it is practicable to model the 2-dimensional probability distribution of signal levels arriving over converging paths. Models have been developed using multiple-path measured data recorded in the UK. Work is ongoing to develop a new fixed-link planning method based on joint signal level (wanted-unwanted) PDFs. However, the methodology for modelling general joint-signal PDFs makes more accurate methods available for other aspects of spectrum management, such as the statistics of combined interfering signals.

N-dimensional PDFs are required for a rigorous treatment of multiple interferers. The theory of N-copulas for non-Gaussian distributions is at an early stage of development. A heuristic approach to modelling interference from high density fixed wireless access systems using 2-copulas was given in [6].

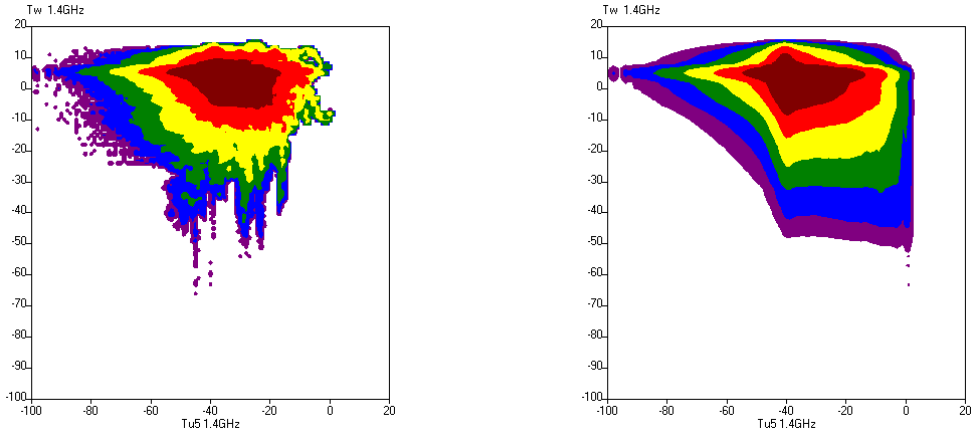

(a) Tw-Tu5

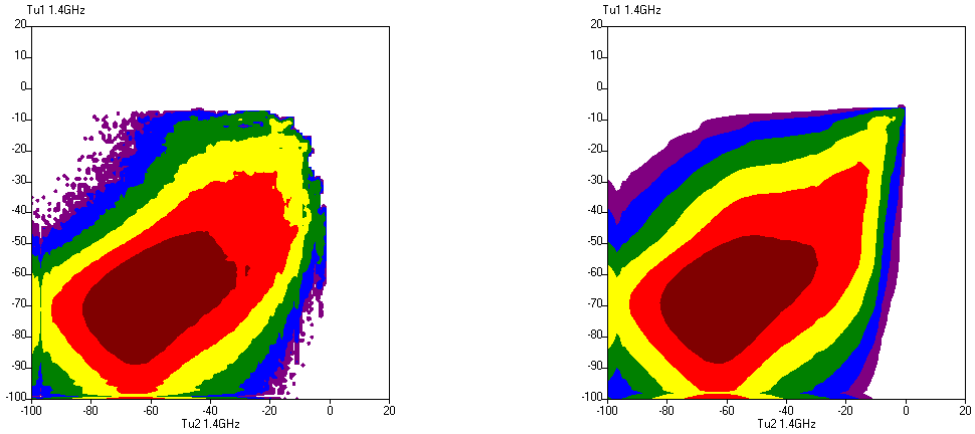

(b) Tu1-Tu2

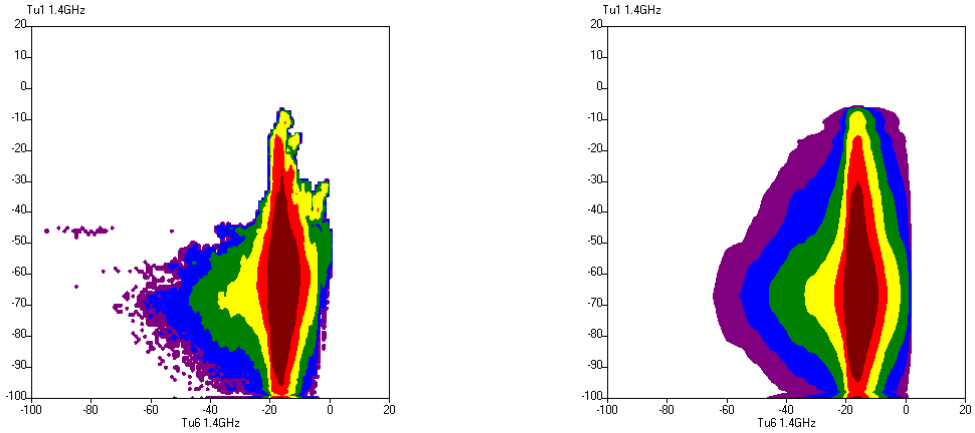

(c) Tu1-Tu6

Figure 10: Comparison of data (left) and model (right)

9. Acknowledgements

This work was funded by Ofcom (and formerly by the Radiocommunications Agency) and the author wishes to thank Ofcom for their support and interest.

10. References

[1] ITU-R Recommendation P.530-11, "Propagation data and prediction methods required for the design of terrestrial line-of-sight systems", 2005

[2] ITU-R Recommendation P.452-11, "Prediction procedure for the evaluation of microwave interference between stations on the surface of the Earth at frequencies above about 0.7 GHz", 2003

[3] Willis M.J. and Craig K.H., "A long term propagation measurement campaign", 9th Int. Symposium on Advanced Radio Technologies, Boulder, Colorado, 2007

[4] Sklar A., "Fonctions de répartition à *n* dimensions et leurs marges", Publ. Inst. Statist. Univ. Paris, 8, pp 229–231, 1959

[5] Nelsen R.B., "An introduction to copulas", Lecture Notes in Statistics Vol 139, Springer Verlag, 1999

[6] Craig K.H., "Theoretical Assessment of the Impact of the Correlation of Signal Enhancements on Area-to-Point Interference", RA Report, 2004: http://www.ofcom.org.uk/research/technology/propagation /interference_mngt/ay4617.pdf

FORM **NTIA-29**
(4-80)

U.S. DEPARTMENT OF COMMERCE
NAT'L. TELECOMMUNICATIONS AND INFORMATION ADMINISTRATION

BIBLIOGRAPHIC DATA SHEET

1. PUBLICATION NO.	2. Government Accession No.	3. Recipient's Accession No.
SP-07-445		

4. TITLE AND SUBTITLE	5. Publication Date
Proceedings of the 2007 International Symposium on Advanced Radio Technologies: February 26-28, 2007	March 2006
	6. Performing Organization Code NTIA/ITS

7. AUTHOR(S)	9. Project/Task/Work Unit No.
Patricia J. Raush, Kristen E. Novik (editors)	6613000-300

8. PERFORMING ORGANIZATION NAME AND ADDRESS	10. Contract/Grant No.
NTIA/ITS.E U.S. Department of Commerce 325 Broadway Boulder, CO 80305	

11. Sponsoring Organization Name and Address	12. Type of Report and Period Covered

14. SUPPLEMENTARY NOTES

15. ABSTRACT (A 200-word or less factual summary of most significant information. If document includes a significant bibliography or literature survey, mention it here.)

16. Key Words (Alphabetical order, separated by semicolons)

17. AVAILABILITY STATEMENT	18. Security Class. (This report)	20. Number of pages
UNLIMITED.		154
	19. Security Class. (This page)	21. Price:

NTIA FORMAL PUBLICATION SERIES

NTIA MONOGRAPH (MG)

A scholarly, professionally oriented publication dealing with state-of-the-art research or an authoritative treatment of a broad area. Expected to have long-lasting value.

NTIA SPECIAL PUBLICATION (SP)

Conference proceedings, bibliographies, selected speeches, course and instructional materials, directories, and major studies mandated by Congress.

NTIA REPORT (TR)

Important contributions to existing knowledge of less breadth than a monograph, such as results of completed projects and major activities. Subsets of this series include:

NTIA RESTRICTED REPORT (RR)

Contributions that are limited in distribution because of national security classification or Departmental constraints.

NTIA CONTRACTOR REPORT (CR)

Information generated under an NTIA contract or grant, written by the contractor, and considered an important contribution to existing knowledge.

JOINT NTIA/OTHER-AGENCY REPORT (JR)

This report receives both local NTIA and other agency review. Both agencies' logos and report series numbering appear on the cover.

NTIA SOFTWARE & DATA PRODUCTS (SD)

Software such as programs, test data, and sound/video files. This series can be used to transfer technology to U.S. industry.

NTIA HANDBOOK (HB)

Information pertaining to technical procedures, reference and data guides, and formal user's manuals that are expected to be pertinent for a long time.

NTIA TECHNICAL MEMORANDUM (TM)

Technical information typically of less breadth than an NTIA Report. The series includes data, preliminary project results, and information for a specific, limited audience.

For information about NTIA publications, contact the NTIA/ITS Technical Publications Office at 325 Broadway, Boulder, CO, 80305 Tel. (303) 497-3572 or e-mail info@its.bldrdoc.gov.

This report is for sale by the National Technical Information Service, 5285 Port Royal Road, Springfield, VA 22161,Tel. (800) 553-6847.